Characterisation of Microvascular and Myocardial Function Changes In Meningococcal Disease

Thesis submitted in accordance with the requirements of the University of Liverpool for the degree of Doctor in Medicine

Fauzia Paize

June 2011

Declaration

This thesis is the result of my own work. The material contained within this thesis has not been presented, nor is being presented for any other degree.

Longitudinal data analysis was carried out by Dr Gerwyn Green and Professor Peter Diggle at the University of Lancaster. Logistic regression analysis in Chapter 3 was carried out by Dr Gerwyn Green at the University of Lancaster.

Viral detection for human herpes virus 6 and human herpes 7 was carried out by Kate Ward at University College London. Viral detection was carried out by Malcolm Guiver Meningococcal reference unit, Manchester.

Bacterial load analysis was carried out by Malcolm Guiver, Meningococcal reference unit, Manchester.

Quantification of Cardiac Troponin I was carried out at the Royal Liverpool Hospital NHS Trust, Biochemistry department. Cardiac Troponin T and procalcitonin determination were carried out by the Alder Hey Children's NHS Foundation Trust, Biochemistry department.

Dedication

To my husband Stu for his unfailing support, encouragement, love and belief in me at all times. This work could not have been completed without him.

Acknowledgements

I would like to thank the Meningitis Research Foundation for funding my period of research.

Thanks to my supervisors Professor Hart, Alistair Thomson, Chris Parry and Enitan Carrol. A special thanks to Professor Hart for his kindness, encouragement and guidance, at all times until his death. His conduct as a supervisor was exemplary and he is sadly missed.

Thanks also to my friends Paul McNamara and Kevin Southern whose mentorship and support throughout the project was beyond that expected for a research fellow not under their supervision.

Thanks to Ian Sinha and Helen Michaels for their contribution in image analysis.

This work could not have been carried out without the co-operation of the patients and their parents and I would like to thank them for their participation. I would also like to thank the medical and nursing staff of the Alder Hey Children's NHS Foundation Trust Emergency Department and the Paediatric Intensive Care Units at the Alder Hey Children's NHS Foundation Trust and the Royal Manchester Children's Hospital for their diligence in informing me of participants to recruit to the study.

Abstract

Meningococcal disease (MCD) is the most common infective cause of mortality in children in the United Kingdom. It is the most common cause of sepsis-induced purpura fulminans in children accounting for 10% of cases.

Between January 2007 and April 2008 45 children with suspected meningococcal disease were prospectively recruited to an observational study. These children were recruited from two-centres, Alder Hey Children's NHS Foundation Trust and the Royal Manchester Children's Hospital NHS Trust. This prospective study aimed to provide further understanding into the haemodynamic response in meningococcal disease, evaluating abnormalities in the macro- and microcirculation in children admitted to intensive care. In addition this study aimed to evaluate the performance characteristics of a new method of detecting infection in children, the Activated Partial Thromboplastin Time (aPTT) waveform.

During the prospective study 33 children were classed as confirmed meningococcal disease, and the other 12 were children with a presumed viral illness. There were 17 children (52%) with severe disease as defined by a Glasgow Meningococcal Septicaemia Prognostic Score (GMSPS) of ≥ 8. 20 children were ventilated and admitted to PICU (60%). There were no deaths.

A significant difference in aPTT TL18 between MCD patients and those with presumed viral illnesses and controls was found. There was no significant difference between children with a presumed viral illness and

controls. This shows that the lower the admission aPTT TL18 (the more severe the BPW) the higher the probability of needing intensive care support.

The aPTT waveform analysis as a simple, rapid and robust diagnostic marker in the detection of meningococcal sepsis that has translational potential in facilitating prompt diagnosis and real-time monitoring of patients with critical illnesses.

Side stream dark field imaging can be utilised in healthy awake and anaesthetised children to obtain sublingual microcirculatory images and establish normal values for disease free children. Images can be evaluated manually and it has been shown that good inter- and intraobserver agreement is possible.

Side stream dark field imaging can also be utilised in children with MCD to evaluate microcirculation dysfunction. A significant reduction in admission microcirculatory measurement was found in children with severe MCD when compared to both anaesthetised and healthy awake controls. These differences were no longer significant pre-extubation showing that microcirculatory recovery occurred alongside clinical recovery. The degree of microcirculatory dysfunction was found to predict the duration of ventilatory requirement, irrespective of the stage of illness at the time of admission to PICU is present in children with MCD. Longitudinal data analysis demonstrated that as the microcirculation improves over time lactate, pCO_2 and FiO_2 all decrease and base excess, pH and urine output all increase over time.

A relationship exists between the microcirculation and vasoactive mediators. In children with severe MCD requiring mechanical ventilation there is release of the cell adhesion molecules E-selectin, Intercellular adhesion molecule-1 (ICAM-1) and vascular adhesion molecule-1 (VCAM-1) when compared to children with MCD who do not require ventilation and PICU support. Children with severe MCD requiring mechanical ventilation also release more nitric oxide (NO) when compared to children with MCD who do not require ventilation and PICU support. A negative correlation exists between admission NO levels and the microvascular flow index for capillaries (MFIc) and longitudinal analysis showed that as the MFIc recovers NO release reduces over time. Longitudinal analysis has shown that as MFIc recovers over time the levels of ICAM-1, NO, IL-1Ra, IL-6 and IL-8 all reduce over time.

Children with severe MCD and septic shock have myocardial cell injury and cardiac systolic and diastolic dysfunction. 60% of the 20 children with confirmed MCD cases, requiring ventilatory support on PICU had abnormal cardiac troponin (cTn) values. None of the children with a presumed viral illness or those with a confirmed diagnosis of MCD who did not require admission to PICU had an elevated cardiac troponin T (cTnT) or cardiac troponin I (cTnI). 50% of children admitted to PICU had systolic dysfunction as measured on echocardiography as the fractional shortening and a rise in cTn. Two of the ventilated children had raised cTn values but normal cardiac systolic function. Positive correlations exist between peak cTn levels and indicators of disease severity including severity assessment scores, duration of inotropic and ventilatory support and hospital stay. 37% of the children receiving mechanical ventilation had abnormal diastolic function at admission as assessed by the Ea wave of the tissue doppler

imaging echocardiography (TDI). Levels of N-Terminal Pro Brain Natriuretic Peptide (NT-proBNP) were significantly higher in all children with MCD compared to those with a presumed viral illness and controls. NT-Pro BNP levels correlate with disease severity and declines as clinical recovery occurs in children with severe MCD. Admission NT-Pro BNP levels predict left ventricular filling pressure as assessed by the E/Ea ratio of TDI even when accounting for children presenting at different times in their illness.

Table of Contents

List of figures		1
List of tables		5
Abbreviations		7
Chapter 1: Introduction		**13**
1.1	General Background	14
1.2	Epidemiology	16
1.3	The Meningococcus	19
1.4	Pathophysiology	21
1.4.1	Endotoxin and cytokines	22
1.4.2	Endothelial dysfunction	25
1.4.3	Cardiac dysfunction	26
1.4.4	Coagulopathy	27
1.5	Diagnosis	29
1.6	Clinical manifestations and management	31
1.6.1	Signs and symptoms	31
1.6.2	Management	32
1.6.2.1	Emergency Department management	33
1.6.2.2	Inotropes	34
1.6.2.3	Management on PICU	35
1.6.2.4	Adjunctive therapy	37
1.6.2.5	Novel therapies	37
1.7	The Microcirculation and Tissue Perfusion	39

1.8	Tissue perfusion assessment	41
1.8.1	Near Infrared Spectroscopy (NIRS)	41
1.8.2	Laser doppler flowmetry	43
1.8.3	Gastric tonometry	43
1.8.4	Sublingual Capnometry	44
1.8.5	Intravital Microscopy	44
1.9	Orthogonal Polarisation Spectral imaging and Side Stream Darkfield Imaging	44
1.10	OPS and SDF in monitoring the microcirculation in sepsis	45
1.11	Monitoring of the Macrocirculation in Sepsis	49
1.11.1	Troponin	51
1.11.2	N-Terminal Pro Brain Natriuretic Peptide	53
1.12	Aims of current prospective study	56

Chapter 2: Methods and materials **57**

2.1	Patient Recruitment	58
2.1.1	Study Design	58
2.1.2	Notification of cases and controls	59
2.1.3	Assessment of patients	61
2.1.4	Disease severity assessment	61
2.1.5	Definitions	65
2.1.6	Patient Inclusion Criteria	66
2.1.7	Patient Exclusion Criteria	66
2.2	Blood Sampling	66
2.2.1	Blood sample separation and storage	68

2.3	Analysis of blood samples	68
2.3.1	aPTT waveform analysis	68
2.3.2	Quantification of Procalcitonin	69
2.3.3	Quantification of endothelial cell adhesion molecules	69
2.3.3.1	ICAM-1	69
2.3.3.1a	Materials	69
2.3.3.1b	Method	70
2.3.3.1c	Performance characteristics of the assay	70
2.3.3.2	VCAM-1	71
2.3.3.2a	Materials	71
2.3.3.2b	Method	73
2.3.3.2c	Performance characteristics of the assay	73
2.3.3.3	P-Selectin	73
2.3.3.3a	Materials	73
2.3.3.3b	Method	74
2.3.3.3c	Performance characteristics of the assay	75
2.3.3.4	E-Selectin	75
2.3.3.4a	Materials	75
2.3.3.4b	Method	75
2.3.3.4c	Performance characteristics of the assay	76
2.3.4	Quantification of cytokines	76
2.3.4a	Materials	76
2.3.4b	Reagent Preparation	77
2.3.4c	Assay Procedure	77
2.3.5	Quantification of Nitric Oxide Metabolites	81

2.3.5a	Materials	81
2.3.5b	Method	84
2.3.5c	Calculation of Results	85
2.3.5d	Performance characteristics of the assay	85
2.3.6	Quantification of NT ProBNP	85
2.3.7	Quantification of Cardiac Troponin I and Cardiac Troponin T	85
2.3.8	Quantification of Bacterial Load and viral detection	86
2.4	Microcirculation visualisation	87
2.5	Echocardiography	90
2.5.1	Systolic function	90
2.5.2	Diastolic function	90
2.5.3	Global function	91
2.6	Statistical Methods	91

Chapter 3: Diagnostic efficacy of Activated Partial Thromboplastin Time (aPTT) waveform and Procalcitonin analysis in paediatric meningococcal sepsis **94**

3.1	Introduction	95
3.2	Subjects and Methods	97
3.2.1	aPTT waveform and PCT analysis	97
3.2.2	Full blood count and CRP analysis	98
3.2.3	Statistical analysis	100
3.3	Results	100
3.3.1	Test performance in the diagnostic groups	101

3.3.2	Probability of admission to PICU	109
3.3.3	Serial monitoring	111
3.5	Discussion	114
3.6	Conclusion	117

Chapter 4: The microcirculation in normal children using Side Stream Dark Field Imaging **118**

4.1	Introduction	119
4.1.1	Outcome measures from microcirculation images	120
4.1.2	Histology and anatomy of the tongue	123
4.2	Materials and Methods	125
4.2.1	Patients recruited	125
4.2.2	Microcirculation visualisation	125
4.2.3	SDF image analysis	126
4.2.4	Statistical analysis	131
4.3	Results	131
4.3.1	Inter- and Intraobserver repeatability	138
4.3.1.1	Image attainment	138
4.3.1.2	Image analysis	141
4.4	Discussion	145
4.4.1	Limitations	148
4.4.2	An approach to automated microcirculation image analysis	148
4.5	Conclusion	150

Chapter 5: The Microcirculation in Meningococcal Disease **51**

5.1	Introduction	152
5.1.2	The microcirculation in childhood sepsis	153
5.2	Method	153
5.2.1	Patients	153
5.2.2	Echocardiography	153
5.2.3	Statistics	154
5.3	Results	154
5.3.1	Agreement	157
5.3.2	Microcirculatory variables	160
5.3.3	Predicting outcome	167
5.3.4	Longitudinal Data Analysis	170
5.4	Cardiac comparative group	175
5.5	Discussion	176
5.6	Conclusion	180

Chapter 6: Vasoactive mediators and the microcirculation in meningococcal disease **181**

6.1	Introduction	182
6.1.2	Vasoactive mediators	182
6.1.2.1	Cell Adhesion Molecules	182
6.1.2.2	Nitric oxide	183
6.2	Method	185
6.2.1	Statistics	185

6.3	Results	186
6.3.1	ICAM-1	186
6.3.2	VCAM-1	188
6.3.3	P-Selectin	190
6.3.4	E-Selectin	192
6.3.5	Nitric oxide	195
6.3.6	Cytokines	199
6.4	Discussion	200
6.5	Conclusion	203

Chapter 7: Cardiac function in meningococcal disease **204**

7.1	Introduction	205
7.1.1	Assessment of cardiac function in sepsis	206
7.1.1.1	Biomarkers	206
7.1.1.2	Cardiac systolic, diastolic and global function assessment	208
7.1.1.3	Cardiac output measurement	217
7.2	Method	220
7.2.1	Patients	220
7.2.2	Echocardiography	221
7.2.3	Troponin	221
7.2.4	NT-Pro BNP	221
7.2.4a	Reconstitution	222
7.2.4b	Method	222
7.2.4c	Performance characteristics of the assay	223
7.2.5	Cytokine determination	223
7.2.6	Statistics	223

7.3	Results	224
7.3.1	Cardiac Troponin and systolic function	224
7.3.2	NT-Pro BNP and Diastolic function	231
7.3.3	Global function	242
7.3.4	Cardiac output and Index	244
7.3.5	Agreement	247
7.4	Discussion	249
7.4.1	Cardiac Troponin and systolic function	249
7.4.2	NT-Pro BNP, Diastolic function and Global function	251
7.4.3	Cardiac output and index	253
7.5	Conclusion	256

Chapter 8: Conclusions **257**

8.1	Summary of conclusions from the studies	258
8.2	Future research	259
8.2.1	Targeted anti-inflammatory therapy	259
8.2.2	Vasoactive agents	260
8.2.3	Novel microcirculation therapies	261
8.2.4	Improvement of Cardiac function	262
8.3	Conclusions	263

References **265**

List of figures

Figure 1.1	Mortality rate from 1996 to 2004 in children and adults	18
Figure 1.2	Electron micrograph of a meningococcus showing blebbing	20
Figure 1.3	Schematic representation of the relationship between oxygen delivery and oxygen consumption in tissue	40
Figure 2.1	Serial dilution of VCAM-1 Standard for standard curve determination	72
Figure 2.2	Serial dilution of Multiplex standard for standard curve determination	80
Figure 2.3	Serial dilution of Nitrite or Nitrate Standard for standard curve determination	83
Figure 2.4	The Microscan	89
Figure 3.1	Normal and Biphasic waveform profiles	99
Figure 3.2	Bar chart representing differences in aPTT waveforms, as quantified by the light transmittance level at 18 seconds (TL18) between the diagnostic groups	103
Figure 3.3	Receiver Operator Characteristic Curve for aPTT waveform TL18, PCT and CRP for detecting MCD at hospital admission	105
Figure 3.4	Pointwise 95% confidence band for the probability of a child requiring admission to PICU given their aPTT TL18 measurement	110
Figure 3.5	Serial aPTT waveform changes as quantified by light transmittance levels at 18 seconds (TL18) on a child with severe MCD who required a below knee amputation	112
Figure 3.6	Serial levels of protein C and antithrombin III in a child with severe MCD who had a below knee amputation	113
Figure 4.1A	Schematic to illustrate OPS imaging	122
Figure 4.1B	Schematic to illustrate SDF imaging	122
Figure 4.2	The superimposition of lines upon the SDF image to determine capillary density, proportion of perfused vessels and perfused vessel density	129

Figure 4.3	Quadrant division of an image to determine the Microvascular flow index (MFI) score	130
Figure 4.4	Box and whisker plot demonstrating the difference in capillary density between awake children and anaesthetised children.	133
Figure 4.5	Scatter plot demonstrating the relationship between capillary density and weight in all control children	134
Figure 4.6	Bland Altman plot for intraobserver repeatability in obtaining SDF images	139
Figure 4.7	Bland Altman plot for interobserver repeatability in obtaining SDF images	140
Figure 4.8	Bland Altman plot for intraobserver agreement in the calculation of capillary density in healthy children	143
Figure 4.9	Bland Altman plot for interobserver agreement in the calculation of capillary density in healthy children	144
Figure 5.1	Bland-Altman plot of assessment of capillary density by two independent observers in children with MCD	159
Figure 5.2	Bar chart showing change in mean MFI and MFIc in children with MCD over time	162
Figure 5.3	Bar chart showing change in mean percentage of perfused vessels in children with MCD over time	163
Figure 5.4	Bar chart showing change in mean capillary density in children with MCD over time	164
Figure 5.5	Bar chart showing change in mean perfused vessel density in children with MCD over time	165
Figure 5.6	Bar chart showing change in mean heterogeneity index in children with MCD over time	166
Figure 6.1	Admission ICAM-1 levels per diagnostic group	187
Figure 6.2	Admission VCAM-1 levels per diagnostic group	189
Figure 6.3	Admission P-Selectin levels per diagnostic group	191

Figure 6.4	Admission E-Selectin levels per diagnostic group	193
Figure 6.5	MFI for capillaries and NO at admission	196
Figure 6.6	Heterogeneity index and NO at admission	197
Figure 7.1	Echocardiographic M-mode recording to measure Fractional Shortening	209
Figure 7.2	Tissue Doppler velocity curve in a healthy volunteer. Apical 4-chamber view	213
Figure 7.3A	Schematic of Doppler flow velocity to represent the time intervals necessary to derive the left ventricular Tei index	216
Figure 7.3B	Time intervals illustrated on a TDI trace taken from the lateral aspect of the left ventricular wall	216
Figure 7.4	Principles of cardiac output calculation using echocardiography	219
Figure 7.5	Median peak cTnI and cTnT per time point with interquartile ranges in 20 children with severe MCD	226
Figure 7.6	Box and whisker plot indicating NT-Pro BNP levels at admission between the diagnostic groups	234
Figure 7.7	Box and whisker plot showing changed in NT-Pro BNP levels over time in children with severe MCD	235
Figure 7.8	Changes in mean TDI Ea wave and E/Ea ratio in children with severe MCD over time (with standard error bars)	237
Figure 7.9	Scatter plot showing the relationship between NT-Pro BNP and left ventricular pressure as evaluated by the E/Ea ratio	241
Figure 7.10	Changes in mean Tei index in children with severe MCD over time	243
Figure 7.11	Scatter plot to display relationship between admission cardiac output and systemic vascular resistance in 20 children with severe MCD	245
Figure 7.12	Scatter plot to display relationship between admission cardiac index and systemic vascular resistance in 20 children with severe MCD	246

Figure 7.13 Bland Altman plot to show agreement between two independent observers in the assessment of fractional shortening 248

List of tables

Table 2.1	Glasgow Meningococcal Septicaemia Prognostic Score	62
Table 2.2	Pediatric Risk of Mortality III Score	63
Table 2.3	Pediatric Logistic Organ Dysfunction score	64
Table 2.4	Details of included participants in each study	93
Table 3.1	Characteristics of included participants	102
Table 3.2	Correlation between aPTT TL18 and PCT at admission and clinical and laboratory variables	104
Table 3.3	Performance characteristics of variables for detecting meningococcal disease in children presenting with a fever and a non-blanching rash	108
Table 4.1	Demographic data for 40 control children used to determine normal microcirculatory values using SDF	132
Table 4,2	Correlation coefficients between capillary density and weight, age and body surface area	136
Table 4.3	Multiple Linear Regression Analysis of factors affecting capillary density	137
Table 5.1	Demographic data for the study population	155
Table 5.2	Characteristics of included participants at admission	156
Table 5.3	Inter- and intraobserver agreement for flow scoring for calculation of MFIc and MFI	158
Table 5.4	Spearman Rank Correlation coefficients between all microcirculatory outcome variables measured	161
Table 5.5	Correlations between admission microcirculation variables and markers of illness severity	168
Table 5.6	Multiple linear regression analysis was used to assess the independent predictor ability of MFIc for the duration of ventilation in hours	169
Table 5.7	Longitudinal analysis comparing changes in microcirculation variables with MFIc over time	171
Table 5.8	Admission correlations between clinical and biochemical measurements of tissue perfusion and MFIc and Longitudinal analysis comparing changes clinical and biochemical measurements of tissue perfusion with MFIc over time	172
Table 5.9	Admission correlations between laboratory markers and MFIc and Longitudinal analysis comparing changes in laboratory markers with MFIc over time	173

Table 5.10	Admission correlations between haemodynamic variables and MFIc and Longitudinal analysis comparing changes in haemodynamic variables with MFIc over time	174
Table 6.1	Correlation table for microcirculatory variables and vasoactive mediators at admission	194
Table 6.2	Longitudinal analysis comparing changes of laboratory variables with MFIc over time	198
Table 7.1	Demographic table of 20 children admitted to PICU with severe MCD	227
Table 7.2	Correlations of peak cTnI and cTnT with various clinical parameters	228
Table 7.3	Multiple Linear Regression Analysis of factors affecting peak Troponin T	230
Table 7.4	Characteristics of included participants	233
Table 7.5	Diastolic echocardiographic measurements in children with severe MCD at admission to PICU	236
Table 7.6	Correlation table for admission and peak NT-Pro BNP levels	239
Table 7.7	Multiple Linear Regression Analysis of factors affecting the relationship between admission NT-Pro BNP levels and the E/Ea ratio	240

Abbreviations

AH	Alder Hey Children's Foundation Trust
ANP	Atrial natriuretic peptide
aPTT	Activated partial thromboplastin time
AT III	Antithrombin III
AUC	Area under the curve
BE	Base excess
BMR	Basal metabolic rate
BNP	Brain natriuretic peptide
BPI	Bactericidal permeability-increasing protein
BPW	Biphasic waveform
BSA	Body surface area
cAMP	3'5'-cyclic adenosine monophosphate
CPB	Cardiopulmonary bypass
CD	Capillary density
CI	Cardiac index
CI	Confidence Internal
CK-MB	Creatine kinase skeletal muscle isoenzyme
CK-MM	Cardiac isoenzyme
CO	Cardiac output
CO_2	Carbon dioxide
CRP	C-reactive protein
CSF	Cerebrospinal fluid
cTnI	Cardiac troponin I

cTnT	Cardiac troponin T
CVC	Central venous catheter
CVP	Central venous pressure
Dao	Systolic aortic diameter
DBP	Diastolic blood pressure
DIC	Disseminated intravascular coagulation
DVD	Digital Video Discs
ECG	Electrocardiogram
ECLIA	Electro-Chemical-Luminescence ImmunoAssay
ED	Emergency Department
EDTA	Ethylene-diamine-tetra-acetic acid
EGDT	Early goal directed therapy
ELISA	Enzyme-Linked Immunosorbent Assay
ET	Ejection time
FiO_2	Fractional inspired oxygen
FS	Fractional shortening
GE	General Electrical
GMSPS	Glasgow Meningococcal Septicaemia Prognostic Score
GP	General Practitioner
HA1A	Human monoclonal antibody to endotoxin
HHV6	Human Herpes Virus 6
HHV7	Human Herpes Virus 7
HI	Heterogeneity index
ICAM-1	Intercellular adhesion molecule-1
ICT	Isovolumic contraction time
ICU	Intensive care unit

IL-1	Interleukin-1
IL-10	Interleukin-10
IL-13	Interleukin-13
IL-1Ra	Interleukin-1 receptor antagonist
IL-1β	Interleukin-1 β
IL-6	Interleukin-6
IL-8	Interleukin-8
iNOS	Inducible nitric oxide synthase
INR	International Normalized Ratio
IQR	Interquartile range
IRT	Isovolumic relaxation time
LiDCO	Lithium dilution *cardiac output*
LOS	Lipooligosaccharide
LPS	Lipopolysaccharide
LV	Left ventricular
LVEDV	Left ventricular end diastolic volume
LVESV	Left ventricular end systolic volume
MAP	Mean arterial pressure
MAS	Microvision Analysis Software
MCD	Meningococcal Disease
MD2	Myeloid differentiation factor
MFI	Microvascular Flow Index
MFIc	Microvascular Flow Index for capillaries
mm	Millimetre
MRU	Meningococcal Reference Unit
NIRS	Near Infrared Spectroscopy
nm	Nanometer

NO	Nitric Oxide
NPV	Negative predictive vale
NT-Pro BNP	N-Terminal Pro Brain Natriuretic Peptide
OPS	Orthogonal Polarisation Spectral
PACs	Pulmonary artery catheters
PAI	Plasminogen activator inhibitor
PAOP	Pulmonary artery occlusion pressure
PC	Protein C
PCR	Polymerase Chain Reaction
PCT	Procalcitonin
PEEP	Positive end expiratory pressure
PELOD	Pediatric Logistic Organ Dysfunction Score
PiCCO	Pulse Contour Cardiac Output Monitoring
PICU	Paediatric Intensive Care Unit
PPV	Percentage of perfused vessels
PPV	Positive Predictive Value
PRAM	Pressure recording analytical method
PRISM III	Pediatric Risk of Mortality score III
PT	Prothrombin time
PVD	Perfused vessel density
rBPI	Recombinant bactericidal permeability-increasing protein
RMCH	Royal Manchester Children's Hospital NHS Trust
ROC	Receiver operator characteristics
SBP	Systolic blood pressure
$ScvO_2$	Central venous oxygen saturations
SDF	Sidestream darkfield imaging

*sia*D	Meningococcal sialyltransferase gene
sIL-6R	Soluble Interleukin-6 receptor
$ScvO_2$	Central venous oxygen saturations
SPSS	Statistical Package for Social Sciences
SSD	Serum standard diluent
SV	Stroke volume
SvO_2	Mixed venous oxygen saturations
SVR	Systemic vascular resistance
Taq	*Thermophilus aquaticus*
TDI	Tissue Doppler imaging
TF	Tissue factor
TFPI	Tissue factor pathway inhibitor
TL18	Transmittance level at 18 seconds
TLR	Toll like receptor
TLR4	Toll like receptor 4
TMB	Tetramethyl benzidine
TnC	Troponin C
TNF	Tumour Necrosis Factor
TNFR	Tumour necrosis factor alpha receptor
TnI	Troponin I
TnT	Troponin T
TOE	Transoesophageal echocardiography
tPA	Tissue plasminogen activator
UK	United Kingdom
USCOM	Ultrasound Cardiac Output Monitor
VCAM-1	Vascular cell adhesion molecule-1
VLDL	Very low density lipoprotein

VTI	Velocity time integral
WCC	White cell count

Chapter 1

Introduction

1.1 General Background

Meningococcal disease (MCD) is the most common infective cause of mortality in children in the United Kingdom (UK) (Heyderman, Ben-Shlomo et al. 2004). It is the most common cause of sepsis-induced purpura fulminans in children accounting for 10% of the total number of cases of purpura fulminans.

MCD has a wide spectrum of clinical presentation with early symptoms in children often mimicking those of self limiting viral illnesses. It is a highly unpredictable disease. Some children require only minimal supportive clinical measures but others develop fulminant sepsis, leading to a rapid clinical decline and the need for intensive care support. If not detected and treated promptly and appropriately MCD can rapidly lead to death in this group of patients.

Severe MCD causes a rapid progression of disease. Successful management of the disease is dependent on early identification of symptoms by care givers and health care workers and prompt resuscitation. In a prospective paediatric intensive care (PICU) based study describing management of children with MCD in the Netherlands over an 18 year period (Maat, Buysse et al. 2007), survival of children presenting to their unit with MCD correlated with year of admission with a significant reduction in the case fatality rate during the study period. The authors attributed this improvement in outcome to more effective strategies

for resuscitation and intensive care management. These findings are consistent with the significant reduction in mortality seen in MCD in the UK. The causes of this improvement in outcome are multifactorial (Booy, Habibi et al. 2001; Thorburn, Baines et al. 2001; Thorburn and Baines 2002). Figure 1.1 displays a graph of the change in mortality rates seen in MCD from 1996 to 2004. MCD is an important cause of long term morbidity including neurodevelopmental impairment. (Fellick, Sills et al. 2001) Survivors of invasive disease may sustain permanent sequelae. This includes hearing impairment, seizures, limb or digit amputation, tissue loss, chronic renal impairment, developmental delay and psychosocial problems, (Fellick, Sills et al. 2001; Belthur, Bradish et al. 2005; Slack, Hawkins et al. 2005). Bache et al. studied orthopaedic sequelae in 143 children with MCD (Bache and Torode 2006). Twenty one children died, and among the 122 survivors 40 had skeletal, vascular, or cutaneous sequelae. Seventeen patients lost tissue secondary to ischemia, 6 patients lost digits from their hands or feet and 5 underwent limb amputation. Sixteen children developed partial or complete epiphyseal growth arrest leading to angular deformities or short limbs. This study highlights some of the devastating consequences of MCD.

1.2 Epidemiology

The incidence of MCD can be as high as 500 per 100 000 population a year in developing countries during epidemics (Tikhomirov, Santamaria et al. 1997). In developed countries including the UK and United States of America, the incidence is 1 to 5 per 100 000 population a year with a mortality rate ranging from 5% to 25 % (Faust, Levin et al. 2001; Harrison, Pass et al. 2001; Heyderman, Ben-Shlomo et al. 2004). In the UK severe MCD has a higher incidence in males and a winter peak. Meningococcal

infections are however seen throughout the year. MCD has its highest incidence in children under the age of 5 years with another peak in teenagers and young adults.

Serogroups A, B, C, W135, and Y account for the majority of cases of MCD throughout the world (Rosenstein, Perkins et al. 2001). Invasive infection in Africa and Asia continue to be attributed to serogroup A infections (Kvalsvig and Unsworth 2003). More recently the incidence of serogroup W135 has increased, particularly in a region of sub-Saharan Africa called the "meningitis belt" which extends from The Gambia to Ethiopia. During epidemics, the local incidence of the disease in some sub-Saharan African regions may approach 1000 cases per 100,000 population (Molesworth, Thomson et al. 2002; Pollard and Maiden 2003). In the UK, serotype Group B disease has historically been the most common pathogen to cause invasive disease. The incidence of Group C disease increased in the late 80's and early 90's and caught up with Group B incidence. This prompted the development of the Meningococcal C vaccine.

In November 1999, the UK became the first country to incorporate the Meningococcal C vaccine into a national immunisation programme. Following this introduction, disease attack rates fell in vaccinated children, carriage rates decreased and the incidence declined among the unvaccinated, suggesting the development of herd immunity (Handford S 2007). Despite the clear effect of the meningococcal C conjugate vaccine, the vast majority of invasive disease remains the group B serotype (Gray, Trotter et al. 2006). Unfortunately the widespread use of an effective group B vaccine is many years away. Serogroup B polysaccharide is poorly immunogenic in humans probably explained by its structural identity to a

glycoprotein found on human tissues (Lifely, Roberts et al. 1991). A reduction in the incidence of serotype group B disease has been seen in the UK (Gray, Trotter et al. 2006) . This may be attributable to a virulence shift in the organism causing not only less disease but less severe disease.

In an effort to reduce mortality in the UK policies have been designed to raise awareness at every step of the patient journey. Public awareness had been increased with the help of charities such as the Meningitis Research Foundation. This has involved education encouraging parents to seek medical help early for children with a high temperature and a non-blanching rash (identified using the 'glass or tumbler test') and the importance of receiving the meningococcal serogroup C conjugate vaccine. In primary care, general practitioners (GP) have been made aware of the presenting clinical features and the need to administer penicillin to children prior to transfer to hospital (Hahne, Charlett et al. 2006).

Figure 1.1. Mortality rate from 1996 to 2004 in children and adults. Taken from 'Meningococcal infection in England 1996 to 2004. Mortality trends' Health Protection Agency

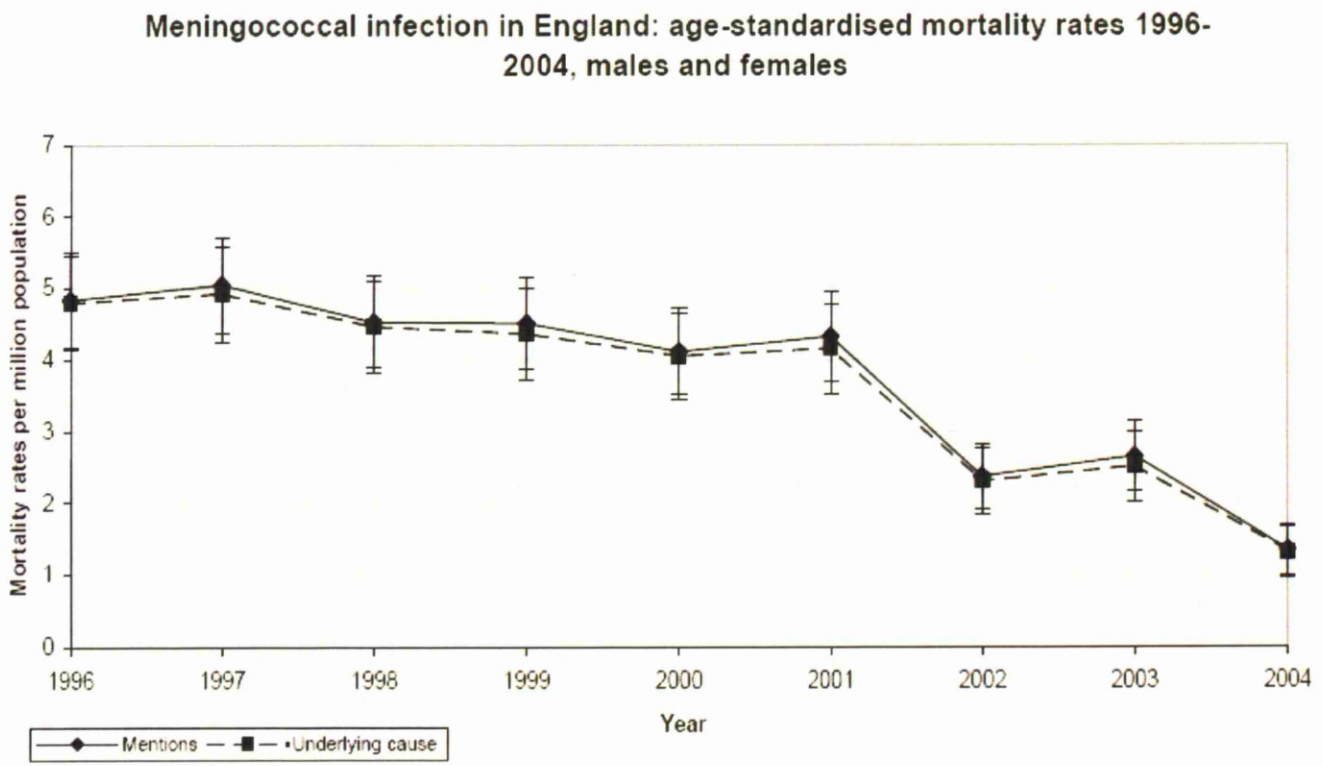

1.3 The Meningococcus

Neisseria meningitides (the meningococcus) is an encapsulated, oxidase positive, Gram negative diplococcus. It is a strictly human pathogen and its transmission is by contact with respiratory secretions. The cell wall of the meningococcus is organised into layers. The innermost layer is a cytoplasmic membrane which is covered by a peptidoglycan cell wall. Overlying this is the outer membrane which consists of lipooligosaccharide (LOS) molecules. This LOS has a hydrophilic and a hydrophobic portion. The immunotype of the meningococcus is determined by the hydrophilic oligosaccharide portion. The active part of endotoxin is determined by the hydrophobic portion. Type IV pili are incorporated into the outer membrane. This outer membrane is over synthesised compared to the other structures during in vivo growth of the meningococcus. This causes 'blebbing' (Figure 1.2) in which structures are released from the organism which contain endotoxin, a critical factor in meningococcal virulence (Hart and Rogers 1993).

Meningococci are separated into several serogroups (A, B, C, 29-E, H, I, K, L, W-135, X, Y, Z) according to their capsular polysaccharide antigens. Only A, B, C, W135 and Y are considered clinically important. The bacteria can be further serotyped, sero-subtyped, and immunotyped on the basis of outer-membrane proteins and lipopolysaccharide expression (Hart and Rogers 1993).

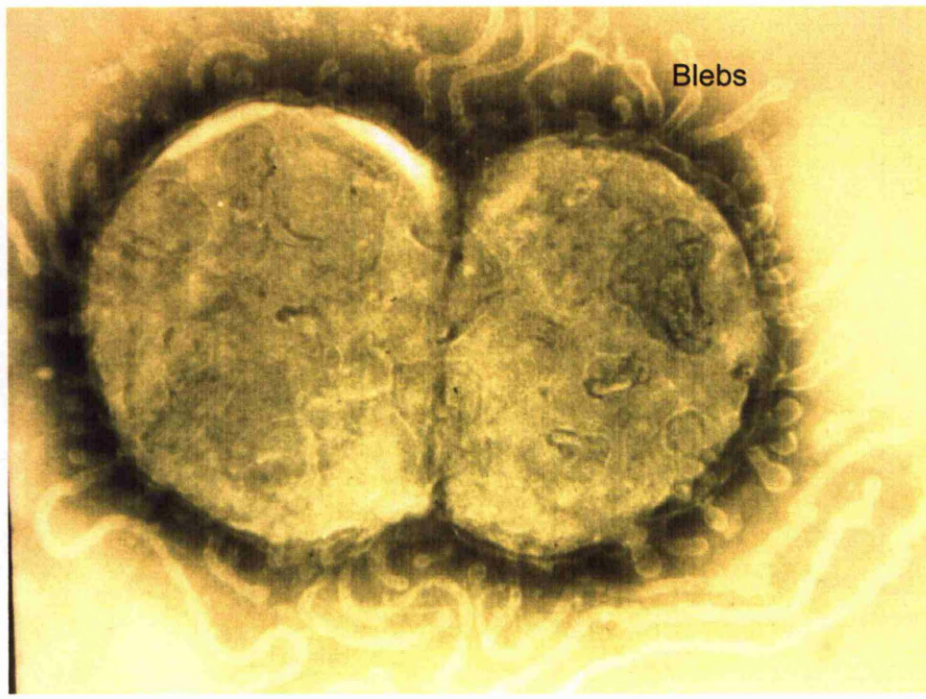

Figure 1.2. Electron micrograph of a meningococcus showing blebbing Courtesy of Professor Hart (own image).

1.4. Pathophysiology

The meningococcus can cause a wide spectrum of disease including septicaemia, meningitis or most frequently a combination of these two (Riordan, Thomson et al. 1995), conjunctivitis, arthritis, pneumonia and pericarditis. The host inflammatory response, consisting of the activation of cytokine cascade systems and the release of intercellular pro- and anti-inflammatory mediators, acts to neutralise the meningococcus and its toxic products. However this response can be exaggerated leading to tissue damage within the host.

Invasive infection starts initially with nasopharyngeal colonization. Colonisation occurs asymptomatically in 10-20% of the population (Stephens, Hoffman et al. 1983; Stephens 1999; Glitza, Ehrhard et al. 2008). The Meningococcus binds to the microvillous surfaces of non-ciliated columnar mucosal cells of the nasopharynx causing colonisation (Stephens, Hoffman et al. 1983). Stephens et al showed that the meningococcus became surrounded by elongated microvilli and then was observed inside intracellular vacuoles. Subsequent studies demonstrated that the bacteria does not open the tight junctions between epithelial cells but invades the host cell by transcytosis. These events are controlled by the interactions between virulence factors of the meningococcus, cognate host cell receptors and signalling between pathogen and host at numerous stages of the adhesion cascade. The outermembrane adhesion proteins such as Opa and Opc are also of importance in adherence to epithelial surfaces (Merz and So 1997; Merz, Enns et al. 1999; Merz and So 2000). Invasive disease results when translocation occurs across the nasopharyngeal mucosa.

1.4.1. Endotoxin and cytokines

The clinical features and sequelae observed in patients with severe MCD are directly related to endotoxin release and the resulting complex interactions between host and bacterial factors. The host response results in a cascade of pro and anti-inflammatory cytokine production. The concentration of endotoxin has a dose response relationship with disease severity and fatality (Brandtzaeg, Mollnes et al. 1989; Waage, Brandtzaeg et al. 1989). The levels of pro-inflammatory cytokines are significantly increased early in the disease and are also associated with disease severity and outcome (Waage, Halstensen et al. 1987; Westendorp, Langermans et al. 1995; Zhou, Arthur et al. 2001).

Toll-like receptors (TLR) are pattern recognition receptors that recognise pathogen associated molecular patterns produced by pathogens. They are part of the innate immune response. TLR4 is the major endotoxin signalling receptor and, with its co-factor myeloid differentiation factor (MD2), triggers gene transcription and the production of proinflammatory cytokines and chemokines by macrophages, monocytes and endothelial cells (Emonts, Hazelzet et al. 2003).

Experimental and clinical data have shown that the major proinflammatory cytokines upregulated in MCD are tumour necrosis factor (TNF), Interleukin-1 beta (IL-1β), Interleukin-6 (IL-6) and Interleukin-8 (IL-8), with the predominant anti-inflammatory cytokine being Interleukin-10 (IL-10) (Girardin, Roux-Lombard et al. 1992; Hackett, Thomson et al. 2001; Emonts, Hazelzet et al. 2003; Bjerre, Brusletto et al. 2004). These cytokines are produced by a range of cell types including neutrophils,

macrophages, dendritic cells and epithelial cells (Van Amersfoort, Van Berkel et al. 2003).

Tumour necrosis factor is released early in MCD followed by IL-6 release 1-4 hours later (Waage, Halstensen et al. 1989). TNF enhances antimicrobial activity of monocytes, macrophages and neutrophils, downregulates thrombomodulin expression on endothelial cells and hence contributes to the procoagulant state (Waage, Halstensen et al. 1987; Emonts, Hazelzet et al. 2003). TNF binds to cell surface receptors. These can then be released forming a pool of free soluble TNF receptors which can either inhibit or prolong the actions of TNF (Girardin, Roux-Lombard et al. 1992; van Deuren, van der Ven-Jongekrijg et al. 1995). IL-1β acts in a similar way to TNF. It has chemotactic activity for neutrophils and concentrations are raised in MCD, with higher levels being associated with mortality (Girardin, Grau et al. 1988).

IL-6 production results in synthesis of acute-phase proteins (Hazelzet, van et al. 1994). It also causes proliferation and antibody production by B-cells and has been shown to be a modulator of myocardial dysfunction associated with MCD (Pathan, Hemingway et al. 2004). High levels of IL-6 in the presence of Interleukin-1 (IL-1) are associated with fatality and levels of IL-6 are significantly higher in children with septic shock than in those with meningitis alone or meningitis and septicaemia (Girardin, Grau et al. 1988; Casey, Balk et al. 1993). IL-6 exerts many of its effects via the soluble IL-6 receptor. It has recently been shown that severe MCD is associated with a reduction in soluble IL-6 receptor levels in relation to disease severity. Disease severity is inversely related to IL-6 levels

(Pathan, Williams et al. 2005) and soluble IL-6 receptor levels return to normal with clinical recovery.

IL-8 is a potent chemoattractant. It causes activation of neutrophils and is involved in neutrophil-mediated vessel wall injury (Baggiolini, Walz et al. 1989). Levels have been demonstrated to be elevated in MCD (Halstensen, Ceska et al. 1993). Muscle damage is mediated via TNF and IL-8 in MCD, as estimated by creatine kinase skeletal muscle isoenzyme (CK-MM) and cardiac isoenzyme (CK-MB) concentrations. CK-MM correlated significantly with TNF and IL-8 (Carrol, Thomson et al. 2002).

Counter regulatory cytokines release quickly follows the cascade of pro-inflammatory cytokines. These anti-inflammatory cytokines include IL-1 receptor antagonist (IL-1Ra), soluble IL-6 receptors (sIL-6R), IL-10 and Tumour necrosis factor alpha receptors TNFRs (Van Zee, Kohno et al. 1992; Gerard, Bruyns et al. 1993). IL-10 levels have been shown to be related to outcome (Derkx, Marchant et al. 1995) and correlate with pro-inflammatory cytokines (Riordan, Marzouk et al. 1996). IL-10 is a potent inhibitor of cytokine production and suppresses the procoagulant activity induced by endotoxin at the surface of human monocytes (Gerard, Bruyns et al. 1993; Pradier, Gerard et al. 1993). This complex cascade of immune modulators is released in order to neutralise micro-organisms and their toxic products. However, the process can sometimes be overwhelming leading to serious tissue damage.

1.4.2 Endothelial dysfunction

The endothelium is the cellular interface between circulating blood and underlying tissue. A well functioning, healthy endothelium is vital not only to the continual adjustments of vascular tone, but for the regulation of white cell movement from blood to tissue and maintenance of the equilibrium between the anticoagulant and the antithrombotic state in blood flow (Pearson 2000). The healthy vascular endothelium is lined by the endothelial glycocalyx, a network of membrane-bound proteoglycans and glycoproteins.

The release of endotoxin and cytokines such as TNF and IL-1 in sepsis activates vascular endothelial cells. This leads to alterations in the structure and function of endothelial cells and separation of the tight junctions between endothelial cells leading to capillary leakage, intravascular fluid and high molecular protein loss. (Klein, Shennan et al. 1992; Lampugnani, Caveda et al. 1993) If not corrected by therapeutic intervention circulatory collapse will occur, leading to septic shock due to a low systemic vascular resistance.

Nitric oxide (NO) is produced as a result of cytokine stimulation of endothelial cells in sepsis. NO is a potent vasodilator and has also been found to impair cardiac function further exacerbating the adverse circulatory response (Balligand, Kelly et al. 1993; Balligand, Ungureanu et al. 1993). Endothelial damage can also be caused by other factors. The adherence of activated neutrophils and platelets to endothelial cells can cause dysfunction of the cells directly. (Bone 1991; Finn, Naik et al. 1993; Varani and Ward 1994) Additionally, the endothelial glycocalyx itself has been

shown to become dysfunctional following exposure to TNF and endotoxin in animal models. (Chappell, Hofmann-Kiefer et al. 2008; Marechal, Favory et al. 2008)

Endothelial activation by circulating pro-inflammatory cytokines leads to the release of a number of mediators which can be measured in the central circulation. There is increased expression of endothelial adhesion molecules, including P-selectin, intercellular adhesion molecule-1 (ICAM-1), vascular cell adhesion molecule-1 (VCAM-1) and E-selectin (Carlos and Harlan 1994; Jakobsen, Morris-Jones et al. 1994; Bruserud, Akselen et al. 1995). Levels of E-selectin and ICAM-1 have been shown to be elevated in children with MCD (Baines, Marzouk et al. 1999). In small vessels, leukocyte adhesion may contribute to disordered microvascular flow and potentially increase the inflammatory response within these local capillary beds by mediating the release of pro-inflammatory cytokines, reactive oxygen species, proteases and other inflammatory mediators. Ultimately endothelial dysfunction leads to increased vascular permeability and profound interstitial oedema. Without supportive management to counteract the pathophysiological processes there will be persistent hypovolaemia followed by impaired microvascular blood flow, organ dysfunction and death.

1.4.3 Cardiac dysfunction

The primary cause of circulatory collapse in MCD is thought to be peripheral circulatory impairment, myocardial involvement, however, is also crucial in determining the patient's outcome (Hardman and Earle 1969; Monsalve, Rucabado et al. 1984; Mercier, Beaufils et al. 1988; Thiru, Pathan et al. 2000; Briassoulis, Narlioglou et al. 2001; Pathan, Sandiford et

al. 2002). When myocardial dysfunction is severe it will lead to vascular collapse and impaired tissue perfusion culminating in multiple organ failure. Boucek et al performed echocardiography in 12 children with MCD, finding impairment of the left ventricular function in seven (Boucek, Boerth et al. 1984). Three of these children died. Children with normal cardiac function survived. Cardiac dysfunction preceded clinical collapse in several of the children.

The cause of this dysfunction is not fully elucidated. Acidosis, hypoxia, electrolyte imbalances are likely to contribute and are known to be associated with severe MCD. A myocardial depressant factor may also be present (Pathan, Sandiford et al. 2002). Pathan et al found that exposing rat myocytes to serum from a child with MCD impaired contraction. Recombinant IL-6 induced dose-dependent myocardial depression on the rat myocyte. They also found that TNF had little effect on myocyte contractility and that adding TNF to the IL-6 did not increase the myocardial depressant effect. They concluded that IL-6 is a mediator of myocardial depression in meningococcal disease, and concentrations of serum IL-6 strongly predicted the degree of myocardial dysfunction and severity of disease in children with meningococcal septic shock (Pathan, Hemingway et al. 2004).

1.4.4 Coagulopathy

The most severe manifestation of coagulopathy is disseminated intravascular coagulation (DIC), a pathological activation of coagulation. It is a complex and frequently fatal condition associated with gross abnormalities of thrombosis, haemostasis, vascular function and inflammation. Multiple microvascular thrombi form leading to the

consumption of all available coagulation proteins and platelets resulting in abnormal bleeding.

Tissue plasminogen activator (tPA) catalyzes the conversion of plasminogen to plasmin and is the major enzyme responsible for fibrinolysis. Levels of tPA have been shown to be related to outcome and disease severity. Voss et al. showed that activation of coagulation is accompanied by an activation of fibrinolysis in the microcirculation. They also demonstrated that increased levels of inhibitors of fibrinolysis (tPA and plasminogen activator inhibitor (PAI)) induce a decrease of the fibrinolytic capacity of the blood (Voss, Matthias et al. 1990). Significant differences in the initial levels of tPA in survivors and non-survivors with meningococcal septic shock have not been demonstrated (Hazelzet, Risseeuw-Appel et al. 1996; Kornelisse, Hazelzet et al. 1996).

Tissue factor (TF) is a protein present in subendothelial tissue, platelets and leukocytes. It is needed for the initiation of thrombin formation from prothrombin. Endotoxin and TNF release lead to production of tissue factor. Increased levels of tissue factor have been demonstrated in circulating monocytes isolated from blood of patients with MCD. The highest values were found in non-survivors (Osterud and Flaegstad 1983). There is also a reduction of plasma tissue factor pathway inhibitor (TFPI), which is a potent inhibitor of the TF-dependent coagulation system. (Eling, Stephens et al. 2001)

Levels of natural antithrombotics including Protein C (PC), antithrombin III (AT III) levels and protein S are markedly decreased in severe MCD. The decrease in AT III, protein C and protein S levels is associated with the presence of DIC and poor outcome. Thrombin normally binds to thrombomodulin on the endothelial surface. This leads to protein C activation which acts with protein S to inactivate coagulation factors, as well as downregulating PAI. Severe MCD impairs these processes (Powars, Rogers et al. 1987; Brandtzaeg, Sandset et al. 1989; Fourrier, Lestavel et al. 1990; Faust, Levin et al. 2001). Recombinant activated Protein C inhibits activated coagulation factors and could be beneficial in the management of severe MCD. This was demonstrated in a study of adults with severe sepsis (Bernard, Vincent et al. 2001). A randomised controlled trial of the administration of a recombinant form of human activated protein C recruited 477 children with sepsis, including 237 receiving placebo and 240 in the treatment arm. The use of recombinant activated protein C failed to reduce morbidity or mortality significantly and there were numerically more intracranial bleeding events in the group receiving recombinant activated protein C (Nadel, Goldstein et al. 2007).

1.5. Diagnosis

The clinical diagnosis of children with severe MCD is usually clear to the health care professional due to the fast evolution of clinical signs such as a spreading purpuric rash and shock requiring intensive volume resuscitation. In some cases of severe disease and in less severe manifestations the diagnosis may be less clear. The gold standard for confirmation of the presence of the meningococcal bacteria is the polymerase chain reaction test (PCR) (Carrol, Thomson et al. 2000; Hackett, Carrol et al. 2002). This is more sensitive than blood cultures, which require viable bacteria to give a

positive result. Blood cultures may give a false negative result if the child has been receiving antibiotics prior to hospital arrival. PCR will detect both viable and non-viable organisms. The drawback of PCR is that most hospitals do not have the capacity to perform this investigation. Samples must be transported to the Meningococcal Reference Unit laboratory for analysis. The PCR analysis is not time consuming, but a result can take several days to be relayed back to the referring hospital because of delays in transporting the sample.

A rapid, easily accessible investigation for the detection of early sepsis in children would be of great benefit in paediatric clinical practice particularly in the Accident and Emergency department. Children frequently attend hospital with a non-blanching rash and a fever. Although some of these children will have meningococcal sepsis some will have a viral infection (e.g. Human Herpes Viruses 6 (HHV6) or 7 (HHV7), or the Enteroviruses) which may also cause a non-blanching rash and a fever leading to 48 hours of unnecessary intravenous antibiotics. As many of the clinical symptoms of early bacterial illnesses mimic those of a non-specific viral infection, a test that could aid doctors in deciding whether a child has a significant bacterial infection would be of value.

C-reactive protein (CRP) is the main biochemical indicator used currently for the detection of sepsis in children but has limitations. A lack of sensitivity means that a CRP cannot be used to exclude all bacterial infection (Marzouk, Bestwick et al. 1993; Sanders, Barnett et al. 2008). The role of procalcitonin (PCT) in the identification of sepsis in both adults and children has been extensively studied. It has been shown to be a better diagnostic marker of early sepsis with a higher specificity that CRP in

critically ill children. CRP as well as PCT could be used to identify early sepsis (Simon, Gauvin et al. 2004; Arkader, Troster et al. 2006; Rey, Los et al. 2007). PCT has been shown to be a better diagnostic and prognostic marker in MCD when compared to CRP (Bohuon, Assicot et al. 1998; Bohuon and Gendrel 1999; Carrol, Newland et al. 2002; Carrol, Newland et al. 2005; Chalumeau, Leroy et al. 2007).

Adult studies have shown the presence of a biphasic wave form in the aPTT test in severe infection and this has been suggested as a marker for the early detection of infection (Downey, Kazmi et al. 1997; Toh, Ticknor et al. 2003; Dempfle, Lorenz et al. 2004). Chopin et al (Chopin, Floccard et al. 2006) found that the biphasic waveform was more accurate than PCT and CRP for differentiating patients with severe sepsis and septic shock, with 90% sensitivity and 92% negative predictive value. The result on day 3 of intensive care admission had a specificity of 91% and negative predictive value of 98% for predicting sepsis-related mortality. There have been no paediatric studies of the biphasic waveform in sepsis and an aPTT test is not a routine investigation in children with suspected infection. The aPTT waveform could potentially be used as a prognostic and diagnostic marker in paediatric patients on intensive care units.

1.6 Clinical manifestations and management

1.6.1 Signs and symptoms

The commonest presentations of MCD are meningitis alone (15-50% of cases), meningitis and septicaemia (40-50%) or septicaemia alone (10-36%) (Riordan, Marzouk et al. 1995; Kirsch, Barton et al. 1996). The classic features of meningococcal septicaemia are fever and a spreading

non-blanching rash in an ill child (Thomson APJ 2000). If purpura is present in a child who is clearly unwell and has a fever then meningococcal disease is very likely. The classic features may be preceded by a few days of a non-specific viral illness. Up to 30% of children with meningococcal disease present with a non-specific maculopapular rash. This type of rash will blanch. However the majority will have a non-blanching rash present as well (Marzouk, Thomson et al. 1991). Features of meningitis include fever, headache, loss of appetite, vomiting, drowsiness, photophobia and neck stiffness but these be absent in infants and small children. A non-blanching rash can also be present but a small group present with classic features of meningitis and no rash. In this clinical situation the diagnosis is confirmed at lumbar puncture. The diagnosis is relatively straightforward when the older patient presents in this manner. A younger child however may display more insidious signs such as poor feeding, irritability and maybe a bulging fontanelle. The clinical presentation of children with a rapidly progressing septicaemia is shock, tachycardia, poor peripheral perfusion, tachypnoea, oliguria and hypotension. Patients with pure septicaemia generally have a more severe and rapid progression.

1.6.2. Management

A study by Ninis et al determined three factors that were independently associated with an increased risk of death in children with MCD (Ninis, Phillips et al. 2005). These were failure to be looked after by a paediatrician, failure of sufficient supervision of junior staff, and failure of staff to administer adequate inotropes. When complications were not recognised this was also a significant risk factor for death, although this was not independent of the absence of paediatric care (Ninis, Phillips et al.

2005). A skilled multidisciplinary paediatric team in the resuscitation, stabilisation and transfer of any child requiring intensive care support is clearly paramount and if performed poorly will lead to worse outcomes (Peters, Petros et al. 2002).

1.6.2.1 Emergency Department management

All critically ill children should follow a structured algorithm of care as taught in Acute Paediatric Life Support training commencing with assessment of airway, breathing, circulation, and disability (Theilen, Wilson et al. 2008). Effective management relies on the early recognition of the illness in a shocked child followed by swift, aggressive fluid resuscitation and antibiotic administration. A third generation cephalosporin such as cefotaxime or ceftriaxone is the preferred initial therapy. Ceftriaxone monotherapy once daily may be used if parenteral agents containing calcium (such as intravenous calcium, parenteral nutrition, or Hartmann's solution), have not been used in the preceding 48 hours (Callaghan, Buckee et al. 2008; Theilen, Wilson et al. 2008). Early, aggressive fluid resuscitation is associated with improved survival in paediatric septic shock (Carcillo, Davis et al. 1991). Initial therapy with 20ml/kg of colloid as a bolus is required and repeated as necessary. Fluid administration should be titrated to clinical markers of cardiac output including heart rate, capillary refill and level of consciousness (Carcillo, Davis et al. 1991). If signs of shock persist after 40-60 ml/kg of fluid resuscitation, there is a significant risk of pulmonary oedema and elective intubation and ventilation is recommended, even in the absence of signs of respiratory failure (Carcillo and Fields 2002; Theilen, Wilson et al. 2008). Children not responding to 60 ml/kg of initial fluid resuscitation have 'fluid refractory shock' and require intubation, mechanical ventilation and the administration of inotropic agents.

Intubation and ventilation protects the airway, reduces the risk of pulmonary oedema, facilitates adequate oxygenation and ventilation, and reduces the work of breathing and oxygen consumption (Ledingham and McArdle 1978; Theilen, Wilson et al. 2008).

1.6.2.2. Inotropes

Inotropic support is frequently necessary in order to maintain end-organ tissue perfusion. Appropriate inotrope selection is only one facet of the effective management of the critically ill child with shock. The Surviving Sepsis Campaign international guidelines for the management of severe sepsis and septic shock recommend dopamine as the first choice of inotrope to support the paediatric patient with hypotension refractory to fluid resuscitation in an emergency department setting (Dellinger, Levy et al. 2008). The administration of dobutamine as an initial inotrope should be reserved for patients who still have features of low cardiac output following fluid resuscitation, but who have a normal blood pressure and clinical evidence of elevated systemic vascular resistance (SVR). These features are a prolonged capillary refill, cool extremities and a widened core-peripheral temperature gap.

The inotropes should ideally be administered through a central venous catheter, but may also be infused through an intraosseous line. Powered intraosseous access devices such as the EZ-IO® device allow secure vascular access to be obtained within 60 seconds and facilitate the administration of inotropes in the Emergency Department (ED) or General Paediatric areas. Patients requiring inotropic support should have an in-dwelling arterial, and urinary catheter sited and should be referred to a PICU. Children not responding to this level of therapy have 'fluid refractory-

dopamine resistant shock' and require the administration of additional inotropic agents.

1.6.2.3 Management on PICU

The choice of inotropic and vasoactive agents, such as whether to commence dopamine or dobutamine first and the decision to commence adrenaline or noradrenaline, is determined by clinical examination and an estimation of the cardiac output (CO). In most cases physical examination and therapeutic end points, which can be applied in any clinical setting, are adequate to guide management although cardiac output monitors may also be employed in PICU.

Therapeutic end points in the management of shock should include normalisation of the heart rate, a capillary refill time of less than 2 seconds, normal volume pulses with no differential between peripheral and central pulses, warm extremities with a modest core-peripheral temperature gap, urine output >1 ml/kg/hr and normal mental status. Blood gas measurement should show a decreasing lactate and an improving base deficit. Central venous pressure should be maintained at 8-12 mmHg. Central venous ($ScvO_2$) and mixed venous (SvO_2) oxygen saturations are measurements of the relationship between oxygen consumption and oxygen delivery in the body and are easily measured therapeutic end points in the management of shock. Normal values for $ScvO_2$ will be slightly higher than the SvO_2 as blood has not mixed with the venous blood from the coronary sinus. In shock the therapeutic end point for $ScvO_2$ should be $\geq$ 70% and $\geq$ 65% for the SvO_2 (Arkader, Troster et al. 2006). Oliveria et al. showed that utilising a goal-directed therapy strategy in children and adolescents with septic shock using the endpoint of a $ScvO_2 \geq$ 70% had a significant and additive

impact on the outcome of these children in terms of fewer new organ dysfunctions and less mortality (de Oliveira, de Oliveira et al. 2008)

In the child with 'fluid refractory-dopamine resistant shock' typical choices for a 'second-line' inotrope would be adrenaline for the child with low blood pressure and high SVR (so-called 'cold shock') or noradrenaline for the child with low blood pressure and low SVR (so-called 'warm shock'). Children with a persistent low cardiac output state with high SVR despite fluid resuscitation and inotropic support may benefit from vasodilator or inodilator therapy, particularly if the arterial blood pressure is relatively well maintained. A typical choice in this circumstance would be a type III phosphodiesterase inhibitor such as milrinone (Lindsay CA 1998).

When cardiac output monitoring is available the cardiac index can be measured and other parameters such as the systemic vascular resistance calculated. These devices have become more reliable and less invasive over time; pulmonary artery catheters are now rarely used in PICU, and have largely been superseded by less invasive thermodilution systems such as Pulse Contour Cardiac Output Monitoring (PiCCO), Lithium dilution cardiac output (LiDCO) and the more recently developed pressure recording analytical method (PRAM) devices. The Ultrasound Cardiac Output Monitor (USCOM) is a non-invasive transcutaneous continuous wave Doppler ultrasound with software that calculates cardiac output, stroke volume and systemic vascular resistance and additional parameters such as cardiac power, stroke work and oxygen delivery. It is non-invasive and so ideal for use in children and has been used in paediatric critical care studies (Brierley and Peters 2008). As this is not an automated method of measuring haemodynamics a level of operator error is inevitable.

Therapeutic end points include the cardiac index (CI – CO corrected for body surface area) >3.3 and <6.0 l/min/m^2 with normal coronary perfusion pressure (mean arterial pressure minus central venous pressure) for age. Frequent re-assessment of children with shock is necessary as the haemodynamic profile of critically ill children rapidly changes, particularly during the early phase of their illness.

1.6.2.4 Adjunctive therapy

Profound derangements in metabolism associated with MCD may contribute to a worsening of clinical condition, including myocardial depression (Nadel, Levin et al. 1995). Anaemia and deranged glucose and electrolyte regulation are common and need active correction (Britto, Nadel et al. 1996; Goldhill 1997; Weisinger and Bellorin-Font 1998; Baines, Thomson et al. 2000). Adult data suggested that strict blood glucose control has a favourable effect on mortality (van den, Wouters et al. 2001). Day et al. showed a significant associated between outcome and peak glucose level in children with MCD (Day, Haub et al. 2008). Correction of DIC with fresh frozen plasma, platelets and cryoprecipitate may be required. Recombinant activated protein C administration in paediatric sepsis has not been shown to be of benefit by the RESOLVE study. This may have been due to the heterogeneous population that was recruited and the outcome measures used (Nadel, Goldstein et al. 2007). Further studies using activated protein C in paediatric sepsis would be welcomed.

1.6.2.5 Novel therapies

A double-blind, randomized, placebo-controlled trial of a human monoclonal antibody to endotoxin (HA1A) in the treatment of children with MCD

demonstrated no significant reduction in the 28-day all-cause mortality rate when compared to placebo (Derkx, Wittes et al. 1999).

Bactericidal permeability-increasing protein (BPI) is a potent bactericidal protein produced by neutrophils. It is stored in the azurophilic granules and is also expressed on the cell surface. The bactericidal activity of BPI is caused by the strong affinity of BPI for LOS (Weiss, Elsbach et al. 1978). In addition to bactericidal capacity, BPI also neutralizes LOS activity in vitro and in vivo (Marra, Wilde et al. 1992). A double-blind, randomized, placebo-controlled trial of recombinant bactericidal permeability-increasing protein (rBPI) showed an improved outcome with fewer amputations, decreased blood product transfusions and improved functional outcome but was not sufficiently powered to detect a reduction in mortality (Giroir, Scannon et al. 2001). Recombinant tissue plasminogen activator may reduce peripheral necrosis and minimise the risk of amputation in children with MCD, but its use in patients with severe MCD and purpura fulminans was associated with a high risk of intracranial haemorrhage and therefore its use is not routinely recommended (Zenz, Zoehrer et al. 2004).

The CORTICUS trial is the largest prospective randomised controlled trial to date to study the effects of low dose replacement steroids in adults with sepsis (Sprung, Annane et al. 2008). There was no improvement in survival or reversal of shock in patients given hydrocortisone in the presence or absence of adrenal insufficiency. However when shock was reversed, the time to shock reversal was quicker in those patients treated with hydrocortisone. Replacement steroids are being increasingly used in children with refractory septic shock. There is however no clear evidence

supporting their use. As a small proportion of children with MCD have adrenal insufficiency (Bone, Diver et al. 2002) administration of low dose maintenance steroids in patients with unresponsive shock is logical (Riordan, Thomson et al. 1999).

1.7 The Microcirculation and Tissue Perfusion

The microcirculation is the interface between blood and tissue and is vital to maintain cell function and survival. Under diseased conditions when the circulation becomes compromised, cells will receive insufficient quantities of vital substances and the build up of waste products will cause toxic effects. Cell activity within a tissue bed determines the demand for substances and waste removal. Increased demand must be met by increased exchange of substances between the capillary blood supply and the tissue bed. This exchange can be limited either by the rate of transport across the capillary walls or by the quantity of a substance available in the capillary blood supply.

The maintenance of an adequate supply of oxygen to all tissues is vital to ensure tissue viability. Human tissues have a limited capacity for anaerobic metabolism and although some cells can produce energy anaerobically for a short time, it is inefficient. Maintaining adequate tissue perfusion and tissue oxygenation is, therefore, an important goal in the clinical management of any critical illness. When the demand for oxygen by the tissues is met by the supply of oxygen to tissue adequate tissue oxygenation can occur. The relationship between oxygen delivery and oxygen consumption in a tissue can be represented by Figure 1.3.

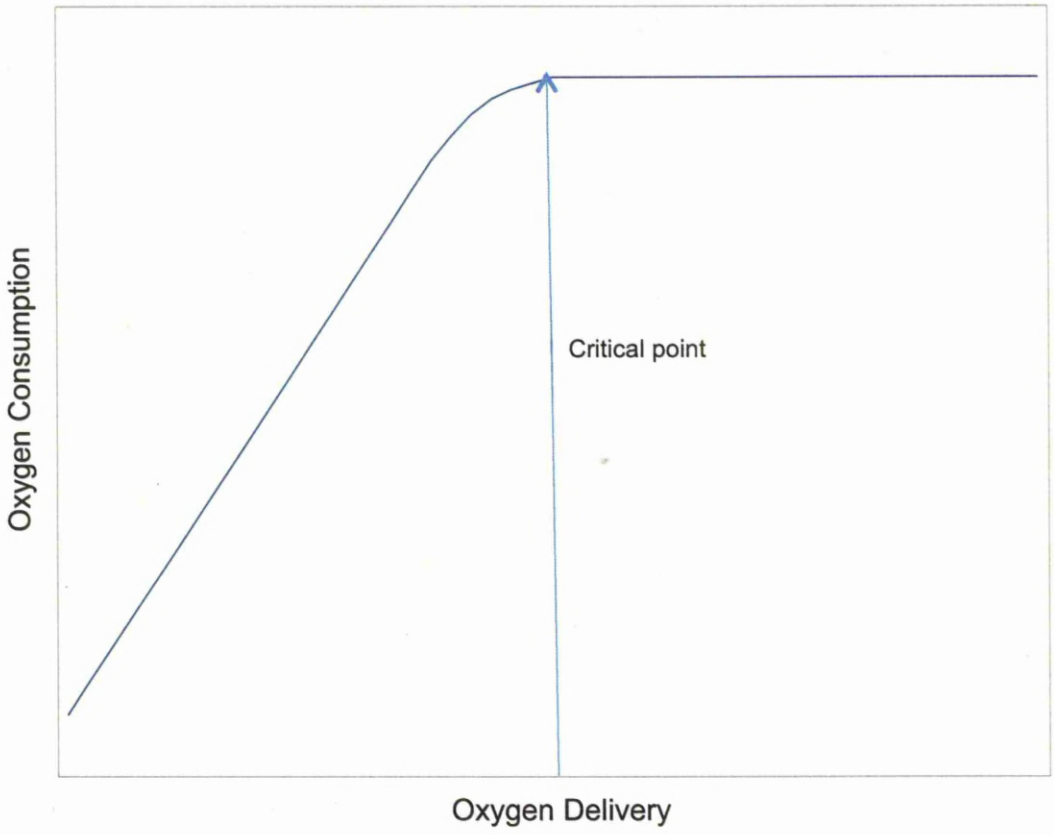

Figure 1.3. Schematic representation of the relationship between oxygen delivery and oxygen consumption in tissue.

At high levels of oxygen delivery tissue oxygen requirements are met and changes in the rate of delivery have no effect on the rate of consumption. (Leach and Treacher 1992; Treacher 1998) Oxygen consumption is assumed to be supply independent. At low levels of oxygen delivery, tissue oxygen requirements are not met. This leads to changes in oxygen delivery which are matched by changes in oxygen consumption, oxygen consumption is said to be supply dependant and tissue hypoxia occurs. This biphasic model of the relationship between oxygen delivery and oxygen consumption has been demonstrated in animals and in humans (Kolar and Jansky 1984). The rate of oxygen delivery at which oxygen consumption changes from being supply dependant to being supply independent is known as the critical oxygen delivery. The aim of intensive care is to maintain oxygen delivery at or above the critical oxygen delivery to ensure adequate tissue oxygenation (Leach and Treacher 1998).

Tissue delivery of oxygen is by the arterial blood and is mostly carried bound to haemoglobin. Tissue oxygen delivery therefore relies on the haemoglobin concentration of blood, the oxygenation of the arterial blood and the rate of flow of that blood through the tissues.

1.8 Tissue perfusion assessment

The quantification of tissue perfusion in critical illness has been attempted by various methods in addition to previously used markers such as capillary refill time, base deficit, lactate and urine output.

1.8.1 Near Infrared Spectroscopy (NIRS)

NIRS is a non-invasive continuous method to evaluate peripheral tissue oxygen metabolism. The first observations of spectroscopy of tissues using

near infrared light were made by Jobsis in 1977 (Jobsis 1977). He noted that the penetration of tissue by light with a wavelength shorter than 700nm is poor, due to increased scattering at short wavelengths, and that light with a wavelength longer than 1300nm is absorbed within a few millimetres by tissue water. However between these two wavelengths, in the near infrared, light penetrates tissue well. It can therefore be used with computer analysis of spectra in the near-infrared range, 680 to 800 nm, to determine tissue haemoglobin oxygen saturation. This technique has shown lower tissue haemoglobin oxygen saturation values in adult septic shock (Poeze 2006; Skarda, Mulier et al. 2007; Mulier, Skarda et al. 2008). NIRS may therefore be a reasonable non-invasive indicator of systemic oxygen delivery in severe sepsis. The first application in paediatrics was in 1985 in the bedside monitoring of cerebral oxygenation in sick preterm infants (Brazy, Lewis et al. 1985; Brazy, Lewis et al. 1985). Further studies have been performed in paediatric and neonatal practice although mainly in the areas of brain injury or congenital heart defect surgery (Fallon, Roberts et al. 1994; Toet, Flinterman et al. 2005; Kirshbom, Forbess et al. 2007; Subbaswamy, Hsu et al. 2008). A limitation of NIRS is that it is necessary to perform continuous monitoring during a therapeutic or experimental intervention or a particular clinical event in order to determine the effect on oxygenation or haemodynamics. Also the method is limited to the outer cortex of the brain with a penetrable depth of 25 mm, it is time consuming to assemble and there are motion artefacts when measuring. NIRS is not routinely used in clinical practice and has not been evaluated in children with MCD.

1.8.2. Laser doppler flowmetry

Laser doppler uses a laser of a wavelength of 770–790 nm, which is directed onto the skin surface. It is a repeatable method of studying microvascular reactivity function (Yvonne-Tee, Rasool et al. 2005). Light that is reflected off a piece of stationary tissue undergoes no shift. Light that is reflected off cells that have a velocity like red blood cells undergoes a Doppler shift. The degree to which this Doppler shift occurs is proportional to the velocity of the cells. The light is then randomly reflected back onto a photodetector. This calculates the mean velocity of the cells within the tissue. Studies in adults have shown microvascular abnormalities in sepsis using this method (Knotzer, Maier et al. 2007). Laser doppler has not been used to investigate childhood sepsis.

1.8.3. Gastric tonometry

Gastric tonometry measures carbon dioxide (CO_2) production. Gastric CO_2 rises in states of low perfusion because of anaerobic metabolism and/or decreased clearance (Friedman, Berlot et al. 1995; Baines 2001; Marik 2005). A nasogastric tube with a CO_2 permeable balloon is placed into the stomach to measure gastric CO_2. Carbon dioxide from the gastrointestinal tract diffuses into the balloon over a period of 30 to 90 minutes, and the CO_2 of the balloon content is then analyzed once removed. It has been shown to be an effective way of assessing tissue perfusion in children with severe MCD (Baines 2001). Its limitations are that the tube can be difficult to place, must be placed each time a reading is to be taken, and can cause discomfort. Additionally gastric enteral nutrition can produce gastric hypersecretion and lower the pH (Marik and Lorenzana 1996).

1.8.4. Sublingual Capnometry

Sublingual capnometry is performed with a silicone-covered disposable probe filled with a fluorescent dye. The probe is placed under the tongue for 5 to 10 minutes. This allows CO_2 to diffuse into the dye. A light is then transmitted into the dye via an optic fibre and the amount of fluorescence is analysed (Marik 2005). It can detect microcirculatory changes in adults with severe sepsis but has not been studied in children (Weil, Nakagawa et al. 1999; Boswell and Scalea 2003; Marik and Bankov 2003; Creteur 2006).

1.8.5 Intravital Microscopy

Intravital microscopy has contributed significantly to the understanding of leukocyte-endothelial cell interactions in-vivo (Smedegard, Bjork et al. 1985). It is used to track the movements of white cells through the inflammatory microcirculation in real time. The method requires sections of tissue to be illuminated with light and is appropriate for animal studies but could not be used to obtain real time images of the microcirculation in humans.

1.9 Orthogonal Polarisation Spectral imaging and Side Stream Darkfield Imaging

Orthogonal polarization spectral (OPS) imaging was first introduced in 1999 as a method of assessing tissue perfusion. OPS and sidestream darkfield imaging (SDF) are incorporated into a small, hand held device that non-invasively visualises the microcirculation. OPS uses polarised light of a wavelength within the haemoglobin absorption spectrum (e.g. 548 nm) and red blood cells appear dark when visualised on a computer screen. An objective lens focuses the light onto a region of approximately 1 mm in diameter (Groner, Winkelman et al. 1999). The polarised light is scattered

by the tissue and the majority is reflected back from the tissue surface. The reflected light is collected by the objective lens. A polarization filter orthogonal to the original beam of light eliminates the scattered reflected light but retains the light that remains polarised. High contrast images of the microcirculation are formed by the absorbing red blood cells that are close to the mucosal surface giving real- time images of microcirculatory blood flow. A thin layer of mucosal tissue is needed for image attainment.

OPS has been superseded by SDF imaging which uses the same principle of OPS but without polarised light. Instead light-emitting diodes are incorporated into the image attainment probe resulting in higher quality images. Both techniques enable images to be obtained at the bed-side most conveniently by placing the imaging probe sublingually in a fashion similar to an oral thermometer (Groner, Winkelman et al. 1999; Nadeau and Groner 2001). Images can be obtained from any mucosal surface and video sequences have been obtained from the brain surface, stomas and tumour surfaces (Thomale, Schaser et al. 2001; Pahernik, Harris et al. 2002; Boerma, Mathura et al. 2005) OPS imaging, after validation (Mathura, Vollebregt et al. 2001), was introduced into surgery giving the first direct observations of the microcirculation of human internal organs (Groner, Winkelman et al. 1999; Mathura, Vollebregt et al. 2001; Pennings, Bouma et al. 2004).

1.10 OPS and SDF in monitoring the microcirculation in sepsis

The regulatory mechanisms controlling microcirculatory perfusion are multifactorial. The endothelial cells lining the microvessels sense blood flow and metabolic and regulatory substances to modulate smooth muscle cell tone and capillary recruitment (Vallet 2002). The endothelium is vital in

regulating coagulation and immune function, which directly affect microcirculatory function. Sepsis significantly disrupts endothelial and microcirculatory function (De Backer and Dubois 2001; De Backer, Creteur et al. 2002; Spronk, Zandstra et al. 2004). Blood flow becomes abnormal with some capillaries having low flow or even stagnant blood flow within them while others have normal to abnormally high blood flow (De, Creteur et al. 2002; Spronk, Zandstra et al. 2004). Functionally vulnerable microcirculatory units become hypoxic, leading to an oxygen extraction deficit (Lam, Tyml et al. 1994; Sinaasappel, van et al. 1999; Goldman, Bateman et al. 2004) and varying degrees of functional shunting occur, more severely in sepsis than in haemorrhage (Ince and Sinaasappel 1999; Sinaasappel, van et al. 1999). In consequence, monitoring of systemic haemodynamic-derived and oxygen-derived variables may not detect such microcirculatory dysfunction.

In sepsis, the microcirculatory endothelial cells are unable to perform their regulatory function (Lidington, Tyml et al. 2002; Vallet 2002). The precise nature of this reaction within the endothelial cells has not been fully elucidated and could well be an adaptive response. Contributing factors include the NO system which is severely disturbed by heterogeneous expression of inducible nitric oxide synthase (iNOS) in different areas of organ beds, causing pathological shunting (Revelly, Ayuse et al. 1996; Morin, Unno et al. 1998). Activated leucocytes generate reactive oxygen species that directly disrupt microcirculatory structures, cellular interactions and coagulation (Cerwinka, Cooper et al. 2003; Martins, Kallas et al. 2003; Victor, Rocha et al. 2004). These, and other inflammatory mediators, alter barrier function in the microcirculation, leading to tissue oedema and further oxygen extraction deficit.

Several studies have investigated the microcirculation in adults with severe sepsis. The first, by De Backer et al., found a lower proportion of perfused small vessels (capillaries) and a lower capillary density when compared to controls and that these changes were more severe in non-survivors (De, Creteur et al. 2002). Studies visualising the sublingual microcirculation in adult sepsis have directly correlated the degree of microcirculatory distress with disease severity, mortality and response to therapy (Spronk, Ince et al. 2002; Sakr, Dubois et al. 2004). Sakr and colleagues showed that in adults microcirculatory dysfunction left uncorrected for 24 hours was the single most important independent factor predicting patient outcome. Only one paediatric study has been published using OPS imaging in sepsis. Top et al. showed that there was poor microcirculatory recovery in non-survivors of paediatric sepsis (Top, Ince et al. 2011)

The dysfunctional capillary blood flow associated with sepsis is characterized by sluggish or obstructed blood flow in the smallest capillaries with near to normal flow in the larger microcirculatory vessels. The relevance of the redistribution of oxygen to the pathophysiology of sepsis is uncertain. Fluid resuscitation, while correcting systemic haemodynamics, can leave areas of the microcirculation hypoxic (Ince and Sinaasappel 1999; Goldman, Bateman et al. 2004). In adult septic shock the sublingual microcirculation remained sluggish after pressure-guided resuscitation, despite the endothelial vasodilatory response being intact (De, Creteur et al. 2002). Sublingual OPS imaging in septic patients demonstrated that resuscitation of mean arterial pressure (MAP) and CO alone is not enough to resuscitate the microcirculation (Sakr, Dubois et al. 2004; Boerma, Mathura et al. 2005). There is increasing evidence that

organ function improves and mortality decreases when resuscitation also improves microcirculatory flow.

A number of strategies are suggested for resuscitating the microcirculation in septic patients. While vasopressor therapy alone is insufficient, the combination of adequate volume resuscitation, vasopressor agents and blood transfusion ensure adequate global oxygen delivery. This targeted strategy improves organ function and survival as demonstrated by the work of Rivers and colleagues (Rivers, Nguyen et al. 2001; Rivers, Nguyen et al. 2004; Otero, Nguyen et al. 2006; Rivers 2006). SDF and OPS imaging have been incorporated into the concept of goal directed therapy (Trzeciak, Dellinger et al. 2006; Trzeciak, Dellinger et al. 2007). These studies confirmed that early microvascular dysfunction is more severe in non-survivors despite the utilisation of goal directed therapy on cardiovascular variables and is also more severe in those patients with global cardiovascular dysfunction.

If enhanced microcirculatory flow is essential for oxygen transport and this may be achieved by vasodilator agents, it can be hypothesised that vasodilator therapy will improve both regional perfusion and oxygen availability during sepsis. Several animal studies have suggested that prostacyclin preferentially protects vessels in the microcirculation (Muller, Schmidtke et al. 1987; Bouskela and Rubanyi 1995). Clinical studies have shown that prostacyclin improves microvascular skin blood flow and global oxygen variables such as oxygen delivery and consumption in septic patients (Pittet, Lacroix et al. 1990; Pittet, Lacroix et al. 1992). Nitric oxide has also been shown to stabilise the microcirculation in animal models (Nishida, McCuskey et al. 1994; Gundersen, Saetre et al. 1996). In the

study by Spronk in adult septic patients , OPS imaging revealed that there was enhanced microcirculatory blood flow with nitroglycerin after pressure-guided resuscitation (Spronk, Ince et al. 2002).

There are limitations to using OPS and SDF imaging in the assessment of the microcirculation in sepsis. Obtaining sublingual images may not be representative of other organs. It has been shown that sublingual and gut microvascular blood flow had a similar response when exposed to endotoxin (and resulting shock) implying that the sublingual circulation is a good central area for images to be obtained (Fries, Weil et al. 2006). The area of tissue being visualised is very small leading to the possibility of pressure effects affecting the area of blood flow being visualised. Image attainment and analysis is largely subjective resulting in possible bias.

Although correction of hypotension is an important clinical target in the management of MCD, the use of vasopressor therapy to achieve this could be detrimental to microcirculatory perfusion and oxygenation. In this complex situation new clinical techniques for monitoring the microcirculation could significantly improve management.

OPS imaging and SDF could be used to target management or be used as a criteria for inclusion in clinical trials. Assessment of the microcirculation in MCD by using SDF or OPS could have an impact on the management of the disease.

1.12 Monitoring of the Macrocirculation in Sepsis

The characteristic 'macro'-haemodynamic feature of fulminant adult meningococcal sepsis is hyperdynamic shock, with increased cardiac

output and reduced peripheral resistance (Parker, Shelhamer et al. 1987). The cardiovascular features of sepsis in children may be different from those of critically ill adults. Children with sepsis have a low indexed CO, a low vascular resistance alone, or combined cardiac and vascular dysfunction (Ceneviva, Paschall et al. 1998). Furthermore, the cardiovascular pathophysiology may change during the evolution of sepsis requiring changes in therapy and the need for continuing monitoring if possible. Peters et al. demonstrated that the haemodynamic patterns of fluid-resistant paediatric septic shock differs according to the underlying cause. Children with central venous catheter (CVC) infections having a different pattern of septic shock, compared with those with community acquired infections. A greater proportion of CVC infections presented with a low systemic vascular resistance index and high cardiac index whereas a normal or low cardiac index was predominant in children with community acquired sepsis (Brierley and Peters 2008).

Studies investigating the microcirculation in severe illness must also look at cardiac function. Two-dimensional echocardiography is valuable for examining sepsis induced cardiac dysfunction (Boucek, Boerth et al. 1984; Mercier, Beaufils et al. 1988; Hagmolen of ten, Wiegman et al. 2000; Briassoulis, Narlioglou et al. 2001). Echocardiography assesses both cardiac systolic and diastolic function. Reliable estimates of cardiac output and when corrected for body surface area, cardiac index, can be calculated. When this data, although subjective, is combined with clinical haemodynamic variables reasonable estimates of systemic vascular resistance can be produced.

Haemodynamic information available from pulmonary artery catheters (PACs) has been helpful in understanding MCD. Children with MCD have a lower CO despite a higher pulmonary artery occlusion pressure (PAOP) and CO does not increase in response to volume loading in MCD, compared with other forms of Gram negative sepsis (Monsalve, Rucabado et al. 1984). Furthermore SVR in survivors is abnormally high. This suggests that there may be a specific problem with cardiac performance in those children who die (Mercier, Beaufils et al. 1988). Similar information can be obtained from thermodilution catheters. The insertion of PACs or thermodilution devices is uncommon in paediatric critical care. They are invasive, a possible source of infection and thrombus may form at the catheter site. Laboratory investigations and non-invasive methods of assessing haemodynamic dysfunction, such as echocardiography, could give more information on the state of the cardiovascular system in sepsis.

1.12.1 Troponin

Changes in the intracellular calcium concentration control cardiac and skeletal muscle activity. A rise in intracellular calcium causes muscle contraction, and a decrease, muscle relaxation. Troponin is a component of thin filaments (along with actin and tropomyosin) and is the protein to which calcium binds to accomplish this regulation. Damaged myocytes release cardiac troponins (cTn). Troponin has three subunits, Troponin C (TnC), Troponin I (TnI), and Troponin T (TnT). When calcium binds to TnC, the structure of the thin filament changes. This causes myosin to attach to thin filaments and produces force and/or movement, which results in muscle contraction. If levels of calcium are absent or low, tropomyosin interferes with this action of myosin (Clark 2002). This then leads to muscles remain relaxed. Individual subunits serve different functions:

- **Troponin C** binds to calcium ions to produce movement;
- **Troponin T** binds to tropomyosin, interlocking them to form a troponin- tropomyosin cross-bridge formation;
- **Troponin I** binds to actin in thin myofilaments to hold the troponin-tropomyosin complex in place (Clark 2002)

Troponin measurement has replaced the measurement of cardiac enzymes for the detection of cardiac cell death due to a myocardial infarction in adults. In 2000 both the European Society of Cardiology and the American College of Cardiology recommended replacing the traditional CK-MB with cardiac troponins cTnT and cTnI as markers of a myocardial infarction. They are more sensitive markers of myocardial damage than CK-MB (Gerhardt, Katus et al. 1991; Hawkins and Tan 1999; Alpert, Thygesen et al. 2000). cTnT levels are detectable as early as three hours following a myocardial infarction, peaking between 10-20 hours and remain elevated for up to 20 days (Katus, Remppis et al. 1991; Uji, Sugiuchi et al. 1992; Murthy and Karmen 1997; Wu, Feng et al. 1998) despite a half-life in blood of approximately two hours (Gerhardt, Katus et al. 1991) The persistence of a raised cTnT level does not necessarily represent continuing myocyte death or damage as it may be due to the ongoing release of cTnT from previously damaged myocytes into blood.

Increased troponin levels have been observed in diseases other than myocardial infarction. Viral myocarditis can produce myocyte damage and raised troponin (Narula, Southern et al. 1991; Dec, Waldman et al. 1992; Narula, Khaw et al. 1993). Patients with pericarditis can have involvement of the epicardium with myocyte injury and cTnI is elevated in approximately one third of these patients (Brandt, Filzmaier et al. 2001). Bodor et al found that patients with Duchenne muscular dystrophy and polymyositis had

raised serum levels of cTnT and concluded that cTnT is found in regenerating muscle (Bodor, Survant et al. 1997). High levels of cTnT have been found in a young dialysis population indicating that cTnT is expressed in the skeletal muscle of dialysis patients or that there is possible cardiac damage from ongoing hypertension (McLaurin, Apple et al. 1997).

Elevated cTnT and cTnI have been found in adults with sepsis and have been shown to correlate with ejection fraction and mortality. They have also been shown to correlate with TNF, sTNFR levels, IL-6 and ICAM-1 in sepsis (Spies, Haude et al. 1998; Fernandes, Akamine et al. 1999; Turner, Tsamitros et al. 1999; Ammann, Fehr et al. 2001; Ammann, Maggiorini et al. 2003; Mehta, Khan et al. 2004). cTnI has been found to be elevated in MCD. In a study by Thiru et al 62% of children admitted to PICU with MCD has a raised cTnI troponin I and cTnI levels correlated with disease severity scores, inotropic support and cardiac function in that a lower ejection fraction was seen in children with a raised cTnI (Thiru, Pathan et al. 2000). These findings have been reproduced by other paediatric studies investigating MCD (Briassoulis, Narlioglou et al. 2001; Gurkan, Alkaya et al. 2004). The pathophysiological process involved in the release in cardiac troponins in sepsis is not clear.

1.12.2 N-Terminal Pro Brain Natriuretic Peptide

Of recent interest in monitoring cardiac performance are the natriuretic peptides. Atrial natriuretic peptide (ANP) was the first member of the natriuretic peptides to be isolated. This group of neuropeptides include brain natriuretic peptide (BNP), and C-type natriuretic peptide (Levin, Gardner et al. 1998). The pro-hormones of ANP and BNP split into the inactive N-terminals, NT-Pro ANP and NT-Pro BNP. The biologically active COOH-terminals are the ANP and BNP peptides. ANP is the dominant

peptide released by the cardiac atria and BNP, the ventricles. Both are produced in response to increased myocardial wall stress and improve myocardial performance due to their potent natriuretic and vasorelaxant activity (Krupicka, Janota et al. 2008). The natriuretic peptides are now a validated marker in the diagnosis of heart failure in adults as they are early markers of myocardial dysfunction (Maisel, Krishnaswamy et al. 2002; Sirithunyanont, Leowattana et al. 2003; Machado, Falcao et al. 2004; Wang, Larson et al. 2004). They are sensitive and specific and measurement is rapid and reasonably cheap (Collinson, Barnes et al. 2004) There has been recent interest in the measurement of NT-Pro BNP in sepsis to detect poor cardiac function. Chua et al noted that six patients admitted to intensive care with septic shock had markedly elevated levels of NT-Pro BNP within 6 hours of admission (Chua and Kang-Hoe 2004). In a larger study of adults admitted to intensive care with severe sepsis and congestive cardiac failure, those with severe sepsis or septic shock had highly elevated levels of BNP and NT-Pro BNP and despite significant hemodynamic differences that these levels were comparable with patients admitted due to acute heart failure (Rudiger, Gasser et al. 2006). BNP has also been shown to be inversely related to cardiac index in critically ill adults (Witthaut, Busch et al. 2003). NT-Pro BNP is measured rather than BNP because the different pathways of peptide clearance mean that the half-life of NT-proBNP is longer than BNP (Hall 2005). Levels of NT-Pro BNP in severe sepsis have also shown to predict outcome. Varpula et al found significantly higher values in non-survivors and NT-Pro BNP was an independent prognostic marker of mortality in adults with severe sepsis and septic shock. (Varpula, Pulkki et al. 2007).

NT-Pro BNP has been measured in children with cardiac dysfunction (Nir and Nasser 2005; Nasser, Perles et al. 2006; Geiger, Hammerer-Lercher et al. 2007). Fried et al were the first group to assess whether NT-Pro BNP levels could differentiate paediatric patients with critical illnesses due to sepsis from those with acute left ventricular dysfunction from other causes. They found that NT-Pro BNP levels were elevated in patients with sepsis but were significantly higher in patients with acute left ventricular dysfunction from known congenital cardiac disease. NT-Pro BNP levels of patients with sepsis and impaired systolic function were not different from those of patients with sepsis and normal systolic function measured with echocardiography. In a further group of patients, not admitted to PICU, attending or admitted to hospital with a self limiting viral illness, levels of NT-Pro BNP were significantly lower than the two groups admitted to PICU (Fried, Bar-Oz et al. 2006). A larger study found that children with septic shock had an elevated BNP level on admission to PICU when compared with healthy children and PICU controls. They also found that BNP measured at 12 hrs had a strong positive correlation with Pediatric Risk of Mortality III score and a strong negative correlation with fractional shortening as a measure of echocardiographic cardiac dysfunction (Domico, Liao et al. 2008). There have been no studies that have investigated NT-Pro BNP production in children with MCD.

1.12 Aims of current prospective study

1. To determine whether activated Partial Thromboplastin Time waveform analysis and Procalcitonin could be used as early diagnostic markers in sepsis.

2. To assess the microcirculation of normal healthy children using side-stream dark-field imaging to validate its use in children.

3. To visualise the microcirculation in children with severe meningococcal disease using side-stream dark-field imaging.

4. To correlate microcirculatory variables of children with severe MCD with disease severity, cardiac function and plasma vasoactive endothelial mediators and cytokines.

5. To study cardiac systolic and diastolic function in children with severe meningococcal disease using echocardiography and determine the relationship between plasma cardiac troponin and NT Pro-BNP with cardiac function in children with severe MCD.

Chapter 2

Materials and Methods

2.1 Patient Recruitment

2.1.1 Study Design

The study was a two-centre, prospective, observational study. The study was conducted at Alder Hey Children's NHS Foundation Trust (AH) and the Royal Manchester Children's Hospital NHS Trust (RMCH). The Research and Development Committees at both hospitals granted approval for the study. Ethical Committee approval was obtained from the South Sefton Research Ethics Committee in November 2006. The study was carried out between January 2007 and April 2008, at AH and March 2007 and April 2008 at RMCH. The AH and RMCH admit children from the North west of England (or Merseyside and Greater Manchester) and North Wales. Both serve as tertiary centres admitting children to the regional PICU from other districts including North Wales, Lancashire and the Lake District.

Of the 45 children in the prospective study 33 were classed as confirmed meningococcal disease, and the other 12 were children with a presumed viral illness. 17 (38%) were male and 28 were female (62%). The age range was from 0.16 to 15.17 years, median age 2.16 years, interquartile range (IQR) 0.92 to 4.33 years. There were 17 children (52%) with severe disease as defined by a Glasgow Meningococcal Septicaemia Prognostic Score (GMSPS) of ≥ 8. 20 children were ventilated and admitted to PICU (60%). Blood was taken from a control population of 23 children who were group of well patients undergoing elective dental surgery. Of the 23 control children, 12 (52%) were male and 11 (48%) female. The age range was from 0.25 to 11 years, median age 2.5 years, interquartile range (IQR) 0.6 to 4.4 years.

As this study also evaluated a new technique for visualisation of the microcirculation control children were recruited to assess 'normal' images. Three groups were recruited. The first were children attending for routine general surgery. Twenty children were recruited 10 (50%) were male and 10 (50%) female. The age range was from 0.75 to 4.5 years, median age 2.5 years, interquartile range (IQR) 0.75 to 4.5 years. The second group were older children who could co-operate with image attainment. Twenty children were recruited 11 (55%) were male and 11 (45%) female. The age range was from 8.2 to 11.2 years, median age 10.4 years, interquartile range (IQR) 8.2 to 10.4 years. The third group were children who were attending hospital for cardiac surgery The median age of the children was 2.1 years (IQR 0.7 to 2.6), 5 (50%) were male and 5 (50%) female.

2.1.2 Notification of cases and controls

The Research Fellow was notified whenever a child with suspected meningococcal septicaemia or meningitis was admitted to the Emergency department (ED), or if the Regional PICU Transport Teams at AH or RMCH had received a referral from a district general hospital for admission to PICU. Once notified, the Research Fellow attended as soon as possible after the arrival to hospital. In the majority of cases this was within one hour of being contacted. Notification was by the doctors involved in these children's clinical care. In the case of PICU admissions, the Research Fellow saw the child on arrival to PICU, and subsequently followed their course throughout their hospital stay.

Admissions via the ED at AH were seen in the ED, and their subsequent course followed throughout their hospital stay. Children referred as having

possible or probable MCD, but who were later felt to have an alternative diagnosis were also recruited. Their hospital progress was followed in an identical way as the confirmed cases. These children were used as a separate clinical group and were assumed to have a viral infection. Blood samples were sent for viral analysis including PCR for adenovirus, enterovirus, HHV6, HHV7, influenza A and B, cytomegalovirus, parovovirus and rubella. This group was included for determination of blood analytes and gene expression studies.

The control population was recruited from a group of well patients undergoing elective surgery for non-infective conditions at AH. Patients were identified by discussing prospective theatre lists with hospital theatre co-ordinators and anaesthetists. On arrival to AH, these patients and their parents were approached regarding entry into the study. Control patients who had clinical symptoms of an acute illness in the last 2 weeks were excluded, as were patients where there was evidence on examination of a possible systemic infection. No control patients who were excluded on the basis of above.

Children for the cardiac surgery comparative group was recruited from list of children listed for cardiac surgery at AH. Patients were identified by discussing prospective theatre lists with hospital theatre co-ordinators and anaesthetists. These patients and their parents were approached regarding entry into the study the day prior to surgery. Only children who were undergoing surgery requiring cardiac bypass were included.

2.1.3 Assessment of patients

Children were recruited into the study once the Research Fellow had obtained informed consent or assent from the parents or children themselves. Informed consent entailed the details of this study being explained to the patients and parents and written information being supplied. Those giving informed consent were told that even if consent was given if could be withdrawn at any time. Demographic data, duration and nature of symptoms, severity of disease assessments, clinical assessment, laboratory results, SDF image recording, echocardiography recording and outcome were recorded on a specifically designed proforma.

2.1.4 Disease severity assessment.

For each patient a prospective GMSPS (Sinclair, Skeoch et al. 1987; Thomson, Sills et al. 1991), the Pediatric Logistic Organ Dysfunction Score (PELOD) (Leteurtre, Martinot et al. 2003; Lacroix and Cotting 2005) and the Paediatric Risk of Mortality III (PRISM III) (Pollack, Ruttimann et al. 1988) were calculated at admission as detailed in Tables 2.1, 2.2 and 2.3 respectively. Inotrope score was also calculated using the following equation:

[1 x (dopamine dose + dobutamine dose) + 100 x (epinephrine dose + norepinephrine dose)] (Skippen and Krahn 2005)

CLINICAL SIGNS OR SYMPTOMS	SCORE
Low BP ▪ Age <4, <75mmHg ▪ Age >4, <85mmHg	3
Skin / rectal temp. difference > 3°C	3
GCS ≤ 8 or deterioration 3 points	3
Deterioration last hour	2
Absence of meningism	2
Extending/widespread petechiae	1
Base deficit > -8	1

Table 2.1. Glasgow Meningococcal Septicaemia Prognostic Score

	Infant	Child	Value	Score
Systolic blood pressure (BP, mmHg)	≤40	≤50	7	
	40-54	50-64	6	
	55-65	65-75	2	
	130-160	150-200	6	
	≥160	≥200	7	
Diastolic BP (mmHg)	≥110	≥110	6	
Heart Rate	≥160	≥150	4	
	≤90	≤80	4	
Respiratory Rate	61-90	51-70	1	
	≥90	≥71	5	
PaO2/FiO2 (mmHg)	200-300		2	
	≤200		3	
PaCO2 (mmHg)	51-65		1	
	≥65		5	
Glasgow Coma Score	≤8		6	
Pupillary reaction	Unequal or dilated		4	
	Fixed dilated		10	
PT / APTT	1.5x control PT ≥ 22.5 APTT ≥ 54		2	
Billirubin (μmol/L)	≥60		6	
Potassium (mmol/L)	≤3.0		5	
	3-3.5		1	
	6.5-7.5		1	
	≥7.5		5	
Calcium (mmol/L)	≤1.75		6	
	1.75-2.00		2	
	3-3.75		2	
	≥3.75		6	
Glucose (mmol/L)	≤2.2		8	
	2.2-3.3		4	
	13.9-22.2		4	
	≥22.2		8	
Bicarbonate (mmol/L)	≤16		3	
	≥32		3	
Total			Max 76	

Table 2.2. Pediatric Risk of Mortality III Score

	Scoring system			
	0	1	10	20
Organ dysfunction and variable				
Neurological				
Glasgow coma score	12–15	7–11	4–6	3
	and		**or**	
Pupillary reactions	Both reactive	NA	Both fixed	NA
Cardiovascular				
Heart rate (beats/min)				
<12 years	≤195	NA	>195	NA
≥12 years	≤150	NA	>150	NA
	and		**or**	
Systolic blood pressure (mm Hg)				
<1 month	>65	NA	35–65	<35
1 month–1 year	>75	NA	35–75	<35
1–12 years	>85	NA	45–85	<45
≥12 years	>95	NA	55–95	<55
Renal				
Creatinine (μmol/L)				
<7 days	<140	NA	≥140	NA
7 days–1 year	<55	NA	≥55	NA
1–12 years	<100	NA	≥100	NA
≥12 years	<140	NA	≥140	NA
Respiratory				
PaO_2 (kPa)/FIO_2 ratio	>9·3	NA	≤9·3	NA
	and		**or**	
$PaCO_2$ (kPa)	≤11·7	NA	>11·7	NA
	and			
Mechanical ventilation§	No ventilation	Ventilation	NA	NA
Haematological				
White blood cell count ($\times 10^9$/L)	≥4·5	1·5–4·4	<1·5	NA
	and	**or**		
Platelets ($\times 10^9$/L)	≥35	<35	NA	NA
Hepatic				
Aspartate transaminase (IU/L)	<950	≥950	NA	NA
	and	**or**		
Prothrombin time (or INR)	>60 (<1·40)	≤60 (≥1·40)	NA	NA

Table 2.3. Pediatric Logistic Organ Dysfunction score

2.1.5 Definitions

Children were recruited if presenting with fever and a non blanching rash. Cases were classified as either confirmed, probable or possible cases (Stuart, Monk et al. 1997):

- *Confirmed cases* – Clinical cases with microbiological confirmation of *Neisseria meningitidis* infection, either positive cultures from a normally sterile site (blood, cerebrospinal fluid (CSF) or joint fluid), or a positive meningococcal PCR from normally sterile sites.

- *Probable cases* – Clinical diagnosis of meningococcal meningitis or septicaemia without confirmation. The clinician managing the case considers that meningococcal disease is the likeliest diagnosis. In the absence of an alternative diagnosis a feverish, ill patient with a petechial or purpuric rash was regarded as a probable case.

- *Possible cases* – The clinician managing the case considers that diagnoses other than meningococcal disease were as likely. This included cases treated with antibiotics whose probable diagnosis is viral meningitis.

- *Presumed viral illness* – A possible case where *Neisseria meningitidis* infection has been excluded via blood or CSF culture from normally sterile sites and a negative meningococcal PCR from normally sterile sites.

2.1.6 Patient Inclusion Criteria

Prospective demographic data regarding diagnostic test results were collected on all patients referred to the Research Fellow with a diagnosis of possible MCD. Age was limited to 3 months to 16 years. Blood sampling was not undertaken if patients had been treated for 24 or more hours before consent could be obtained. These children were not included in any analysis.

2.1.7 Patient Exclusion Criteria

Patients with an underlying immune deficiency or congenital abnormalities that could have adversely affected outcomes were excluded from the data analysis - there were no patients in this group.

2.2 Blood Sampling

Blood samples in patients were collected as soon as possible after admission to hospital. For patients admitted to the general paediatric wards, samples were obtained at admission. For patients admitted to PICU samples were obtained at admission, 12, 24, and 72 hours, where possible, from indwelling arterial lines. Blood samples were taken for the determination of meningococcal bacterial load, viral detection, cytokines list) VCAM, ICAM, P-selectin, E-selectin, NO, cTnT, cTnI, NT-Pro BNP, PCT and aPTT waveform analysis. Blood samples taken at admission consisted of the following:

Three millilitre blood samples were collected into a 5mL Ethylene-diamine-tetra-acetic acid (EDTA) tube and placed immediately on ice for bacterial load, viral detection, cytokine, VCAM-1, ICAM-1, NO, P-selectin, E-selectin, cTnT, cTnI and NT-Pro BNP estimation. The blood pellet that remained after separation of plasma from the spun EDTA sample was used for bacterial load analysis. 1.3mls of blood was placed into a citrated tube for aPTT waveform analysis. Blood samples taken at 12, 24, and 72 hours consisted of 3 millilitre blood samples were collected into a 5mL Ethylene-diamine-tetra-acetic acid (EDTA) tube and placed immediately on ice

Coagulation samples are taken daily from children in intensive care into citrate tubes. These samples are processed by the haematology laboratory at AH and RMCH. The citrated blood is centrifuged 4000 x g for 5 minutes at room temperature and the plasma removed. Once the coagulation studies have been carried out the plasma remaining is frozen at -70 °C and if there is no further clinical use for the sample the laboratory disposes of it after 7 days. These samples were retrieved from the Haematology laboratories at AH and RMCH after the 7 days for serial aPTT waveform analysis.

Control patients undergoing elective surgery routinely had a cannula inserted in the anaesthetic room prior to surgery and it was during this procedure that 5mL of blood was obtained for cytokine estimation, VCAM-1, ICAM-1, NO, P-selectin, E-selectin, cTnT, cTnI, NT-Pro BNP and aPTT waveform analysis.

2.2.1 Blood sample separation and storage

Blood analysis for clinical purposes was performed in the haematology, biochemistry and microbiology laboratories at AH and RMCH. Separation was performed by centrifugation of the 3 ml EDTA samples at 4000 x g for 5 minutes at 4 °C and the serum decanted with fine tipped disposable Pasteur pipettes into a sterile container. 250 microlitre plasma aliquots were then pipetted into 2.0ml Nalgene cryogenic vials using Eppendorf micropipettes and the pellet was separated into a further cryogenic vial. Separation was performed by centrifugation of the 1.3 ml citrate sample at 4000 x g for 5 minutes at room temperature. The citrate plasma was decanted with fine tipped disposable Pasteur pipettes into a 2.0ml cryogenic vial. The samples were then all frozen at –70 °C until analysed. This occurred within 30 min of sampling. Citrate samples were analysed by the haematology laboratories at AH and RMCH as part of clinical coagulation studies. Frozen citrated plasma was stored in the haematology laboratories for 7 days following blood sampling. After 7 days if the sample was no longer needed for clinical purposes, it was retrieved from the laboratory for aPTT waveform analysis. The results of blood analysis are included in Chapters 3, 6 and 7.

2.3. Analysis of blood samples

2.3.1 aPTT waveform analysis.

Plasma aPTT waveform analysis was determined on the MDA 180 (Organon Teknika, Cambridge, United Kingdom) analyzer using Platelin LS. The methodology for this is described in chapter 3.

2.3.2. Quantification of Procalcitonin.

PCT was measured using an automated immunofluorescent assay: the BRAHMS PCT sensitive KRYPTOR kit and the BRAHMS KRYPTOR machine.

2.3.3 Quantification of endothelial cell adhesion molecules.

VCAM-1, ICAM-1 and P Selectin concentrations were measured using commercially produced Enzyme-Linked Immunosorbent Assay (ELISA) marketed by R&D Systems, Minneapolis, Minnesota, USA. E-Selectin concentrations were measured using commercially produced ELISAs marketed by Hycult Biotechnology. All samples and standards were assayed in duplicate in 96 well plates. All samples and controls were diluted 1:20 with sample diluent. For all assays a standard curve was constructed from the standard values using commercially available software and sample concentrations were obtained from this standard curve. The concentration of a sample was taken from the mean of the two wells.

2.3.3.1. ICAM-1

2.3.3.1a Materials

Wash Buffer - 20 mls of Wash Buffer concentrate was diluted with distilled water to prepare 500 mls of Wash Buffer.

ICAM-1 Standard - The sICAM-1 standards were reconstituted with 1.0 ml of distilled water. The vials were allowed to sit at room temperature for at least 10 minutes prior to use. Concentrations were: 0, 1.56, 3.13, 6.25, 12.5, 25, 50 ng/ml.

ICAM-1 Control - The sICAM-1 control was reconstituted with 500 µl of distilled water. The vial was allowed to sit at room temperature for at least 10 minutes prior to use.

ICAM-1 Conjugate concentrate - 250 µl of the conjugate concentrate was pipetted into the bottle of conjugate diluent and gently mixed.

Stop solution.

2.3.3.1b Method

100µl of ICAM-1 diluted conjugate was pipetted to each well.

100µl of standard, control, or sample was pipetted into each well.

An adhesive plate was covered was applied and incubated for 1.5 hours at room temperature

Each well was aspirated and washed using an autowasher with 400µl of wash buffer. This step was repeated five times for a total of 6 washes.

After the last wash any remaining wash buffer was removed by inverting the plate and blotting it against clean paper towels.

100 µl of substrate solution was pipetted into each well.

The plate was incubated for 30 minutes at room temperature, protected from light.

100 µl of stop solution was pipetted into each well.

The optical density of each well was read within 30 minutes, using a microplate reader set to 450 nm subtracting the blank well absorbance from all other values.

2.3.3.1c Performance characteristics of the assay

The inter-assay coefficient of variation of 4.4-6.8 % and an intra-assay coefficient of variation of 3.6-5 %.

2.3.3.2 VCAM-1

2.3.3.2a Materials

Wash Buffer - 20 mls of Wash Buffer concentrate was diluted with distilled water to prepare 500 mls of Wash Buffer.

Substrate Solution - Colour Reagents A and B were mixed together in equal volumes and used within 15 minutes.

Calibrator Diluent – 20 mls of calibrator diluent concentrate was diluted with 80 mls of distilled water to prepare 100 mls of calibrator diluent.

VCAM-1 Standard - The VCAM-1 standard vial was reconstituted with 1.0 ml of distilled water. This reconstitution produces a stock solution of 400 ng/ml and was allowed to sit for a minimum of 15 minutes with gentle agitation prior to making dilutions.

500 µl of calibrator diluent was pipetted into each tube. The stock solution was used to produce a dilution series (Figure 6.3). Each tube was thoroughly mixed before the next transfer. The 200 ng/mL standard served as the high standard. The calibrator diluent served as the zero standard (0 ng/mL).

Stop solution.

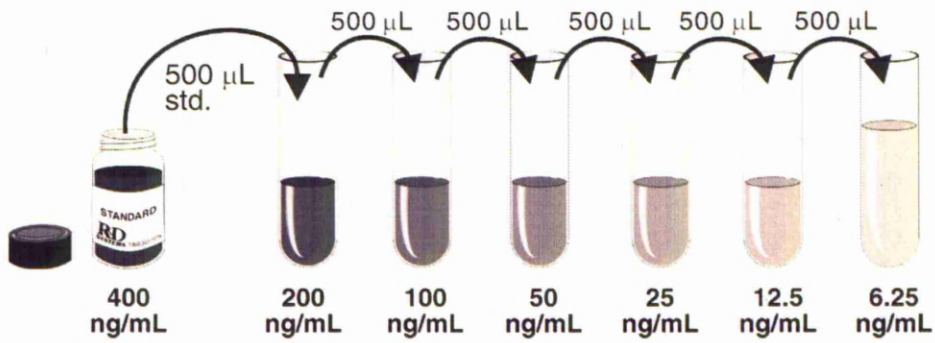

Figure 2.1 Serial dilution of VCAM-1 Standard for standard curve determination

2.3.3.2b Method

100µl of sVCAM-1 diluted conjugate was pipetted to each well.

100µl of standard, control, or sample was pipetted into each well.

The plate was covered with the adhesive strip and incubated for 1.5 hours at room temperature

Each well was aspirated and washed using an autowasher with 400µl of wash buffer. This step was repeated three times for a total of 4 washes. After the last wash any remaining wash buffer was removed by inverting the plate and blotting it against clean paper towels.

100 µl of substrate solution was pipetted into each well.

The plate was incubated for 20 minutes at room temperature, protected from light.

50 µl of stop solution was pipetted into each well.

The optical density of each well was read within 30 minutes, using a microplate reader set to 450 nm subtracting the blank well absorbance from all other values.

2.3.3.2c Performance characteristics of the assay

The inter-assay coefficient of variation of 5.5-8.7 % and an intra-assay coefficient of variation of 2.3-3.6%.

2.3.3.3. P-Selectin

2.3.3.3a Materials

Wash Buffer - 20 mls of Wash Buffer concentrate was diluted with distilled water to prepare 500 mls of Wash Buffer.

P-Selectin Standard - The P-Selectin standards were reconstituted with 1.0 ml of distilled water. The vials were allowed to sit at room temperature for at

least 10 minutes prior to use. Concentrations were: 0, 1.56, 3.13, 6.25, 12.5, 25, 50 ng/ml.

P-Selectin Control - The P-Selectin control was reconstituted with 500 µl of distilled water. The vial was allowed to sit at room temperature for at least 10 minutes prior to use.

P-Selectin Conjugate concentrate - 250 µl of the conjugate concentrate was pipetted into the bottle of conjugate diluent and gently mixed.

Stop solution.

2.3.3.3b Method

100µl of P-Selectin diluted conjugate was pipetted to each well.

100µl of standard, control, or sample was pipetted into each well.

The plate was covered with the adhesive strip and incubated for 1hour at room temperature.

Each well was aspirated and washed using an autowasher with 300µl of wash buffer. This step was repeated two times for a total of 3 washes.

After the last wash any remaining wash buffer was removed by inverting the plate and blotting it against clean paper towels.

100 µl of substrate solution was pipetted into each well.

The plate was incubated for 15 minutes at room temperature, protected from light.

100 µl of stop solution was pipetted into each well.

The optical density of each well was read within 30 minutes, using a microplate reader set to 450 nm subtracting the blank well absorbance from all other values.

2.3.3.3c Performance characteristics of the assay

The inter-assay coefficient of variation of 7.9-9.9 % and an intra-assay coefficient of variation of 5.1-5.6 %.

2.3.3.4 E-Selectin

E-Selectin concentrations were measured using commercially produced ELISAs marketed by Hycult Biotechnology.

2.3.3.4a Materials

Vial of tetramethylbenzidine (TMB)

Wash Buffer - 40 mls of Wash Buffer concentrate was diluted with distilled water to prepare 960 mls of Wash Buffer. 5ml of a concentrated magnesium and calcium solution was added.

E-Selectin Standard - The E-Selectin standards were reconstituted with 1.0 ml of distilled water. The vials were allowed to sit at room temperature for at least 10 minutes prior to use. Concentrations were: 0, 3.2, 16, 80, 400, 2000, 10,000 pg/ml.

E-Selectin tracer was reconstituted with 1.0 ml of distilled water and 11 mls of wash buffer added.

E-Selectin streptavidin-peroxidise conjugate was reconstituted with 1.0 ml of distilled water and 24 mls of wash buffer added and gently mixed.

Stop solution.

2.3.3.4b Method

100µl of standard, control, or sample was pipetted into each well.

An adhesive plate cover was applied and incubated for 2 hours at 18-25 °C

Each well was aspirated and washed using an autowasher with 200µl of wash buffer. This step was repeated three times for a total of 4 washes.

100µl of E-Selectin diluted tracer was pipetted to each well.

An adhesive plate cover was applied incubated for 1 hour at 18-25 °C

Each well was aspirated and washed using an autowasher with 200µl of wash buffer. This step was repeated three times for a total of 4 washes.

100µl of E-Selectin diluted streptavidin-peroxidise conjugate was pipetted to each well. An adhesive cover was applied to the plate and incubated for 1 hour at 18-25 °C. Each well was aspirated and washed using an autowasher with 200µl of wash buffer. This step was repeated three times for a total of 4 washes.

100µl of E-Selectin TMB substrate solution was pipetted to each well.

The plate was covered with the adhesive strip and incubated for 20-30 minutes at room temperature.

100 µl of stop solution was pipetted into each well.

The optical density of each well was read within 30 minutes, using a microplate reader set to 450 nm subtracting the blank well absorbance from all other values.

2.3.3.4c Performance characteristics of the assay

The inter-assay coefficient of variation of 3.9-7.8 % and an intra-assay coefficient of variation of 4.2-4.9 %.

2.3.4 Quantification of cytokines

Cytokine determination was carried out using Luminex technology in the Bio-plex Protein Array System marketed by Bio-Rad.

2.3.4a. Materials

Bio-Plex® Human 27-plex Multi-Cytokine Standard

Bio-Plex® Human 27-Plex Multi-Cytokine Beads

Bio-Plex® Human 27-plex Multi-Cytokine, Biotin

Bio-Plex® Streptavidin-Phycoerythrin

Bio-Plex® Cytokine Assay Buffer

Bio-Plex® Stop Solution

Bio-Plex® 96-well Filter Plate

2.3.4b. Reagent Preparation

Human 27-plex Multi-Cytokine Standard was resuspended in 1ml of serum standard diluent (SSD). It was vortexed on medium speed for 15 seconds and placed on ice for 5 minutes. This was standard A which was serially diluted (1:4) as shown in Figure 2,2. Bio-Plex® Streptavidin-Phycoerythrin was diluted 1:12.5 in Bio-Plex® Cytokine Assay Buffer using the mixing vial provided - 200µL in 2.6 ml.

2.3.4c. Assay Procedure

25µl of Bio-Plex® Cytokine Assay Buffer was pipetted into each well, vortexed, and a vacuum was applied to the bottom of plate. The bottom of plate was blotted on clean paper towel.

25µl of SSD + 15µL sample were pipetted into each well and the plate incubated at room temperature on a plate shaker for 20 minutes.

The Bio-Plex® Human 27-plex Multi-Cytokine Beads were vortexed at high speed for 15 sec.

25µl of bead solution was pipetted into each well. A plate cover was placed upon the plate and the plate incubated for 2 hours in the dark at room temperature on a plate shaker.

A vacuum was applied to the bottom of the filter plate. 50µl of Bio-Plex® Cytokine Assay Buffer was pipetted into each well and vacuum extracted. This wash step was repeated twice to make a total of 3 washes. The bottom of plate was blotted onto a clean paper towel following the final wash.

75µl of Bio-Plex® Cytokine Assay Buffer was pipetted into each well. A plate cover was applied and the plate was vortexed at low speed on a plate shaker.

25µl Bio-Plex® Human 27-plex Multi-Cytokine biotin was pipetted into each well. A plate cover was applied and the plate vortexed at low speed. It was then incubated for 1.5 hour in the dark at room temperature on a plate shaker.

A vacuum was applied to the bottom of the filter plate. 50µl of Bio-Plex® Cytokine Assay Buffer was pipetted into each well and vacuum extracted. This wash step was repeated twice to make a total of 3 washes. The bottom of plate was blotted onto a clean paper towel following the final wash.

25µl of diluted Bio-Plex® Streptavidin-Phycoerythrin was pipetted into each well. A plate cover was applied and the plate vortexed at low speed. It was then incubated for 30 minutes in the dark at room temperature on a plate shaker.

25µl of Bio-Plex® Stop Solution was pipetted into each well, the plate vortexed gently on a plate shaker and incubated for 5 minutes at room temperature in the dark.

A vacuum was applied to the bottom of the filter plate. 50µl of Bio-Plex® Cytokine Assay Buffer was pipetted into each well and vacuum extracted. This wash step was repeated twice to make a total of 3 washes. The bottom of plate was blotted onto a clean paper towel following the final wash.

125µl of sheath fluid was pipetted into each well, the plate vortexed at low speed and placed on a plate shaker for 1 minute.

Results were read on a Luminex 100 System. The concentration of each cytokine in the sample was automatically calculated from a standard curve derived from serial dilutions of the cytokine standard using the Bio-Plex Manager software.

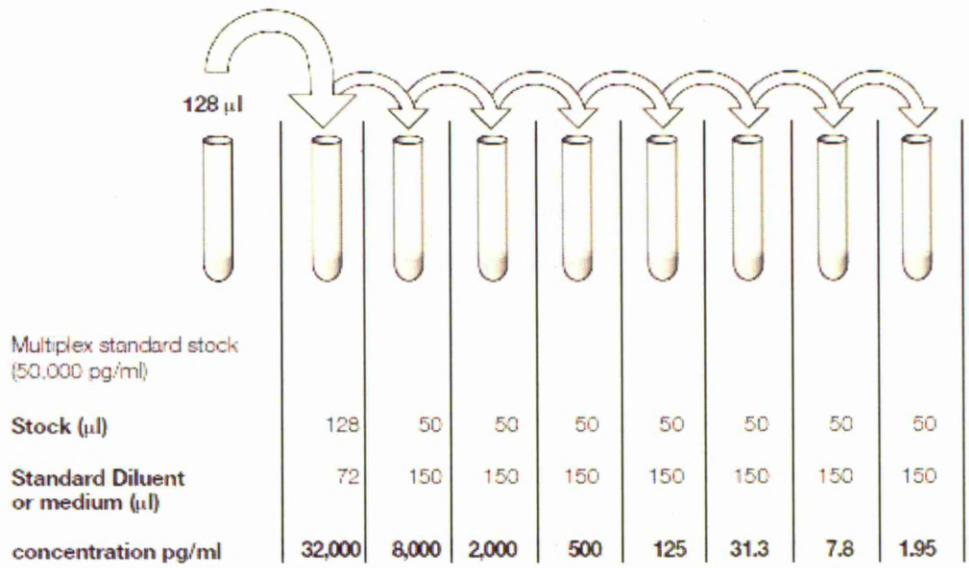

Figure 2.2 Serial dilution of Multiplex standard for standard curve determination

2.3.5. Quantification of Nitric Oxide Metabolites

Nitric oxide metabolite concentrations were measured by the Griess reaction using a commercially produced, 96 well plate, enzyme reduction assay marketed by R&D Systems Minneapolis, Minnesota, USA. Samples were 10,000 molecular weight filtered using 10,000 molecular weight cut-off filters. Samples and Controls were diluted 1:2 in assay buffer before being assayed (10 µl sample + 10 µl assay buffer) and were assayed in duplicate.

2.3.5a Materials

Reaction Diluent: 30 mls of Reaction Diluent Concentrate was diluted with 300 mls of distilled water to prepare 300 mls of Reaction Diluent to make a 10x solution.

Nitrate Reductase

Reconstitution - Nitrate Reductase was reconstituted with 1.0 ml of Nitrate Reductase Storage Diluent. The solution was vortexed vigorously and allowed to sit for 15 minutes at room temperature. This step was repeated and the solution then used immediately.

Dilution - Immediately before use the Nitrate Reductase was diluted using the following equation:

A. Nitrate Reductase (µl) = (number of wells required + 2) x 5 µl.

B. Reaction Diluent (µl) = volume from step A x 4.

C. Volumes from steps A and B were added to a clean test tube and vortexed.

D. The test tube was placed on ice and use within 15 minutes of dilution.

Nicotinamide adenine dinucleotide. (NADH) Reagent – Reconstituted with 5.0 mls of distilled water. The NADH was allowed to sit for 3 minutes and was gently agitated prior to use.

Nitrite and Nitrate Standard - 900 µl of Reaction Diluent was pipetted into the 200 µmol/l tube. 500 µl of Reaction Diluent was pipetted into the remaining tubes. Using the appropriate 2000 µl mol/l standard stock a dilution series was produced as shown in figure 2.3. The tubes were mixed thoroughly and pipette tips changed between each transfer. The 200 µmol/l standard served as the high standard and the Reaction Diluent served as the blank (0µmol/l).

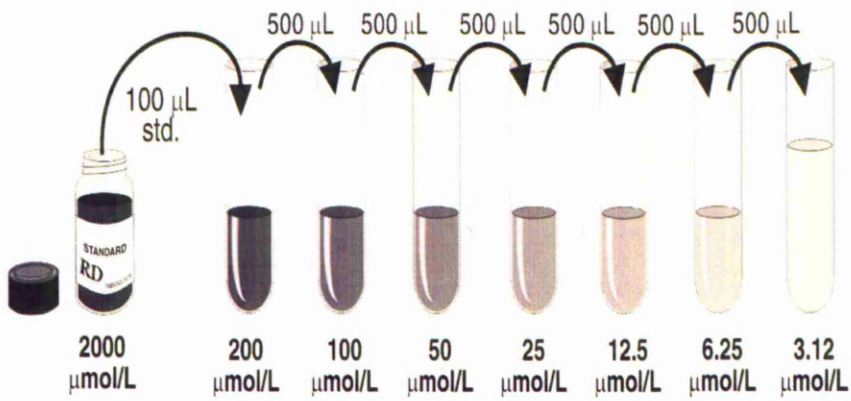

Figure 2.3 Serial dilution of Nitrite or Nitrate Standard for standard curve determination

2.3.5b Method

Nitrite Assay

50µl of Reaction Diluent was pipetted into the blank wells.

50µl of Nitrite Standard or sample was pipetted into the remaining wells.

50µl of Reaction Diluent was pipetted into all wells.

50µl of Griess Reagent I was pipetted into all wells.

50 µl of Griess Reagent II was pipetted to all wells.

The plate was incubated for 10 minutes at room temperature and the optical density of each well was read using a microplate reader set at 540 nm.

Nitrate Reduction Assay

50 µl of Reaction Diluent was pipetted to the Blank wells.

50 µl of Nitrate Standard or sample was pipetted into the remaining wells.

25 µl of NADH was pipetted into all wells.

25 µl of diluted Nitrate Reductase was pipetted into all wells.

The plate was mixed well and incubated for 30 minutes at 37° C.

50 µl of Griess Reagent I was pipetted into all wells.

50 µl of Griess Reagent II was pipetted into all wells.

The plate was incubated for 10 minutes at room temperature.

The optical density of each well was red using a microplate reader set at 540 nm

Calculation of Results

A standard curve was constructed from the standard values using commercially available software and sample concentrations were obtained from this standard curve. The concentration of a sample was taken from the mean of the two wells. The Nitrite assay measures the concentration of endogenous nitrite present in the sample. The nitrate assay measures the total nitrite by converting nitrate to nitrite. To determine the nitrate concentration in the sample, the endogenous nitrite concentration measured from the Nitrite Assay Procedure was subtracted from the converted nitrite concentration measured in this procedure.

2.3.5c Performance characteristics of the assay

The inter-assay coefficient of variation of 3.4 -4.6% and an intra-assay coefficient of variation of 1.6-2.5%.

2.3.6. Quantification of NT ProBNP

Concentrations of plasma NT ProBNP were measured using commercially produced ELISAs marketed by Biomedica Gruppe, Austria. Full methodology is described in chapter 7.

2.3.7. Quantification of Cardiac Troponin I and Cardiac Troponin T

cTnI and cTnT were measured by an automated Troponin I and T STAT (Short Turn Around Time) assay, using Elecsys 10:10 apparatus, Roche Diagnostics GmbH, Mannheim. This involves an Electro-Chemical-Luminescence ImmunoAssay (ECLIA).

2.3.8. Quantification of Bacterial Load and viral detection

Nucleic acid extraction was performed at the Meningococcal Reference Unit (MRU) by the automated Qiagen MDX system (Roche Applied Science, Indianapolis, IN) using robotics, precision pipetters, and silica matrix to purify RNA. The samples were dissolved and simultaneously stabilised by incubation with a buffer containing denaturing agents and proteinase K. Several washing steps remove the unbound substances leaving the nucleic acids bound to the surface of the silica matrix. The purified nucleic acids were then eluted with 100 µL elution buffer. PCR detection of meningococcal, pneumococcal, *Haemophilus influenzae* type b, adenovirus, enterovirus, influenza A and B, cytomegalovirus and paraecho virus, was performed on the extracted samples. Meningococcal DNA was quantified to enable determination of bacterial load. Meningococcal DNA detection and quantification was performed on all samples using the Taqman PCR on the ABI PRISM 7500 Sequence Detection System (Perkins-Elmer Applied Biosystems 7500 automated PCR platform, Norwalk, Connecticut) using a fluorescence-based closed tube system. Quantification of bacterial load was calculated from the cycle threshold values.

Detection of human herpesviruses 6 and 7 rubella, measles and parvovirus B19 was carried out at the Department of Virology, University College Hospital, London by PCR.

2.3. Microcirculation visualisation

Sublingual microcirculatory visualisation was carried out using SDF imaging. The SDF device used to obtain images was the Microscan™. (Fig 2.1) The device was linked to a computer via a Canopus™ ADVC 110 device which converts analogue video to digital capturing from a FireWire port. The WinDV™ programme, a Windows™ application for capturing videos from digital video device into Audio Video Interleave files, was used to capture the images. This enabled real time visualisation of the sublingual microcirculation on the computer screen. The images were stored anonymously onto Digital Video Discs (DVD). Due to the level of co-operation needed for image attainment only children with MCD who required ventilation were recruited for microcirculatory visualisation. Microcirculatory image acquisition was carried out within an hour of admission to PICU then at 6, 12 and 24 hours post admission and 24 hourly thereafter, until extubation. Whenever OPS images were being obtained, the pH, lactate, haematocrit, systolic blood pressure (SBP), diastolic blood pressure (DBP), MAP, CVP, inotropic support, ventilatory support and amount and type of sedation or other medications being administered were recorded. The operating procedure for microcirculatory image acquisition was as follows:

1. The dentition of child was examined to ensure no teeth were loose.
2. Secretions were removed from the surface of the sublingual mucosa with a suction catheter or gauze.
3. A sterile disposable cap was placed on the Microscan™ probe.
4. The probe was positioned on the sublingual mucosal surface.

5. The probe was manoeuvred until the microcirculation came into view.
6. The image was focused
7. Up to 5 video clips, of 20 seconds each, were recorded. It was ensured that both sides of the tongue were visualised.
8. The images were immediately saved to DVD and anonymised.
9. If the child, the child's parents or nursing staff became distressed by the microcirculatory image acquisition the procedure was abandoned. This did not happen at any point.

The adjustments to this methodology for the control groups of children are described in chapter 4.

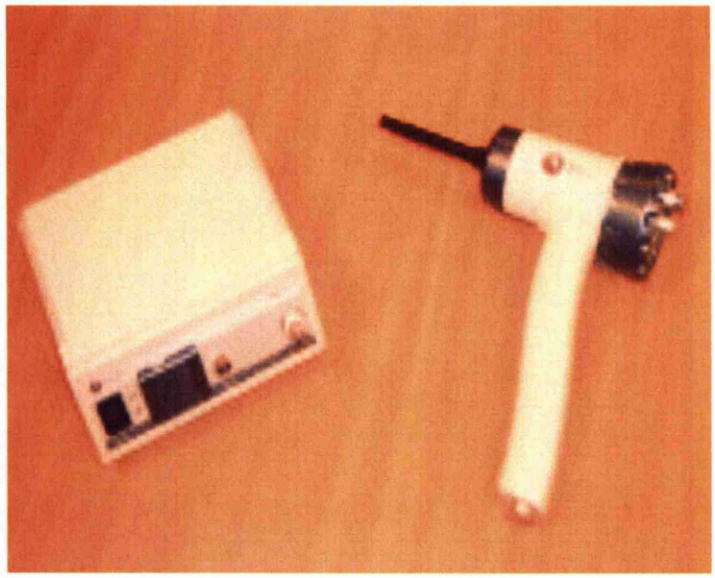

Figure 2.4. The Microscan – own image

2.4. Echocardiography

Transthoracic echocardiographic examination took place with the patient in the supine position or in a left lateral semi-recumbency position. All studies were carried out by the Research Fellow using a GE™ (General Electrical) Vivid 7 Echocardiography machine within 30 minutes of microcirculatory visualisation. An electrocardiogram (ECG) tracing was recorded simultaneously with the echocardiogram. Standard parasternal, apical, and subcostal views were used to detect any cardiac abnormalities in the patients prior to obtaining functional studies. Transducer frequency was 3, 5 or7 MHz depending on the size of the patient. At least three cardiac cycles were recorded for analysis for all measurements.

2.5.1. Systolic function

M-mode echocardiography was performed from the parasternal long axis view. On the M-mode echocardiography, the left ventricular (LV) fractional shortening (FS) was calculated from the LV end diastolic volume (LVEDV) and the LV end systolic volume (LVESV). The FS is 100 X (LVEDV-LVESV)/LVEDV

2.5.2. Diastolic function

Left ventricular diastolic function was estimated from the mitral inflow signal obtained by Doppler echocardiography. Transmitral flow velocity patterns were recorded from the apical 4-chamber view, with the pulsed doppler sample volume being positioned between the tips of the mitral valve leaflets. The early peak flow velocity (E) and atrial peak flow velocity (A) were measured and the E/A ratio calculated.

Tissue Doppler imaging (TDI) was obtained from an apical 4-chamber view to obtain longitudinal annular velocities at the lateral mitral wall annulus, adjacent to the atrioventricular valve hinge point. The maximal velocities of the E, A and S waves were recorded as was the E/Ea ratio. The E/Ea ratio was determined by dividing the peak E velocity from TDI imaging by the peak E wave measured by pulsed doppler readings of transmitral flow velocity patterns.

2.5.3. Global function

The Tei index, defined as the sum of isovolumic contraction and relaxation times divided by LV ejection time, was calculated via pulsed wave doppler and TDI for assessment of global systolic and diastolic left ventricular function.

2.6 Statistical Methods

Parametric tests were used if data followed a normal distribution when plotted as a histogram. Where data did not follow a normal distribution when plotted as a histogram, non-parametric tests were used. Standard statistical tests were used to calculate descriptive results of continuous data which were expressed as mean and standard deviation or median, interquartile range and range. Mann-Whitney U test or the t-test was used to determine rank, and Spearman's correlation coefficient was used for correlations. A p value of less than 0.05 was considered significant. The Bonferroni correction was not utilised for correction of multiple testing on the advice of statistical support. Receiver operator characteristic curves were used to assess diagnostic test performance characteristics. Multiple

logistic regression was used to account for confounding variables. Statistical analysis was performed using Statistical Package for Social Sciences (SPSS) for Windows, version 14.0, R (www.r-project.org), Excel with Analyse-it and Stats Direct software.

Longitudinal data analysis was performed by Gerwyn Green and Peter Diggle at the University of Lancaster. A joint model is postulated for a microcirculatory variable and another variable associating the two procedures via a correlated residual error structure using 'R' (www.r-project.org). As missing data was at random, the missingness can be ignored in the formulation of the likelihood.

A summary of which participants were included in each of the different studies is in Table 2.4

	MCD ventilated	MCD non ventilated	Presumed Viral	Control (blood only)	Cardiac control	Awake control	Anaesthetised control	Total
apter 3. gnostic efficacy of vated Partial omboplastin Time TT) waveform and calcitonin analysis in diatric meningococcal sis	15	9	12	20	0	0	0	56
apter 4. microcirculation in mal children using e Stream Dark Field ging	0	0	0	0	0	20	20	40
apter 5. Microcirculation in ningococcal Disease	20	13	10	23	10	20	20	116
apter 6. oactive mediators and microcirculation in ningococcal disease	20	13	10	23	0	0	0	66
apter 7. diac function in ningococcal disease	20 (19 with longitudinal echocardiograohy)	13	10	23	0	0	0	66

Table 2.4. Details of included participants in each study. Due to amount of blood sample left from certain children after analysis or the method of sample collection or due to technical difficulties, not all of the children that were recruited are included in each study.

Chapter 3

Diagnostic efficacy of Activated Partial Thromboplastin Time (aPTT) waveform and Procalcitonin analysis in paediatric meningococcal sepsis

3.1 Introduction

Severe sepsis is a major cause of childhood morbidity and mortality and accounts for more than 10% of deaths in children aged 4 years or younger in the UK (Bryce, Boschi-Pinto et al. 2005; Hart and Thomson 2006). Meningococcal septicaemia is a rapidly progressive life-threatening infection and remains the most common cause of infection-related deaths in children (Heyderman, Ben-Shlomo et al. 2004). Early recognition and appropriate antibiotic treatment can significantly reduce the morbidity and mortality associated with MCD but diagnosis can be difficult in its early stages. One of the characteristic signs of MCD is a spreading petechial or non-blanching rash but 15% of cases can present with a blanching, maculopapular rash (Marzouk, Thomson et al. 1991). Paediatricians are often concerned that children who present with a non-blanching rash may have MCD, although 90% do not (Wells, Smith et al. 2001; Klinkhammer and Colletti 2008). The relatively well child who presents with fever and a rash can therefore be a diagnostic dilemma for the clinician. These children may be commenced on antibiotic therapy pending the definitive confirmation of MCD by blood culture or PCR. Biomarkers of sepsis, such as PCT, could be useful in this context, and PCT has been found to be sensitive and specific for MCD in children presenting with a fever and a rash (Carrol, Newland et al. 2002; Carrol, Newland et al. 2005). However this test is expensive and not widely available in the UK.

Over the past decade, there has been increasing interest in the biphasic waveform (BPW) abnormality of the aPTT assay as an early marker of sepsis and DIC in adults (Downey, Kazmi et al. 1997; Downey, Kazmi et al. 1998; Fernandes and Giles 2003). The aPTT is a routinely performed test

of intrinsic coagulation and its waveform is the optical profile generated from changes in light transmittance during the process of clot formation (Downey, Kazmi et al. 1997). The aPTT BPW, caused by immediate falls in light transmittance upon plasma recalcification, has been shown to be a sensitive indicator of sepsis and DIC in several studies in adults (Smith, Charles et al. 2004; Chopin, Floccard et al. 2006; Matsumoto, Wada et al. 2006; Hussain, Hodson et al. 2008; Mair, Dunhill et al. 2008; Zakariah, Cozzi et al. 2008). Its diagnostic utility is independent of the aPTT clot time and the mechanism is mediated by complexes between CRP and very low density lipoprotein (VLDL) (Toh, Samis et al. 2002) induced by calcium within the aPTT reagent. These macroscopic complexes increase plasma turbidity to alter light transmittance when measured on the automated coagulation analyser, the MDA II. The aPTT BPW has been shown to be more accurate than either of its components; i.e. CRP and VLDL, for identifying adult patients with severe sepsis and septic shock (Chopin, Floccard et al. 2006).

Although PCT has been studied in children and neonates (Gendrel, Assicot et al. 1996; Carrol, Newland et al. 2002; Van der Kaay, De Kleijn et al. 2002; Carrol, Newland et al. 2005) the aPTT waveform has not. Severe sepsis differs markedly between children and adults (Carcillo and Fields 2002; Dellinger, Levy et al. 2008). Many adults have underlying co-morbidities and there is a significantly higher mortality in adult sepsis (Carcillo and Fields 2002; Levy, Fink et al. 2003; Watson, Carcillo et al. 2003; Dombrovskiy, Martin et al. 2007). The aim of this study is to determine whether an abnormal aPTT waveform is present in children with MCD and whether aPTT waveform analysis can distinguish children with presumed viral illnesses from those with MCD.

3.2 **Subjects and Methods**

Patient recruitment, data collection, and blood sampling were carried out as detailed in Chapter 2. The aPTT waveform analysis and PCT were prospectively evaluated in all patients following informed consent. Clinicians performing the daily clinical assessment were blinded to the results of PCT and aPTT waveform analysis. Laboratory staff performing PCT and aPTT waveform analyses were blinded to the clinical information. Admission levels of PC, AT III, white cell count (WCC), platelet count, lactate and CRP were also determined. Analysis of the aPTT waveform, PC and AT III were possible whenever a coagulation specimen was taken for clinical purposes as it was retrieved from the Haematology laboratory at AH. However, PCT samples were only taken on admission and at 6, 12, 24 and 72 hours post admission.

3.2.1 aPTT waveform and PCT analysis

For aPTT waveform analysis, PC and AT III estimation, plasma was derived from blood collected in 0.105 M trisodium citrate at a ratio of 1 part anticoagulant to 9 parts whole blood, which was separated within 30 minutes and the plasma frozen at -70°C until analysed. The aPTT, including waveform analysis, was determined on the automated MDA II (Trinity Biotech, Ireland) analyzer using Platelin LS, as described in detail elsewhere (Downey, Kazmi et al. 1997; Downey, Kazmi et al. 1998). The MDA II uses a photo-optical detection system and quantifies changes in light transmittance at 580nm following plasma recalcification. Normal and biphasic aPTT waveforms are illustrated in Figure 1. To quantitate the waveform, light transmittance at time 0 is set at 100% and the value recorded 18 seconds later (TL18). This is then taken as the quantitative

index of the abnormality, as previously described (Toh, Ticknor et al. 2003). PC and AT III were quantified using chromogenic assays (bioMérieux, France) on the MDA II.

PCT was measured in plasma using an automated immunofluorescent assay using the BRAHMS PCT sensitive KRYPTOR kit designed for the BRAHMS KRYPTOR machine was utilised, according to the manufacturer's instructions. The intra-assay coefficient of variation of the assay was <5% for values over 0.3 ng/ml and 10% for those around 0.2ng/ml.

3.2.2 Full blood count and CRP analysis

Full blood count and CRP analysis was performed as part of routine management. Whole blood was taken into EDTA for full blood count measurements on the Sysmex SE 9500 analyser (Global Medical Instrumentation Inc., Minnesota, USA). Whole blood was taken into a lithium heparin bottle for CRP estimation and analysed on the automated Architect c8000 (Abbott Diagnostics, Illinois, USA) according to the manufacturer's instructions.

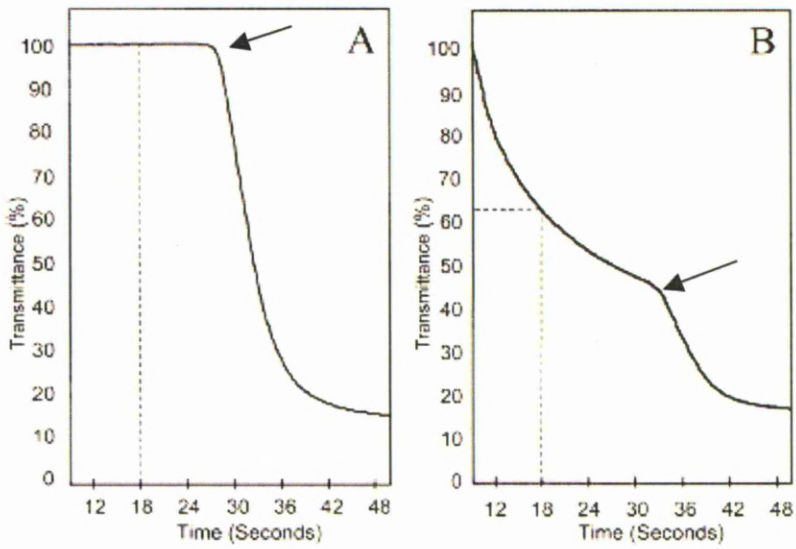

Figure 3.1. Normal and Biphasic waveform profiles

A – Normal aPTT waveform. The first phase is a plateau that shows 100% transmittance. Once clot forms, light transmittance abruptly decreases. The number of seconds until the drop in light transmittance is the aPTT clot-time in seconds.

B - Biphasic aPTT waveform. There is decreasing light transmittance prior to clot formation.

Dashed lines denote the transmittance level at 18 s (TL18) as the quantitative index (In (**A**), TL18=100 and in (**B**), TL18=63).

Clot times (in seconds) are signified by arrows.

3.2.3 Statistical analysis

Statistical differences between diagnostic groups were evaluated by Independent t-test or the Mann-Whitney U test depending on the distribution of data following evaluation of it from histograms. Correlations between the continuous variables were determined using Spearman's correlation coefficient. Values for sensitivity, specificity, positive and negative predictive values (PPV and NPV) of aPTT BPW presence, PCT and CRP concentration for the diagnosis of sepsis were derived from a two-by-two table. Receiver operator characteristic (ROC) plots were used to calculate the area under the curve (AUC) to compare the performance of aPTT waveform analysis, PCT and CRP in detecting MCD. Statistical analyses were carried out using SPSS for Windows (version 14.0), R (www.r-project.org) and StatsDirect software. Logistic regression analysis was performed with binary values for PICU admission to examine for relationships with variables that may contribute to predicting the need for PICU admission. This analysis was carried out by the Medical Statistics Department at the University of Lancaster.

3.3 Results

Fifty six children were included in the study. Thirty six children were admitted with fever and a rash and there were 20 healthy control children. The median age for the children with fever and rash was 2.16 years [IQR 0.89 – 4.53] and there were 13 males (33%). Twenty four of the 36 children (64%) had proven MCD whilst the other 12 (36%) had a presumed viral illness . Of the 24 children with MCD, 15 (71%) required PICU support. All the children survived but one required a limb amputation. The duration of hospital stay ranged from 1 to 30 days with a median of 5.5 days [IQR 3 to 8 days]. Characteristics of the participants are shown in Table 3.1. Normal

range determination on 20 healthy children attending for dental procedures under general anaesthetic showed a mean plasma TL18 value of 99.6% (99.0%-100.1%), with a mean coefficient of variation of 0.004%. The plasma PCT levels in these children were all found to be < 0.2 ng/ml.

3.3.1 Test performance in the diagnostic groups

There was a significant difference in aPTT TL18 between MCD patients and those with presumed viral illnesses ($p<0.001$) and controls ($p<0.0005$). There was no significant difference between children with a presumed viral illness and controls, $p = 0.14$ (Figure 3.2). There was also a significant difference in aPTT TL18 and PCT between children who required ventilation and those who did not ($p<0.0001$) as well as children with MCD presenting in septic shock and those who did not ($p<0.0001$). With regard to PC and ATIII, there was a significant difference between the MCD group and both the presumed viral illness and control groups ($p<0.05$). Whilst there was a significant difference in ATIII between those children with MCD who required ventilation and those who did not ($p<0.05$), no significance was seen with PC ($p=0.06$).

A significant inverse correlation was found between aPTT TL18 and PCT and length of PICU stay overall length of hospital stay, total duration of ventilation, time on inotropic support and resuscitation volume as well as CRP, PELOD, Maximum GMSPS and PRISM III scores. There was no correlation between TL18 and WCC and lactate. There was a positive correlation between PCT and lactate (Table 3.2).

	All MCD	MCD ventilated	MCD not ventilated	Presumed viral	Control
otal number	24	15	9	12	20
ge at dmission in ears [IQR]	2.98 [1.08 to 4.42]	2.16 [0.69 to 4.75]	3.96 [1.02 to 5.37]	1.58 [0.67 to 2.5]	2.16 [0.69 to 4.75]
ex nale %]	9 [39.1%]	5 [33.3%]	4 [44.4%]	3 [25.0%]	9 [45%]
laximum MSPS QR]	8 [3 to 12]	11 [9 to 12]	3 [2 to 3]	3 [2 to 3]	--
PTT TL18 (%) QR] ıormal range 98%)	93.8 [90.4 to 98.0]	91.9 [90.1 to 95.7]	98.0 [94.7 to 99.0]	99.4 [99.3 to 99.9]	99.7 [99.4 to 99.5]
CT (ng/ml) QR] ıormal range 5ng/ml)	61.8 [29.8 to 267.6]	169.5 [47.5 to 371.9	23.5 [5.8 to 41.2]	0.1 [0.2 to 0.4]	0.04 [0.02 to 0.06]
RP (mg/l) QR] ıormal range 4mg/l)	91 [70 to 174.6]	142.5 [107 to 200]	75.8 [50.8 to 122.4]	10.4 [4 to 37.1]	All <4
/CC ($x10^6$/l) QR] ıormal range .3-10.8 $x10^6$/l)	21.3 [13.6 to 26.2]	20.7 [5.8 to 25.3]	23.7 [15.8 to 30.2]	15.9 [9.9 to 19.8]	--
latelet count $x10^9$/l) QR] ıormal range 50 to 400 10^9/l)	226 [134 to 367]	182 [120 to 248]	322 [241 to 429]	301 [264 to 416]	--
rotein C %)[IQR] ıormal range 0-130%)	28.3 [21.4 to 41.3]	25.9 [19.1 to 29.9]	47.5 [29.5 to 67.5]	66.1 [50.0 to 76.8]	92.6 [84.1 to 104.7]
ntithrombin I (%)[IQR] ıormal range 0-130%)	55.8 [51.5 to 76.1]	51.6 [46.9 to 54.8]	91.9 [72.1 to 106.8]	101.8 [80.3 to 114.6]	109 [101.6 to 114.9]

Table 3.1. Characteristics of included participants (results expressed as median IQR])

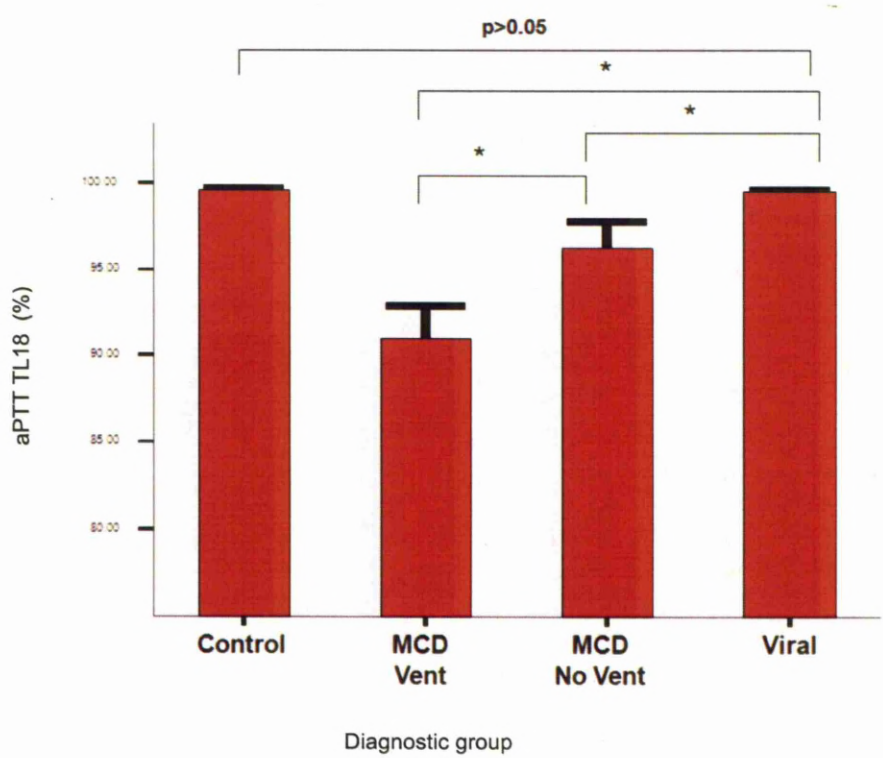

Figure 3.2. Bar chart representing differences in aPTT waveforms, as quantified by the light transmittance level at 18 seconds (TL18) between the diagnostic groups. * $p<0.05$

MCD vent = Children with MCD who required ventilation; MCD No Vent = Children with MCD who did not require ventilation.

Characteristics	Admission aPTT TL18		Admission PCT	
	R	P value	R	P value
Duration of Hospital Stay (days)	-0.61	<0.0001	0.83	<0.0001
Duration of PICU stay (days)	-0.65	<0.0001	0.8	<0.0001
Duration of ventilatory requirement (hours)	-0.66	<0.0001	0.8	<0.0001
Duration of inotropic requirement (hours)	-0.63	<0.0001	0.83	<0.0001
Resuscitation Volume (ml/kg)	-0.78	<0.0001	0.79	<0.0001
CRP	-0.7	< 0.0001	0.54	<0.005
White Cell Count	-0.05	0.75	0.12	0.95
Lactate	0.16	0.53	0.68	<0.005
Maximum GMSPS	-0.68	<0.0001	0.8	<0.0001
PRISM III	-0.73	<0.0001	0.73	<0.0001
PELOD	-0.68	<0.001	0.73	<0.0001

Table 3.2. Correlation between aPTT TL18 and PCT at admission and clinical and laboratory variables (r=Spearman Rank Correlation)

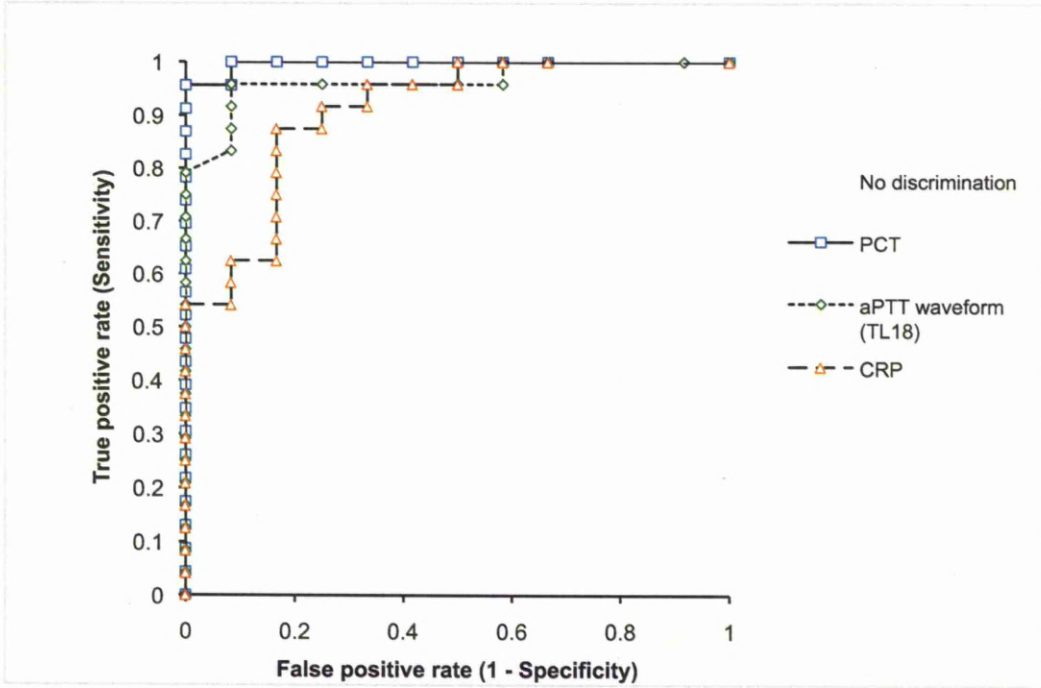

Figure 3.3. Receiver Operator Characteristic Curve for aPTT waveform TL18, PCT and CRP for detecting MCD at hospital admission.

AUC: PCT 0.99, TL18 0.96, CRP 0.91.

In order to determine the discriminatory value of aPTT waveform, PCT and CRP levels for detecting MCD, a ROC curve of admission values was constructed (Figure 3.3). The optimum cut-off value of TL18 selected for detection of invasive meningococcal infection was 99.2%. This is equivalent to a slope 1 level of -0.08, another quantitative measure of the aPTT BPW that has been reported by others. Using this value, a BPW was present in 23 out of the 36 patients (64%) at the time of admission. Twenty two patients with a diagnosis of MCD had a TL18 below 99.2%; representing 96% of the total number of children diagnosed with MCD. One child with a diagnosis of MCD had a TL18 above 99.2% (99.81%) and one had a TL18 of exactly 99.2%. Neither child required mechanical ventilation and their length of hospital stays were 5 and 3 days, respectively. Neither had received intramuscular benzyl penicillin or any other antibiotic prior to hospital admission and GMSPS were 2 and 3 respectively, indicating that they were at the less severe end of the MCD spectrum. Their PCT values were 32.6 ng/ml and 31.42 ng/ml respectively. One child who did not have a positive microbiological diagnosis had a BPW with a TL18 of 98.4%. This child's admission CRP was 115mg/L and PCT was 0.02 ng/ml. Blood and throat cultures and PCR for *Neisseria meningitidis, Haemophilus influenzae b* and *Streptococcus pneumoniae* were negative. This child received 5 days of intravenous antibiotics. However there was no eventual confirmed diagnosis. The diagnosis in this child was that of a self-limiting illness. Virology investigations were negative. Two children were positive for HHV7, both had normal aPTT waveforms, PCT and CRP.

The sensitivity and specificity for detecting MCD using aPTT TL18 were 0.91 and 0.92 respectively with a NPV of 0.87 (Table 3.3). Table 3.3 shows the comparative values for PCT and CRP. The cut-off value of PCT for a diagnosis of MCD using the ROC curve for this cohort was ≥ 11.5 ng/ml. Using this threshold value, 23 patients had an abnormal PCT concentration on admission. Of these, 22 patients (96%) had a diagnosis of MCD. This gave a sensitivity of 0.96 and specificity of 1, with a NPV of 0.92 (Table 3.3). If a cut-off value of <0.5ng/ml were used as in previous studies (Harbarth, Holeckova et al. 2001; Bugden, Coles et al. 2004), the result would be an increased sensitivity but reduced specificity (Table 3). Combining both the presence of a BPW and an abnormal PCT (defined as <0.5 ng/ml) minimally affected sensitivity and specificity.

	aPTT TL18 (cut off 99.2%)	PCT (cut off 11.5ng/ml)	PCT (cut off 0.5ng/ml)	CRP (cut off 10g/dl)	aPTT TL18 (cut off 99%) and PCT(cut off 0.5ng/ml)
AUC (95% CI)	0.96 (0.31 to 1)	0.99 (0.8 to 1)	--	0.91 (0.82 to 0.99)	--
Sensitivity (95% CI)	0.91 (0.72 to 0.99)	0.96 (0.78 to 0.99)	1 (0.86 to 1)	0.87 (0.66 to 0.97)	0.96 (0.85 to 0.99)
Specificity (95% CI)	0.92 (0.64 to 1)	1 (0.73 to 1)	0.83 (0.52 to 0.98)	0.85 (0.55 to 0.98)	0.79 (0.58 to 0.93)
Positive predictive value (95% CI)	1 (0.84 to 1)	1 (0.85 to 1)	0.92 (0.75 to 0.99)	0.91 (0.72 to 0.95)	0.9 (0.78 to 0.97)
Negative predictive value (95% CI)	0.87 (0.6 to 0.98)	0.92 (0.64 to 0.99)	1 (0.69 to 1.0)	0.79 (0.49 to 0.95)	0.9 (0.69 to 0.99)
Likelihood ratio for positive test (95% CI)	3 (1.6 to 7.09)	Infinity (3.94 to infinity)	6 (2.18 to 20.9)	5.25	4.6 (2.36 to 10.38)
Likelihood ratio for negative test (95% CI)	0	0.04 (0 to 0.2)	0 (0 to 0.17)	0.15	0.05 (0.01 to 0.18)

Table 3.3. Performance characteristics of variables for detecting meningococcal disease in children presenting with a fever and a non-blanching rash.

3.3.2 Probability of admission to PICU

Logistic regression analysis was undertaken to examine the relationship between PICU admission and aPTT TL18 with binary values for admission to PICU. Testing the null hypothesis of no association between the logit of requiring intensive care and aPTT TL18 gave a p-value of <0.01. Figure 3.4 shows a 95% confidence band for the probability of a child being admitted to PICU given their TL18 value. This shows that the lower the admission aPTT TL18 (the more severe the BPW) the higher the probability of needing intensive care support.

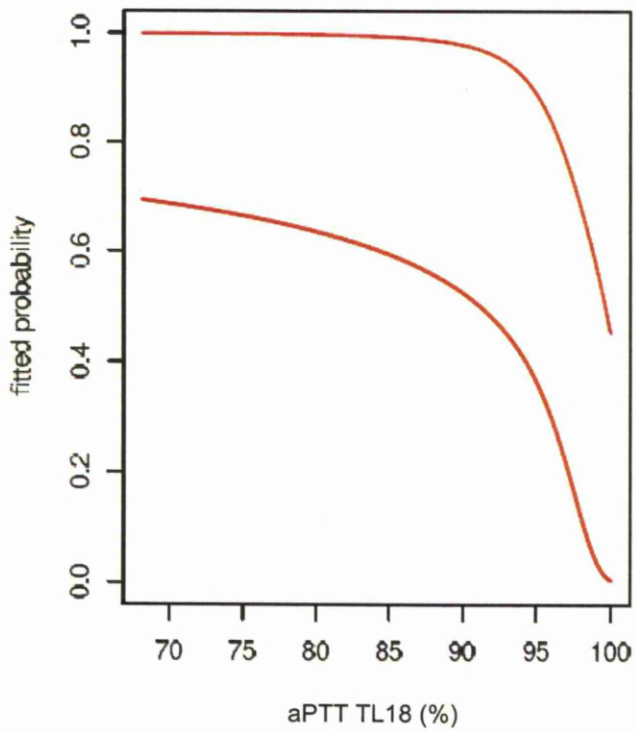

Figure 3.4. Pointwise 95% confidence band for the probability of a child requiring admission to PICU given their aPTT TL18 measurement.

3.3.3 Serial monitoring

Figure 3.5 shows the serial aPTT TL18 changes in a 2 year old girl who was admitted to PICU with severe MCD. Admission GMSPS was 12, PRISM III was 22 and PELOD was 23, indicating a severe disease process with a high probability of mortality. She required inotropic support and haemodialysis due to renal failure. Widespread purpura fulminans developed within 24 hours and it was evident that she would have limb and tissue loss in the event of survival. The aPTT waveform was abnormal on admission (TL18=96.3%) and this progressively decreased until day 5 (TL18=76.5%), whilst she remained in a critical state. After day 5, her ventilatory requirements began to fall and she was extubated on day 7. Improvement in the aPTT TL18 correlated with this progress. She required haemofiltration until day 13 and a left sided below knee amputation was carried out on day 14 due to dry gangrene. Following this, her clinical picture remained poor and her abnormal aPTT TL18s continued until day 20. At this point she had to return to theatre for tissue debridement and a further skin graft. Subsequently she improved and was discharged home after a total hospital stay of 30 days. Her aPTT TL18 levels normalised from day 23 onwards. Her PCT values at admission and 6, 12, 24 and 72 hours post admission are shown in Figure 3.5. Serial PC and AT values over the same time frame are shown in Figure 3.6.

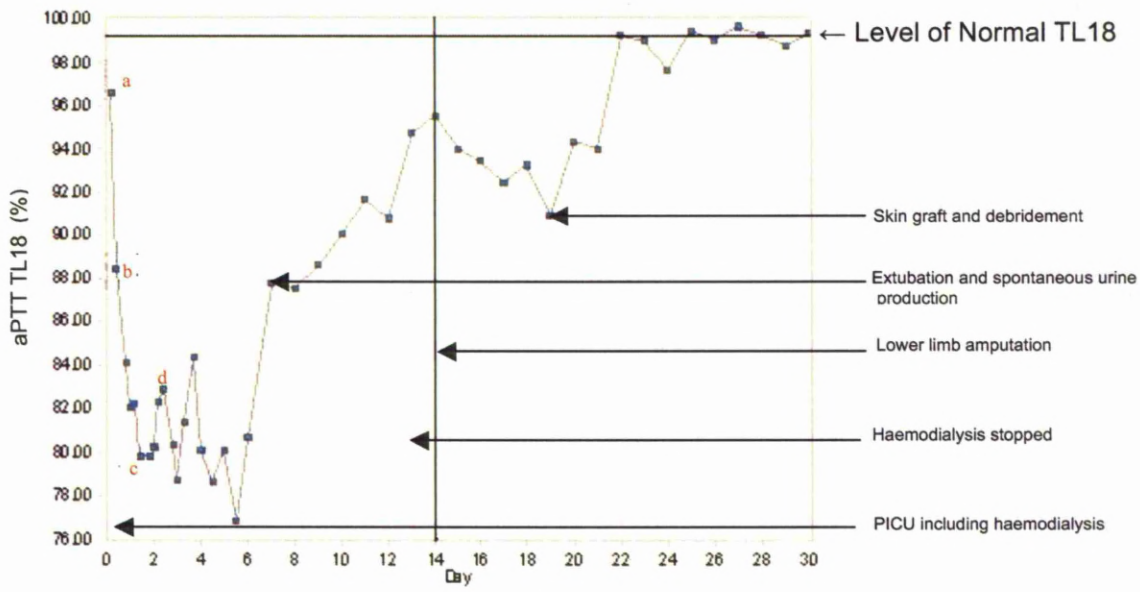

Figure 3.5. Serial aPTT waveform changes as quantified by light transmittance levels at 18 seconds (TL18) on a child with severe MCD who required a below knee amputation.

Procalcitonin values: a=254.8 ng/ml at admission, b=914.8 ng/ml at 12 hours, c=2584 ng/ml at 24 hours and d=985.3 ng/ml at 72 hours post admission.

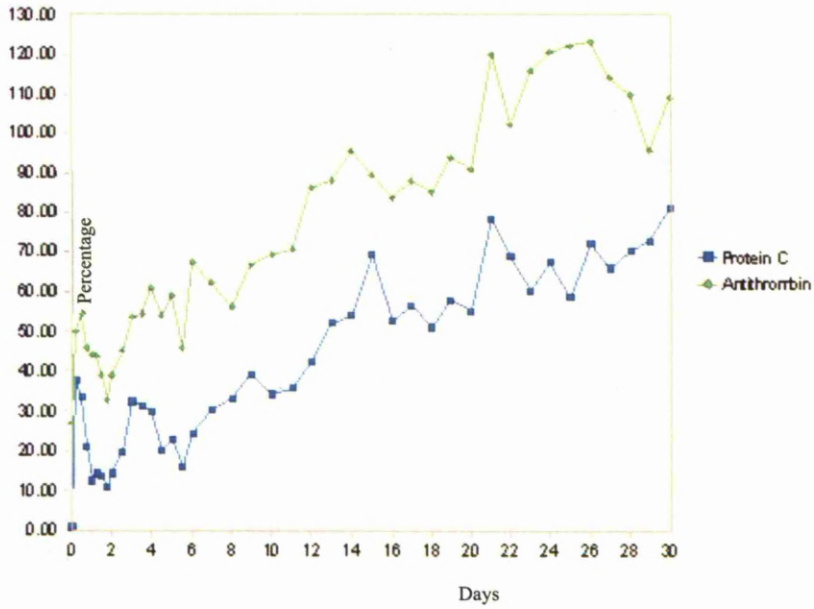

Figure 3.6. Serial levels of protein C (normal range 70-130%) and antithrombin III (normal range 80-130%) in a child with severe MCD who had a below knee amputation on day 14.

3.4 Discussion

This is the first study exploring aPTT waveform analysis in children with sepsis. We demonstrate that the aPTT waveform is abnormal in children with MCD, which is an example of serious bacterial sepsis. As has been shown in adults, aPTT waveform analysis could be a novel method for detecting sepsis in children. The presence of a biphasic aPTT waveform in the initial investigation of a child presenting with a fever and a spreading, non-blanching or petechial rash has a high sensitivity and specificity for the diagnosis of MCD at a level that is similar to PCT. Furthermore, the strong correlation between the extent of waveform abnormality and the likelihood of PICU admission indicates that the aPTT waveform analysis could be a useful adjunctive tool to identify children with MCD who are stable at admission but may deteriorate whilst on the ward and eventually require PICU support. This is in keeping with findings in adult studies (Smith, Charles et al. 2004; Hussain, Hodson et al. 2008; Mair, Dunhill et al. 2008), which have additionally highlighted the strong association of the BPW with mortality (Toh, Ticknor et al. 2003). We were unable to demonstrate this in children as there were fortunately no deaths in our study population.

In a disease with a rapidly progressive clinical course such as severe MCD (Thorburn and Baines 2002), it is important that diagnostic tests are not only accurate but also simple, rapid and inexpensive to perform. As waveform analysis is an adjunct to a standard test of coagulation, the aPTT test, it offers considerable practical advantage. Furthermore, studies in adult patients have demonstrated its ability to identify sepsis early in its clinical course. Zakariah *et al* reported that in 72% of patients, a BPW was present one day before or at the time of diagnosing sepsis (Zakariah, Cozzi et al. 2008) and Toh *et al* found that in 34% of 336 septic patients, the BPW

preceded diagnosis by 18 hours (Toh, Ticknor et al. 2003). As early detection followed by prompt treatment of sepsis can significantly improve outcome, this could be important. Implicit in the translational value of any laboratory marker in sepsis is the ability to monitor response to treatment. The degree of aPTT waveform abnormality appears to correlate closely with the clinical condition in Figure 3.5. Even after amputation, the presence of the abnormal waveform appeared to be a harbinger of the need for further clinical intervention. Subsequent return to theatre for debridement of the amputation stump ultimately led to clinical recovery and normalisation of the aPTT waveform. This is a single case illustration and use of the aPTT waveform for clinical monitoring requires further testing. The changes in TL18 in this child may reflect changes in the underlying molecular mechanism, which is a calcium-dependent complex between CRP and VLDL. This complex has been identified *in vivo* in patients with sepsis (Toh, Samis et al. 2002) and whilst its pathogenic relevance remains to be fully elucidated, there is evidence of its ability to significantly enhance thrombin pro-coagulant activity (Dennis, Downey et al. 2004). The BPW provides a better predictor of sepsis than CRP alone, confirming findings in adult patients (Toh, Ticknor et al. 2003; Chopin, Floccard et al. 2006).

In this study, we also reconfirm the value of PCT as a useful diagnostic marker in MCD (Carrol, Newland et al. 2002; Leclerc, Leteurtre et al. 2002; Carrol, Newland et al. 2005; Casado-Flores, Blanco-Quiros et al. 2006; Mills, Lala et al. 2006). PCT is not commonly used as a diagnostic test in the UK as it is expensive and requires purchase of an additional analyser. A combination of PCT and the aPTT waveform analysis has increased specificity for the identification of sepsis in critically ill adults (Zakariah, Cozzi et al. 2008). This was not demonstrated here, possibly due to the

sample size. A clear correlation between PCT changes and clinical events has yet to been demonstrated, although the mortality rate and multi-organ failure in adults on ICU has been shown to increase markedly when the PCT level increased day-to-day (Giamarellos-Bourboulis, Mega et al. 2002; Jensen, Heslet et al. 2006). Most studies have concentrated on admission PCT levels for detecting sepsis in cohorts with known morbidities (Uzzan, Cohen et al. 2006; Jensen, Lundgren et al. 2007). In some non-survivors, PCT levels may actually decrease as the disease worsens (Claeys, Vinken et al. 2002; Gibot, Cravoisy et al. 2005).

The very high negative predictive values of the aPTT BPW and PCT for MCD, mean that they could be useful in ruling out sepsis in children presenting with fever and a spreading petechial rash or mixed spreading petechial and blanching rash. These children are often given parenteral antibiotics until meningococcal infection can be excluded. A diagnostic test that could reliably exclude serious bacterial infection could reduce hospital admissions and the associated clinical as well as financial costs of unnecessary antibiotic use. The aPTT waveform analysis could also be of use within the community for early detection of infection. However practically this would be difficult in terms of blood collection and processing and children may well be referred to hospital anyway due to their symptoms.

Our study has a number of limitations. It included only a small number of children and those with MCD mostly required PICU intervention. Although we only studied children with MCD, it is an excellent paradigm of sepsis as it is a clearly defined disease entity caused by a single organism. The samples that were taken on admission to PICU may not be representative

of all admissions to the A&E department due to the different stages in the disease process at presentation. Before recommending aPTT waveform analysis as a screening tool studies of its relevance for sepsis detection in an A&E setting are required. Additionally, the aPTT waveform requires further study across the whole spectrum of childhood sepsis caused by other pathogens and alternative reasons for admission to PICU. Finally, whilst the aPTT waveform can be determined at no additional cost as part of the aPTT clot-time measurement, its availability requires the MDA II analyser.

3.5 Conclusion

This study supports the value of aPTT waveform analysis and PCT as a simple, rapid and robust diagnostic marker of meningococcal sepsis. The BPW test has translational potential to facilitate prompt diagnosis and allow real-time monitoring of the patient.

Chapter 4

The microcirculation in normal children using Side Stream Dark Field Imaging

4.1 Introduction

Clinicians have been unable to directly assess the microcirculation until relatively recently. It is now possible with Orthogonal polarisational spectral imaging (OPS) and Sidestream darkfield imaging (SDF) technology (Figure 4.1). OPS was the first to be invented and was produced by Cytometrics (Philadelphia, United States of America). The instrument was called the CYTOSCAN™. The same company patented the HEMOSCAN™ which again used OPS technology but also incorporated a complex algorithmic analysis of the images produced. This enabled this particular device to calculate systemic haemoglobin concentrations. The purpose was to estimate a full blood count without the removal of blood from a patient (Nadeau 2000). The Cytoscan II was also produced but production ceased in 2003 when the company was sold to Rheologics Incorporated (Pennsylvania, United States of America) who discontinued production of both instruments.

These devices had been validated previously, mainly in comparison with 'gold standard' devices such as intravital microscopy. They had also been used for the examination of the microcirculation in different structures such as the colon, pancreas and tumour surfaces in animals (Groner, Winkelman et al. 1999; Harris, Sinitsina et al. 2000; Biberthaler, Langer et al. 2001; Langer, Biberthaler et al. 2001; Langer, Harris et al. 2001; Harris, Sinitsina et al. 2002; Langer, Born et al. 2002; Pahernik, Harris et al. 2002; von Dobschuetz, Biberthaler et al. 2003; Heger M 2005). There were also validation studies in humans (Mathura, Vollebregt et al. 2001)

These earlier devices were followed by the development of the Microscan™ by Microvision Medical (Amsterdam, Holland). This instrument uses SDF technology and provides real-time video images of the microcirculation using a 5x objective giving a screen magnification of x 326 (Ince 2005). It uses light emitting diodes instead of polarised light at a wavelength of 530nm which is absorbed by red cells. A comparison of SDF and OPS, for the validation of SDF, showed that SDF is superior for visualising the microcirculation producing clear and easy to analyse images (Goedhart 2007).

4.1.1 Outcome measures from microcirculation images

Image attainment using OPS and SDF imaging gives a video recording of real time capillary and venular blood flow. For valid outcome measurements to be made from these recordings a robust process of image analysis must be developed. This process should be repeatable, easy to learn and carry out and quick to perform.

There are no fully automated computer software methods for analyzing the video images. Outcome measure methods have been developed and validated in adult studies by two independent groups. The group of De Backer, based in Brussels, developed a semi-quantitative analysis of OPS images. Three equidistant horizontal and three equidistant vertical lines were superimposed upon the moving image (De Backer, Creteur et al. 2002). The vascular density of the area of tissue being observed could then be calculated as vessels per millimetre by counting the number of vessels crossing the lines. Flow categories were also assigned to each vessel type and from this measurements of capillary density (CD), the percentage of perfused vessels (PPV) and perfused vessel density (PVD) were

calculated/derived. This method has is very time consuming and has an element of subjectivity in the assignment of flow categories.

Boerma and colleagues in Holland developed an alternative method of analysis, the Microvascular Flow Index (MFI) (Boerma, Mathura et al. 2005). This is a semi-quantitative analysis in which the video image is divided into four quadrants and assigned flow categories per vessel diameter for the majority of vessels in the video sequence. The MFI can be calculated quickly and it is a much faster analysis that the method of De Backer et al. However it does not take into account functional capillary density and so misses a large amount of information that can be obtained from microcirculatory images.

De Backer's group developed software (Microvision Analysis Software, Microvision Medical, Amsterdam, Netherlands) that attempts to produce a more quantitative analysis of OPS and SDF derived flow images. This software has been designed for stabilisation of the image, vessel size identification and blood flow velocity determination which is carried out by constructing space-time diagrams from the centreline intensity of vessels in subsequent video frames. It allows the user to derive duration, width and blood velocity of individual vessel segments, so creating a detailed report of vascular variables. However this software is not user friendly, is time consuming and still involves a significant amount of user manipulation of the images. As it is not a fully automated process error can be introduced and there is no 'normal' data that has been produced from its use.

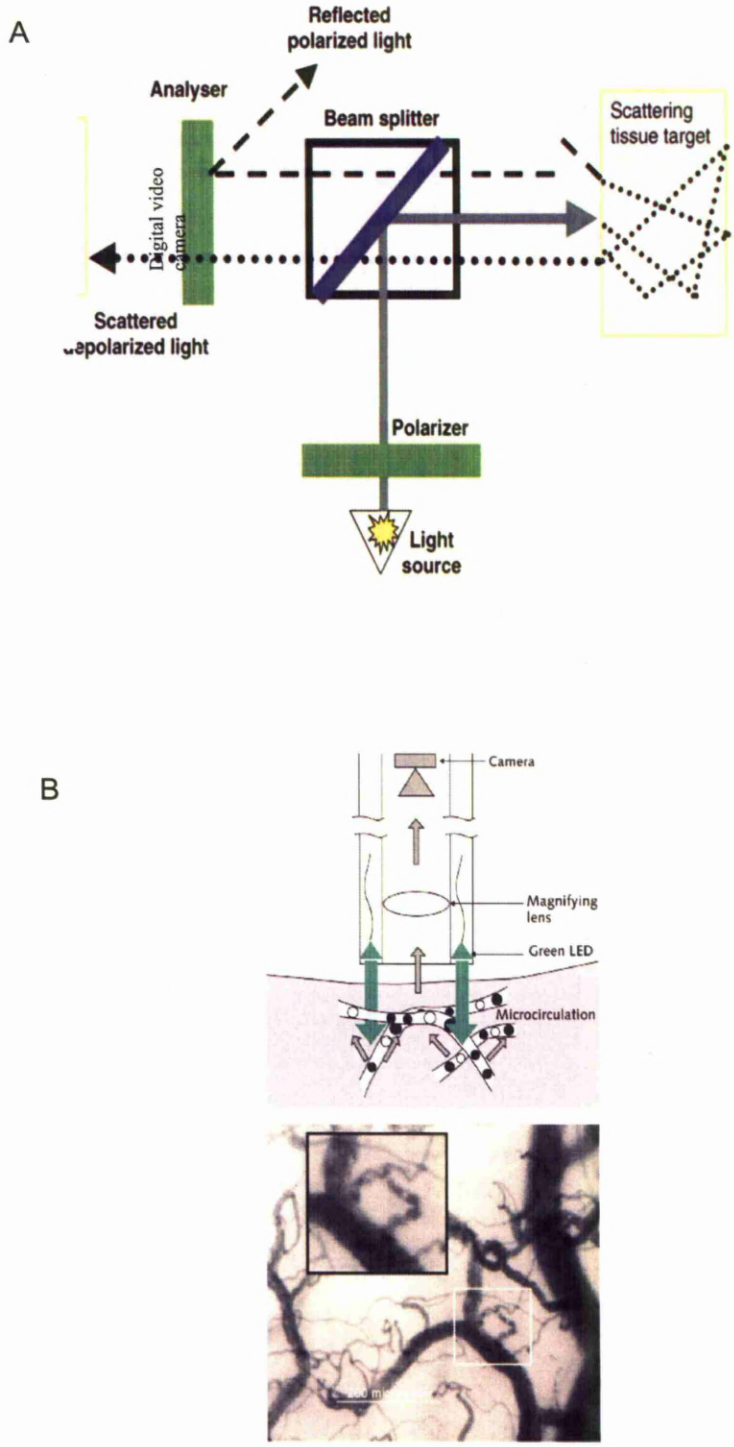

Figure 4.1. A; Schematic to illustrate OPS imaging. B; Schematic to illustrate SDF imaging

De Backer's group have also developed a heterogeneity score of microvascular blood flow (De Backer, Creteur et al. 2002). Five areas of sublingual tissue are visualised. Between the five areas, the coefficient of variation of blood flow is calculated as the standard deviation of the five values of blood flow divided by their mean value. A heterogeneity index (HI) has also been used by an American group led by Trzeciak (Trzeciak, Dellinger et al. 2007). Five images are taken at the same time point and the lowest site flow velocity score is subtracted from the highest site flow velocity score. This value is then divided by the mean of the flow velocity scores of all of the sublingual sites. The higher the value the more heterogeneous the blood flow is between the images.

Trzeciak's group was the first to incorporate all of the microvascular analysis methods in their study of septic adults. This led to a round table conference and a consensus statement advising that all of the methods described be used in the assessment of the microcirculation using OPS and SDF (De Backer, Hollenberg et al. 2007).

4.1.2 Histology and anatomy of the tongue

OPS and SDF imaging is undertaken by placing the probe sublingually. Although this is for convenience there are other reasons why this is appropriate. The tongue begins to form at approximately the same time as the palate and is mainly composed of skeletal muscle. The tongue extends past the posterior border of the mouth and travels into the oropharynx. The lingual artery, a branch of the external carotid artery, gives the blood supply to the tongue and the floor of the mouth. Blood supply to the tongue also comes from the tonsillar branch of the facial artery and the ascending

pharyngeal artery (Snell 2003; Alan Stevens 2004). The sublingual area shares its' embryological origin with the splachnic mucosa (Alan Stevens 2004). Splachnic hypoperfusion is known to be an early indicator of systemic hypoperfusion (Povoas, Weil et al. 2001). Additionally the sublingual region of the oral mucosa is very thin which is why it is an ideal place for OPS images to be taken.

One previous study has used OPS imaging in children with sepsis. No normal control data was reported in this study (Top, Ince et al.). There have been no reported studies using SDF in the assessment of microcirculatory flow in children. No data therefore exists regarding microcirculatory variables in a paediatric population. This chapter examines the use of SDF imaging in normal, healthy children and reports the microcirculatory outcome measures found.

4.2 Materials and Methods

4.2.1 Patients recruited

Two groups of children were eligible for inclusion in the study. The first group were children under the age of 6 yrs attending AH for routine surgery of a non-infective pathology, during a 12 month period. The second group were children over the age of 6 who were selected from a cohort of well children of colleagues from AH. All children had weight, blood pressure, heart rate, respiratory rate measured. Surface area was calculated from the weight as height was not always possible to measure (Sharkey, Boddy et al. 2001). Haematocrit was measured in anaesthetised patients on an arterial blood gas prior to SDF image acquisition.

4.2.2 Microcirculation visualisation

Microcirculatory real-time images were obtained in children under the age of 6 years once they had been anaesthetised. Children were anaesthetized using isoflurane, remifentanyl and propofol. Secretions were initially removed using gauze if necessary. The SDF images were obtained sublingually using the MicroScan™. The probe of the MicroScan™ was covered with a sterilized disposable cap to prevent direct contact between the instrument and the patient, and a different cap was used for each patient. The covered probe was placed under the tongue and manoeuvred until the microcirculation was visible. The MicroScan™ was then focused to give a clear image. In order to minimise the effect of pressure, once an adequate view of the microcirculation had been achieved the probe was advanced in the same area until the red cell flow was partially or completely occluded. The probe was then retracted from the mucosal surface until contact with the tissue was lost. The probe was then gently advanced to make contact with the mucosal surface, re-focused if necessary, and the

image recorded. Video output was visualized on a monitor and images stored as described in Chapter 2.

Two different investigators obtained the images on each anesthetised child. At least five areas of sublingual tissue were chosen for analysis by each investigator and a continuous image lasting for 15-20 seconds each was recorded. The images were taken over a 10-15 minute period prior to the child's surgery once a stable anaesthetic state was reached. The 10-15 minute time period was adopted so that any technical difficulties (for example excessive saliva) could be overcome without affecting the time frame for preparation for surgery.

The investigator explained the principles of obtaining the images and minimising the effect of pressure to the group of children aged over 6.
They were then allowed to hold the MicroScan™ themselves and obtain images. Again, at least five tissue areas were selected by the children themselves under the guidance of the investigator and a continuous image lasting for 20 seconds was recorded.

4.2.3 SDF image analysis

Video clips were coded and then analysed by observers blinded to the clinical condition of the child (whether they were anaesthetised or not). Each video clip was analysed by two observers independently, off line to determine the interobserver agreement. For the intraobserver agreement of image analysis, video clips were duplicated, recoded and again analysed off line. When the two observers had analysed all images, if there was disagreement the images were discussed between the observers to agree

a final consensus assessment of that particular image for use in statistical analysis.

The Microvision Analysis Software (MAS) software was used to stabilise the images prior to analysis. Where movement within the image was excessive and MAS could not stabilise the image, a shortened loop of video image was used for analysis without stabilisation. The MAS software was also used to analyse the size of vessels so that the correct vessel diameter was chosen for the calculation of capillary density and the assignment of flow categories.

CD, PPV and PVD were calculated by applying a Perspex sheet with three equidistant horizontal and three equidistant vertical lines superimposed upon it across the video sequence displayed on the computer screen (Figure 4.2). The three horizontal lines represented 1 mm of tissue surface each, the three vertical lines represented 0.7 mm each. Capillary density was calculated as the number of vessels less than 20 microns in diameter crossing these lines divided by the total length of the lines (5.1 mm). This gave the number of capillaries per millimetre of tissue. Flow categories were then assigned to each vessel type and defined as continuous, intermittent (this included flow that was stopping and starting and reversed blood flow), or absent for more than 50% of the video sequence. The PPV was calculated as the number of capillaries with continuous flow divided by the total number of capillaries per mm. The PVD was calculated by multiplying the CD by the PPV and gives a representation of total functional vessel density. The mean of all images was used for analysis.

The MFI was ascertained for each image by first dividing the image into 4 quadrants using MAS. Flow scores were assigned per quadrant for each vessel diameter (Figure 3.3). The vessel size cut-offs were: small, less than 25 microns; medium, 26 to 50 microns and large, 51 to 100 microns. The flow categories are 0 for no flow, 1 for intermittent flow, 2 for sluggish flow and 3 for continuous flow. The MFI is assigned by visualisation of each quadrant and assigning flow categories per vessel size for the majority of that group of vessels. The flow category assigned per vessel diameter is then totalled for the 4 quadrants and divided by the number of quadrants in which the vessel type is present. An MFI value can be determined for each vessel type and for the overall image with a score in the range 0-3.

The HI was calculated by subtracting the lowest site flow velocity score from the highest site flow velocity score of all of the images taken at the same time point. This value was divided by the mean flow velocity calculated from all of the images.

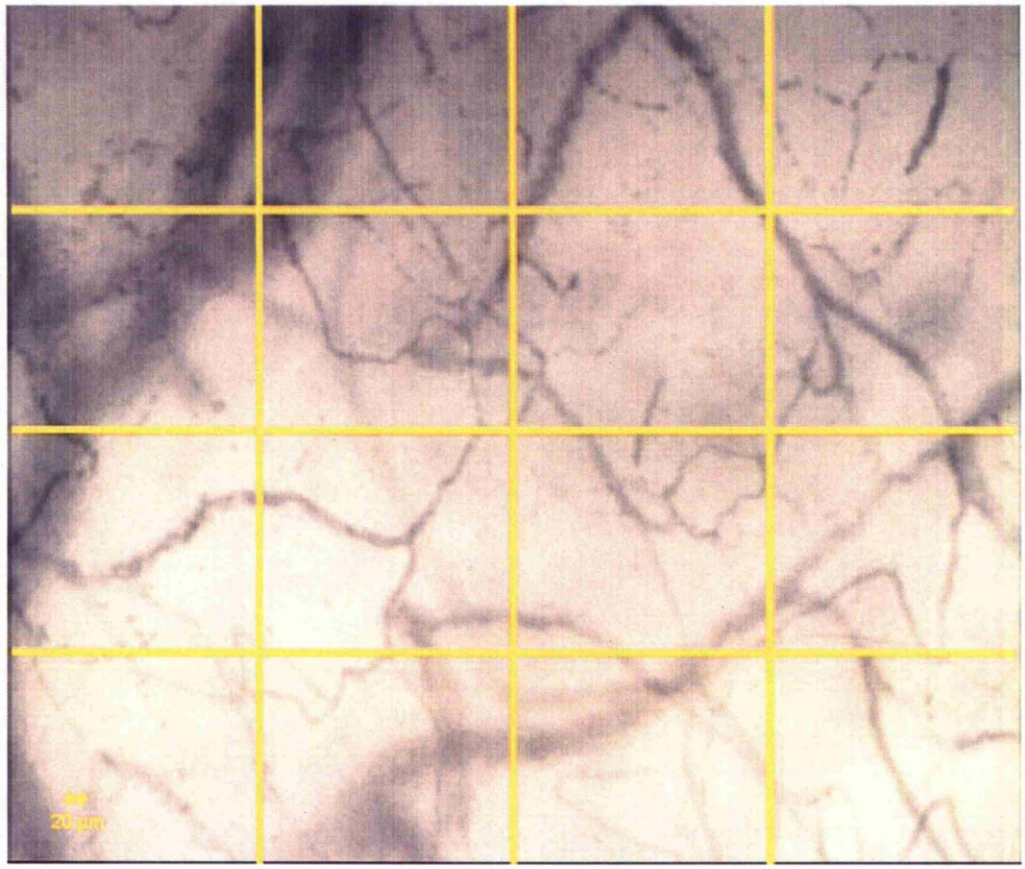

Figure 4.2. The superimposition of lines upon the SDF image to determine capillary density, proportion of perfused vessels and perfused vessel density in accordance with the scoring system by De Backer (De Backer, Creteur et al. 2002). Taken from How to evaluate the microcirculation: report of a round table conference. Crit Care. 2007;11(5):R101.

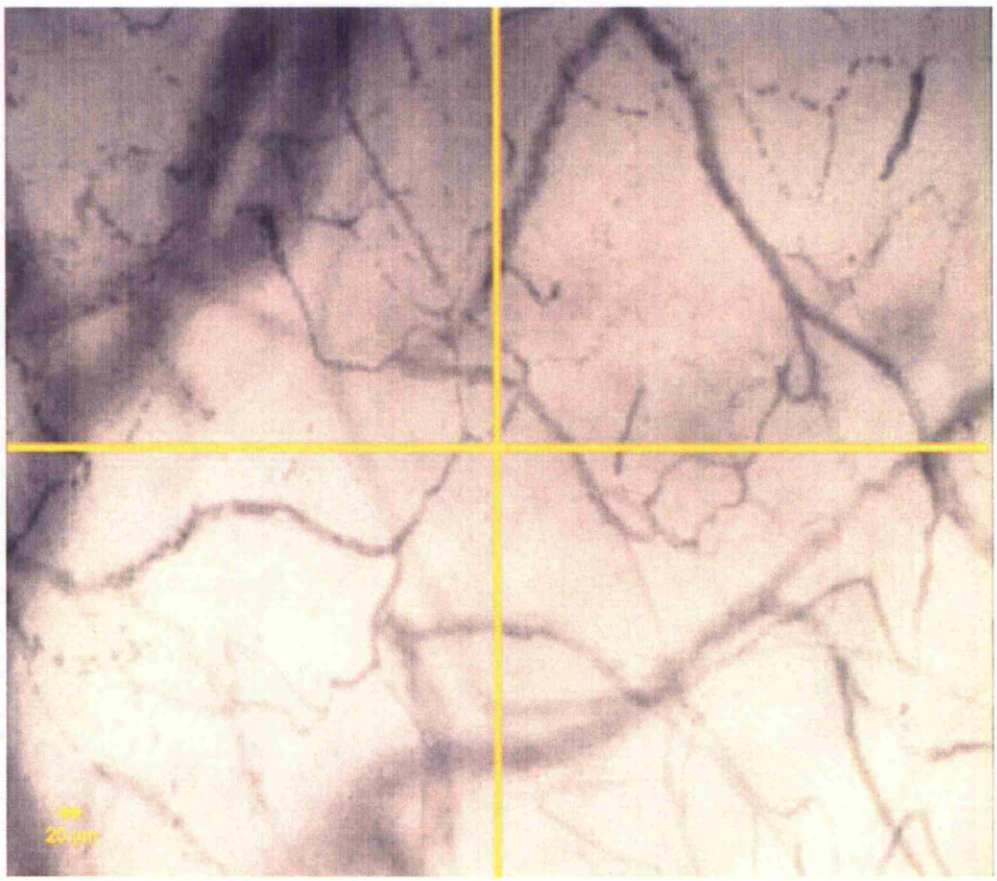

Figure 4.3. Quadrant division of an image to determine the Microvascular flow index (MFI) score in accordance with Boerma et al (Boerma, Mathura et al. 2005). Taken from: How to evaluate the microcirculation: report of a round table conference. Crit Care. 2007;11(5):R101.

4.2.4 Statistical analysis

Intra- and interobserver agreement was determined by Bland–Altman plots and the repeatability coefficient for continuous variables and by kappa (κ) cross tables for categorical variables. These analyses were performed for both image attainment (obtaining the video image) and image analysis (analysing the video image). Statistical analyses were performed using Analyse-It Software v.1.62 for Microsoft Excel (Analyse-It Software, Leeds, UK) and SPSS v. 14.0 (SPSS Inc., Chicago, IL, USA). Spearman's rank correlation coefficient, multiple linear regression and univariate analysis were used to investigate the relationship between explanatory and outcome variables.

4.3 Results

Forty children were studied, twenty anaesthetised children and twenty awake children. None of the awake children had any previous medical history and the anaesthetised children had no co-morbidity other than the condition for which they were requiring surgery. There were 10 males (50%) and 10 females (50%) in each group. Demographics for the groups are shown in Table 4.1. All of the children had normal blood pressures, heart rate and respiratory rate for their age. The anaesthetised children all had a normal haematocrit and oxygen saturation level at time of image acquisition.

The mean number of capillaries per millimetre of tissue was 5.59 capillaries for awake children (standard deviation 0.76) and 6.56 per mm of tissue for anaesthetised children (standard deviation 0.78). There was a significant difference between the two groups ($p<0.01$, mean difference 0.97 (CI -1.46 to -0.47)) Independent t-test (Figure 4.4).

Diagnosis	Age range in years	Median Age in years [IQR]	Median weight in kilograms [IQR]	Median Surface area in meters^2 [IQR]	Diagnoses in anaesthetised patients	Total
Awake	6.5 to 16	10.7 [5.8 to 15.6]	29.6 [19.6 to 39.6]	1.05 [0.7 to 1.8]		20
Anaesthetised	0.4 to 5.9	2.5 [0.75 to 4.5]	11.5 [3.2 to 19.8]	0.5 [0.2 to 0.8]	Spinal cord untethering	10
					Scaphocephaly repair	4
					Trigonocephaly repair	3
					Brachycephaly repair	3

Table 4.1. Demographic data for 40 control children used to determine normal microcirculatory values using SDF

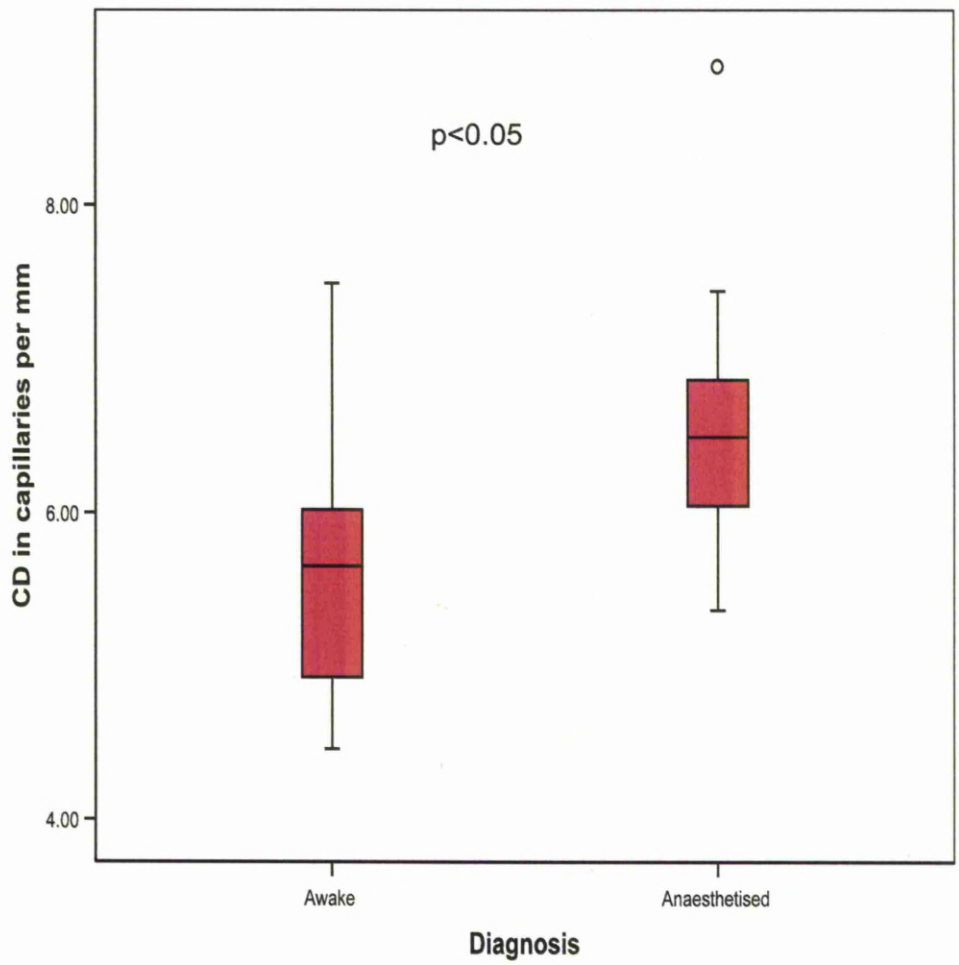

Figure 4.4. Box and whisker plot demonstrating the difference in capillary density between awake children and anaesthetised children.

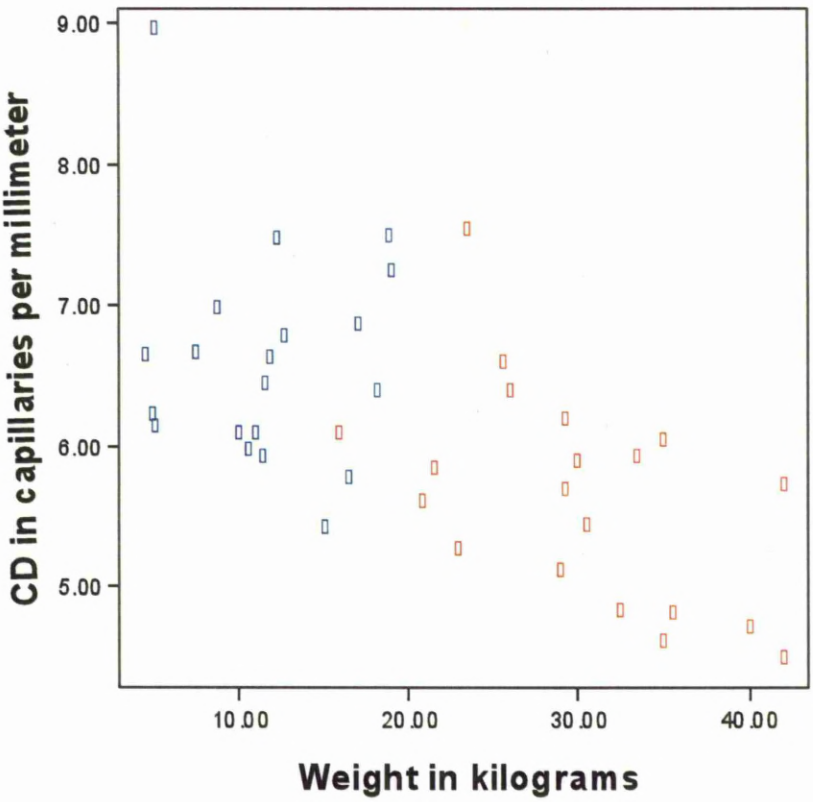

Figure 4.5. Scatter plot demonstrating the relationship between capillary density and weight in all control children. Blue= anaesthetised; Red= awake children.
R= -0.61, p<0.0001

There were significant correlations between capillary density and age, sex, weight and body surface area (Table 4.2). Step-wise multiple linear regression showed that only weight was an independent factor affecting capillary density (Table 4.3). Univariate analysis of variance accounting for anaesthetic agent found the relationship between weight and capillary densitiy remained significant ($p<0.05$)

As this study investigated normal microcirculation in children it was unsurprising that the mean MFI for all images for large and small vessels was 3, the highest score possible and the heterogeneity index was 0 for all participants. The mean PPV from all images was 1 (or 100%), however 11 participants (28%) - 6 anaesthetised and 5 awake, had a PPV of 0.99. As the PVD is calculated by multiplying the CD by the PPV, the results for CD and PVD will be identical in this healthy population with normal microcirculatory blood flow. The following analysis will therefore be based upon CD.

	Spearman rank correlation coefficient	P value
Weight (kg)	-0.6	<0.0001
Age (years)	-0.61	<0.0001
Body Surface Area (m^2)	-0.62	<0.0001

Table 4,2 Correlation coefficients between capillary density and weight, age and body surface area

Predictor variable	B coefficient	P value	95% CI
Weight (Kilograms)	-0.61	<0.001	-0.07 to -0.03
Sex	0.03	0.83	-0.14 to 0.9
Age (years)	-0.18	0.75	-0.01 to 0.12
Body surface Area	0.36	0.78	-0.05 to 0.76

Table 4.3. Multiple Linear Regression Analysis of factors affecting capillary density Adjusted R Square= 0.36, F=22.8, $p<0.0001$ (using stepwise model)

4.3.1. Inter- and Intraobserver repeatability

4.3.1.1 Image attainment.

Intraobserver agreement

Observer 1 obtained at least 5 images from each of the 20 anaesthetised patients. The four best images were chosen for analysis. A Bland–Altman plot of the two pairs of images taken by observer 1 show the limits of agreement (Figure 4.8). The 95% confidence interval for the lower limit is -2.3 to -1.2 and for the upper is 1.7 to 2.8. The 95% repeatability coefficient was 2.8 capillaries per mm. This means that the value within which the differences between two images attained by observer 1 is expected to be 2.8 capillaries per mm for 95% of subjects.

Interobserver agreement

For the 20 anaesthetised patients, four images were chosen that had each been obtained by observer 1 and observer 2 from each participant. A Bland–Altman plot of the 80 images shows the limits of agreement (Figure 4.9). The 95% confidence interval for the lower limit was -2.3 to -1.5 and for the upper is 2.0 to 2.9. The 95% repeatability coefficient was 3 capillaries per mm. This means that the value within which the differences between two images attained by two observers is expected to be 3 capillaries per mm for 95% of subjects.

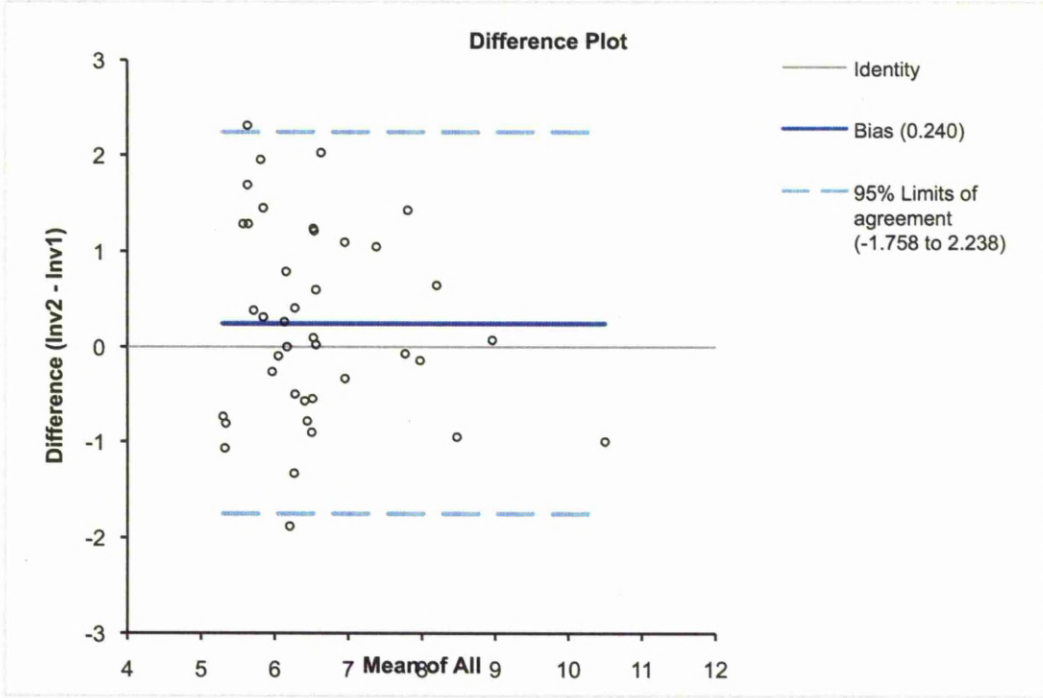

Figure 4.6 Bland Altman plot for intraobserver repeatability in obtaining SDF images

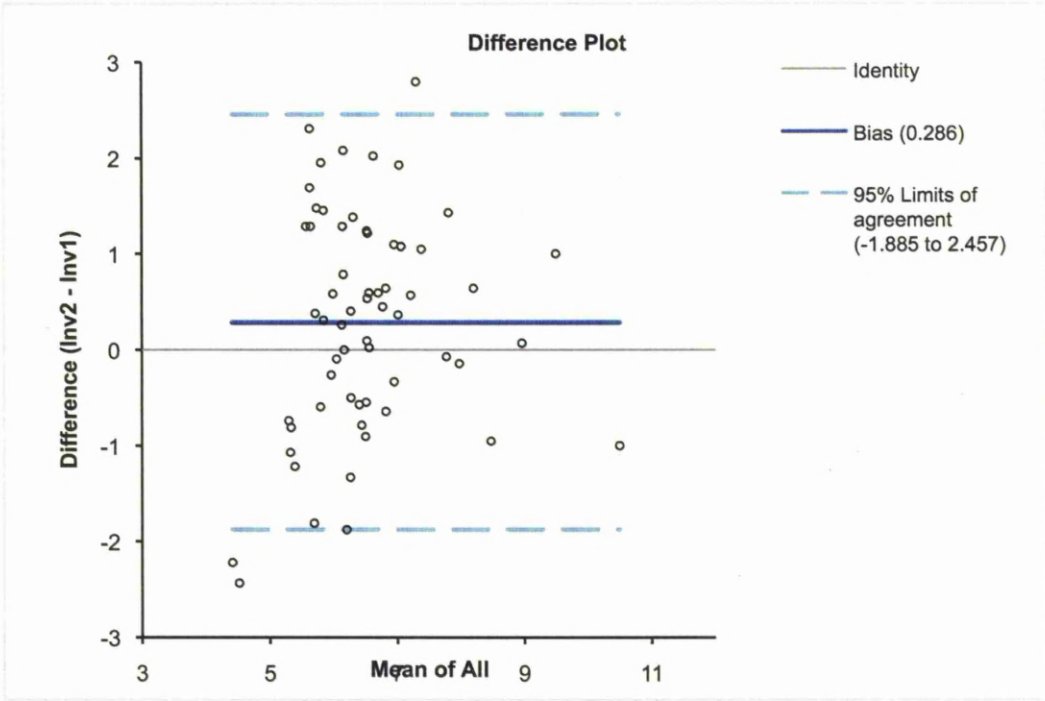

Figure 4.7 Bland Altman plot for interobserver repeatability in obtaining SDF images

4.3.1.2 Image analysis

The four best images in terms of focus and stability were chosen for image analysis from each participant. Kappa analysis of agreement for categorical variables for both inter- and intraobserver repeatability was 1 for both awake and anaesthetised images as all vessel sizes in all quadrants had continuous flow and therefore scored '3'.

Intraobserver agreement

The mean baseline CD from 4 images from all 40 subjects (160 images) measured by observer 1 was 6.08 capillaries per mm (95% CI 5.9 to 6.3). For the second measurement by observer 1, from the duplicated images, this was 6.06 capillaries per mm (95% CI 5.9 to 6.3). The mean difference between the first and second measurements was 0.2 capillaries per mm (95% CI -0.25 to 0.29). A Bland–Altman plot constructed from the data shows that the limits of agreement are narrow with respect to the mean CD and there is no evidence of bias within the graph (Figure 3.7). The 95% confidence interval for the lower limit is -0.51 to -0.39 and for the upper is 0.35 to 0.47. The narrow 95% limits indicate good intraobserver agreement. To further assess the agreement, the 95% repeatability coefficient was calculated and found to be 0.6. This means that the value within which the differences between two replicated images analysed by the same person is expected to be 0.6 capillaries for 95% of subjects.

Interobserver agreement

Four possible paired comparisons could be made between observer 1 and observer 2 from the 4 images taken from each participant. The mean baseline CD from 4 images from all 40 subjects (160 images) measured by

observer 1 was 6.08 capillaries per mm (95% CI 5.9 to 6.3). The mean baseline CD from 4 images from all images measured by observer 2 was 6.12 capillaries per mm (95% CI 5.9 to 6.3). The mean difference between the measurement between observer 1 and observer 2 was -0.04 capillaries per mm (95% CI -0.31 to 0.23). A Bland–Altman plot of the data shows that the limits of agreement are narrow with respect to the mean CD and there is no evidence of bias within the graph (Figure 3.8). The 95% confidence interval for the lower limit is -1.13 to -0.85 and for the upper is 0.92 to 1.2 and indicates good interobserver agreement. The 95% repeatability coefficient was 1.45 capillaries per mm. This means that the value within which the differences between two replicated images analysed by two observers is expected to be 1.45 capillaries per mm for 95% of subjects.

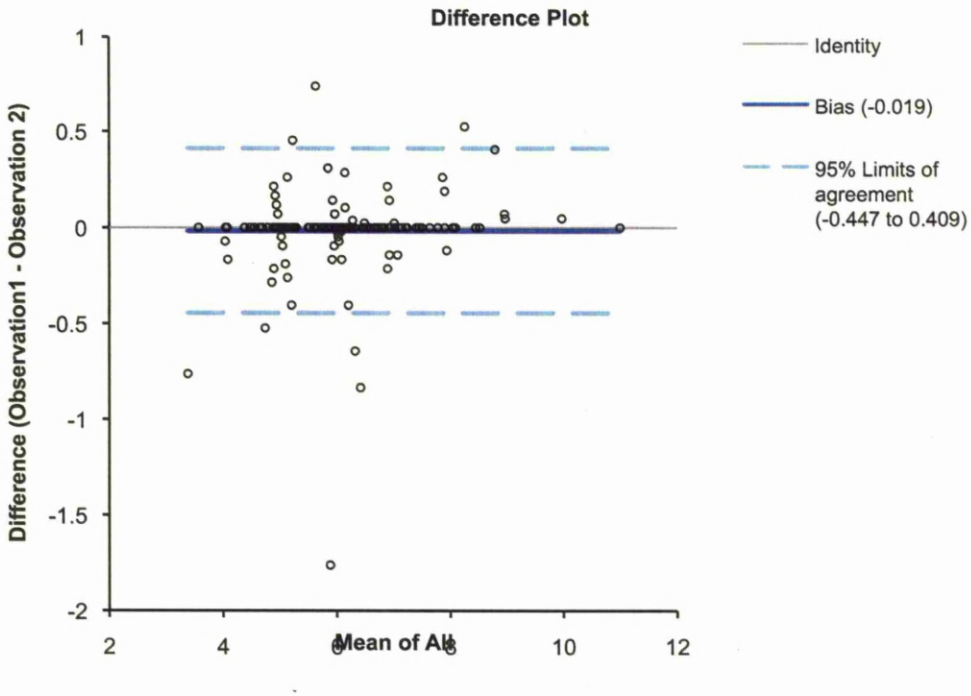

Figure 4.8.Bland Altman plot for intraobserver agreement in the calculation of capillary density in healthy children.

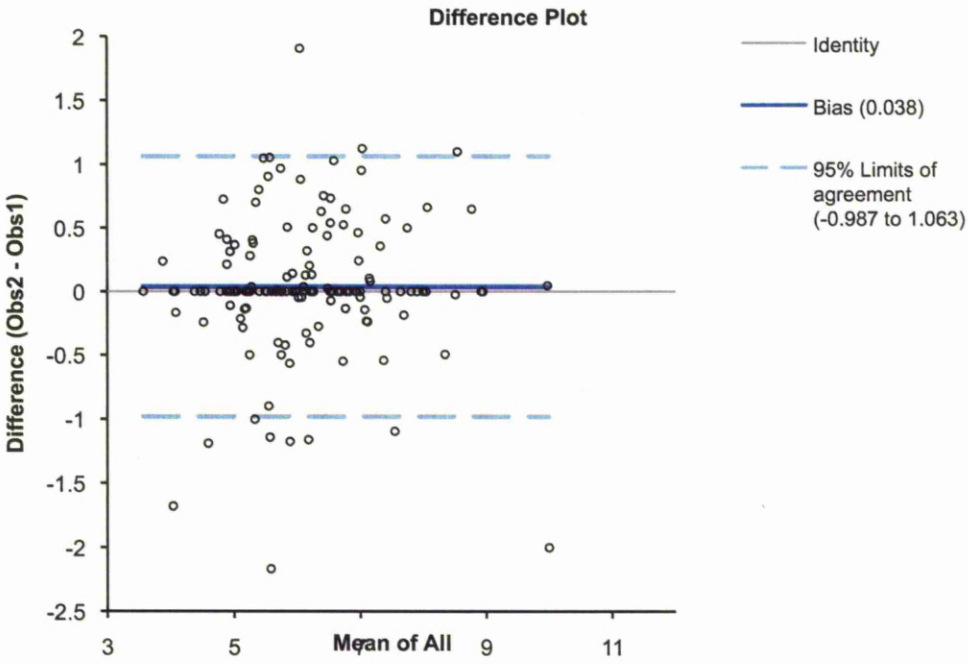

Figure 4.9. Bland Altman plot for interobserver agreement in the calculation of capillary density in healthy children.

4.4 Discussion

In this chapter the normal values for the manual assessment of microcirculation variables in children have been documented and shown good intra- and interobserver agreement. The values for image analysis are good with narrow 95% CI limits of agreement. The values for image attainment were not as good with wider 95% CI limits of agreement.

To ensure a wide spectrum of ages for the determination of normal microcirculation variables, it was necessary to recruit children who were anaesthetised. SDF imaging results in a video image representing a 1mm by 0.7 mm area of sublingual tissue. A significant degree of cooperation is required to obtain clear, focused images that are steady for 20 second on multiple occasions. This would not be possible in a young child as there would be significant movement in the tissue area being visualised and obstructions of view of the microcirculation due to saliva. The younger children (under 6 years of age) were therefore under the influence of anaesthetic agents whilst the older children were able to cooperate with the procedure.

Anaesthetic agents can cause significant haemodynamic alterations. Studies of propofol in animals (Goodchild and Serrao 1989) and humans (Claeys, Gepts et al. 1988) have shown minor degrees of hypotension and depression of cardiac contractility. Animal studies, using intravital microscopy have shown that anaesthetic agents such as propofol, thiopental and etomidate have a vasodilatory effect on the microcirculation (Holzmann, Schmidt et al. 1995; Bazin, Dureuil et al. 1998; Brookes, Reilly et al. 2004) but some agents, like isoflurane and ketamine, can cause

vasoconstriction (Grundmann, Zissis et al. 1997; Brookes, Reilly et al. 2004). Propofol has also been shown to reduce the oxygen extraction capabilities in dogs (Walley 1996)

De Backer et al conducted a prospective study of 15 women anaesthetised with propofol. (Koch, De Backer et al. 2008). They assessed the sublingual microcirculation before, during, and after propofol infusion using orthogonal polarization spectral imaging. They found that during propofol administration, systemic haemodynamic and oxygenation variables were unchanged, but that the CD and the PVD were significantly reduced by 17%. These microcirculatory alterations resolved three hours after the completion of the propofol infusion. It was not possible to determine a baseline CD measurement in children prior to the anaesthetic, this type of analysis was not possible. However, a large number of capillaries with poor perfusion were not observed when analysing the images taken from anaesthetised children with a minimum PPV of 0.99. Propofol was used in these children but it may be that they respond differently to the anaesthetic agent or that the microcirculation changes require prolonged anaesthetic exposure. The results in adults suggest that the CD found in the younger age group might underestimate the values in awake infants and young children.

The relationship between weight and CD is not surprising. The need to consider size in children of different ages is well illustrated by the example of drug prescribing. Drug dose calculations are most commonly based on weight in kilograms (BNF 2005) although body surface area is a more satisfactory index of drug requirements than body weight or age, particularly during infancy and childhood (Lack and Stuart-Taylor 1997). A

"third size model" using an exponent of weight is weight$^{3/4}$. This is called the allometric 3/4 power model (Kleiber and Rogers 1961) and has been found useful in normalizing a large number of physiological parameters including basal metabolic rate (BMR) and oxygen consumption (Dawson 2005; Weibel and Hoppeler 2005).

It is possible to show that in almost all species including humans, the log of BMR and resting oxygen consumption plotted against the log of body weight produces a straight line with a slope of ¾ (Weibel and Hoppeler 2005). This exponential function remains the same between a 7 gram mammal and a horse of over 500 kilograms (Weibel and Hoppeler 2005). Explanations for this model vary and are still debated. Kleiber's explanation is based on changes in body composition with size and concludes that the concentration of `active protoplasm' declines with size (Kleiber and Rogers 1961). Another theory is a structural explanation as the cross sectional area of an animal increases as a 3/4 power function of weight (McMahon 1973). The maximum power a muscle can produce depends on its cross-sectional area. Thus, if the metabolic rate of an organism is proportional to the power production of its muscles, then metabolic rate rises with muscle cross-sectional area and weight$^{3/4}$. West et al. attempted to use fractal geometry to mathematically explain this relationship and by using the distributive nature of vascular networks in animals again arrived at the ¾ power scaling rule (West, Brown et al. 1999). Recently others have argued that this relationship changes between rest and exercise and that no single power law relationship between metabolic rate and body size is appropriate (Darveau, Suarez et al. 2002).

One of the most important roles of the capillary is oxygen transfer to tissues. If the oxygen consumption rate of mammals follows the ¾ power law as has been suggested (Bishop 1999; Dodds, Rothman et al. 2001) , then the smaller the body mass, per area of muscle mass, more capillaries and a higher concentration of intracellular mitochondria will be needed to meet oxygen demand. A study involving muscle dissection of various mammals found that capillary density was proportional to the size of the mammal, corroborating this point (Schmidt-Nielsen and Pennycuik 1961).

4.4.1 Limitations

This technology has limitations, particularly the possible effects of contact pressure. Excessive pressure of the SDF probe upon the tissue can affect blood flow and may have contributed to a slight reduction of PPV that was seen in both control groups. This small reduction was however slight and may in fact be the norm in healthy children. This limitation can be overcome by experience. Lateral movement of tissue (or probe) will affect the video image and a smooth, continuous video sequence may not be possible. To visualise capillary and venular flow patterns and density effectively a static piece of tissue area is the ideal. This is difficult due to the small area of tissue examined by the SDF probe. A further limitation of this study is that, for the purposes of comparison with children with MCD, age matched controls were not possible for non anaesthetised children. Although preferable to assess the microcirculation in healthy unanaesthetised children , the level of co-operation needed to obtain high quality sublingual images is lacking in a child less than 6 years of age.

4.4.2. An approach to automated microcirculation image analysis

Future work should aim for fully automated image analysis. Ideally the velocity of red cells should be calculated in a manner that removes any user manipulation Microcirculation image analysis is not yet available, although there have been attempts to solve the difficulties.

The videos to be analysed are recorded at 25 frames per second and are about 500 frames in length. In each frame red blood cells may appear as isolated objects or as collections of blood cells. Blood vessel walls cannot be visualised with this technology and are defined by the movement of red cells through them. In order to determine the speed of blood flow in a vessel, a cell (or group of cells) must be followed from frame to frame and the capillaries should be in an orthogonal plane to the lens, which is not always the case. Knowing the spatial scale of the image and the time interval between frames, the displacement of a cell in pixels per frame can be converted to a speed in micrometers per second. Video images may seem stable to the naked eye but when there is a significant amount of tissue or probe movement, it is difficult to identify each individual red blood cell in successive frames. There are tissue movements with respiration and vascular pulsations, which may be increased by mechanical ventilation and administration of inotropes in sick ICU patients. It is therefore important to stabilise each frame so that the capillary networks appears to be static over the duration of the video. Quantification of blood flow velocity requires a sequence of stable video images.

Following the motion of all cells over all frames allows the vessel network to be mapped out. This network is broken into separate segments as the speed of blood flow cannot be defined at a junction between vessels. The diameter of each segment is noted so that blood flow values can be

categorised later into capillaries (diameter < 10 μm), venules and veins. Each non-linear vessel segment needs to be straightened to make subsequent speed analysis possible. For each vessel in turn, the cells visible in each frame are displayed in a 'space-time' diagram. If the cells are imaged clearly, this diagram exhibits features whose orientation is related to flow speed. If the cells are static then the features are aligned with the time axis of the diagram. Cells with higher speeds produce features at larger angles with respect to the time axis. The speed can be calculated every two seconds (giving approximately 10 values for a 20-second video). If the vessel segment is long then speeds can be calculated at different positions along the vessel length.

The result of the analysis is speed data for each vessel and is therefore a function of time and the position of an individual red blood cell along the vessel. This data can be reduced to a 'score' that can be compared with that produced by the manual analysis that has been carried out here. This software development is ongoing and the hope is that it will generate a quick, reliable set of microcirculatory values at the bedside, that aid clinical decision making.

4.5 Conclusion

Side stream dark field imaging can be used in healthy awake and anaesthetised children to obtain high quality images of the microcirculation and normal values for children have been established. Manual analysis of the images produced has good inter- and intra-observer agreement but a fully automated and user-friendly image analysis software system would be a superior and faster method of evaluation. Its use in critically ill children would therefore be appropriate.

Chapter 5

The Microcirculation in Meningococcal Disease

5.1 Introduction

Severe sepsis is characterized by systemic inflammation and widespread tissue injury. It involves widespread vasodilatation, increased microvascular permeability, and leukocyte attraction to affected tissue areas. Organ dysfunction can vary from mild impairment to complete organ failure (Dellinger, Levy et al. 2008). One reason for this variation is the extent to which the microcirculation has been affected by the inflammatory process. Normal blood flow in capillaries ensures the delivery of oxygen to cells, appropriate tissue oxygenation and the removal of waste products. The microcirculation is defined as a network of blood vessels less than 100 μm in diameter. These blood vessels consist of venules, capillaries and arterioles. Oxygen, nutrients and waste products are exchanged between the circulating blood and cells of various tissue types under normal circumstances. In severe sepsis poor tissue perfusion is attributable to abnormal capillary blood flow (Ince 1999; Ince and Sinaasappel 1999). Surrogate measures of tissue perfusion have been used to assess the degree of microcirculatory dysfunction. These include blood lactate, arterial blood base deficit, gastric and sublingual capnography and urine output (De Backer 2003).

Intravital microscopy in animal models has given a large amount of information about the microcirculatory response to sepsis including evidence of major alterations in microvascular vessel density and flow patterns (Ellis, Bateman et al. 2002; Bateman and Walley 2005). In most circumstances intravital imaging technology cannot be used in humans. OPS and SDF technology, however, can be used to visualise some areas of the microcirculation in humans (Groner, Winkelman et al. 1999; De Backer and Dubois 2001; De Backer, Creteur et al. 2002; Spronk, Ince et

al. 2002). Although still a research tool, microcirculatory imaging can provide real time, bedside images in the investigation of human sepsis and has been utilised in studies of severe sepsis in adults and children (Top, Ince et al.).

5.1.2 The microcirculation in childhood sepsis

This chapter examines the use of SDF imaging in children with severe MCD and describes the microcirculatory measures used and the abnormalities found.

5.2 Method

5.2.1 Patients

Patient recruitment, data collection, sublingual microvascular visualisation, echocardiography and blood sampling and analysis were carried out as detailed in Chapter 2. Control subjects were children who had blood taken during routine surgery. The 40 children from the previous chapter were controls for the microcirculatory variables. As an additional comparative group, the sublingual microcirculation was visualised on 10 children pre and post cardiac surgery. The sublingual microcirculation was visualised using SDF in these children while they were anaesthetised, approximately 10-15 minutes prior to cardiac surgery, within one hour of completion of surgery and three hourly until extubation. Echocardiography was not performed on these children and blood was not taken from them. Analysis of SDF images was carried out as described in Chapter 4.

5.2.2 Echocardiography

Systolic and diastolic cardiac function measurements, cardiac output and index were calculated using the methods described in Chapter 2.

5.2.3 Statistics

Data are presented as median and IQR or mean and standard deviation where appropriate. Correlations between variables were determined using Spearman rank correlation coefficient. A p value of <0.05 was considered statistically significant. Inter- and intraobserver agreement for measurements of SDF images by two independent observers is expressed as Kappa coefficients and Bland-Altman plots. Statistical analyses were carried out using SPSS for Windows (version 14.0), (SPSS,Inc., Chicago, Illinois) and Analyse-It Software v.1.62 for Microsoft Excel (Analyse-It Software, Leeds, UK). Longitudinal analysis was carried out by the Medical Statistic Department at the University of Lancaster.

5.3 Results

After informed consent, admission plasma samples were obtained from 43 children who were reported to the research fellow as 'suspected MCD'. This included 33 children subsequently confirmed to have MCD and 10 with presumed viral illness. Sequential plasma samples were available from 20 of the 33 MCD children. Twenty-three children had blood taken during routine surgery to act as controls. Demographic details for these children are shown in Tables 5.1 and results of investigations in Table 5.2. There was no mortality and 2 children required limb amputations. One child required haemofiltration.

	MCD ventilated	MCD not ventilated	Presumed viral	Control
Total number	20	13	10	23
Age at admission in years [IQR]	2.16 [0.69 to 4.75]	3.1 [1.02 to 5.37]	1.58 [0.67 to 2.5]	2.5 [0.74 to 4.5]
Sex [male %]	5 [25%]	4 [30.7%]	3 [30%]	9 [39.1%]
Maximum GMSPS [IQR]	11 [9 to 12]	3 [2 to 3]	3 [2 to 3]	--
Admission PELOD [IQR]	11 [5.1 to 16.8]	0	0	--
Admission PRISM III [IQR]	20 [17.2 to 22.5]	3 [0 to 3]	3 [0 to 3]	--
Admission Inotrope score [IQR]	17.5 [6 to 77.5]	0	0	--
Duration of hospital stay (days) [IQR]	10 [7.3 to 15.5]	5 [3 to 7]	3 [2 to 5]	--
Duration of rash (hours) [IQR]	2 [1-7]	1 [1-5.5]	4.5 [2-7.5]	--

Table 5.1. Demographic data for the study population.

	MCD ventilated	MCD not ventilated	Presumed viral	Control	p value
Total number	20	13	10	23	
CRP (mg/l) [IQR] (normal range <4mg/l)	142.5 [107 to 200]	75.8 [50.8 to 122.4]	10.4 [4 to 37.1]	All <4	*NS †<0.05 ‡<0.05
WBC ($x10^6$/l) [IQR] (normal range 4.3-10.8 $x10^6$/l)	20.7 [5.8 to 25.3]	23.7 [15.8 to 30.2]	15.9 [9.9 to 19.8]	--	* NS † NS ‡N/A
Platelet count ($x10^9$/l) [IQR] (normal range 150 to 400 $x10^9$/l)	182 [120 to 248]	322 [241 to 429]	301 [264 to 416]	--	*<0.001 †NS ‡N/A
aPTT [IQR] (normal range 22-34 seconds)	44.1 [39.3 to 55.7]	39.5 [34.1 to 39.6]	33.4 [31.4 to 35.1]	30.4 [29.1 to 34.2]	*<0.05 † NS ‡ NS
PCT (ng/ml) [IQR] (normal range <5ng/ml)	169.5 [47.5 to 371.9]	23.5 [5.8 to 41.2]	0.1 [0.2 to 0.4]	0.04 [0.02 to 0.06]	*<0.0001 †<0.005 ‡<0.05
IL-1Ra (pg/ml) [IQR]	5107 [683 to 8388]	245.5 [76 to 1115.8]	86.2 [68 to 308.1]	39.6 [12.9 to 56.5]	*<0.005 †NS ‡<0.001
IL-6 (pg/ml) [IQR]	3771 [1651 to 11140]	523.5 [100.8 to 2838.9]	61.0 [12.9 to 73.4]	34.0 [24 to 59.9]	*<0.05 †<0.05 ‡NS
IL-8 (pg/ml) [IQR]	643.0 [137.5 to 1434.0]	328.5 [76.1 to 619.8]	26.6 [5.1 to 74]	44.0 [34.3 to 73.7]	*NS †<0.05 ‡NS
IL-10 (pg/ml) [IQR]	187 [70 to 519]	146.9 [28.2 to 1562.5]	33.0 [14.6 to 162.2]	47.8 [23.8 to 66]	*NS † NS ‡ NS
TNF (pg/ml) [IQR]	316 [193 to 373]	66.8 [43.8 to 115.9]	26.0 [19.5 to 40.8]	43.9 [28.8 to 57.6]	*<0.0001 †<0.005 ‡ NS
Bacterial load in copies per ml [IQR]	320,000 [61,000 to 1,020,000]	7800 [3000 to 32000]	--	--	*<0.05 †N/A ‡N/A

5.3.1 Agreement

There were 618 video images available for the assessment of agreement from the 20 children with MCD who required ventilation. The Kappa coefficients and weighted Kappa coefficients for intra- and inter-observer repeatability are shown in Table 5.3, indicating excellent agreement.

For the 20 children with MCD four images were chosen that had each been analysed by observer 1 and observer 2 for each time point. A Bland–Altman plot constructed from the image analysis (Figure 5.1) shows the limits of agreement. The 95% limit of agreement for the lower limit is -2.1 (95% confidence interval -2.2 to -1.8). The 95% limit of agreement for the upper limit is 1.8 (95% confidence interval 1.6 to 1.9). The 95% repeatability coefficient was 2.6 capillaries per mm. This means that the value within which the differences between two images attained by two observers is expected to be 2.6 capillaries per mm for 95% of subjects.

	Kappa coefficient	CI	Weighted Kappa coefficient	CI
MFI for capillaries (MFIc)				
Interobserver	0.83	0.80 to 0.86	0.80	0.70 to 0.83
Intraobserver	0.88	0.86 to 0.89	0.80	0.72 to 0.85
MFI for all vessels (MFI)				
Interobserver	0.85	0.83 to 0.87	0.88	0.86 to 0.89
Intraobserver	0.88	0.86 to 0.89	0.80	0.72 to 0.85

Table 5.3. Inter- and intraobserver agreement for flow scoring for calculation of MFIc and MFI

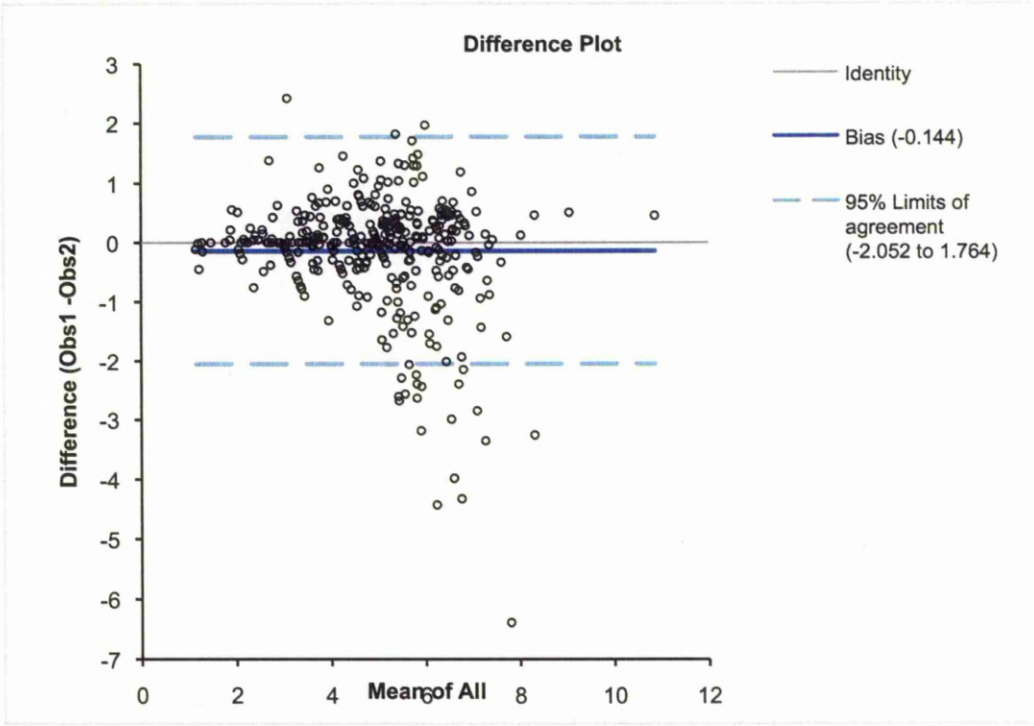

Figure 5.1. Bland-Altman plot of assessment of capillary density by two independent observers in children with MCD

5.3.2 Microcirculatory variables

Table 5.4 shows the relationship between microcirculation measurements taken from each of the 618 video sequences. There are strong positive correlations between MFI and MFIc, PPV, PVD and a strong negative correlation between MFI and HI. There is a significant but weaker positive correlation between MFI and CD and PPV. As PPV is a function of CD this relationship is not surprising. Almost identical correlation coefficients were found when MFIc was used instead of MFI for the analyses (Table 5.4)

A significant reduction in admission MFI, MFIc, PPV, CD, and PVD were found in children with severe MCD when compared to both anaesthetised ($p<0.05$) and healthy awake controls ($p<0.005$) (Figures 5.2, 5.3, 5.4, 5.5 and 5.6). These differences were no longer significant pre-extubation showing that microcirculatory recovery occurred alongside clinical recovery.

Microcirculatory outcome variable	MFIc	MFI	CD	PPV	PVD	HI
MFIc	1					
MFI	1 p<0.0001	1				
CD	0.5 p<0.0001	0.49 p<0.0001	1			
PPV	0.76 p<0.0001	0.75 p<0.0001	0.45 p<0.0001	1		
PVD	0.77 p<0.0001	0.67 p<0.0001	0.91 p<0.0001	0.63 p<0.0001	1	
HI	-0.89 p<0.0001	-0.85 p<0.0001	-0.24 NS	-0.68 p<0.0001	-0.21 NS	1

Table 5.4. Spearman Rank Correlation coefficients between all microcirculatory outcome variables measured.

HI - Heterogeneity index, NS – not significant

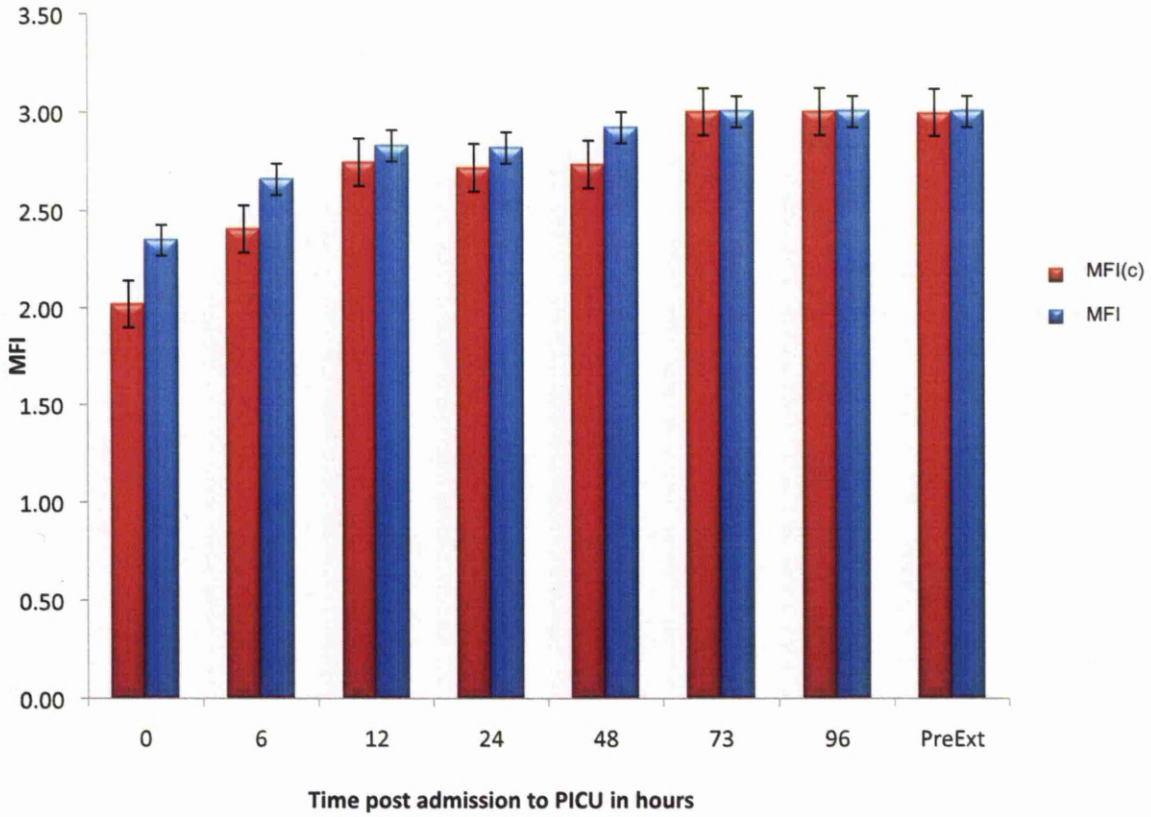

Figure 5.2. Bar chart showing change in mean MFI and MFIc in children with MCD over time (with standard error bars)

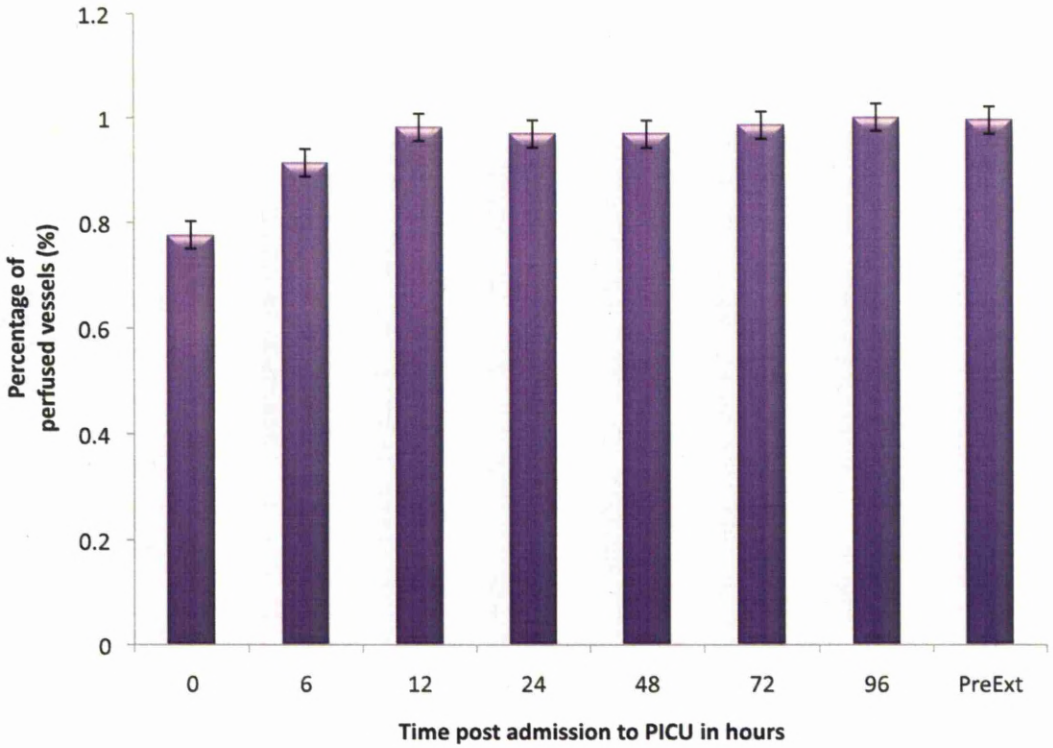

Figure 5.3. Bar chart showing change in mean percentage of perfused vessels (PPV) in children with MCD over time (with standard error bars).

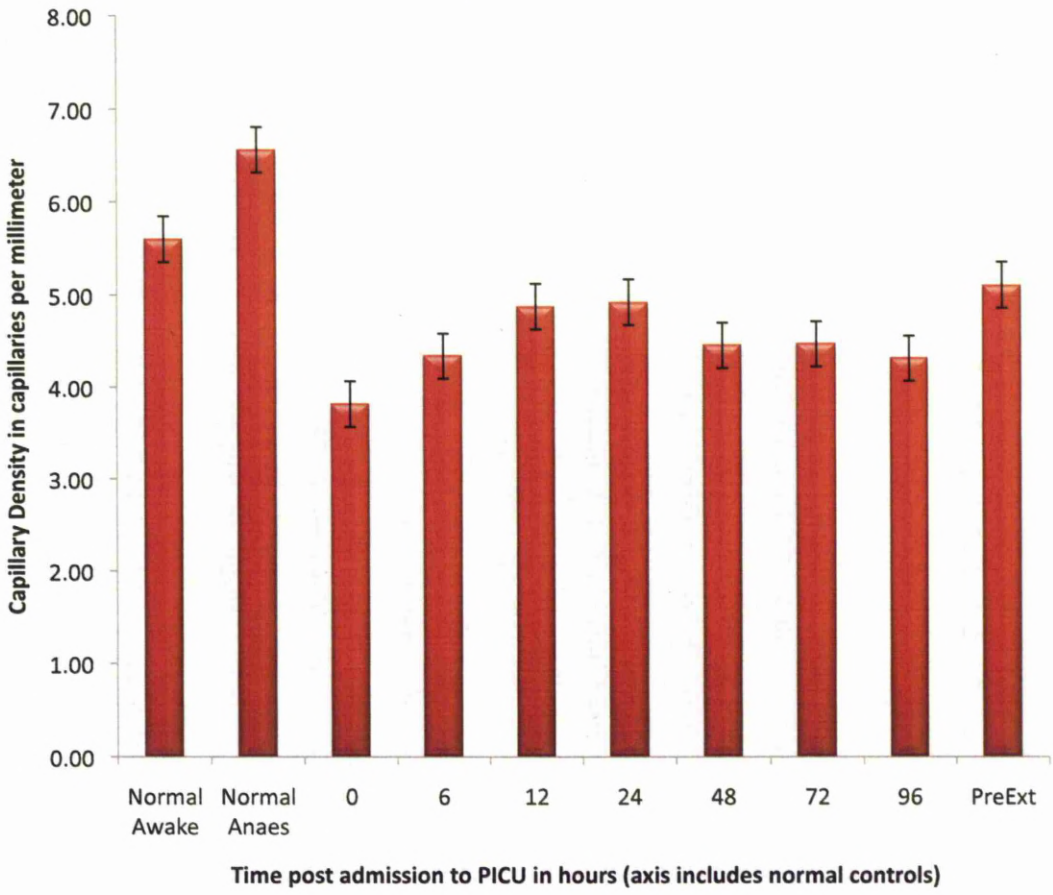

Figure 5.4. Bar chart showing change in mean capillary density (CD) in children with MCD over time (with standard error bars). Mean values for PVD in awake and anaesthetised control children are also included.

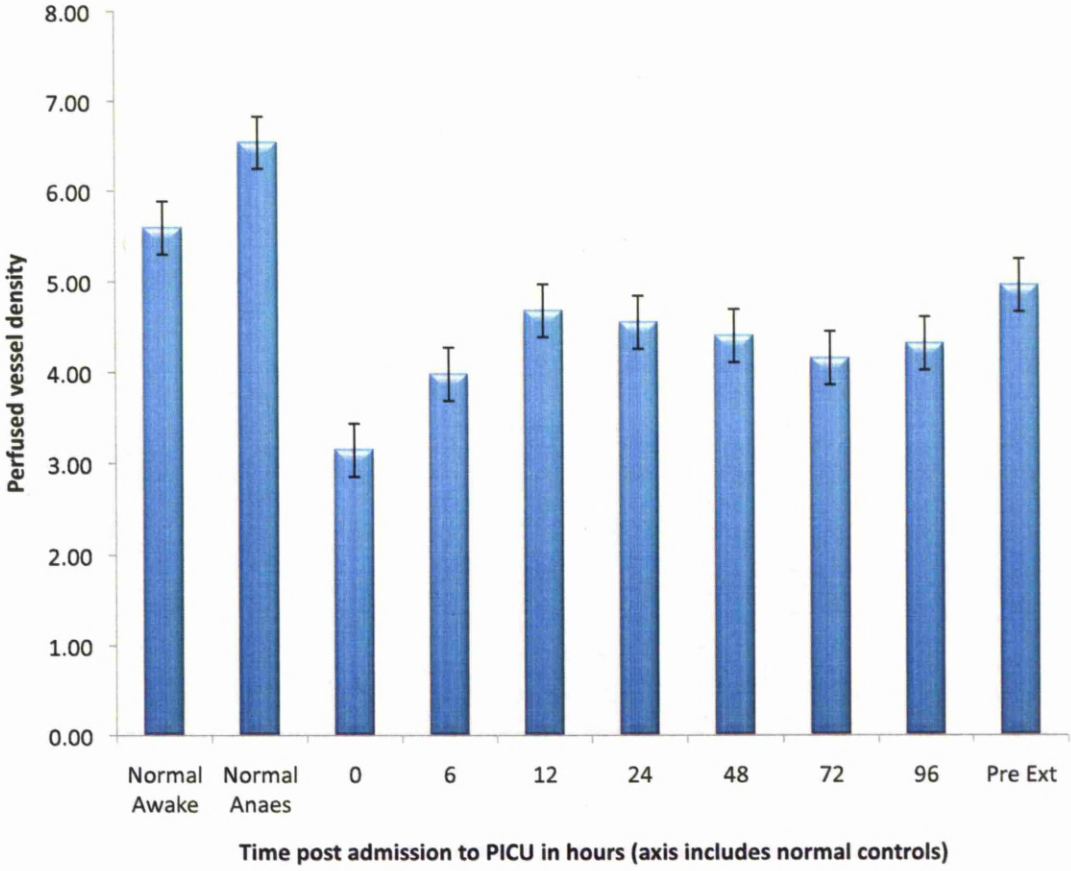

Figure 5.5. Bar chart showing change in mean perfused vessel density (PVD) in children with MCD over time (with standard error bars). Mean values for PVD in awake and anaesthetised control children are also included.

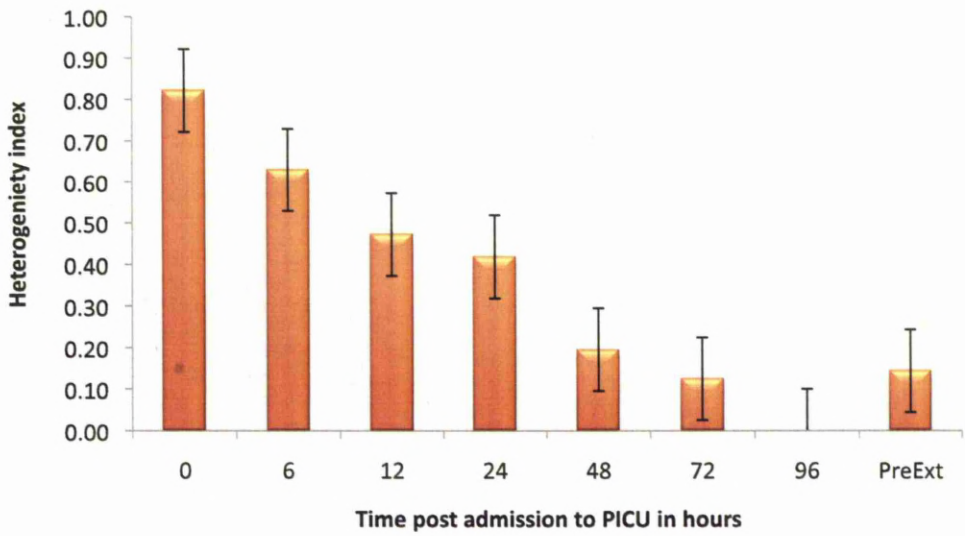

Figure 5.6. Bar chart showing change in mean heterogeneity index (HI) in children with MCD over time (with standard error bars)

5.3.3 Predicting outcome

Table 5.5 show the relationship between admission microcirculation measurements and assessments of illness severity. It shows a significant negative correlation between MFI and MFIc and volume of fluid resuscitation needed, total duration of time the child was ventilated and required inotropic support, admission inotrope score and the PELOD score.

To account for children presenting to PICU at different points in their illness, multiple linear regression analysis was used to assess the independent predictive ability of MFIc for the duration of ventilation in hours after adjustment for duration of illness, defined as the duration of rash prior to PICU admission and the duration of ventilation prior to PICU admission. MFIc was chosen for use in the analysis as was deemed to be the most pertinent microcirculatory variable due to its ease of ascertainment and analysis from an SDF image. The results show that MFIc predicts the duration of ventilatory requirement, irrespective of the stage of illness at the time of admission to PICU (Table 5.6).

Covariate	MFI	MFIc	CD	PPV	PVD	HI
Duration of Hospital stay (days)	r=-0.28 NS	r=-0.3 NS	r=-0.4 NS	r=-0.15 NS	r=-0.3 NS	r=0.4 NS
Duration of PICU stay (days)	r=0.39 NS	r=0.39 NS	r=-0.25 NS	r=-0.24 NS	r=-0.11 NS	r=0.4 NS
Bacterial load	r=-0.31 NS	r=-0.31 NS	r=-0.2 NS	r=0.06 NS	r=0.03 NS	r=0.3 NS
Volume of resuscitation fluid	r=-0.52 p<0.05	r= -0.54 p<0.05	r= -0.2 NS	r=-0.46 p<0.05	r= -0.19 NS	r= 0.35 NS
Duration of ventilation (hours)	r=-0.48 p<0.05	r= -0.48 p<0.05	r= 0.06 NS	r= -0.27 NS	r=-0.08 NS	r=0.45 p<0.05
Duration of inotropic support (hours)	r=-0.56 p<0.05	r= -0.49 p<0.05	r= -0.19 NS	r= -0.16 NS	r=0.15 NS	r= 0.36 NS
PELOD	r=-0.58 p<0.05	r=-0.53 p<0.05	r= -0.04 NS	r= -0.15 NS	r= 0.1 NS	r=0.5 p<0.05
PRISM III	r= -0.18 NS	r= -0.12 NS	r= -0.19 NS	r= -0.19 NS	r= -0.19 NS	r= 0.01 NS
Peak GMSPS	r=-0.48 p<0.05	r=-0.47 p<0.05	r=0.01 NS	r=-0.15 NS	r=0.13 NS	r=0.4 NS
Inotrope score	r= -0.75 p<0.001	r= -0.74 p<0.001	r=-0.1 NS	r=-0.62 p<0.05	r=0.001 NS	r=0.67 p<0.01

Table 5.5. Correlations between admission microcirculation variables and markers of illness severity

Predictor variable	B coefficient	P value	95% CI
Total Duration of ventilation	-0.56	<0.05	-0.01 to -0.15
Duration of rash prior to hospitalisation	0.41	0.9	-0.04 to 0.5
Duration of ventilation prior to admission	0.21	0.9	-0.01 to 0.002

Table 5.6. Multiple linear regression analysis was used to assess the independent predictor ability of MFIc for the duration of ventilation in hours

Adjusted R Square= 0.34, F=9.7, p<0.01 (using stepwise model)

5.3.4 Longitudinal Data Analysis

The longitudinal data analysis for microcirculation variables is shown in Table 5.7 and reports the estimated correlation parameter p between each time-varying covariate and the measured microcirculation (MFIc was the microcirculation parameter used for the analysis). All microcirculation variables changed over time alongside MFIc when MFIc was used as the comparative variable. This relationship is strongest with MFI, PPV and HI.

Table 5.8 shows admission correlations and longitudinal analysis comparing changes in clinical and biochemical measurements of tissue perfusion in the 20 children with MFIc over time. It demonstrates that as MFIc improves over time lactate, pCO_2 and FiO_2 all decrease. Base excess, pH and urine output all correlate with an increase in MFIc over time. Table 5.9 shows that aPTT, INR and PCT all decreased over time alongside MFIc. Haemodynamic variables are shown in Table 5.10 and although the inotrope score decreased over time in relation to MFIc, there was no change in cardiac systolic function, as assessed by FS, or cardiac index.

Covariate	$\hat{p}$	CI
MFI	0.91	0.69 to 1.1
CD	0.29	0.03 to 0.55
PPV	0.66	0.43 to 0.88
PVD	0.34	0.1 to 0.58
Heterogeneity index	-0.75	-0.53 to -0.97

Table 5.7. Longitudinal analysis comparing changes in microcirculation variables with MFIc over time. $\hat{p}$=estimated correlation parameter

Covariate	MFIc	$\hat{P}$	CI
Lactate	r=-0.59 p<0.05	-0.52	-0.74 to -0.3
pH	r=0.2 NS	0.29	0.03 to 0.55
Base excess	r=0.17 NS	0.3	0.03 to 0.6
pO_2	r=0.24 NS	0.04	-0.33 to 0.41
pCO_2	r=-0.39 NS	-0.27	-0.5 to -0.02
Bicarbonate	r=0.11 NS	-0.04	-0.31 to 0.22
FiO_2	r=-0.38 NS	-0.35	-0.57 to -0.13
Urine output	r=0.3 NS	0.22	0.01 to 0.43

Table 5.8. Admission correlations between clinical and biochemical measurements of tissue perfusion and MFIc and Longitudinal analysis comparing changes clinical and biochemical measurements of tissue perfusion with MFIc over time. $\hat{p}$=estimated correlation parameter

Covariate	MFIc	$\hat{p}$	CI
aPTT	r=-0.23 NS	-0.46	-0.69 to -0.23
INR	r=-0.57 p<0.05	-0.37	-0.59 to -0.15
Fibrinogen	r=0.39 NS	-0.001	-0.76 to 0.76
Haemoglobin	r=-0.13 NS	-0.21	-0.4 to 0.01
Haematocrit	r=-0.3 NS	-0.1	-0.68 to 0.24
WCC	r=0.36 NS	0.002	-0.36 to 0.36
Neutrophil	r=0.33 NS	0.04	-0.22 to 0.29
Platelet	r=0.22 NS	-0.07	-0.35 to 0.21
CRP	r=0.58 p<0.05	0.2	-0.60 to 0.03
PCT	r=-0.36 NS	-0.37	-0.6 to -0.14
Glucose	r=0.11 NS	0.25	-0.03 to 0.53

Table 5.9. Admission correlations between laboratory markers and MFIc and Longitudinal analysis comparing changes in laboratory markers with MFIc over time.

$\hat{p}$ = estimated correlation parameter

Covariate	MFIc	$\hat{p}$	CI
Inotrope Score	r=-0.74 p<0.01	-0.46	-0.71 to -0.21
MAP	r=0.05 NS	-0.14	-0.4 to 0.14
CVP	r=-0.02 NS	-0.08	-0.3 to 0.13
Fractional shortening	r=0.08 NS	0.17	-0.07 to 0.41
Cardiac Index	r=-0.23 NS	-0.2	-0.44 to 0.04
SVR	r=0.15 NS	-0.04	-0.26 to 0.18

Table 5.10. Admission correlations between haemodynamic variables and MFIc and Longitudinal analysis comparing changes in haemodynamic variables with MFIc over time. $\hat{p}$ = estimated correlation parameter

5.4 Cardiac comparative group

Of the 10 children undergoing cardiac surgery, 4 children had ventricular septal defects, 4 had completion of Fontan circulation from complex congenital cyanotic cardiac defects and 2 had supravalvular aortic stenosis repair. The median age of the children was 2.1 years (IQR 0.7 to 2.6), 50% were male. The median time to extubation from the completion of surgery was 52 hours (interquartile range 3.8 to 68 hours).

There was no significant difference between pre-surgical microcirculatory findings and those taken from anaesthetised controls. A significant reduction of CD, MFI, PPV and PVD were found in all children 1 hour following surgery when compared to anaesthetised ($p<0.05$) and awake controls ($p<0.05$). These differences were no longer significant 3 hours after this time point. There were significant correlations between cardiopulmonary bypass time and MFI ($r= -0.73$, $p<0.05$) and PPV ($r= -0.62$, $p<0.05$) and aortic cross clamp time and MFI ($r= -0.78$, $p<0.01$) and PPV ($r= -0.76$, $p<0.05$). Two of these children were not receiving any inotropic support when microvascular abnormalities were seen. The other 8 were receiving milrinone at the time in image acquisition.

No significant difference was found between admission values for MFIc ($p=0.23$), MFI ($p=0.23$), CD ($p=0.5$), PPV ($p=0.4$) and PVD ($p=0.4$) for children with MCD and the same microcirculatory values for children who were 1 hours post cardiac surgery. A significant reduction in admission CD ($p<0.05$), MFI ($p<0.05$), PPV ($p<0.05$) and PVD ($p<0.05$) was seen in children with MCD when compared to children 3 hours post cardiac surgery in the 6 children that remained ventilated 3 hours post operatively.

5.5 Discussion

These results confirm excellent intraobserver and interobserver agreement in the assessment of microcirculation SDF images from children with MCD. This chapter demonstrates that microcirculation variables can predict the duration of ventilatory requirement, irrespective of the stage of illness at the time of admission to PICU and that the microcirculatory dysfunction present in children with severe MCD recovers alongside clinical recovery. As a useful comparative group this study has also shown that the systemic inflammatory response seen in children post operatively from cardiac surgery requiring cardiopulmonary bypass produces similar sublingual microcirculatory changes to children with MCD. These changes were shown to be shorter in duration when compared to children with severe sepsis indicating more severe microcirculatory disruption in children with MCD.

De Backer et al. showed a significant decrease in CD and PPV in adults with severe sepsis with the most severe changes being associated with mortality (De Backer, Creteur et al. 2002). Sakr et al. used OPS to assess the microcirculation in adults and showed that PPV that did not improve over time in non-survivors (Sakr, Dubois et al. 2004). The findings here show a clear relationship between microcirculatory dysfunction and severity of illness in children. Sakr et al. stated that the persistence of significant microcirculatory dysfunction was the most accurate haemodynamic predictor of mortality when compared with commonly used methods of global hemodynamic assessment. They concluded that poor tissue perfusion of organs could be identified using OPS imaging and this would allow for more targeted therapy to improve microcirculatory blood flow and

reduce mortality (Sakr, Dubois et al. 2004). Trzeciak et al. found microcirculatory abnormalities in patients with severe sepsis treated with early goal directed therapy (EGDT) which were more severe in non-survivors than in survivors and in patients with cardiovascular dysfunction (Trzeciak, Dellinger et al. 2007). EGDT is a technique used in adult and some paediatric critical care, involving early monitoring of superior vena cava oxygen saturation ($ScvO_2$) and a treatment algorithm. Adjustments of cardiac preload, afterload, and contractility are made to within tight target ranges in order to balance oxygen delivery with oxygen demand in patients with a high risk of morbidity and mortality (Rivers, Nguyen et al. 2001; Rivers, Nguyen et al. 2004; Rivers 2006). The only paediatric study to date used OPS imaging to examine the microcirculation of 21 children with sepsis from a variety of aetiologies. This study demonstrated that in children with septic shock the persistence of microcirculation abnormalities was associated with a poor outcome. This was despite adequate resuscitation and support of systemic haemodynamics (Top, Ince et al.). The buccal mucosa was examined in this study which is not a common place to obtain microcirculation images as detailed in the majority of the adult literature.

The reasons for the occurrence of microcirculation abnormalities in severe sepsis are complex and the precise mechanisms remains unclear. Multiorgan dysfunction is associated with endothelial cell injury leading to tissue hypoxia. A disruption in global oxygen delivery alters the metabolic regulation of tissue oxygen delivery contributing to organ dysfunction leading to a cycle of tissue destruction. The profound hypotension seen in septic shock will lead to vascular shutdown contributing to the microcirculation problems. Hypotension is in part a result of the

microvascular changes, including increased permeability and the shunting of blood. Reactive oxygen species and vasoactive substances including NO cause damage to red blood cells, affecting their normally smooth journey through the vessels of the microcirculation (Lominadze and McHedlishvili 1999). Red blood cells are able to change their shape as they move through narrow capillaries. If this ability to change shape is lost, red blood cells become rigid resulting in impaired perfusion and oxygen delivery in peripheral tissues. Rigid red blood cells can be caused by NO release and may block microvessels directly (Parthasarathi and Lipowsky 1999).

This study has shown correction of coagulopathy alongside microcirculatory recovery. A large randomised study called the RESOLVE (REsearching severe Sepsis and Organ dysfunction in children: a gLobal perspectiVE) trial to investigate the efficacy and safety of Drotrecogin alfa (activated PC) was published in 2007 (Nadel, Goldstein et al. 2007). 477 patients were enrolled; 237 received placebo, and 240 Drotrecogin alfa. No significant difference was found between the groups in 28-day mortality and serious bleeding events were similar between groups. This study however enrolled a wide spectrum of paediatric patients with sepsis. With a more specific criterion for trial entry, such as using an MFI cut off of 2 in conjunction with other entry criteria, a positive effect of Drotrecogin alfa may have been seen.

Vasopressors have a vasoconstrictor effect which may have an effect on capillary function. An increase in systemic vascular resistance would increase blood pressure but at the expense of poor blood flow through capillaries. The inverse relationship shown here between microcirculation

variables and inotrope score could be explained by this. Alternatively it may be because the sicker the patient is the worse the microcirculatory flow is and hence the need for more inotropes. Cardiopulmonary bypass (CPB) induces a systemic inflammatory response. Studies in adults have shown microcirculatory abnormalities after cardiac surgery. Our study confirms this. Microcirculatory dysfunction was seen in children following cardiac surgery both in children who were and children who were not on inotropes. This would indicate that inotropic agents play a minor part, if at all in microcirculation abnormalities in children with MCD.

A limitation of this work is that there are insufficient time points to compare cardiac patients with children with MCD in longitudinal analysis. This also highlights the speed at which the microcirculation recovered in the cardiac comparison group indicating that the nature of the insult and the effect of the inflammatory cascade is more potent in sepsis. However, eight of the children in the cardiac comparison group were receiving milrinone at the time of image acquisition, an agent that has been shown in a small case series of MCD to be of benefit (Rich, West et al. 2003). Milrinone is an inodilator that improves left ventricular diastolic relaxation by selectively inhibiting III phosphodiesterase isoenzyme in both cardiac and vascular muscle which increases myocardial contractility. A different response is seen in vascular smooth muscle where vasodilation occurs due to a reduced sensitivity of the muscle to calcium influx (Shipley, Tolman et al. 1996; Duggal, Pratap et al. 2005). These influences on the microcirculation may also contribute to improved microcirculatory blood flow in the children in the cardiac comparison group.

Another cellular entity to consider is the endothelial cell glycocalyx. This is a surface matrix that lines the luminal surface of all blood vessels and consists of glycolipids, glycoproteins, and proteoglycans (Taylor and Gallo 2006). The glycocalyx plays a protective role for the capillary wall. Studies have shown that the haematocrit, flow resistance, permeability, coagulation, and leukocyte adhesion may all be regulated by the glycocalyx (Vink and Duling 1996; Pries and Kuebler 2006). Marechal et al. demonstrated that administration of intravenous LPS into rats induced microvascular dysfunction due to loss of the endothelial glycocalyx which improved when activated protein C was administered, limiting degradation of the glycocalyx (Marechal, Favory et al. 2008). It is highly likely that a mechanism such as this will be fundamental in the pathogenesis of microvascular dysfunction associated with severe sepsis in humans.

A limitation of this work is that the image analysis is manual and time consuming if all microcirculation variables are computed. A recent study has found that MFI can be reasonably quickly estimated at the bedside by a suitably experienced individual. For microcirculation measurements from SDF to be used to maximse clinical care and as an endpoint for resuscitation, the outcome measures derived from the images must be assessed quickly

5.6 **Conclusion**

These results have shown that the assessment of the microcirculation in children is possible and interpretation of images is repeatable. The findings are pertinent to the diagnosis, management and prognosis of septic shock in children. A new part of the circulation has been visualised in children for the first time.

Chapter 6

Soluble mediators and the microcirculation in meningococcal disease

6.1 Introduction

6.1.2 Vasoactive mediators

A normally functioning endothelium is a requirement for efficient tissue perfusion. Sepsis is a process of intravascular inflammation. The normal response to this is a complex immunologic cascade that ensures a rapid response to neutralise the bacterial invasion. An inadequate immunologic defence may allow infection to become established. Alternatively an excessive or poorly regulated response may harm the host by an exaggerated release of inflammatory mediators. Cytokines and immune modulators mediate the clinical manifestations of sepsis leading to continued activation of leukocytes, macrophages, and lymphocytes. All of these processes can create a destructive immunologic imbalance.

6.1.2.1 Cell Adhesion Molecules

The attraction of activated leucocytes to areas of tissue damage and infection is a vital part of the host immune response to eradicate infection. It involves a three stage process. Leucocytes initially roll along the vascular endothelium. They then adhere to the endothelium and migrate across it. Leucocyte rolling is mediated through the expression of selectins on the surfaces of leucocytes and the endothelium. This is regulated by pro-inflammatory cytokines. The selectins are three proteins which are designated by their prefixes P (platelet), E (endothelial) and L (leucocyte). The rolling of leucocytes along the endothelium is mediated by P-selectin and E-selectin (both expressed on the endothelium) and L-selectin which is present on the surfaces of leucocytes (Carlos and Harlan 1994; Tedder, Steeber et al. 1995; Frenette and Wagner 1996; Frenette and Wagner 1996). Activation is triggered by factors, including IL-8, and causes the

adhesion of leucocytes to the endothelium surface through the binding of β2 integrins to ICAM-1 (Xu, Gonzalo et al. 1994). IL-8 is a powerful chemoattractant and activator of neutrophils. Strong adherence of leucocytes to the endothelium causes migration into tissue between endothelial tight junctions.

Adult studies have demonstrated that disease severity in sepsis is related to an increase in the expression of adhesion molecules. Cowley et al found that E-selectin, ICAM-1 and VCAM-1 were all raised with the highest levels found in patients with multi-organ failure (Cowley, Heney et al. 1994). Gando et al demonstrated that levels of E-selectin, ICAM-1 and VCAM-1 were higher in adults with sepsis related DIC than those with sepsis but no evidence of DIC. They found no difference in P-selectin levels between the two groups (Gando, Kameue et al. 2005). These findings have also been documented in paediatric studies (Whalen, Doughty et al. 2000; Krueger, Heinzmann et al. 2007). In one study, ICAM-1 and E-selectin were found to be raised in children with MCD when compared to children who presented to hospital with a fever and a rash with no eventual diagnosis of MCD. The highest levels were found in children with severe MCD as assessed by the GMSPS. P-selectin was not raised and was lower in children who died. VCAM-1 was not measured in this study (Baines, Marzouk et al. 1999).

6.1.2.2 Nitric oxide

Vascular endothelium and smooth muscle cells produce nitric oxide (NO) from inducible nitric oxide synthase (iNOS). This is mediated by pro-inflammatory mediators including endotoxin, TNF and IL-1. NO has been shown, in experimental models, to have a key role in the fall in systemic

vascular resistance underlying the hypotension and myocardial dysfunction in septic shock (Umans, Wylam et al. 1993; Wang, Ba et al. 1995; Rees, Monkhouse et al. 1998). Refractory hypotension is a prominent feature of severe MCD with children unresponsive to treatment with fluids, inotropes and conventional vasoconstrictors. NO synthesis requires the presence of L-arginine. Theoretically administration of an analogue of L-arginine (L-N monomethylarginine) should block production of NO and restore vascular tone in septic shock. A multi-centre, randomised, placebo-controlled, double-blind study in adult septic shock showed increased mortality in human septic shock in those given L-N monomethylarginine (Lopez, Lorente et al. 2004). There was an increased proportion of deaths due to refractory shock in the L-N monomethylarginine treatment group. This implied that in some patients, treatment with L-N monomethylarginine provoked a paradoxical worsening of the circulatory failure or myocardial dysfunction. The authors attributed the increased mortality in the L-N monomethylarginine treated group to a possible overcorrection of vascular tone resulting in an excessive increase in ventricular afterload compounded by inadequate inotropic support. Additionally a previously unrecognized primary effect of L-N monomethylarginine of worsening myocardial performance may have been present. NO depresses cardiac contractility and the ability of the myocardium to relax, thus maximising end diastolic filling and coronary artery perfusion. Nitric oxide also reduces responsiveness to β-adrenergic agents (Balligand, Kelly et al. 1993; Balligand, Ungureanu et al. 1993; Brady 1993; Brady and Poole-Wilson 1993; Brady, Warren et al. 1993; Grocott-Mason and Shah 1998).

Nitric oxide is a highly labile molecule and cannot easily be measured directly. The metabolites nitrite and nitrate can be measured in plasma as

an index of nitric oxide concentrations. High nitrate and nitrite levels have been reported in hypotensive children with septic shock (Wong, Carcillo et al. 1996). In a study specific to MCD peak and admission nitrate and nitrite levels were highest in the children with severe meningococcal disease when compared to those with less severe disease (Baines, Stanford et al. 1999).

There have been no studies investigating the relationship between the microcirculation and vasoactive mediators in sepsis.

6.2 Method

Patient recruitment, data collection, sublingual microvascular visualisation and blood sampling and analysis were carried out as detailed in Chapter 2.

6.2.1 Statistics

Data are presented as median and IQR and mean and standard deviation where appropriate. Correlations between variables were determined using Spearman rank correlation coefficient. Comparison between diagnostic groups was carried out using the Mann Whitney U test. A p value of <0.05 was considered statistically significant. Statistical analyses were carried out using SPSS for Windows (version 14.0), (SPSS,Inc., Chicago, Illinois). Longitudinal analysis was carried out by the Medical Statistic Department at the University of Lancaster using the MFI for capillaries (MFIc) as the factor that other variables are related to as described in Chapter 2. As the findings in Chapter 5 demonstrated a close relationship between MFI and MFIc, only MFIc is used in statistical analysis in this chapter.

6.3 Results

After informed consent, admission plasma samples were obtained from 43 children who were reported to the research fellow as 'suspected MCD'. MCD was confirmed in 33 and 10 had a presumed viral illness. Sequential plasma samples were available from 20 of the children with MCD. Twenty-three children who had blood taken during routine surgery were controls. the demographic features of these children are as described in Chapter 5.

6.3.1 ICAM-1

The median admission ICAM-1 levels per diagnostic group were: 273.9 ng/ml for controls (IQR 255.9 to 352.8); 246 ng/ml for presumed viral illness (IQR 146 to 473.9); 594.7 ng/ml for MCD non-ventilated (IQR 363.5 to 697.4) and 890.6 ng/ml for children with MCD requiring ventilation (IQR 816.7 to 986) (Figure 6.4). The admission ICAM-1 levels were significantly higher in children with MCD than those with a presumed viral illness ($p<0.01$) and controls ($p<0.01$). Children ventilated with MCD had higher admission ICAM-1 levels than those who did not ($p<0.05$). There were negative correlations between admission ICAM-1 levels and admission MFIc and PPV. There were positive correlations between ICAM-1 and HI (Table 6.1). Table 6.2 shows that there was a weak reduction of ICAM-1 over time in parallel with MFIc.

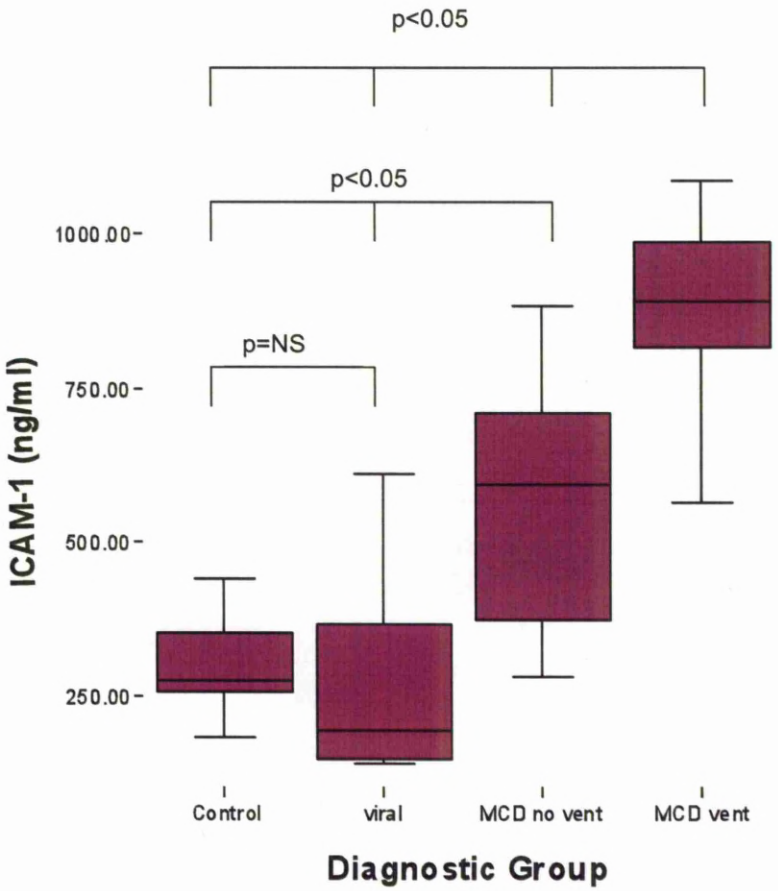

Figure 6.1. Admission ICAM-1 levels per diagnostic group

Viral – presumed viral illness

MCD no vent – children with MCD who did not require ventilation at admission to hospital

MCD Vent– children with MCD did not require ventilation at admission to hospital

6.3.2 VCAM-1

The median admission VCAM-1 levels per diagnostic group were: 406 ng/ml for controls (IQR 251.9 to 694.7); 1177.2 ng/ml for presumed viral illness (IQR 791 to 1517.4); 1465 ng/ml for MCD non-ventilated (IQR 1331.9 to 1662.6) and 1930 ng/ml for children with MCD requiring ventilation (IQR 1664 to 2023.6) (Figure 6.5). The admission VCAM-1 levels were significantly higher in children with MCD than those with a presumed viral illness ($p<0.01$) and controls ($p<0.01$). Children ventilated with MCD had higher admission VCAM-1 levels than those who did not ($p<0.05$). There were negative correlations between admission VCAM-1 levels and MFIc and PPV. There was a positive correlation between VCAM-1 and HI (Table 6.1). Table 6.2 shows that there was no relationship between VCAM-1 and MFIc over time.

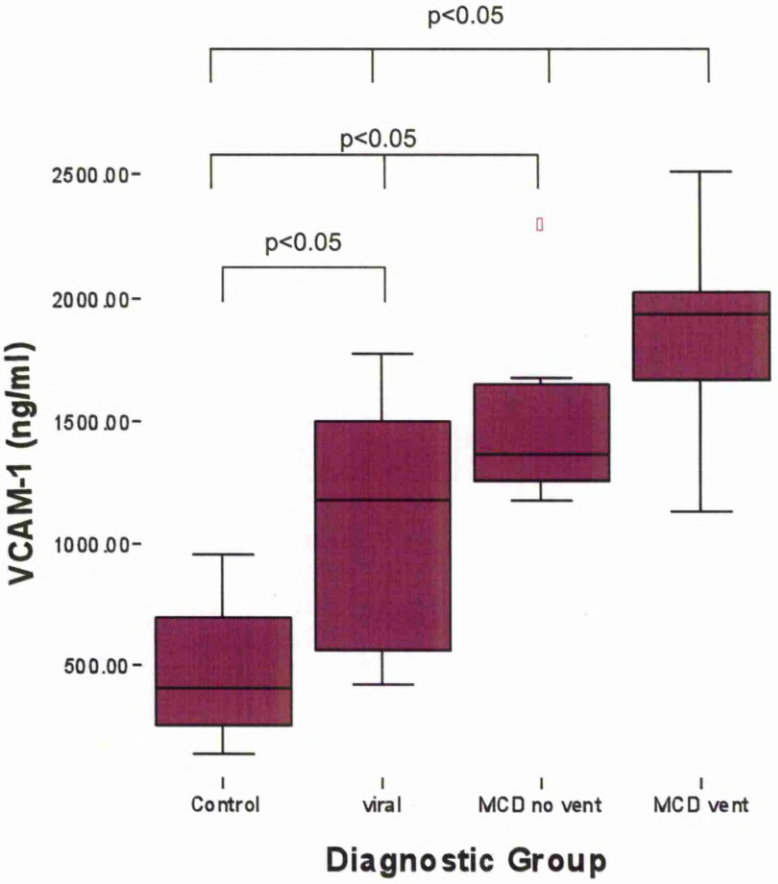

Figure 6.2. Admission VCAM-1 levels per diagnostic group

Viral – presumed viral illness
MCD no vent – children with MCD who did not require ventilation at admission to hospital
MCD Vent– children with MCD did not require ventilation at admission to hospital

6.3.3 P-Selectin

The median admission P-Selectin levels per group were: 62.8 ng/ml for controls (IQR 47.3 to 77.4); 61.7 ng/ml for presumed viral illness (IQR 30.8 to 107.9); 117.6 ng/ml for MCD non-ventilated (IQR 56.6 to 130.5) and 92.9 ng/ml for children with MCD requiring ventilation (IQR 68.9 to 98.9) (Figure 6.6). There was no significant difference in admission P-Selectin values between the diagnostic groups. There were no correlations between admission P-Selectin levels and the microcirculatory variables (Table 6.1). Table 6.2 shows that there was no relationship between P-Selectin and MFIc over time.

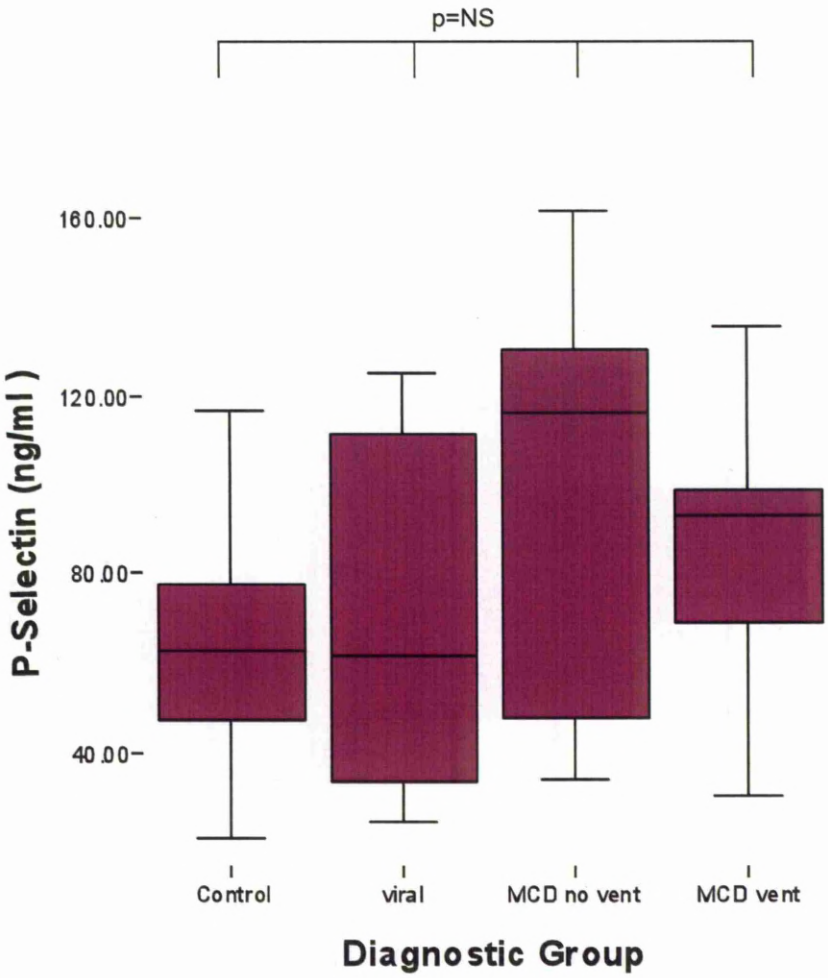

Figure 6.3. Admission P-Selectin levels per diagnostic group

Viral – presumed viral illness
MCD no vent – children with MCD who did not require ventilation at admission to hospital
MCD Vent– children with MCD did not require ventilation at admission to hospital

6.3.4 E-Selectin

The median admission E-Selectin levels per group were: 102 ng/ml for controls (IQR 91.3 to 118.5); 94.5 ng/ml for presumed viral illness (IQR 50.7 to 113.3); 202 ng/ml for MCD non-ventilated (IQR 160.5 to 298.3) and 397.6 ng/ml for children with MCD requiring ventilation (IQR 300 to 450.8) (Figure 6.7). The admission E-Selectin levels were significantly higher in children with MCD than those with a presumed viral illness ($p<0.001$) and controls ($p<0.001$). Children ventilated with MCD had higher admission E-Selectin levels than those who did not ($p<0.001$). There were strong negative correlations between admission E-Selectin levels and MFIc and PPV. There was a strong positive correlation between E-Selectin and HI (Table 6.1). Table 6.2 shows that there was no relationship between E-Selectin and MFIc over time.

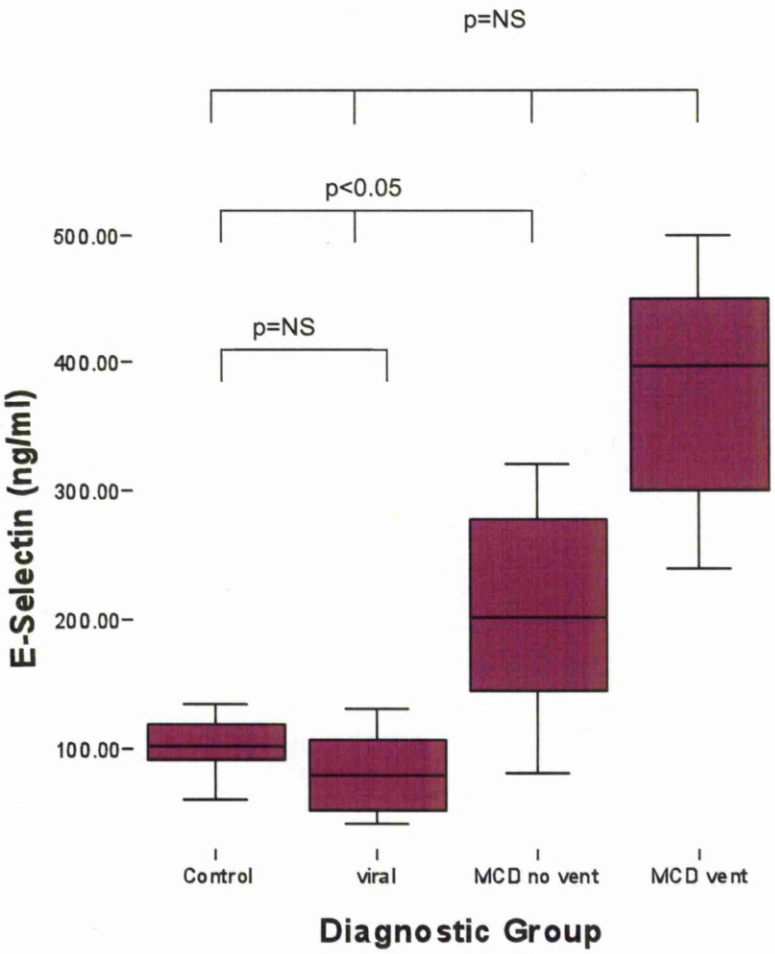

Figure 6.4. Admission E-Selectin levels per diagnostic group

Viral – presumed viral illness

MCD no vent – children with MCD who did not require ventilation at admission to hospital

MCD Vent– children with MCD did not require ventilation at admission to hospital

	MFIc	CD	PPV	PVD	HI
ICAM-1	r= -0.78 p<0.01	r= -0.1 NS	r= -0.59 p<0.01	r= -0.1 NS	r= 0.67 p<0.01
VCAM-1	r= -0.75 p<0.01	r= -0.1 NS	r= -0.52 p<0.05	r=0 NS	r= 0.64 p<0.01
E selectin	r= -0.92 p<0.01	r= 0.02 NS	r= -0.66 p<0.01	r=0.01 NS	r= 0.8 p<0.01
P selectin	r= 0.14 NS	r= -0.2 NS	r= 0.05 NS	r=-0.3 NS	r= 0.1 NS
NO	r=-0.56 p<0.05	r=-0.36 NS	r=-0.38 NS	r=-0.23 NS	r=0.67 p<0.001
IL-6	r= -0.61 p<0.01	r= -0.3 NS	r= -0.42 NS	r= -0.21 NS	r= 0.51 p<0.05
IL-8	r= -0.31 NS	r= -0.47 p<0.05	r= -0.48 p<0.05	r= -0.33 NS	r=-0.45 p<0.05
IL-1ra	r= -0.24 NS	r= 0.06 NS	r= -0.2 NS	r= 0.16 NS	r= 0.06 NS
IL-10	r= -0.39 NS	r= -0.43 NS	r= -0.56 p<0.05	r= -0.34 NS	r= -0.52 p<0.05
TNF	r= -0.14 NS	r= -0.2 NS	r= -0.2 NS	r= -0.7 NS	r= 0.06 NS

6.3.5 Nitric oxide

The median admission NO levels per group were: 41.8 nmol/ml for controls (IQR 25.6 to 62.8); 29.7 nmol/ml for presumed viral illness (IQR 24.8 to 37.2); 32.4 nmol/ml for MCD non-ventilated (IQR 19.7 to 41.6) and 70.7 nmol/ml for children with MCD requiring ventilation (IQR 59.9 to 94.3). The admission NO levels were significantly higher in children with MCD than those with a presumed viral illness ($p<0.001$) and controls ($p<0.001$). Children ventilated with MCD had higher admission NO levels than those who did not ($p<0.0001$). There was a negative correlation between admission NO levels and MFIc and a positive correlation between NO and HI (Figures 6.8 and 6.9). Table 6.2 shows that there was a weak reduction of NO over time in parallel with MFIc.

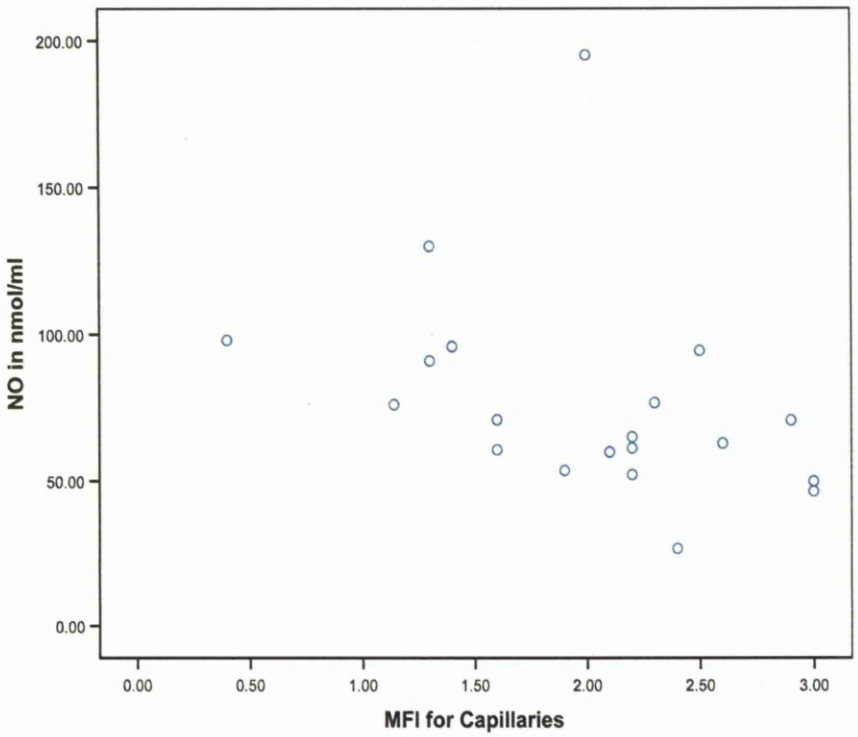

Figure 6.5. MFI for capillaries and NO at admission

Spearman rank correlation r= -0.56, $p<0.05$

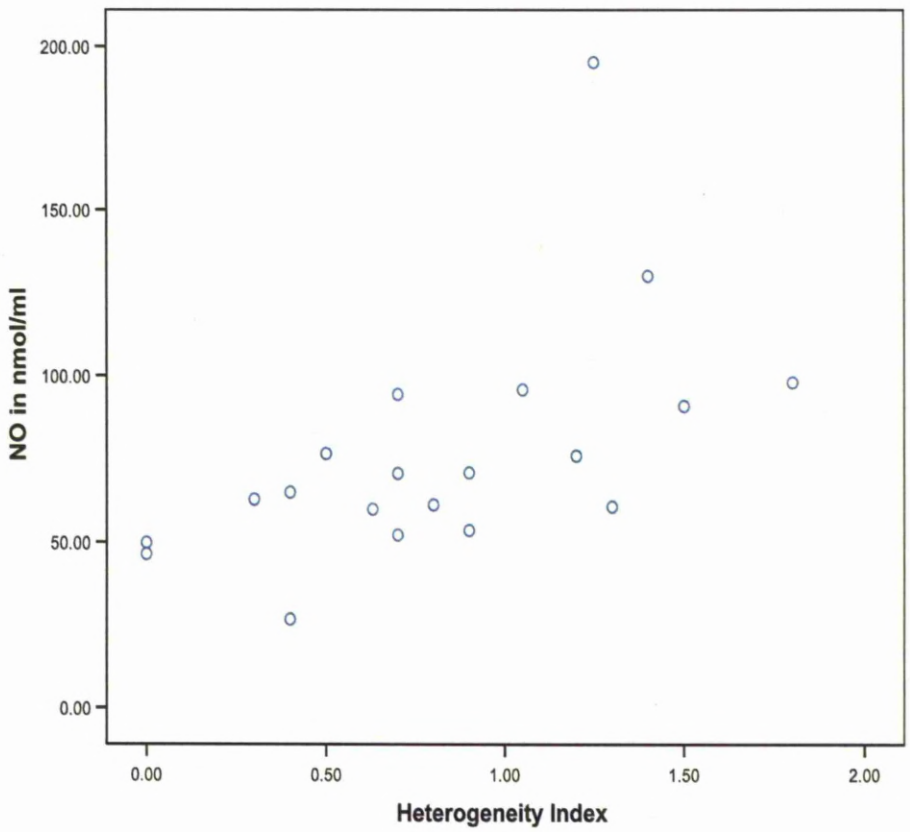

Figure 6.6 Heterogeneity index and NO at admission

Spearman rank correlation r= 0.67, p<0.001

Covariate	$\hat{p}$	CI
ICAM	-0.32	-0.52 to -0.08
VCAM	-0.07	-0.32 to 0.12
P Selectin	0.17	-0.05 to 0.39
E Selectin	-0.15	-0.37 to 0.07
NO	-0.38	-0.6 to -0.16
IL-6	-0.5	-0.72 to -0.28
IL-8	-0.45	-0.67 to -0.23
IL-1ra	-0.44	-0.66 to -0.22
IL-10	-0.2	-0.42 to 0.02
TNF	0.0003	-0.22 to 0.22

Table 6.2. Longitudinal analysis comparing changes of laboratory variables with MFIc over time

6.3.6 Cytokines

The relationship between admission levels of IL-1Ra, IL-6, IL-8, IL-10 and TNF and microcirculation variables and their changes over time in relation to MFIc are shown in Table 6.1 and 6.2 respectively. There were negative correlations between MFIc and IL-6 and also PPV and HI with IL-8 and IL-10.

6.4 Discussion

This study has demonstrated elevated levels of VCAM-1, ICAM-1, E-selectin and NO in children with MCD with the highest levels in ventilated patients. This study has also demonstrated a relationship between the microcirculation and vasoactive mediators in children with MCD.

Sepsis related tissue injury that leads to organ dysfunction and failure cannot be attributed to a single inflammatory mediator. IL-1b, IL-6, IL-8, IL-1Ra, IL-10, TNF, IL-4 and IL-13 have all been shown to be associated with morbidity and mortality in adults and children with sepsis. (Casey, Balk et al. 1993; Koj 1996; Bjerre, Brusletto et al. 2004; Carrol, Thomson et al. 2005). Endotoxin stimulation causes neutrophils to produce TNF and IL-1b which in turn stimulates the production of IL-6, IL-8 and IL-10. TNF and IL-1b induce fever, activates coagulation and trigger the expression of adhesion molecules.

Studies in adults with severe sepsis have shown that the expression of adhesion molecules is associated with disease severity with levels being highest in those patients with multiple organ failure. Cowley et al. demonstrated a relationship between mortality and high E-Selectin levels in adult sepsis (Cowley, Heney et al. 1994). Boldt et al. found that E-Selectin, ICAM-1 and VCAM-1 were all markedly higher in non-surviving than in surviving critically ill patients (Boldt, Wollbruck et al. 1995). The same group demonstrated that adult trauma patients showed lower plasma levels of E-Selectin, ICAM-1 and VCAM-1 than did sepsis patients indicating a more pronounced inflammatory related endothelial activation or damage in sepsis (Boldt, Muller et al. 1996).

These finding have been corroborated by paediatric studies. Whalen et al. showed that plasma VCAM-1 (but not ICAM-1 or E-selectin) was increased in children with sepsis and multi organ failure when compared to children with sepsis and no evidence of multi organ failure. They also demonstrated that ICAM-1 and VCAM-1 concentrations independently predicted multi organ failure. ICAM-1 and VCAM-1 also predicted mortality (Whalen, Doughty et al. 2000). A study specific to MCD recruited 67 children, 40 of whom had mild disease as defined by a GMSPS below 8. The E selectin values in those with severe disease were higher than in those with mild disease. P selectin concentrations were not altered in meningococcal disease, but those who died had lower concentrations. (Baines, Marzouk et al. 1999). More recently Krueger et al. studied VCAM-1, ICAM-1 and E-selectin in ventilated neonatal and paediatric intensive care patients with varying severity of multiorgan dysfunction. Dysfunction of three or more organ systems was associated with a significant increase in VCAM-1 levels. A significant difference in E-selectin serum levels was found between patients with organ failure due to an infectious cause when compared to those with organ failure of non-infectious origin. This study found no relationship between adhesion molecules and mortality although the sample size was much smaller than that of Whalen et al. (Krueger, Heinzmann et al. 2007).

The data as presented here confirms the findings of these studies with the highest values of VCAM-1, ICAM-1 and E-selectin in ventilated patients with MCD. This study also adds new data about the pathophysiological process with the visualisation of the microcirculation. For the first time it has been possible to obtain a real time view of the microvascular

dysfunction in severe childhood sepsis. The data demonstrates a relationship between dysfunctional tissue perfusion and endothelial activation. P-Selectin levels have not been observed to rise in previous studies investigating cell adhesion molecules in sepsis and this is confirmed here. There were also no correlations of P-Selectin with microcirculation variables. This may be because P selectin is stored in Weibel-Palade bodies as a presynthesised molecule within endothelial cells and so is released rapidly in the inflammatory process. Possibly the peak concentration of P-Selectin is missed so that no correlations between it and microcirculation variables are detectable. In comparison E-selectin reaches a maximum at 6 h and returns to baseline at 24 hours post cell line stimulation with endotoxin. Levels of ICAM-1 and VCAM-1 peak between 12 and 24 hours and remain elevated for at least 48 hours (Springer 1994).

The reasons for this relationship between vasoactive mediators and microcirculatory variables are likely to be complex. Truhan et al. examined 17 adult patients with angiographically proven normal coronary arteries and slow coronary flow in all three coronary vessels. They found increased levels of ICAM-1, VCAM-1, and E-selectin in patients with slow coronary flow. They concluded that this may be an indicator of endothelial activation and was likely to be in the causal pathway leading to slow coronary flow (Turhan, Erbay et al. 2005).

A clear relationship between NO and microcirculation variables has been documented in this study. This is consistent with a previous study in 19 children with MCD in which higher levels of nitrates and nitrites (the composite measures of NO) were seen in the more severely affected children and there was a strong positive correlation with PRISM scores

(Baines, Stanford et al. 1999). There are clear alterations in haemodynamic regulation in MCD producing maldistribution of oxygen delivery and arteriovenous shunting. Both processes result in the tissue hypoxia and lactic acidosis seen in severe sepsis. This cellular hypoxia is confounded due to impaired cellular oxygen extraction. In an animal model it is suggested that this occurs via mitochondrial disruption mediated by NO (Loke, McConnell et al. 1999). Mitochondria are the energy suppliers of cells. They are also involved in oxygen sensing and cell death. NO is thought to block the mitochondrial electron transfer chain at its terminal receptor. This then causes cellular hypoxia and an increase in mitochondrial derived reactive oxygen species concentrations (Poderoso, Carreras et al. 1996).

The exact mechanism causing the abnormal capillary blood flow observed using SDF in severe sepsis remains unknown. Hypoxia and hypovolaemia will inevitably play a role. This is the first study to show a relationship between the endothelial activation seen in MCD with abnormal blood flow. Direct endothelial destruction is likely to contribute to the microcirculation abnormalities seen in this study.

6.5 Conclusion

This study has demonstrated that children with severe MCD release cell adhesion molecules and NO into the bloodstream. It has also shown a relationship between these substances and the microcirculation as assessed using SDF imaging. Future work should be directed at elucidating the effects that cell adhesion molecules and NO have upon the endothelium in childhood MCD.

Chapter 7

Cardiac function in meningococcal disease

7.1 Introduction

There are several complex interacting components contributing to the pathophysiology of the haemodynamic instability seen in MCD. Endothelial activation and damage leads to capillary leakage and a reduction in the circulating vascular volume. The inflammatory response to endotoxin released by the meningococcus results in peripheral vasodilatation. Healthy adults injected with endotoxin intravenously, had lower systemic vascular resistance and arterial pressure (Suffredini, Fromm et al. 1989). This study also showed that the cardiac output in these volunteers was high as a result of a reduced afterload, or did not change from baseline readings.

Myocardial dysfunction has been shown to be present and persistent despite the correction of the common physiological disturbances in children with MCD, such as acidosis, electrolyte derangements and hypovolaemia (Mercier, Beaufils et al. 1988). There is evidence of biventricular dilation, reduced ejection fraction and fractional shortening, and a requirement for high infusion rates of inotropes to maintain cardiac output within the normal range (Boucek, Boerth et al. 1984; Mercier, Beaufils et al. 1988; Hagmolen of ten Have, Wiegman et al. 2000; Briassoulis, Narlioglou et al. 2001).

The cause of this dysfunction is unclear (Boucek, Boerth et al. 1984; Mercier, Beaufils et al. 1988; Tavernier, Li et al. 2001). Explanations range from factors influencing cardiac contractility (Krown, Page et al. 1996; Comstock, Krown et al. 1998) to myocyte damage and death (Herbertson, Werner et al. 1996; Pathan, Sandiford et al. 2002). Cytokine production and release of intracellular mediators are likely to play a role, but this has not been fully elucidated.

Pathan et al have shown that that myocardial depression was mediated in part by circulating factors and that the contractility of rat myocytes was suppressed by serum taken from patients with proven MCD. They also showed that myocardial depressant factors were released when whole blood or peripheral blood mononuclear cells of healthy donors are exposed to heat-killed meningococci (Pathan, Sandiford et al. 2002). This group went on to show that elevated IL-6 levels significantly reduced myocyte contractility and was associated with disease severity and myocardial dysfunction in patients with severe MCD (Pathan, Hemingway et al. 2004).

7.1.1 Assessment of cardiac function in sepsis

7.1.1.1 Biomarkers

The release of cTn into blood signifies myocardial necrosis (Katus, Remppis et al. 1991). An elevation of both cTnT and cTnI have been found in sepsis and are associated with a poorer prognosis (Swaanenburg et al. 1998, Turner et al. 1999b, ver Elst et al. 2000, Gunnewiek et al. 2004, Roongsritong et al. 2004, van Bockel et al. 2005). cTnT levels are associated with mortality, cardiac dysfunction and correlate with TNF, IL-6 and sTNFR levels (Turner et al. 1999a, Ammann et al. 2003) and the inter-cellular adhesion marker ICAM-1 in septic adults (Spies, Haude et al. 1998). cTnI levels have been shown to be elevated in children with sepsis and correlate with disease severity scores, the level of inotropic support and evidence of ischaemia on ECG (Thiru, Pathan et al. 2000; Briassoulis, Narlioglou et al. 2001; Gurkan, Alkaya et al. 2004). Release of cTn has been attributed to inflammatory myocardial damage and not ischaemia (Cunnion, Schaer et al. 1986). However, if a dysfunctional microcirculation is present in septic patients, ischaemia may be present in various organs, including the heart (Hersch, Gnidec et al. 1990).

With the discovery that the infusion of myocardial tissue into rats caused diuresis, ANP was the first of the natriuretic peptides to be isolated and is released from cardiac atria (de Bold, Borenstein et al. 1981). Brain natriuretic peptide (BNP) was isolated initially from porcine brains (Sudoh, Kangawa et al. 1988) and subsequently from the ventricles of the heart (Suga, Nakao et al. 1992). The natriuretic peptides lower blood pressure by diuresis and vasodilation, inhibit the renin–angiotensin system, sympathetic outflow, vascular smooth muscle and endothelial cell proliferation (Hunt, Espiner et al. 1996). Both ANP and BNP are released in response to myocyte stretching and are therefore markers of myocardial wall stress (Magga, Marttila et al. 1994). They improve myocardial performance on their release due to their natriuretic properties. NT-Pro BNP is an established biomarker for the diagnosis of heart failure in adults and is considered a (first line) diagnostic tool for congestive heart failure in acute settings and in primary care (Wright, Doughty et al. 2003; Januzzi, Camargo et al. 2005; Januzzi, van Kimmenade et al. 2006).

NT-Pro BNP is a useful laboratory marker in the identification of systolic dysfunction in adults (Charpentier, Luyt et al. 2004; Roch, Allardet-Servent et al. 2005; Tang, Huang et al. 2007; Varpula, Pulkki et al. 2007) and survival in sepsis (Brueckmann, Huhle et al. 2005). Two recent studies found that NT-Pro BNP discriminated between sepsis and non-sepsis related left ventricular failure in children (Domico, Liao et al. 2008) and is a useful tool in predicting septic shock (Fried, Bar-Oz et al. 2006).

7.1.1.2 Cardiac systolic, diastolic and global function assessment

Systolic function

Conventional two-dimensional M-mode echocardiography has been used in paediatric studies to evaluate sepsis related cardiac systolic dysfunction. (Boucek, Boerth et al. 1984; Hagmolen of ten Have, Wiegman et al. 2000; Briassoulis, Narlioglou et al. 2001; Gurkan, Alkaya et al. 2004). These studies have used either fractional shortening (FS) or the ejection fraction (EF) of the left ventricle.

FS measures the difference in left ventricular (LV) diameter during the cardiac cycle. It is calculated using the following formula:

$$\frac{\text{LV end-diastolic diameter} - \text{LV end-systolic diameter}}{\text{LV end-diastolic diameter}}$$

Figure 7.1 shows the measurement of FS. Systolic dysfunction is classified as mild in the range of 27% to 30% and more severe below 27% (Gutgesell, Paquet et al. 1977; Snider AR 1990).

EF measures the volume changes during the cardiac cycle and is determined from the formula:

$$\frac{\text{LV diastolic volume} - \text{LV systolic volume}}{\text{LV diastolic volume}}$$

A value of less than 50% represents systolic dysfunction (Snider AR 1990).

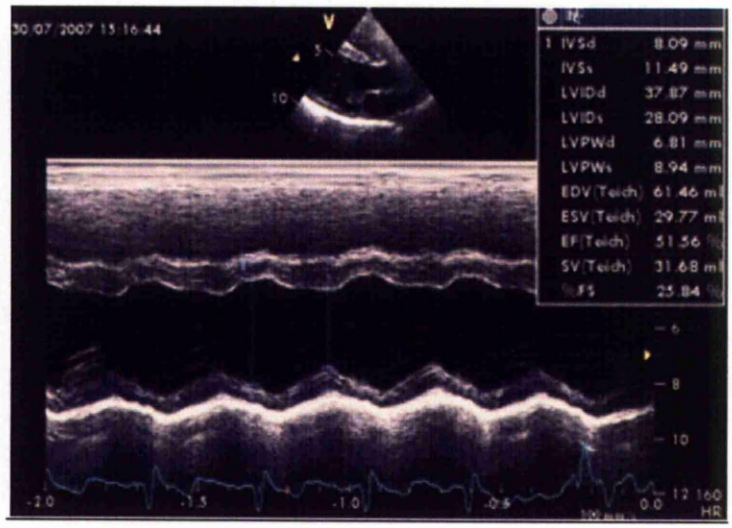

Figure 7.1 Echocardiographic M-mode recording to measure Fractional Shortening. (Own image).

Diastolic function.

Left ventricular filling pressure and diastolic function variables can be derived from flow measurements across the mitral valve at the level of the tips of the mitral valve leaflets. The early mitral peak flow velocity (E wave), atrial peak flow velocity (A wave), and the early mitral to atrial peak flow velocity ratio (E/A) are all methods of LV diastolic function assessment. There are several important factors in Doppler evaluation including sample volume and placement, recording speed, beam alignment and echocardiography machine settings (Appleton, Jensen et al. 1997). The initial abnormality in diastolic dysfunction is loss of the elastic recoil in early diastole. Diastolic dysfunction manifests as abnormal relaxation and there is a lower than normal E/A ratio. If this dysfunction progresses then active myocardial relaxation reduces and ventricular compliance becomes abnormal. In this state mitral inflow Doppler patterns are mildly abnormal. As diastolic dysfunction progresses, the E wave increases and the A wave becomes smaller. This is called the restrictive pattern and if it persists despite manipulation of filling pressure, then it is irreversible and is called stage IV LV diastolic dysfunction. These later changes are chronic and will not be seen in the acute setting such as severe sepsis. (Appleton, Hatle et al. 1988; Appleton, Jensen et al. 1997; Ommen and Nishimura 2003). Different loading conditions have effects on transmitral flow velocity (Wood and Picard 2004). Acute decrease in preload lowers E and A waves. Increase in preload has an opposite effect. The E wave decreases and the A wave increases if afterload is increased (Yamamoto, Redfield et al. 1996).

Tissue doppler imaging (TDI) measures the velocity of the inter-ventricular septum and lateral mitral annulus during the cardiac cycle and provides an

estimate of LV diastolic function (Ommen 2001). Conventional Doppler echocardiography measures blood flow at low amplitude and high frequency. Myocardial tissue velocities, however, have a higher amplitude and lower frequency. The TDI values recorded are a peak systolic annular velocity (Sa), a peak annular velocity during early diastole (Ea) and a peak annular velocity during atrial contraction (Aa) (Hiarada, Orino et al. 2000). These three distinct waveforms can be easily identified. (Figure 7.2).

Several time intervals can be obtained from the mitral annular TDI tracing. The isovolumic relaxation time (IRT) is defined as the time from the end of the systolic waveform to the beginning of the early diastolic velocity (wave). The isovolumic contraction time (ICT) is defined as the time from the end of the diastolic waveform with atrial contraction to start of the systolic velocity (wave). (Figure 7.2). Peak early diastolic myocardial velocity (Ea) is measured at the lateral corner of the mitral valve annulus and is a more reproducible measurement than the septal annular velocity (Sohn, Chai et al. 1997). Ea is a good index of LV relaxation and appears to be less sensitive to alterations in preload (Nagueh, Middleton et al. 1997; Oki, Tabata et al. 1997). These values are age and heart rate specific but normal values to account for this in children have been reported as Z score tables (Roberson, Cui et al. 2007). In combination with pulsed-wave Doppler echocardiography, Nageuh and colleagues showed that the E/Ea ratio (when the Ea is recorded at the lateral mitral annulus) correlates with invasively measured LV filling pressures in adults (Nagueh, Middleton et al. 1997; Nagueh, Mikati et al. 1998). This relationship has been confirmed in children, where patients with an E/Ea ratio of >9.8 have high LV end diastolic pressures (Oyamada, Toyono et al. 2008).

Diastolic dysfunction in septic adults has been investigated in four studies. Three studies used pulsed wave Doppler flow across the mitral valve to assess left ventricular inflow patterns and showed diastolic dysfunction. (Jafri, Lavine et al. 1990; Poelaert, Declerck et al. 1997; Munt, Jue et al. 1998). A recent study used TDI to assess the LV diastolic function of adults with severe sepsis. (Bouhemad, Nicolas-Robin et al. 2008). It confirmed the findings of the previous three studies and showed that the impairment of left ventricular relaxation was reversible but associated with transient increases in cTnI, TNF, IL-8, and IL-10.

No previous studies have evaluated diastolic dysfunction in children with sepsis.

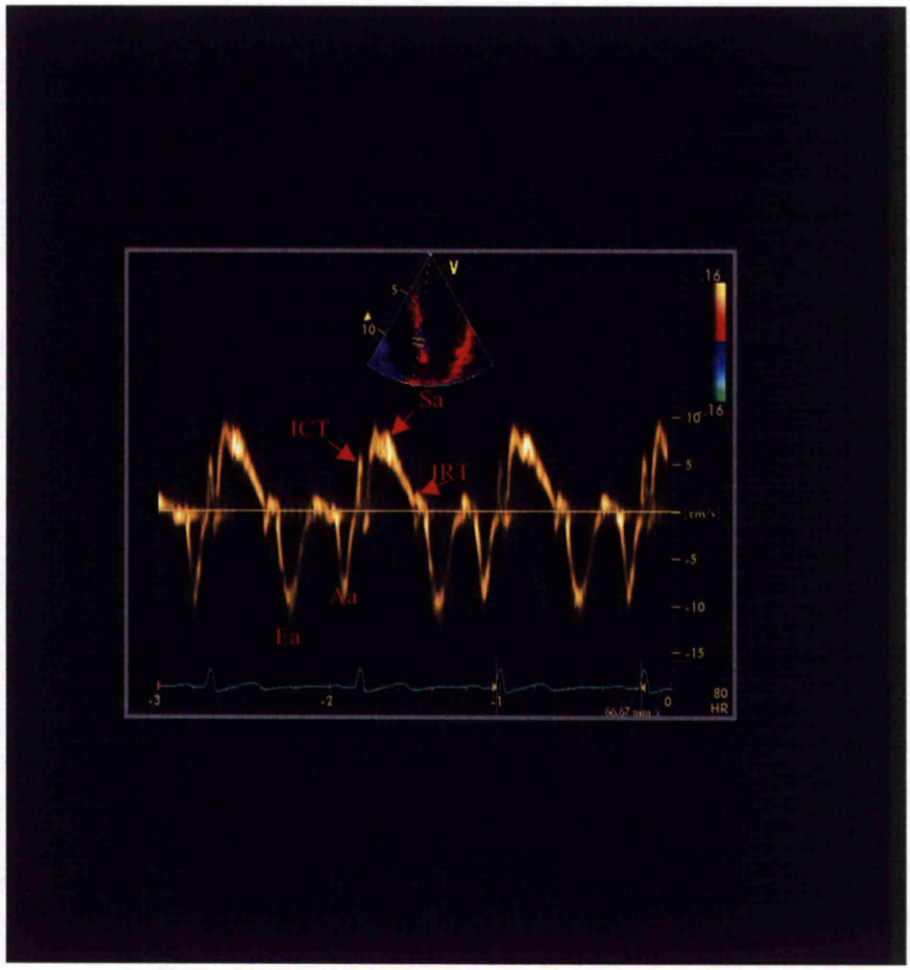

Figure 7.2. Tissue Doppler velocity curve in a healthy volunteer. Apical 4-chamber view. The pulsed wave Doppler sample volume is positioned in the basal interventricular septum. The initial positive excursion represents the isovolaemic contraction time (ICT), Peak systole (Sa) is followed by a positive excursion represents the isovolaemic contraction time (IRT) followed. The negative waves represent early (Ea) and late (Aa) diastole. (Own image).

Global function – Tei index

Systolic and diastolic LV dysfunction can be, and often are, present simultaneously. The indices of cardiac function discussed here were designed to assess either systolic or diastolic function alone. The Tei index evaluates systolic and diastolic function and is also known as the myocardial performance index (Figure 7.3.). The calculation is made from the respective times from the start to the end of transmitral blood flow (interval a) and from the start to the end of aortic ejection (interval b) (Tei 1995; Tei, Ling et al. 1995). Interval *a* is the sum of the ICT, ejection time (ET), and IRT, and *a* - *b* is the sum of ICT and IRT. The ICT is the time interval from the mitral valve closing to the aortic valve opening and IRT is the time from aortic valve closure to mitral valve opening. They are indices of systolic and diastolic function respectively and become prolonged as function deteriorates. The ICT and IRT are both dependent on the heart rate. The ET measurement is determined by stroke volume. It too can be shortened by systolic or diastolic dysfunction. It is also dependent on heart rate. When the ICT is divided by the ET it becomes *independent* of heart rate and a decrease in systolic function can be identified more clearly. Similarly the IRT also becomes independent of the heart rate when divided by the ET. The sum of the ICT/ET and IRT/ET is the Tei index and increases when there is impairment of either systolic or diastolic function (Pellett, Tolar et al. 2004).

The Tei index was initially measured by pulsed wave Doppler ultrasound. A limitation of using pulsed Doppler is that the interval between the end and onset of mitral inflow and ejection time are measured sequentially and not in the same cardiac cycle. Heart rate variability can therefore affect the

findings. TDI enables the simultaneous measurement of both the systolic and diastolic components of the cardiac cycle and in therefore a superior method of evaluating the Tei index. Studies have shown good reproducibility using this method (Harada, Tamura et al. 2002; Cui and Roberson 2006). Normal values have been established for the left ventricle in children and are 0.35 ± 0.03. A value of 0.40 or higher in the left ventricle is abnormal (Eidem, Tei et al. 1998).

No studies in adults or children have evaluated the Tei index in sepsis.

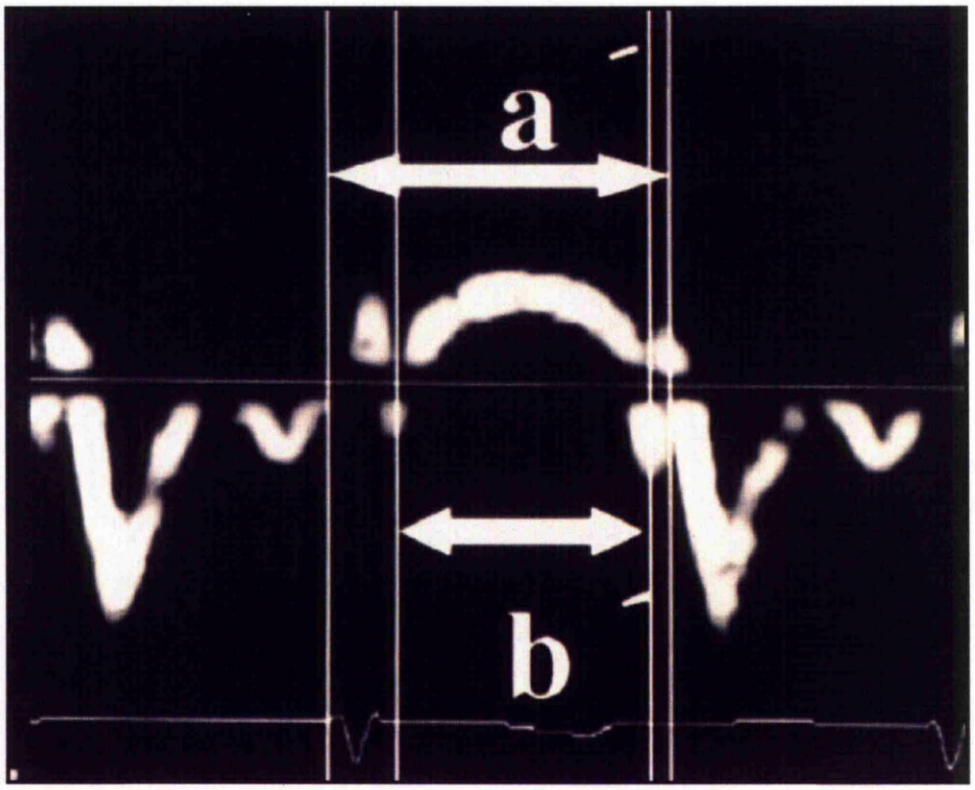

$$\text{Tei index} = \frac{a-b}{b}$$

Figure 7.3

Schematic of Doppler flow velocity to represent the time intervals necessary to derive the left ventricular Tei index. Time interval 'a' is the end of mitral inflow to the start of mitral inflow (of the next cycle), it includes the isovolumic contraction time (ICT), ejection time and the isovolumic relaxation time (IRT). Time interval 'b' is the duration of the ejection time (the left ventricular outflow).

Taken from Pellett, A. et al. (2004). "The Tei index: methodology and disease state values." Echocardiography **21**(7): 669-72.(Pellett, Tolar et al. 2004)

7.1.1.3 Cardiac output measurement

Cardiac output (CO) can be measured non-invasively, using Doppler ultrasound. The measurements needed are the blood velocity in the ascending aorta and the cross sectional area of the aortic valve. The calculation (below) gives the stroke volume and when this value is multiplied by the heart rate gives the CO. This method of evaluating CO has been well validated in adult and child studies (Chew and Poelaert 2003; Brueckmann, Huhle et al.). However CO varies with size and is indexed for body surface area (CO/BSA) to give the cardiac index (CI). The normal (resting) value for cardiac index is between 3 l/min/meter^2 to 5 l/min/meter^2 (Ceneviva, Paschall et al. 1998). Ceneviva et al showed that 60% of a group of children with septic shock had a low cardiac index.

To calculate the volume of blood coming into the ascending aorta from the left ventricle the temporal mean velocity is measured but certain assumptions need to be made. These are that the flow across the aortic valve is laminar, the ultrasound probe is placed in the suprasternal notch such that the Doppler beam is parallel to the flow in the ascending aorta to ensure that maximal velocities are recorded. The mean velocity is calculated from the area under the Doppler curve also known as the velocity time integral (VTI). This is repeated over several cardiac cycles to obtain a mean value. The area under the Doppler curve can be calculated using software incorporated into the echocardiographic machine and is shown in Figure 7.4. The systolic aortic diameter (DAo) then has to be measured using M mode.

From this measurement the aortic cross sectional area can be determined using the formula:

$$\text{Aortic cross sectional area} \times DAo^2$$

Stroke volume is then calculated as follows:

$$\text{VTI} \times \text{Aortic cross sectional area.}$$

CO is calculated by SV x heart rate.

The systemic vascular resistance can be calculated once cardiac output is known using the following formula:

$$\text{Systemic vascular resistance (SVR)} = \frac{MAP - CVP}{CO}$$

Normal values lie between 11 to 15 Woods units.

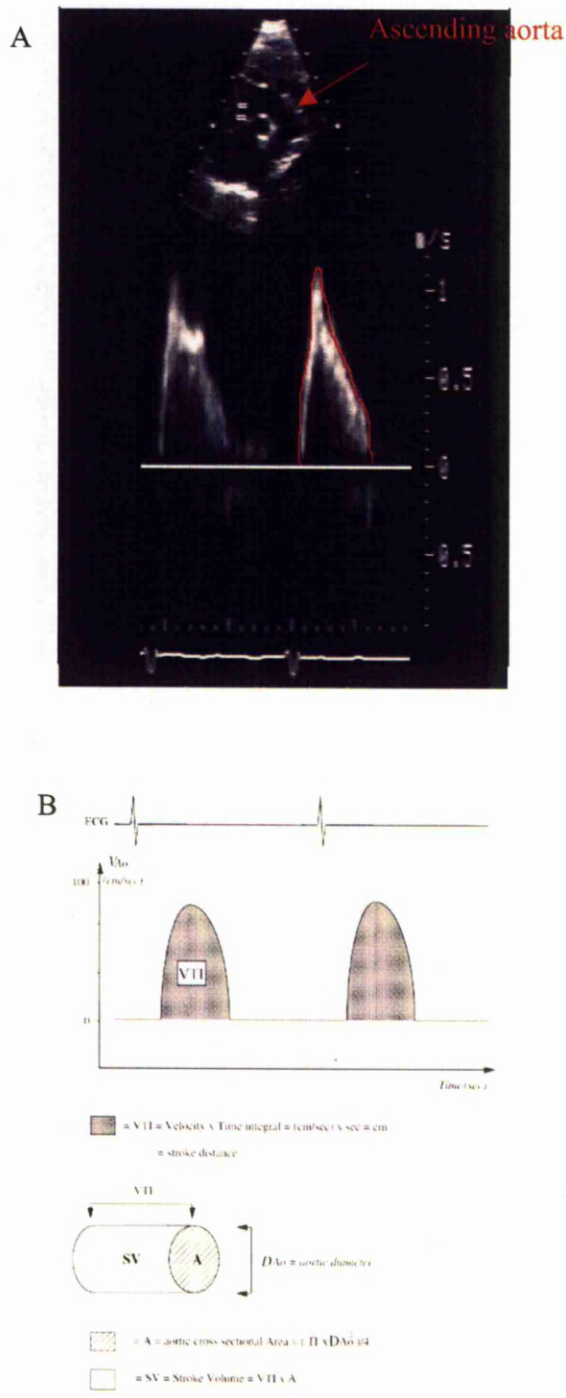

Figure 7.4. Principles of cardiac output calculation using echocardiography.

A. The pulsed wave doppler gate is placed in the ascending aorta. The velocity recording is shown beneath. The velocity recording's outline is traced (red line). The area under the red line indicates the velocity time interval (VTI)

B. Schematic representing the area under the maximum aortic velocity represent the stroke

7.2 Method

7.2.1 Patients

Patient recruitment, data collection and blood sampling are detailed in Chapter 2. Forty three children were recruited due to the diagnosis of 'suspected MCD'. After informed consent, admission and sequential plasma samples were obtained from 23 and 20 children respectively. The 20 children in whom sequential blood sampling was possible were all ventilated and admitted to PICU. In one of these children repeated echocardiography for longitudinal analysis and any measurement of TDI velocities (including admission) were not possible – only an admission echocardiogram was possible. This was due to an acute clinical deterioration during initial echocardiography which was therefore not repeated. Twenty-three children undergoing routine surgery formed the control group.

Sixteen of the 20 children admitted to PICU were ventilated using controlled mechanical ventilation. Tidal volume was set between 6 and 9 ml/kg, and respiratory rate was adjusted by the clinician in charge of the patient to achieve acceptable $PaCO_2$ values. Inspiratory time was between 0.3 and 0.6 seconds, according to the age of the child, set by the treating physician. FiO_2 and positive end expiratory pressure (PEEP) were adjusted to maintain arterial oxygen saturation SaO_2 at ≥ 90% throughout the study period. The remaining 4 children were ventilated using high frequency oscillation. Inspiratory time was fixed at 33% and FiO_2 adjusted to maintain arterial oxygen saturation Sao_2 at >=90% throughout the study period. The mean airway pressure and frequency were adjusted to achieve acceptable PaO_2 and $PaCO_2$ values respectively. All patients were sedated with morphine and midazolam initially. Mean arterial pressure was measured

using an indwelling arterial catheter (Hewlett Packard Hp monitors). CVP was assessed from an indwelling central venous line (Hewlett Packard Hp monitors).

7.2.2 Echocardiography

Systolic and diastolic cardiac function measurements, cardiac output and the Tei index were assessed using the methods described in Chapter 2 and this chapter. An abnormal FS was defined as < 27%. Tissue Doppler values were abnormal if they were 1.5 standard deviations (Z-scores) from the mean as per published results for normal children (Roberson, Cui et al. 2007). Cardiac output was calculated and analysed as described in section 7.1.1.3.

7.2.3 Troponin

cTnI and cTnT were measured by an automated Troponin I and T STAT (Short Turn Around Time) assay, using Elecsys 10:10 apparatus, Roche Diagnostics GmbH, Mannheim. This involves an Electro-Chemical-Luminescence ImmunoAssay (ECLIA). An abnormal result was defined as >0.2 ng/ml for cTnI and >0.01 ng/ml for cTnT.

7.2.4 NT-Pro BNP

Plasma NT ProBNP concentrations were determined using a commercially produced ELISA kit, 96 well plate, Biomedica Gruppe, Austria, according to the manufacturer's instructions.

Samples and Controls were diluted 1:10 in assay buffer before being assayed (10 µl sample + 90 µl assay buffer). The samples were defrosted once only for the assay having been frozen since collection.

7.2.4a Reconstitution

Wash buffer: Diluted with the wash concentrate 1:20 i.e. 50 ml wash buffer + 950 ml distilled water.

Standard: 3 mls of assay buffer was pipetted into the vial and left at room temperature (18-26°C) for 30 min. The reconstituted standard has a concentration of 1,000 fmol/ml. Control: 250 µl of distilled water was pipetted into the vial and left at room temperature for 30 min.

A 1:2 dilution series with the reconstituted standard and Assay buffer was prepared as follows:

Standard1 = reconstituted standard (1.000 fmol/ml)

500 µl Standard1 + 500 µl Assay buffer = Standard2 (500 fmol/ml)

500 µl Standard2 + 500 µl Assay buffer = Standard3 (250 fmol/ml)

500 µl Standard3 + 500 µl Assay buffer = Standard4 (125 fmol/ml)

500 µl Standard4 + 500 µl Assay buffer = Standard5 (62.5 fmol/ml)

500 µl Standard5 + 500 µl Assay buffer = Standard6 (31.25 fmol/ml)

7.2.4b Method

200 µl Assay buffer was placed into the wells marked as blank in duplicate.

200 µl diluted standard, diluted sample or diluted control were placed in duplicate into their respective wells leaving the blank.

50 µl Conjugate was placed into each well, except the blank.

The plate was covered with a plate cover and incubated overnight at 4°C in the dark.

The plate was washed five times with 300µl of diluted wash buffer using an automated plate washer. Any remaining wash buffer was removed by hitting the inverted plate against paper towel after the last wash.

200 µl of substrate was pipetted into each well.

The plate was covered with a plate cover and incubated for 20 min at room temperature in the dark.

50 µl of Stop solution was pipetted into each well.

The absorbance at 450 nm was read immediately, subtracting the blank well absorbance from all other values. A standard curve was constructed from the standard values using commercially available software and sample concentrations were obtained from this standard curve. The concentration of a sample was taken from the mean of the two wells

7.2.4c Performance characteristics of the assay

The minimum detectable concentration of the assay was 5 fmol/ml with an inter-assay coefficient of variation of 4-6.5 % and an intra-assay coefficient of variation of 3.8-4.4 %. A panel of blood donors (n=110) showed a median of 208 fmol/ml (95th percentile 300 fmol/ml).

7.2.5 Cytokine determination

Cytokines were measured using Luminex technology as described in Chapter 5.

7.2.6 Statistics

Data are presented as median and IQR and mean and standard deviation where appropriate. Correlations between variables were determined using Spearman rank correlation coefficient. A p value of <0.05 was considered statistically significant. Receiver operator characteristic (ROC) plots were used to calculate the area under the curve (AUC) to compare the performance of NT-Pro BNP, PCT and CRP in the identification of septic shock in MCD. Inter- and intraobserver agreement for measurements of FS was obtained by selecting 10 random images for two independent

observers to assess. Agreement is expressed as Bland-Altman plots. Statistical analyses were carried out using SPSS for Windows (version 14.0), (SPSS, Inc., Chicago, Illinois) and Analyse-It Software v.1.62 for Microsoft Excel (Analyse-It Software, Leeds, UK).

7.3 Results

Sixty six children were included in this study. Twenty children had severe MCD requiring ventilation and admission to PICU. All of these children had septic shock. Two children required limb amputations but there were no deaths. Thirteen children with MCD did not require intensive care admission, 10 children had a presumed viral illness and there were 23 controls (See Chapter 2).

7.3.1 Cardiac Troponin and systolic function

Among the 43 patients recruited at admission to hospital due to possible diagnosis of MCD, 12 (29%) had an increase in cTnI and cTnT within 24 hours of admission to hospital. cTnT and cTnI were both elevated in these 12 cases, and were highly correlated. (Spearman rank $r=0.98$, $p<0.001$).

All of the children with abnormal cTn values were confirmed MCD cases, receiving ventilatory respiratory support. They represented 60% of the 20 children admitted to PICU with severe MCD. The clinical characteristics of these 20 patients are summarized in Table 7.1. None of the children with a presumed viral illness or those with a confirmed diagnosis of MCD who did not require admission to PICU had an elevated cTnT or cTnI. In patients with a raised cTn the peak concentrations (median, IQR) were 1.0 ng/ml (0.32–2.3 ng/ml) for cTnI and 0.38 ng/ml (0.19–1.0 ng/ml) for cTnT as shown in Figure 7.5.

An increased cTn within 24 hours of admission was seen in 12 children (60%). 10 of the 20 children admitted to PICU had systolic dysfunction and a rise in cTn. Two of the ventilated children had raised cTn values but normal cardiac systolic function. Two children had persistent systolic dysfunction at 6 hours post admission, both with elevated cTn. All children had normal systolic function at 12 hours after admission. The correlations between systolic function, measured by FS, at admission and the peak in cTnT and cTnI were -0.68 ($p<0.001$) and -0.73 ($p<0.005$) respectively.

The demographic, clinical, and biological markers of children admitted to PICU with raised cTnI and cTnT were compared to the PICU patients with normal concentrations (Table 7.1). The two groups differed in the duration and type (inotrope score) of inotropic support administered, duration of ventilatory support, systolic function and the values of cytokine measurements (Table 7.1). The male-to-female ratio did not differ according to cTn status. Patients with elevated cTn values had higher GMSPS scores at admission but not PRISM III or the PELOD scores (Table 7.1). Significant positive correlations were found between peak cTn concentrations and length of hospital and PICU stay, length of ventilatory and inotropic requirement whilst on PICU, disease severity assessments scores, resuscitation volume required, and admission lactate value. (Table 7.2)

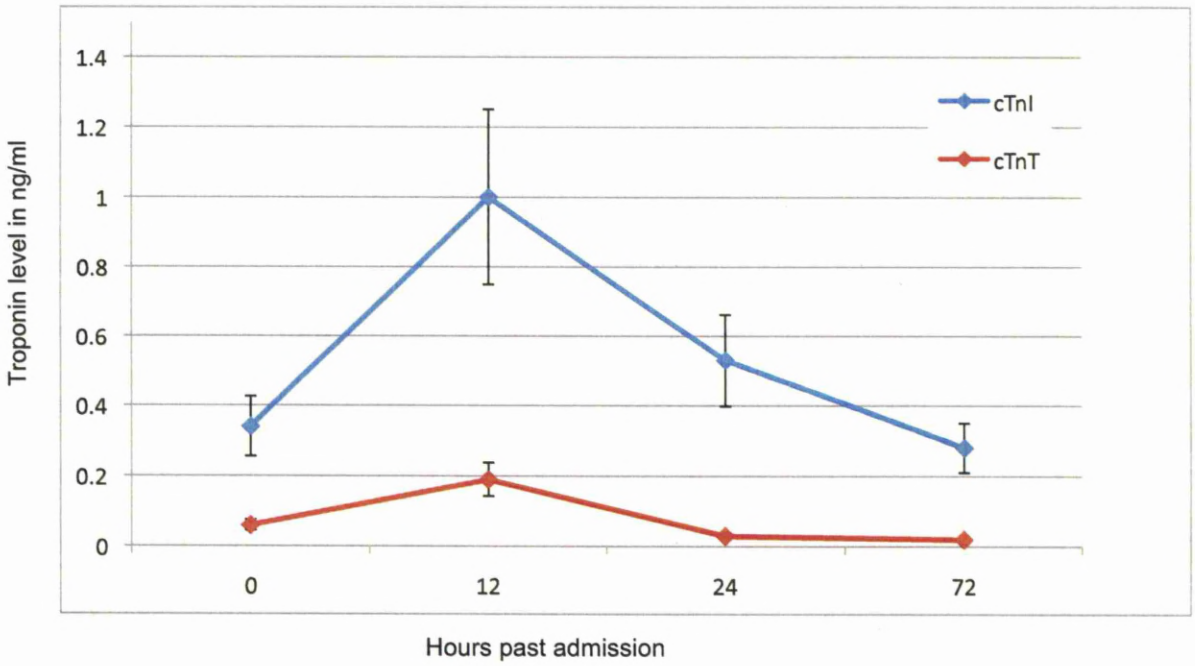

Figure 7.5 Median peak cTnI and cTnT per time point with interquartile ranges in 20 children with severe MCD.

	Raised Troponin	Normal Troponin	p value
Total number	12	8	--
Age in months (range)	2.54 (0.83 to 15.2)	1.42 (0.5 to 15.3)	NS
Sex (male %)	4 (33%)	4 (50%)	NS
GMSPS at admission (IQR)	12 (10 to 14)	9 (3.5 to 12.5)	<0.05
PELOD at admission (IQR)	19 (15 to 22)	12.5 (7 to 17.5)	NS
PRISM III at admission (IQR)	19 (6.3 to 31)	20 (15.5 to 25.5)	NS
Duration of ventilation in hours (IQR)	57 (18 to 96)	30 (17.5 to 42.5)	<0.01
Duration of inotropic requirement in hours (IQR)	40 (23 to 57)	18 (8 to 28.5)	<0.01
Inotrope score at admission	39 (6 to 82)	10 (6 to 22)	<0.01
Resuscitation volume in ml/kg (IQR)	110 (50 to 162)	80 (50 to 110)	NS
FS% at admission (IQR)	22 (15 to 29)	35 (27.5 to 42.5)	<0.001
Cardiac index in litres/m^2/min at admission (IQR)	6.5 (3.5 to 10)	5.9 (3.1 to 8.8)	NS
Peak IL-6 in pg/ml (IQR)	6821.5 (2082.8 to 16242.3)	446.5 (48.3 to 2170.1)	<0.001
Peak IL-10 in pg/ml (IQR)	740.5 (280.5 to 4661.8)	146.9 (38.1 to 834.5)	NS
Peak IL-8 in pg/ml (IQR)	1148.5 (563 to 12158.5)	220 (47.1 to 1456)	<0.01
Peak TNF in pg/ml (IQR)	292.5 (200.8 to 398.6)	68.5 (33.3 to 314)	<0.01

Table 7.1. Demographic table of 20 children admitted to PICU with severe MCD. Results are expressed as medians and interquartile ranges.

	Peak cTnT		Peak cTnI	
	R	**P value**	**R**	**P value**
Duration of Hospital Stay (days)	0.65	<0.0001	0.65	<0.0001
Duration of PICU stay (days)	0.72	<0.0001	0.72	<0.0001
Duration of ventilatory requirement (hours)	0.76	<0.0001	0.76	<0.0001
Duration of inotropic requirement (hours)	0.75	<0.0001	0.75	<0.0001
Resuscitation Volume (ml/kg)	0.67	<0.0001	0.66	<0.01
Lactate	0.63	< 0.0001	0.57	<0.005
Maximum GMSPS	0.67	< 0.0001	0.67	< 0.0001
PRISM III	0.46	<0.01	0.48	<0.005
PELOD	0.6	<0.0001	0.62	<0.0001
Peak Inotrope score	0.6	<0.0001	0.61	<0.01

Table 7.2. Multiple Linear Regression Analysis of factors affecting peak Troponin T

Adjusted R Square= 0.23, $F=7.57$, $p<0.05$ (using stepwise model)

The cTnI and cTnT concentrations were normalised by logarithmic transformation and then entered into a multiple linear regression analysis to assess the independent predictor ability of cTnI and cTnT for duration of ventilatory requirement after adjustment for the following independent variables: age, gender and length of illness. Step-wise multiple linear regression showed that peak cTnT and cTnI were independent factors associated with the duration of ventilation. Excluded from the model were age, sex and length of time of illness (and rash) prior to hospitalisation. The regression model gives the following equation for the estimation of ventilatory time:

Duration of ventilation in hours = 18.6 + 68.3 x (peak cTnT) - 1.36 x (peak cTnI)

Predictor variable	B coefficient	P value	95% CI
Peak cTnT	68.3	<0.001	32 to 104.6
Sex	0.65	0.62	NA
Age (years)	-0.15	0.32	NA
Duration of illness prior to hospitalisation	0.07	0.6	NA
Duration of rash prior to hospitalisation	0.15	0.27	NA

Table 7.3. Multiple Linear Regression Analysis of factors affecting peak Troponin T

Adjusted R Square= 0.23, F=7.57, $p<0.05$ (using stepwise model)

7.3.2 NT-Pro BNP and Diastolic function

NT-proBNP analysis was carried out on plasma samples taken from 66 children at the time of admission to hospital and 12 and 24 hours post admission where possible. Levels of NT-proBNP were significantly higher in all children with MCD compared to those with a presumed viral illness (Mann Whitney U, $p<0.01$) and controls (Mann Whitney U, $p<0.01$) at admission. There was also a significant difference in NT-proBNP between children with MCD who required mechanical ventilation at admission and those that did not as shown in Figure 7.7 (Mann Whitney U, $p<0.05$). Median admission NT-proBNP per group and demographic data are shown in Table 7.4. At 24 hours after admission, levels of NT-Pro BNP in children with MCD who required mechanical ventilation were no longer significantly higher than in those that did not (Mann Whitney U, $p=0.19$).

Two (10%) children of the 20 children with MCD receiving mechanical ventilation had abnormal left ventricular filling pressure patterns with an E/A ratio less than 1 as assessed by pulsed wave Doppler. There was no significant difference in admission and pre-extubation E/A ratios (Table 7.5).

Seven of the 19 children had abnormal diastolic function at admission as assessed by the Ea wave of the TDI tracing being 2 Z-scores below the mean when accounting for heart rate and age. This represented 37% of the children receiving mechanical ventilation. The same 7 children had an E/Ea ratio above 10 indicating abnormally raised LV filling pressure. The two children with an abnormal E/A ratio were included in this group. All of the children who had evidence of diastolic dysfunction also had systolic

dysfunction with an FS of below 27%. A significant difference between admission and pre-extubation values found for Ea velocity and the E/Ea ratio (Table 7.5). Figure 7.9 shows the development of these changes over time.

Both the Ea velocity and the E/Ea ratio correlated with the total duration of inotropic support ($r=-0.71$, $p<0.01$ and $r=0.53$, $p<0.05$ respectively). There was no correlation found with inotrope scores.

	All MCD	MCD ventilated	MCD not ventilated	Presumed viral	Control
Total number	33	20	13	10	23
Sex [male]	13 [39.4%]	8 [40%]	5 [38.5%]	3 [30%]	13 [56.5%]
Age at admission in years [IQR]	2.25 [0.98 to 4.6]	2.16 [0.6 to 4.38]	2.25 [0.84 to 4.8]	1.25 [0.57 to 2.8]	2.5 [0.75 to 4.5]
Admission NT-proBNP in fmol/m [IQR]	1606 [600.0 to 2926.0]	2578 [1715 to 5315.9]	587 [509.3 – 615.0]	381.5 [184.3 – 511.0]	461.8 [365.0 to 537.4]
Admission CRP in mg/l [IQR]	88.8 [45.5 to 148.6]	126.5 [62.6 to 156.2]	60.6 [26.7 to 94.1]	4.7 [4 to 21]	All <4
Maximum GMSPS [IQR]	8 [3 to 12]	11 [9 to 12]	3 [2 to 3]	3 [2 to 3]	--

Table 7.4 Characteristics of included participants (results expressed as median [IQR])

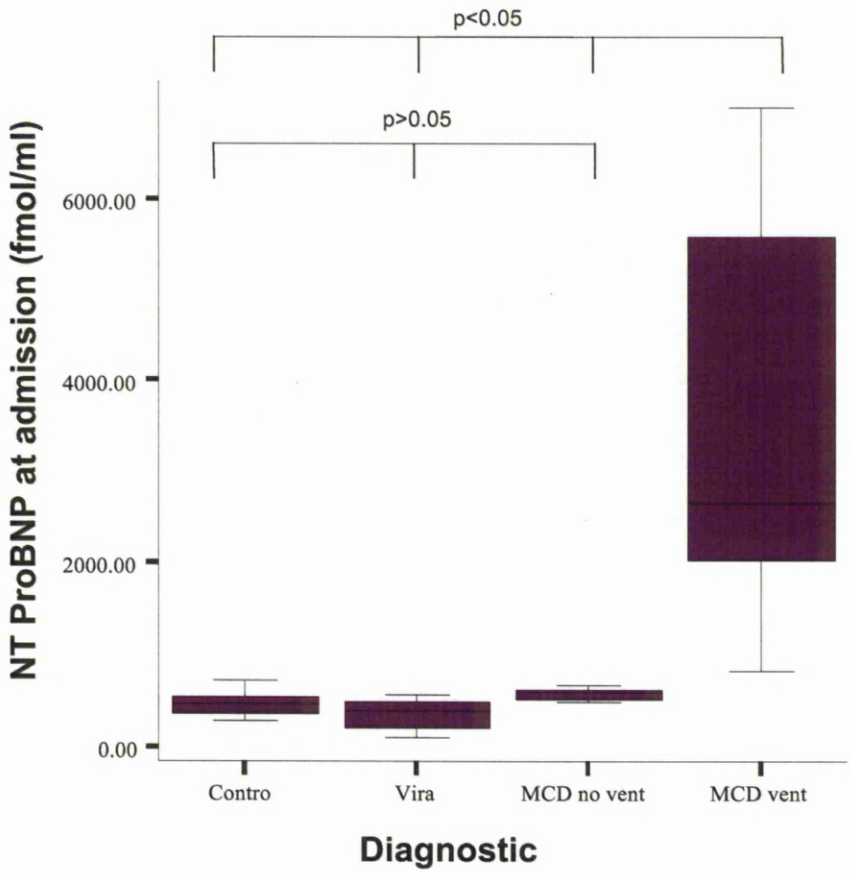

Figure 7.6 Box and whisker plot indicating NT-Pro BNP levels at admission between the diagnostic groups.

MCD no vent = children with confirmed MCD who did not require ventilation. MCD vent = children with confirmed MCD who did require ventilation.

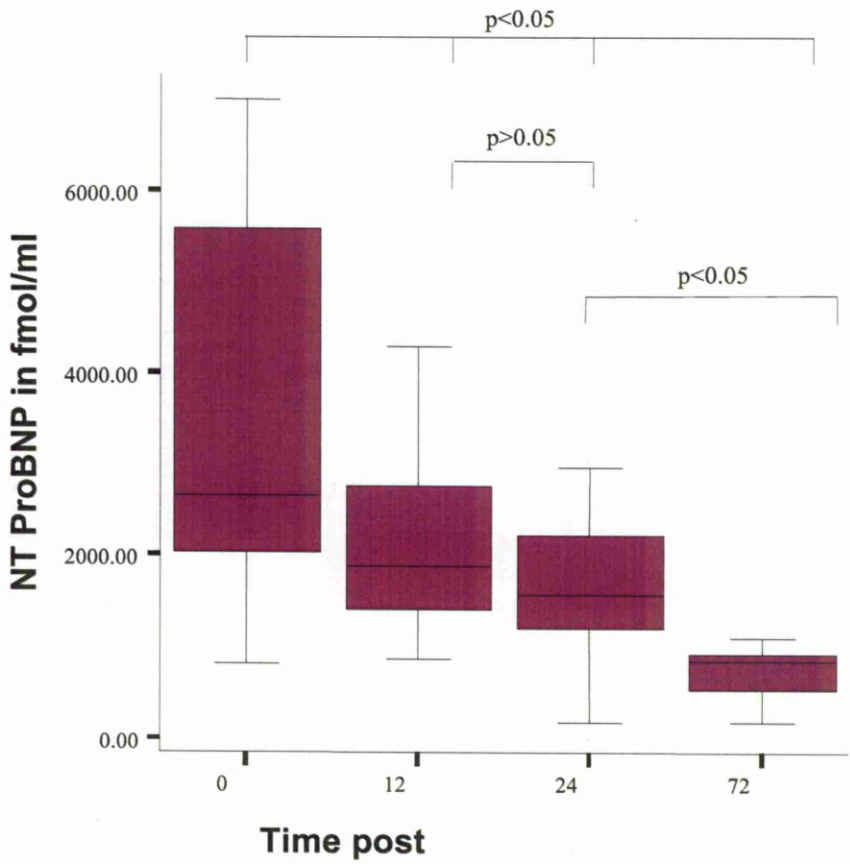

Figure 7.7. Box and whisker plot showing changed in NT-Pro BNP levels over time in children with severe MCD.

	Admission Mean ± SD	Range	Pre-extubation Mean ± SD	Range	p value
Heart rate (beats/min)	153.8±35.8	100-200	130.8±22.7	90-140	0.54
E (cm/sec)	120.7±16.5	88-158	123±17.9	92-169	0.63
A (cm/sec)	71±28	20-130	78.2±21.6	39-135	0.23
E/A	1.52±0.5	0.8-2.7	1.48±0.3	1.2-2.8	0.76
Ea (cm/sec)	10.2±3.8	3-16	12.9±2.6	8-18	<0.05
Aa (cm/sec)	71±28	20-130	72±27	30-150	0.95
Ea/Aa	1.57±0.6	0.4-2.5	2.1±0.9	0.6-4.3	<0.05
E/Ea	9.9±3.7	4-18	7.9±1.5	7-9	<0.05

Table 7.5. Diastolic echocardiographic measurements in children with severe MCD at admission to PICU.

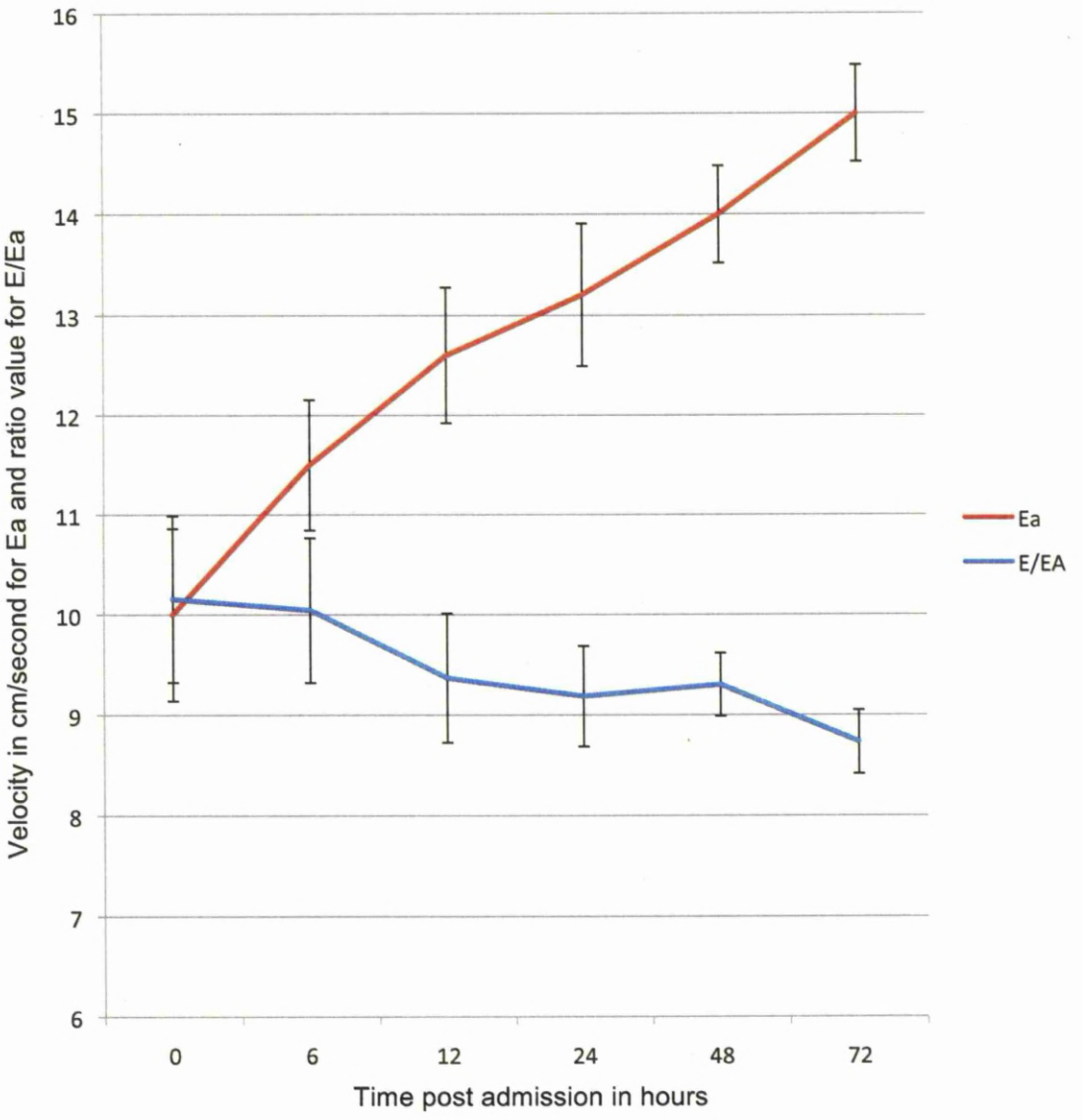

Figure 7.8. Changes in mean TDI Ea wave and E/Ea ratio in children with severe MCD over time (with standard error bars)

There were negative correlations between admission NT-proBNP and FS ($r=-0.45$, $p<0.05$), and Ea ($r=-0.57$, $p<0.05$). These relationships were no longer significant at 24 hours post admission. There was a positive correlation between NT-proBNP and E/Ea ($r=0.71$, $p<0.05$). The relationship is shown in Figure 7.10. There were also positive correlations between admission and peak NT-proBNP and duration of hospital stay, GMSPS and PRISM III, duration of inotropic requirement and resuscitation volume (Table 7.6). 36 of 43 children had peak levels at the time of first measurement. Three children had peak levels at 12 and three at 24 hours post admission.

To account for children presenting to PICU at different points of their illness, multiple linear regression analysis was used to assess the independent predictor ability of NT-Pro BNP for the E/Ea ratio after adjustment for the duration of illness, including the duration of a rash and the duration of time that the child was ventilated prior to PICU admission. The results show that even when accounting for children presenting at different times in their illness admission NT-Pro BNP levels still predict left ventricular filling pressure as assessed by the E/Ea ratio (Table 7.7)

Characteristics	Admission NT-Pro BNP		Peak NT-Pro BNP	
	R	P value	R	P value
Duration of Hospital Stay (days)	0.72	<0.0001	0.78	<0.0001
Duration of PICU stay (days)	0.8	<0.0001	0.79	<0.0001
Duration of ventilatory requirement (hours)	0.82	<0.0001	0.82	<0.0001
Duration of inotropic requirement (hours)	0.82	<0.0001	0.82	<0.0001
Resuscitation Volume (ml/kg)	0.84	<0.0001	0.84	<0.0001
Lactate	0.19	NS	0.17	NS
Admission GMSPS	0.83	<0.0001	0.82	<0.0001
Maximum GMSPS	0.80	< 0.0001	0.80	< 0.0001
PRISM III	0.78	<0.0001	0.79	<0.0001
PELOD	0.76	<0.0001	0.76	<0.0001
Admission Inotrope score	0.27	NS	0.25	NS
Peak Inotrope score	0.30	NS	0.3	NS
Fractional shortening	-0.45	<0.05	-0.44	<0.05
Ea	-0.57	<0.05	-0.6	<0.05
E/Ea	0.71	<0.05	0.7	<0.05

Table 7.6 Correlation table for admission and peak NT-Pro BNP levels.

Predictor variable	B coefficient	P value	95% CI
Admission NT-Pro BNP	0.66	<0.001	0.001 to 0.002
Duration of ventilation prior to PICU admission	-0.2	0.29	-0.3 to 0.99
Duration of rash prior to hospitalisation	0.4	0.051	-0.006 to 1.52

Table 7.7. Multiple Linear Regression Analysis of factors affecting the relationship between admission NT-Pro BNP levels and the E/Ea ratio. Adjusted R Square= 0.58, F=9.2, p<0.01 (using stepwise model)

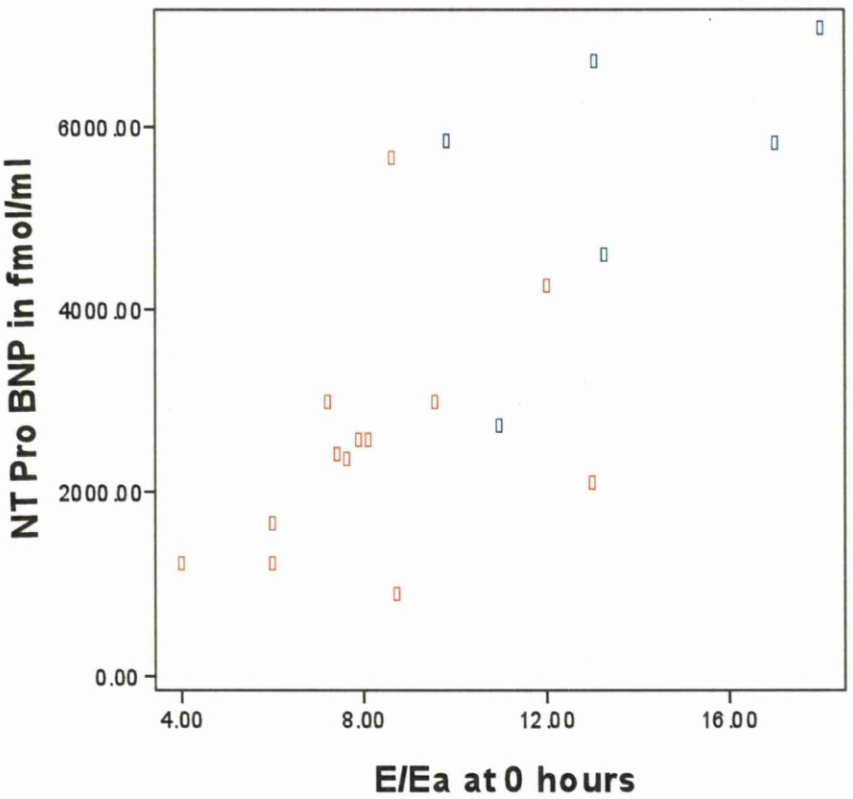

Figure 7.9. Scatter plot showing the relationship between NT-Pro BNP and left ventricular pressure as evaluated by the E/Ea ratio. r=0.71, p<0.05. Blue circles represent patients in septic shock. Red circles represent patients not in septic shock

7.3.3 Global function

The Tei index was greater than 0.40 at the time of admission in 10 children, including the 10 children that had systolic dysfunction and the 7 with diastolic dysfunction. There was a significant difference in the admission and pre-extubation Tei index value for the 19 children ($p<0.05$). Figure 7.12 shows the change in the mean Tei index over time.

There was a negative correlation between the Tei index and FS on admission. ($r=-0.47$, $p<0.05$). Positive correlations were found between the admission Tei index and total durations of ventilation, inotropic support and PICU admission ($r=0.62$, $p<0.05$, $r=0.48$, $p<0.05$ and $r=0.77$, $p<0.05$ respectively). No correlations were found with the Tei index and IL6 ($p=0.38$), IL8 ($p=0.12$), IL10 ($p=0.52$) or TNF ($p=0.39$).

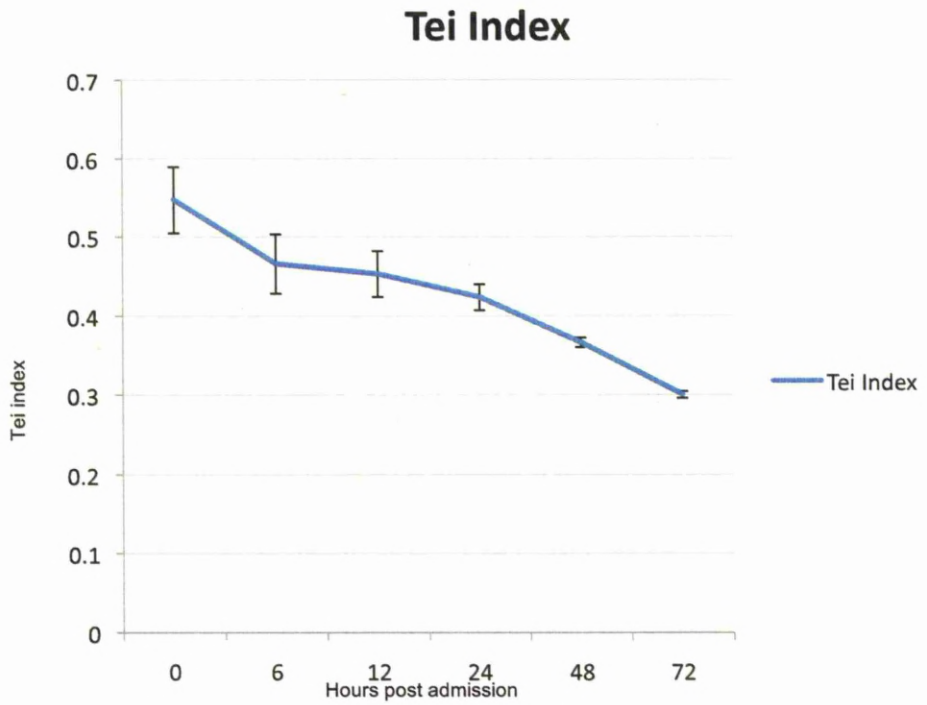

Figure 7.10. Changes in mean Tei index in children with severe MCD over time (with standard error bars)

7.3.4 Cardiac output and Index

Seven out of the 20 children (35%) admitted to PICU had a low cardiac output at the time of admission (less than 3.3 litres per minute). When indexed to take into account BSA only one child (5%) had a low cardiac index (less than 3 l/min/meter^2). Five of the 20 (25%) children had a high cardiac output (more than 5 litres per minute). When indexed to take into account BSA, 13 children (65%) had a high cardiac index (more than 5 l/min/meter^2). One of the two children who subsequently had limb amputations had a high CI and the other a low CI at the time of admission. One of these children did not have any further echocardiography carried out. The CI of the children who did had serial echocardiography normalised alongside clinical recovery.

No correlation were found between admission CI with peak cTnI ($p=0.08$, $p=0.85$ respectively), cTnT ($p=0.08$, $p=0.9$ respectively) or peak NT-Pro BNP levels ($p=0.42$, $p=0.9$ respectively). There was a statistically significant difference found between the admission and pre-extubation values for cardiac output and index for the 19 children ($p<0.05$), with values being high and returning to the normal range. There was also a statistically significant difference found in the admission cardiac output and cardiac index between children with an admission GMSPS above 8 and those below 8 ($p<0.05$ and $p<0.005$ respectively) with higher values being seen in the group with a GMSPS above 8.

Negative correlations were found between admission SVR and CO and CI (Figure 7.15 and Figure 7.16)

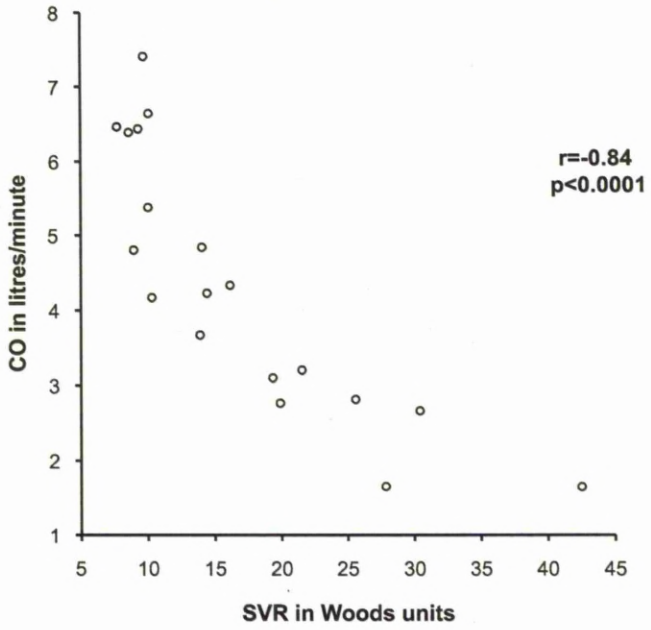

Figure 7.11. Scatter plot to display relationship between admission cardiac output and systemic vascular resistance in 20 children with severe MCD

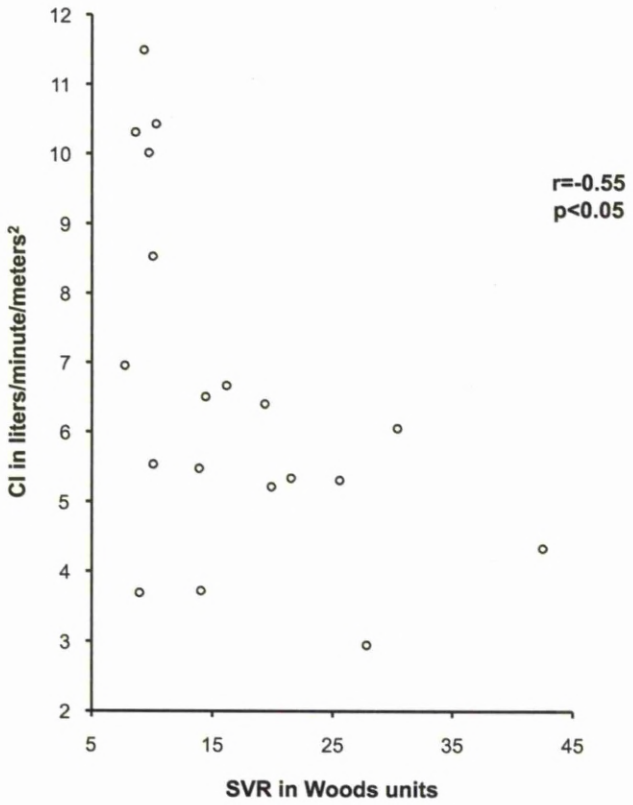

Figure 7.12. Scatter plot to display relationship between admission cardiac index and systemic vascular resistance in 20 children with severe MCD

7.3.5 Agreement

From the 20 ventilated patients ten echocardiographic M-mode images were chosen from a convenient sample and the FS measured by observer 1 and observer 2 independently. A Bland–Altman plot constructed from the 10 images (Figure 7.13) shows the limits of agreement. The 95% confidence interval for the lower limit is -5.1 to -1.3 and for the upper is 2.6 to 4.5. The 95% repeatability coefficient was 1.3%. This means that the value within which the differences between two images analysed by two observers is expected to be 1.3% for 95% of subjects.

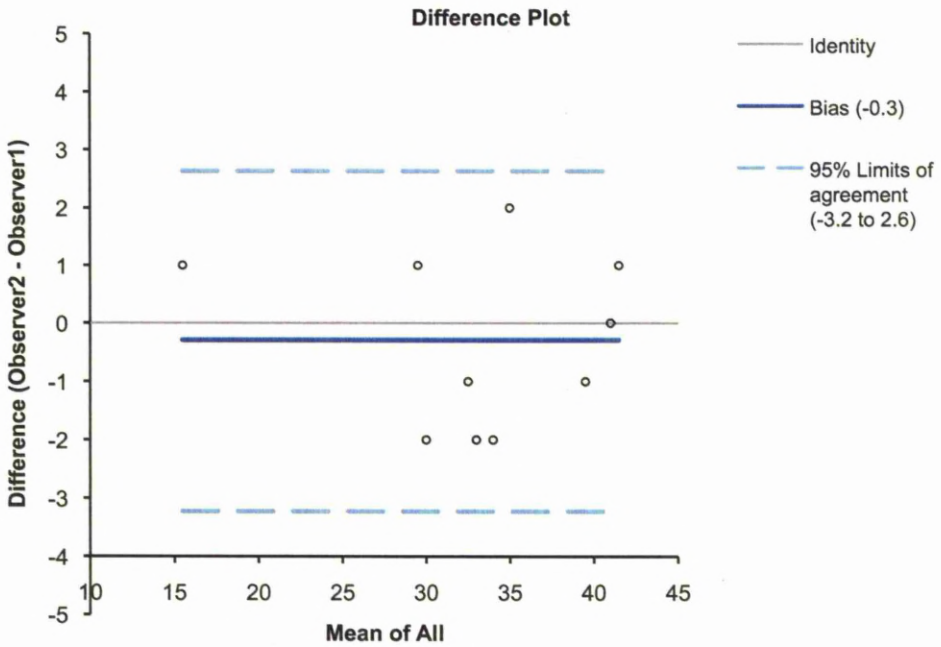

Figure 7.13. Bland Altman plot to show agreement between two independent observers in the assessment of fractional shortening

7.4 Discussion

7.4.1 Cardiac Troponin and systolic function

This study has shown abnormal cardiac systolic function in children with severe MCD which improves alongside clinical recovery and is associated with cTnI and cTnT release. It has also shown significant positive correlations between peak cTn levels and indicators of disease severity including severity assessment scores, duration of inotropic and ventilatory support and hospital stay. These results confirm the finding from other paediatric septic shock and MCD specific studies (Thiru, Pathan et al. 2000; Briassoulis, Narlioglou et al. 2001; Fenton, Sable et al. 2004; Gurkan, Alkaya et al. 2004; Lodha, Arun et al. 2009). None of these studies described how many children had abnormal cTn levels but normal cardiac function. This occurred in two children in this study, who were both transferred from other regional hospitals. Echocardiography may have been performed after the earlier introduction of cardiovascular support had corrected any detectable cardiac dysfunction.

The relationship between myocardial injury and dysfunction and MCD is complex, has not been fully elucidated and may well not be applicable to all forms of bacterial sepsis. Endotoxin stimulates the release of TNF, IL-1β, other pro-inflammatory cytokines and reactive oxygen species, which reduce myocyte contractility (Balligand, Kelly et al. 1993; Balligand, Ungureanu et al. 1993; Kumar, Thota et al. 1996). Studies in rats have demonstrated that sustained infusions of TNF leads to contractile dysfunction and LV dilatation. This was partially reversed by stopping the infusion or by treatment with a TNF antagonist (Bozkurt, Kribbs et al. 1998). Human volunteers demonstrate similar responses when given TNF

infusions (Van der Poll, Romijn et al. 1991; van der Poll, van Deventer et al. 1992). TNF works synergistically with IL-6 in causing an increase in myocyte cell membrane permeability. An intracellular rise of free calcium is the event that couples myocyte electrical excitation with contraction. Calcium ions also play a role in the excitation process itself. Total and ionised calcium has been shown to be reduced in 70% of children with MCD, with a negative correlation between calcium concentration and disease severity (Baines, Thomson et al. 2000). Pathan et al used gene-expression profiling to identify a serum factor causing cardiac dysfunction in MCD. IL-6 was found to cause significant myocardial depression in vitro. When IL-6 was removed from serum samples of patients with MCD and from supernatants of inflammatory cells stimulated by meningococci in vitro, the negative inotropic activity was eliminated. The relationship between IL-6 and myocyte contractility was dose dependent (Pathan, Hemingway et al. 2004).

Aggressive fluid management could lead to left ventricular strain and thus myocyte damage. Alternatively those with most myocyte damage may have the worst cardiac function and therefore need more fluid resuscitation. Children with the most severe meningococcal disease tend to receive the highest fluid volumes during resuscitation. Could fluid therapy contribute to the pathogenesis of myocardial dysfunction? Weisel et al showed that once circulating volume has been restored cardiac damage can continue, suggesting that fluid related damage is unlikely (Weisel, Vito et al. 1977). A dysfunctional microcirculation may contribute to the abnormal cardiac behaviour described in this chapter. Chapters 5 and 6 have shown that the endothelial activation that occurs in MCD results in grossly abnormal microcirculatory blood flow, with the worst seen in the children with the

most severe disease. Regional flow disturbances and abnormal tissue oxygenation associated with septic shock may cause ischaemia in multiple organs, including the heart.

7.4.2 NT-Pro BNP, Diastolic function and Global function

This is the first study to report NT-Pro BNP levels in children with MCD and has shown that NT-Pro BNP levels correlate with disease severity and declines as clinical recovery occurs in children with severe MCD. It is also the first study that has examined diastolic function in children with sepsis and shown a relationship between diastolic dysfunction and NT-Pro BNP levels. The Tei index revealed abnormal global cardiac function, reflecting systolic and diastolic dysfunction in the same subjects on admission. All measures of cardiac function returned to normal values in parallel with clinical recovery. There are no previous studies assessing global function in sepsis.

Few studies have examined diastolic function in sepsis. Jafri et al carried out echocardiography within 24 hours of the onset of septic shock or blood culture positivity in adults (Jafri, Lavine et al. 1990). Systolic function was normal but, using mitral inflow by pulsed wave Doppler, abnormal ventricular filling patterns typical of diastolic dysfunction were shown. Poelaert et al confirmed these findings (Poelaert, Declerck et al. 1997). Munt et al found that in non-survivors compared with survivors of severe sepsis, abnormal left ventricular relaxation occurred (assessed by pulsed-wave Doppler measurement of the left ventricular inflow pattern) (Munt, Jue et al. 1998). Bouhemad et al (Bouhemad, Nicolas-Robin et al. 2008) incorporated TDI into their assessment of adults with septic shock. Patients with septic shock who had systolic dysfunction and cTnI release at

admission had significantly lower Ea values at the mitral annulus than those without these abnormalities. This resolved over time and 7 days after admission there was no difference between the groups. Diastolic dysfunction had not been assessed over time previously. These findings have been confirmed in the current study population. A strong relationship has been shown between NT-Pro BNP levels and LV filling pressure, estimated by the E/Ea ratio. Whether these diastolic abnormalities are a direct consequence of bacteraemia, or represent a compensatory mechanism of the ventricle to allow a larger diastolic volume without a pressure increase that would produce pulmonary oedema, has not been determined.

There have only been two studies where NT-Pro BNP has been measured in children with sepsis. The first compared 10 children with septic shock and 10 children with LV failure on PICU (Fried, Bar-Oz et al. 2006). Both groups underwent echocardiography within the first 24 hours of admission to assess systolic but not diastolic function. The group with LV failure had significantly higher levels of NT-Pro BNP when compared with the group with sepsis. The group with sepsis had higher levels of NT-Pro BNP when compared with 20 children who were admitted to hospital with a febrile illness. Dominico et al. found that children with septic shock had an elevated NT-Pro BNP level at admission when compared to critically ill children without sepsis (Domico, Liao et al. 2008). NT-Pro BNP levels at 12 hrs correlated positively with PRISM III and negatively with FS. The findings presented here support these two paediatric studies. Although elevated NT-Pro BNP levels in MCD might be attributed to the underlying myocardial dysfunction it has also been shown here that NT-Pro BNP

levels are raised in septic patients without shock. This finding has been shown before (Nikolaou, Goritsas et al. 2007) and indicates a direct effect on NT-Pro BNP release due to sepsis alone. In support of this concept LPS and pro-inflammatory cytokines have a direct effect on BNP transcription and translation in cardiomyocytes *in vitro*, (Tomaru Ki, Arai et al. 2002; Ma, Ogawa et al. 2004). Animal studies of severe sepsis have indicated that tissue hypoxia also induces BNP gene transcription (Toth, Vuorinen et al. 1994). An increase in plasma NT-proBNP was seen when *Escherichia coli* endotoxin (LPS) was administered intravenously to 10 healthy adults, aged 20–40 years, with normal medical history, clinical examination, ECG, echocardiography (Vila, Resl et al. 2008). A rise in NT-Pro BNP occurred after LPS administration, peaked at 6 hours and was absent after saline infusion. The NT-proBNP levels correlated with changes in body temperature, heart and CRP, but not blood pressure. This model of systemic infection showed that NT-Pro BNP can be released without cardiac involvement.

It is possible that the volume resuscitation received by children with severe MCD could cause BNP release, by the elevation of both left-sided and right-sided filling pressures. Roch et al however found, in a multivariate analysis, that fluid loading was not a significant predictor of a high NT-proBNP level (Roch, Allardet-Servent et al. 2005).

7.4.3 Cardiac output and index

A higher cardiac output is a consequence of the reduced afterload (Suffredini, Fromm et al. 1989) and in this study has been shown to be strongly correlated with SVR and CO and CI. The cardiac index was found to be high in the majority of children with MCD. This is contrary to the

findings of Monsalve, who recruited adults and children with MCD to a study that evaluated CO with a pulmonary artery catheter using a thermodilution method. They showed a lower CO in patients with MCD despite higher cardiac filling pressures when compared to patients with other forms of Gram-negative sepsis. The study went on to demonstrate that the non-MCD patients were able to increase their CI with an increase in filling pressure, but this response was not seen in the MCD group and suggesting that MCD related cardiac dysfunction is more severe (Monsalve, Rucabado et al. 1984). The discrepancy may have been due to the fact that numbers are smaller in this study or to the use of a non-invasive method of CO measurement as pulmonary artery thermodilution catheters are not routinely used in paediatric critical care. Transthoracic echocardiography is operator dependent and suboptimal alignment with the ascending aorta can affect the CO calculation although would probably not over-estimate it because angle variation would reduce the Doppler signal size.

Another possible source of error is the indexing of CO by dividing by BSA to obtain the CI. This allows comparisons to be made between children of different sizes. However large changes in the CI are seen in the smallest of children and may result in overestimation of the CI. A more appropriate method of adjustment may be that of the allometric scaling as discussed in Chapter 4. This would entail dividing the cardiovascular variable by a body size variable that is raised to a scalar component. So for CO this would be $CI=CO/BSA^{x}$ where x is the scaling component. A study examining the allometric relationship between body size and stroke volume and cardiac output in 970 normotensive adults and children has confirmed this. The study revealed that indexing stroke volume and cardiac output for the first

power of body surface area was acceptable in adults, because the allometric powers detected were close to 1. However this same index calculation in children introduced a significant error, because the power detected by allometric regression was below 1, especially for cardiac output. It recommended that in children, body surface area needs to be raised to the appropriate power, which, for cardiac output, is approximately its square root function (de Simone, Devereux et al. 1997):

When this calculation is applied to the relationship between SVR and this method of cardiac scaling for the current study population, the relationship remains significant with a stronger correlation coefficient ($r=-0.75$, $p<0.001$). Normal ranges for children using this allometric scaling method for critical illness have not however been established.

7.5 Conclusion

This study has found that children with severe MCD and septic shock have myocardial cell injury, which is related to echocardiographic findings of systolic and diastolic dysfunction. The measurement of cTns, NT-proBNP and the transthoracic echocardiographic evaluations made in this group of children has given new information into the haemodynamic changes seen in MCD.

Chapter 8

Conclusions

This thesis describes a series of studies of the haemodynamic responses in the host to invasive meningococcal disease in children. The aims of this thesis were: 1) To determine whether activated Partial Thromboplastin Time waveform analysis and Procalcitonin could be used as early diagnostic markers in sepsis. 2) To assess the microcirculation of normal healthy children using side-stream dark-field imaging to validate its use in children. 3) To visualise the microcirculation in children with severe meningococcal disease using side-stream dark-field imaging. 4) To correlate microcirculatory variables of children with severe MCD with disease severity, cardiac function and plasma vasoactive endothelial mediators and cytokines.5) To study cardiac function using echocardiography and determine the relationship between plasma cardiac troponin and NT Pro-BNP with cardiac function in children with severe MCD.

8.1 Summary of conclusions from the studies

1) This study supports the value of aPTT waveform analysis as a simple, rapid and robust diagnostic marker in the detection of meningococcal sepsis that has translational potential in facilitating prompt diagnosis and real-time monitoring of patients with critical illnesses.

2) This study demonstrated that side stream dark field imaging can be used in healthy awake and anaesthetised children to obtain high quality images of the microcirculation. Normal values for children have also been established. Manual analysis of the images produced has shown good inter- and intraobserver agreement. Automated and user

friendly image analysis software would be a superior and faster method of evaluation. Its use in critically ill children would therefore be appropriate.

3) This study has shown that microcirculation dysfunction is present in children with MCD and that microcirculation outcome variables can be used to predict outcome.

4) This study demonstrated that in children with severe MCD there is release of cell adhesion molecules and NO. It has also shown that there is a relationship between these and microcirculation variables as assessed using SDF imaging.

5) This study found that children with severe MCD and septic shock had myocardial cell injury which was related to echocardiographic findings of systolic and diastolic dysfunction. The measurement of cTns, NT-proBNP and transthoracic echocardiographic evaluation of the haemodynamic effects of MCD could be helpful in guiding PICU interventions in these children.

8.2 Future research

8.2.1 Targeted anti-inflammatory therapy

Drotrecogin alfa (activated protein C; APC) is an endogenous protein that is not only an anticoagulant but also has an anti-inflammatory effect through the inhibition of E-selectin meditated leukocyte adhesion. It also has a role in anti-apoptosis in endothelial cells. These factors make

Drotrecogin alfa a potential agent in the restoration of a healthy microcirculation during sepsis. It has been shown to reduce mortality in severe sepsis in adults (Bernard, Vincent et al. 2001; Ely, Bernard et al. 2002; Ely, Laterre et al. 2003; Vincent, Angus et al. 2003; Abraham, Laterre et al. 2005). A study using OPS imaging to monitor the effects of Drotrecogin alfa in adults with severe sepsis has been carried out. Images were taken at administration of Drotrecogin alfa, four hours later and then daily for a week. Patients receiving Drotrecogin alfa had an increase in the PPV 4 hours after administration (De Backer, Verdant et al. 2006). APC was not found to be beneficial in a large RCT in children with sepsis in the PICU setting. The reason for this may have been the wide inclusion criteria used for study entry (Nadel, Goldstein et al. 2007). If SDF imaging or if aPTT analysis were to be used as a tool to assess entry criteria in such a study a different outcome may be found in terms of mortality and morbidity in children with MCD.

8.2.2 Vasoactive agents

Agents that improve the microcirculation should improve organ function. Vasodilatating agents can improve microcirculatory blood flow. Agents such as sublingual acetylcholine and early studies of intravenous nitroglycerin have been shown to improve microcirculatory blood flow when used together with adequate volume support, inotropes and steroids (De Backer, Creteur et al. 2002; Spronk, Ince et al. 2002). Intravenous nitroglycerin has however recently been shown to have no effect on sublingual microcirculatory blood flow in a randomised controlled trial of nitroglycerin use in early-phase severe sepsis or septic

shock. Vasopressors such as adrenaline and nor-adrenaline could have a detrimental effect upon the microcirculation despite appearing to be beneficial in maintaining blood pressure.

This study has shown high levels of NO production in children with MCD. This is due to iNOS up regulation and can cause arterial hypotension. iNOS inhibition has been shown to cause microvascular dysfunction, by increasing leukocyte adhesion, microthrombosis, and microvascular leakage (Hollenberg, Broussard et al. 2000; Bateman, Sharpe et al. 2008; Trzeciak, Cinel et al. 2008; Bruhn, Correa et al. 2009; Fortin, McDonald et al. 2009). Animal models have shown that exogenous NO may have a role in improving a dysfunctional microcirculation due to its vasodilatory effect and by modulation of leukocyte adhesion (Berger, Gibson et al. 1993; Gundersen, Corso et al. 1998; Chang, Kang et al. 2006; Assadi, Desebbe et al. 2008). Further research in this area needs to be directed at investigating whether inhaled NO can reverse microvascular alterations whilst maintaining haemodynamic equilibrium in MCD.

8.2.3 Novel microcirculation therapies

Randomised trials are needed in children with MCD and severe sepsis of therapies demonstrated to improve microvascular perfusion in adults. The difficultly in undertaking randomised controlled trials in children with severe MCD is the spectrum of disease seen and children will present to a tertiary centre's PICU at different stages of their

illness. Also poor outcomes such as mortality and limb loss are fortunately becoming less common making it near impossible to use as comparative outcome measures. To overcome this, a national multi-centre study being carried out over several years would be needed. Multiple mechanisms lead to cellular dysfunction in sepsis and poor tissue perfusion. Microcirculatory failure is only one of these. Mitochondrial dysfunction plays an important role and can be counteracted by stimulating mitochondrial synthesis with insulin (Lambert, Wang et al. 2004; Remedi, Nichols et al. 2006). It can also be counteracted by reducing the oxidative stress within the mitochondria using antioxidants (Kowluru 2001; Protti and Singer 2006). These methods of therapy are purely investigational and not in clinical use.

8.2.4 Improvement of Cardiac function

This study has confirmed cardiac systolic dysfunction and damage in children with MCD and is the first study to demonstrate diastolic dysfunction. Milrinone is an inodilator, which also improves left ventricular diastolic relaxation. It is a phosphodiesterase isoenzyme inhibitor for both cardiac and vascular muscle. Phosphodiesterase isoenzyme is needed for 3'5'-cyclic adenosine monophosphate (cAMP) breakdown and its inhibition leads to elevated cAMP levels. This results in increased myocardial contractility. Additionally in the vascular smooth muscle, vasodilation occurs due to a reduced sensitivity of the muscle to calcium (Shipley, Tolman et al. 1996). The use of milrinone in children with MCD has been studied in small case series with no improvement in outcome although the interpretation of these studies is

limited by small sample size (Rich, West et al. 2003). No randomised controlled studies have been carried out in an adult or paediatric critical care sepsis setting.

Levosimendan, a drug receiving a large amount of interest, has a calcium sensitizing effects and interacts with potassium channels in the myocyte plasma membrane and in the mitochondria (Toller and Stranz 2006). Levosimendan has been shown to be more effective than dobutamine or milrinone in improving cardiac performance (Pinto, Rehberg et al. 2008). It not only increases stroke volume and cardiac output but improves LV diastolic function and LV filling pressures (Barraud, Faivre et al. 2007; Osthaus, Boethig et al. 2009) . This study has found these parameters to be abnormal in children with MCD making Levosimendan an ideal inotrope to consider in the management of these children.

8.3 Conclusions

Despite improvements in the detection of sepsis and management of MCD, there is no doubt that prevention with appropriate vaccination would reduce mortality and morbidity. We do not fully understand why some children suffer death or disability due to invasive MCD. This thesis has shown new insights into the complex haemodynamic response within a host to invasive MCD. The relationship between microcirculatory and macrocirculatory failure is complex and variable within patients. Macrocirculatory dysfunction may be present without microcirculatory dysfunction and the contrary may also be true. The identification and monitoring of both is important in the management of

these children. The incorporation of these new haemodynamic insights into a novel approach to paediatric critical illness is awaited alongside its impact upon the outcome in these children.

References

Abraham, E., P. F. Laterre, et al. (2005). "Drotrecogin alfa (activated) for adults with severe sepsis and a low risk of death." N Engl J Med **353**(13): 1332-41.

Alan Stevens, J. S. L. (2004). "Human Histology. ." Third Edition. **Mosby**.

Alpert, J. S., K. Thygesen, et al. (2000). "Myocardial infarction redefined--a consensus document of The Joint European Society of Cardiology/American College of Cardiology Committee for the redefinition of myocardial infarction." J Am Coll Cardiol **36**(3): 959-69.

Ammann, P., T. Fehr, et al. (2001). "Elevation of troponin I in sepsis and septic shock." Intensive Care Med **27**(6): 965-9.

Ammann, P., M. Maggiorini, et al. (2003). "Troponin as a risk factor for mortality in critically ill patients without acute coronary syndromes." J Am Coll Cardiol **41**(11): 2004-9.

Appleton, C. P., L. K. Hatle, et al. (1988). "Relation of transmitral flow velocity patterns to left ventricular diastolic function: new insights from a combined hemodynamic and Doppler echocardiographic study." J Am Coll Cardiol **12**(2): 426-40.

Appleton, C. P., J. L. Jensen, et al. (1997). "Doppler evaluation of left and right ventricular diastolic function: a technical guide for obtaining optimal flow velocity recordings." J Am Soc Echocardiogr **10**(3): 271-92.

Arkader, R., E. J. Troster, et al. (2006). "Procalcitonin does discriminate between sepsis and systemic inflammatory response syndrome." Arch Dis Child **91**(2): 117-20.

Assadi, A., O. Desebbe, et al. (2008). "Effects of sodium nitroprusside on splanchnic microcirculation in a resuscitated porcine model of septic shock." Br J Anaesth **100**(1): 55-65.

Bache, C. E. and I. P. Torode (2006). "Orthopaedic sequelae of meningococcal septicemia." J Pediatr Orthop **26**(1): 135-9.

Baggiolini, M., A. Walz, et al. (1989). "Neutrophil-activating peptide-1/interleukin 8, a novel cytokine that activates neutrophils." J.Clin.Invest **84**(4): 1045-1049.

Baines, P. B., O. Marzouk, et al. (1999). "Endothelial cell adhesion molecules in meningococcal disease." Arch Dis Child **80**(1): 74-6.

Baines, P. B., S. Stanford, et al. (1999). "Nitric oxide production in meningococcal disease is directly related to disease severity." Crit Care Med **27**(6): 1187-90.

Baines, P. B., A. P. Thomson, et al. (2000). "Hypocalcaemia in severe meningococcal infections." Arch Dis Child **83**(6): 510-3.

Baines, P. T., APJ; Hart, CA (2001). "Cardiac function and tissue perfusion in children with severe meningococcal disease." Clinical Intensive Care **12**((5,6)): 215 - 221.

Balligand, J. L., R. A. Kelly, et al. (1993). "Control of cardiac muscle cell function by an endogenous nitric oxide signaling system." Proc Natl Acad Sci U S A **90**(1): 347-51.

Balligand, J. L., D. Ungureanu, et al. (1993). "Abnormal contractile function due to induction of nitric oxide synthesis in rat cardiac myocytes follows exposure to activated macrophage-conditioned medium." J Clin Invest **91**(5): 2314-9.

Barraud, D., V. Faivre, et al. (2007). "Levosimendan restores both systolic and diastolic cardiac performance in lipopolysaccharide-treated

rabbits: comparison with dobutamine and milrinone." Crit Care Med **35**(5): 1376-82.

Bateman, R. M., M. D. Sharpe, et al. (2008). "Inhibiting nitric oxide overproduction during hypotensive sepsis increases local oxygen consumption in rat skeletal muscle." Crit Care Med **36**(1): 225-31.

Bateman, R. M. and K. R. Walley (2005). "Microvascular resuscitation as a therapeutic goal in severe sepsis." Crit Care **9 Suppl 4**: S27-32.

Bazin, J. E., B. Dureuil, et al. (1998). "Effects of etomidate, propofol and thiopental anaesthesia on arteriolar tone in the rat diaphragm." Br J Anaesth **81**(3): 430-5.

Belthur, M. V., C. F. Bradish, et al. (2005). "Late orthopaedic sequelae following meningococcal septicaemia. A multicentre study." J Bone Joint Surg Br **87**(2): 236-40.

Berger, J. I., R. L. Gibson, et al. (1993). "Effect of inhaled nitric oxide during group B streptococcal sepsis in piglets." Am Rev Respir Dis **147**(5): 1080-6.

Bernard, G. R., J. L. Vincent, et al. (2001). "Efficacy and safety of recombinant human activated protein C for severe sepsis." N.Engl.J.Med. **344**(10): 699-709.

Bernard, G. R., J. L. Vincent, et al. (2001). "Efficacy and safety of recombinant human activated protein C for severe sepsis." N Engl J Med **344**(10): 699-709.

Berton, C. and B. Cholley (2002). "Equipment review: new techniques for cardiac output measurement--oesophageal Doppler, Fick principle using carbon dioxide, and pulse contour analysis." Crit Care **6**(3): 216-21.

Biberthaler, P., S. Langer, et al. (2001). "In vivo assessment of colon microcirculation: comparison of the new OPS imaging technique with intravital microscopy." Eur J Med Res **6**(12): 525-34.

Bishop, C. M. (1999). "The maximum oxygen consumption and aerobic scope of birds and mammals: getting to the heart of the matter." Proc Biol Sci **266**(1435): 2275-81.

Bjerre, A., B. Brusletto, et al. (2004). "Plasma interferon-gamma and interleukin-10 concentrations in systemic meningococcal disease compared with severe systemic Gram-positive septic shock." Crit Care Med **32**(2): 433-8.

Bjerre, A., B. Brusletto, et al. (2004). "Plasma interferon-gamma and interleukin-10 concentrations in systemic meningococcal disease compared with severe systemic Gram-positive septic shock." Crit Care Med. **32**(2): 433-438.

BNF (2005). "The BNF for children." Drug Ther Bull **43**(11): 84-5.

Bodor, G. S., L. Survant, et al. (1997). "Cardiac troponin T composition in normal and regenerating human skeletal muscle." Clin Chem **43**(3): 476-84.

Boerma, E. C., K. R. Mathura, et al. (2005). "Quantifying bedside-derived imaging of microcirculatory abnormalities in septic patients: a prospective validation study." Crit Care **9**(6): R601-6.

Boerma, E. C., K. R. Mathura, et al. (2005). "Quantifying bedside-derived imaging of microcirculatory abnormalities in septic patients: a prospective validation study." Crit Care **9**(6): R601-R606.

Bohuon, C., M. Assicot, et al. (1998). "[Procalcitonin, a marker of bacterial meningitis in children]." Bull Acad Natl Med **182**(7): 1469-75; discussion 1475-7.

Bohuon, C. and D. Gendrel (1999). "[Procalcitonin: a new marker of bacterial infection. Importance and prospects]." Arch Pediatr **6**(2): 141-4.

Boldt, J., M. Muller, et al. (1996). "Circulating adhesion molecules in the critically ill: a comparison between trauma and sepsis patients." Intensive Care Med **22**(2): 122-8.

Boldt, J., M. Wollbruck, et al. (1995). "Do plasma levels of circulating soluble adhesion molecules differ between surviving and nonsurviving critically ill patients?" Chest **107**(3): 787-92.

Bone, M., M. Diver, et al. (2002). "Assessment of adrenal function in the initial phase of meningococcal disease." Pediatrics **110**(3): 563-9.

Bone, R. C. (1991). "The pathogenesis of sepsis." Ann.Intern.Med. **115**(6): 457-469.

Booy, R., P. Habibi, et al. (2001). "Reduction in case fatality rate from meningococcal disease associated with improved healthcare delivery." Arch.Dis.Child **85**(5): 386-390.

Boswell, S. A. and T. M. Scalea (2003). "Sublingual capnometry: an alternative to gastric tonometry for the management of shock resuscitation." AACN Clin Issues **14**(2): 176-84.

Boucek, M. M., R. C. Boerth, et al. (1984). "Myocardial dysfunction in children with acute meningococcemia." J Pediatr **105**(4): 538-42.

Boucek, M. M., R. C. Boerth, et al. (1984). "Myocardial dysfunction in children with acute meningococcemia." J.Pediatr. **105**(4): 538-542.

Bouhemad, B., A. Nicolas-Robin, et al. (2008). "Isolated and reversible impairment of ventricular relaxation in patients with septic shock." Crit Care Med **36**(3): 766-74.

Bouskela, E. and G. M. Rubanyi (1995). "Effects of iloprost, a stable prostacyclin analog, and its combination with NW-nitro-L-arginine on early events following lipopolysaccharide injection: observations in the hamster cheek pouch microcirculation." Int J.Microcirc.Clin.Exp. **15**(4): 170-180.

Bozkurt, B., S. B. Kribbs, et al. (1998). "Pathophysiologically relevant concentrations of tumor necrosis factor-alpha promote progressive left ventricular dysfunction and remodeling in rats." Circulation **97**(14): 1382-91.

Brady, A. J. (1993). "Nitric oxide synthase activities in human myocardium." Lancet **341**(8842): 448.

Brady, A. J. and P. A. Poole-Wilson (1993). "Circulatory failure in septic shock. Nitric oxide: too much of a good thing?" Br Heart J **70**(2): 103-5.

Brady, A. J., J. B. Warren, et al. (1993). "Nitric oxide attenuates cardiac myocyte contraction." Am J Physiol **265**(1 Pt 2): H176-82.

Brandt, R. R., K. Filzmaier, et al. (2001). "Circulating cardiac troponin I in acute pericarditis." Am J Cardiol **87**(11): 1326-8.

Brandtzaeg, P., T. E. Mollnes, et al. (1989). "Complement activation and endotoxin levels in systemic meningococcal disease." J.Infect.Dis. **160**(1): 58-65.

Brandtzaeg, P., P. M. Sandset, et al. (1989). "The quantitative association of plasma endotoxin, antithrombin, protein C, extrinsic pathway inhibitor and fibrinopeptide A in systemic meningococcal disease." Thromb.Res. **55**(4): 459-470.

Brazy, J. E., D. V. Lewis, et al. (1985). "Monitoring of cerebral oxygenation in the intensive care nursery." Adv Exp Med Biol **191**: 843-8.

Brazy, J. E., D. V. Lewis, et al. (1985). "Noninvasive monitoring of cerebral oxygenation in preterm infants: preliminary observations." Pediatrics **75**(2): 217-25.

Briassoulis, G., M. Narlioglou, et al. (2001). "Myocardial injury in meningococcus-induced purpura fulminans in children." Intensive Care Med. **27**(6): 1073-1082.

Briassoulis, G., M. Narlioglou, et al. (2001). "Myocardial injury in meningococcus-induced purpura fulminans in children." Intensive Care Med **27**(6): 1073-82.

Brierley, J. and M. J. Peters (2008). "Distinct hemodynamic patterns of septic shock at presentation to pediatric intensive care." Pediatrics **122**(4): 752-9.

Britto, J., S. Nadel, et al. (1996). "Severity of illness scores and risk of complication during transfer." Intensive Care Med. **22**(10): 1130-1131.

Brookes, Z. L., C. S. Reilly, et al. (2004). "Differential effects of propofol, ketamine, and thiopental anaesthesia on the skeletal muscle microcirculation of normotensive and hypertensive rats in vivo." Br J Anaesth **93**(2): 249-56.

Brueckmann, M., G. Huhle, et al. (2005). "Prognostic value of plasma N-terminal pro-brain natriuretic peptide in patients with severe sepsis." Circulation **112**(4): 527-34.

Bruhn, F. H., P. B. Correa, et al. (2009). "Blocking systemic nitric oxide production alters neuronal activation in brain structures involved in cardiovascular regulation during polymicrobial sepsis." Neurosci Lett **453**(3): 141-6.

Bruserud, O., P. E. Akselen, et al. (1995). "Serum concentrations of E-selectin, P-selectin, ICAM-1 and interleukin 6 in acute leukaemia patients with chemotherapy-induced leucopenia and bacterial infections." Br.J.Haematol. **91**(2): 394-402.

Bryce, J., C. Boschi-Pinto, et al. (2005). "WHO estimates of the causes of death in children." Lancet **365**(9465): 1147-52.

Bugden, S. A., C. Coles, et al. (2004). "The potential role of procalcitonin in the emergency department management of febrile young adults during a sustained meningococcal epidemic." Emerg Med Australas **16**(2): 114-9.

Callaghan, M. J., C. Buckee, et al. (2008). "Opa protein repertoires of disease-causing and carried meningococci." J Clin Microbiol **46**(9): 3033-41.

Carcillo, J. A., A. L. Davis, et al. (1991). "Role of early fluid resuscitation in pediatric septic shock." JAMA **266**(9): 1242-1245.

Carcillo, J. A. and A. I. Fields (2002). "Clinical practice parameters for hemodynamic support of pediatric and neonatal patients in septic shock." Crit Care Med. **30**(6): 1365-1378.

Carcillo, J. A. and A. I. Fields (2002). "Clinical practice parameters for hemodynamic support of pediatric and neonatal patients in septic shock." Crit Care Med **30**(6): 1365-78.

Carlos, T. M. and J. M. Harlan (1994). "Leukocyte-endothelial adhesion molecules." Blood **84**(7): 2068-2101.

Carrol, E. D., P. Newland, et al. (2002). "Procalcitonin as a diagnostic marker of meningococcal disease in children presenting with fever and a rash." Arch Dis Child **86**(4): 282-5.

Carrol, E. D., P. Newland, et al. (2005). "Prognostic value of procalcitonin in children with meningococcal sepsis." Crit Care Med **33**(1): 224-5.

Carrol, E. D., A. P. Thomson, et al. (2005). "A predominantly anti-inflammatory cytokine profile is associated with disease severity in meningococcal sepsis." Intensive Care Med **31**(10): 1415-9.

Carrol, E. D., A. P. Thomson, et al. (2002). "Myositis in children with meningococcal disease: a role for tumour necrosis factor-alpha and interleukin-8?" J Infect **44**(1): 17-21.

Carrol, E. D., A. P. Thomson, et al. (2000). "Performance characteristics of the polymerase chain reaction assay to confirm clinical meningococcal disease." Arch Dis Child **83**(3): 271-3.

Casado-Flores, J., A. Blanco-Quiros, et al. (2006). "Prognostic utility of the semi-quantitative procalcitonin test, neutrophil count and C-reactive protein in meningococcal infection in children." Eur J Pediatr **165**(1): 26-9.

Casey, L. C., R. A. Balk, et al. (1993). "Plasma cytokine and endotoxin levels correlate with survival in patients with the sepsis syndrome." Ann.Intern.Med. **119**(8): 771-778.

Casey, L. C., R. A. Balk, et al. (1993). "Plasma cytokine and endotoxin levels correlate with survival in patients with the sepsis syndrome." Ann Intern Med **119**(8): 771-8.

Ceneviva, G., J. A. Paschall, et al. (1998). "Hemodynamic support in fluid-refractory pediatric septic shock." Pediatrics **102**(2): e19.

Cerwinka, W. H., D. Cooper, et al. (2003). "Superoxide mediates endotoxin-induced platelet-endothelial cell adhesion in intestinal venules." Am.J.Physiol Heart Circ.Physiol **284**(2): H535-H541.

Chalumeau, M., S. Leroy, et al. (2007). "[Procalcitonin bedside testing in the pediatric emergency department]." Arch Pediatr **14**(6): 529-31.

Chang, Y. S., S. Kang, et al. (2006). "Pretreatment with N-nitro-L-arginine methyl ester improved oxygenation after inhalation of nitric oxide in newborn piglets with Escherichia coli pneumonia and sepsis." J Korean Med Sci **21**(6): 965-72.

Chappell, D., K. Hofmann-Kiefer, et al. (2008). "TNF-alpha induced shedding of the endothelial glycocalyx is prevented by hydrocortisone and antithrombin." Basic Res Cardiol.

Charpentier, J., C. E. Luyt, et al. (2004). "Brain natriuretic peptide: A marker of myocardial dysfunction and prognosis during severe sepsis." Crit Care Med **32**(3): 660-5.

Chew, M. S. and J. Poelaert (2003). "Accuracy and repeatability of pediatric cardiac output measurement using Doppler: 20-year review of the literature." Intensive Care Med **29**(11): 1889-94.

Chopin, N., B. Floccard, et al. (2006). "Activated partial thromboplastin time waveform analysis: a new tool to detect infection?" Crit Care Med **34**(6): 1654-60.

Chopin, N., B. Floccard, et al. (2006). "Activated partial thromboplastin time waveform analysis: a new tool to detect infection?" Crit Care Med. **34**(6): 1654-1660.

Chua, G. and L. Kang-Hoe (2004). "Marked elevations in N-terminal brain natriuretic peptide levels in septic shock." Crit Care **8**(4): R248-50.

Claeys, M. A., E. Gepts, et al. (1988). "Haemodynamic changes during anaesthesia induced and maintained with propofol." Br J Anaesth **60**(1): 3-9.

Claeys, R., S. Vinken, et al. (2002). "Plasma procalcitonin and C-reactive protein in acute septic shock: clinical and biological correlates." Crit Care Med **30**(4): 757-62.

Clark, P. K. a. M. L. (2002). "Clinical Medicine."

Collinson, P. O., S. C. Barnes, et al. (2004). "Analytical performance of the N terminal pro B type natriuretic peptide (NT-proBNP) assay on the Elecsys 1010 and 2010 analysers." Eur J Heart Fail **6**(3): 365-8.

Comstock, K. L., K. A. Krown, et al. (1998). "LPS-induced TNF-alpha release from and apoptosis in rat cardiomyocytes: obligatory role for CD14 in mediating the LPS response." J Mol Cell Cardiol **30**(12): 2761-75.

Cowley, H. C., D. Heney, et al. (1994). "Increased circulating adhesion molecule concentrations in patients with the systemic inflammatory response syndrome: a prospective cohort study." Crit Care Med **22**(4): 651-7.

Creteur, J. (2006). "Gastric and sublingual capnometry." Curr Opin Crit Care **12**(3): 272-7.

Cui, W. and D. A. Roberson (2006). "Left ventricular Tei index in children: comparison of tissue Doppler imaging, pulsed wave Doppler, and M-mode echocardiography normal values." J Am Soc Echocardiogr **19**(12): 1438-45.

Cunnion, R. E., G. L. Schaer, et al. (1986). "The coronary circulation in human septic shock." Circulation **73**(4): 637-44.

Darveau, C. A., R. K. Suarez, et al. (2002). "Allometric cascade as a unifying principle of body mass effects on metabolism." Nature **417**(6885): 166-70.

Dawson, T. H. (2005). "Modeling of vascular networks." J Exp Biol **208**(Pt 9): 1687-94.

Day, K. M., N. Haub, et al. (2008). "Hyperglycemia is associated with morbidity in critically ill children with meningococcal sepsis." Pediatr Crit Care Med **9**(6): 636-40.

De Backer, D. (2003). "Lactic acidosis." Minerva Anestesiol **69**(4): 281-4.

De Backer, D., J. Creteur, et al. (2002). "Microvascular blood flow is altered in patients with sepsis." Am J Respir Crit Care Med **166**(1): 98-104.

De Backer, D. and M. J. Dubois (2001). "Assessment of the microcirculatory flow in patients in the intensive care unit." Curr Opin Crit Care **7**(3): 200-3.

De Backer, D., S. Hollenberg, et al. (2007). "How to evaluate the microcirculation: report of a round table conference." Crit Care **11**(5): R101.

De Backer, D., C. Verdant, et al. (2006). "Effects of drotrecogin alfa activated on microcirculatory alterations in patients with severe sepsis." Crit Care Med **34**(7): 1918-24.

De, B. D., J. Creteur, et al. (2002). "Microvascular blood flow is altered in patients with sepsis." Am.J.Respir.Crit Care Med. **166**(1): 98-104.

de Bold, A. J., H. B. Borenstein, et al. (1981). "A rapid and potent natriuretic response to intravenous injection of atrial myocardial extract in rats." Life Sci **28**(1): 89-94.

de Oliveira, C. F., D. S. de Oliveira, et al. (2008). "ACCM/PALS haemodynamic support guidelines for paediatric septic shock: an outcomes comparison with and without monitoring central venous oxygen saturation." Intensive Care Med **34**(6): 1065-75.

de Simone, G., R. B. Devereux, et al. (1997). "Stroke volume and cardiac output in normotensive children and adults. Assessment of relations with body size and impact of overweight." Circulation **95**(7): 1837-43.

Dec, G. W., Jr., H. Waldman, et al. (1992). "Viral myocarditis mimicking acute myocardial infarction." J Am Coll Cardiol **20**(1): 85-9.

Dellinger, R. P., M. M. Levy, et al. (2008). "Surviving Sepsis Campaign: international guidelines for management of severe sepsis and septic shock: 2008." Intensive Care Med **34**(1): 17-60.

Dempfle, C. E., S. Lorenz, et al. (2004). "Utility of activated partial thromboplastin time waveform analysis for identification of sepsis and overt disseminated intravascular coagulation in patients admitted to a surgical intensive care unit." Crit Care Med **32**(2): 520-4.

Dennis, M. W., C. Downey, et al. (2004). "Prothrombinase enhancement through quantitative and qualitative changes affecting very low density lipoprotein in complex with C-reactive protein." Thromb Haemost **91**(3): 522-30.

Derkx, B., A. Marchant, et al. (1995). "High levels of interleukin-10 during the initial phase of fulminant meningococcal septic shock." J.Infect.Dis. **171**(1): 229-232.

Derkx, B., J. Wittes, et al. (1999). "Randomized, placebo-controlled trial of HA-1A, a human monoclonal antibody to endotoxin, in children with meningococcal septic shock. European Pediatric Meningococcal Septic Shock Trial Study Group." Clin.Infect.Dis. **28**(4): 770-777.

Dodds, P. S., D. H. Rothman, et al. (2001). "Re-examination of the "3/4-law" of metabolism." J Theor Biol **209**(1): 9-27.

Dombrovskiy, V. Y., A. A. Martin, et al. (2007). "Rapid increase in hospitalization and mortality rates for severe sepsis in the United States: a trend analysis from 1993 to 2003." Crit Care Med **35**(5): 1244-50.

Domico, M., P. Liao, et al. (2008). "Elevation of brain natriuretic peptide levels in children with septic shock." Pediatr Crit Care Med **9**(5): 478-83.

Downey, C., R. Kazmi, et al. (1997). "Novel and diagnostically applicable information from optical waveform analysis of blood coagulation in disseminated intravascular coagulation." Br J Haematol **98**(1): 68-73.

Downey, C., R. Kazmi, et al. (1998). "Early identification and prognostic implications in disseminated intravascular coagulation through transmittance waveform analysis." Thromb Haemost **80**(1): 65-9.

Duggal, B., U. Pratap, et al. (2005). "Milrinone and low cardiac output following cardiac surgery in infants: is there a direct myocardial effect?" Pediatr Cardiol **26**(5): 642-5.

Eidem, B. W., C. Tei, et al. (1998). "Nongeometric quantitative assessment of right and left ventricular function: myocardial performance index in normal children and patients with Ebstein anomaly." J Am Soc Echocardiogr **11**(9): 849-56.

Eling, M., A. C. Stephens, et al. (2001). "Tissue factor pathway inhibitor (TFPI) levels in the plasma and urine of children with meningococcal disease." Thromb Haemost **85**(2): 240-4.

Ellis, C. G., R. M. Bateman, et al. (2002). "Effect of a maldistribution of microvascular blood flow on capillary O(2) extraction in sepsis." Am J Physiol Heart Circ Physiol **282**(1): H156-64.

Ely, E. W., G. R. Bernard, et al. (2002). "Activated protein C for severe sepsis." N Engl J Med **347**(13): 1035-6.

Ely, E. W., P. F. Laterre, et al. (2003). "Drotrecogin alfa (activated) administration across clinically important subgroups of patients with severe sepsis." Crit Care Med **31**(1): 12-9.

Emonts, M., J. A. Hazelzet, et al. (2003). "Host genetic determinants of Neisseria meningitidis infections." Lancet Infect Dis **3**(9): 565-77.

Fallon, P., I. G. Roberts, et al. (1994). "Cerebral blood volume response to changes in carbon dioxide tension before and during cardiopulmonary bypass in children, investigated by near infrared spectroscopy." Eur J Cardiothorac Surg **8**(3): 130-4.

Faust, S. N., M. Levin, et al. (2001). "Dysfunction of endothelial protein C activation in severe meningococcal sepsis." N Engl J Med **345**(6): 408-16.

Fellick, J. M., J. A. Sills, et al. (2001). "Neurodevelopmental outcome in meningococcal disease: a case-control study." Arch Dis Child **85**(1): 6-11.

Fenton, K. E., C. A. Sable, et al. (2004). "Increases in serum levels of troponin I are associated with cardiac dysfunction and disease severity in pediatric patients with septic shock." Pediatr Crit Care Med **5**(6): 533-8.

Fernandes, B. and A. Giles (2003). "An abnormal activated partial thromboplastin time clotting waveform is associated with high mortality and a procoagulant state." Lab Hematol **9**(3): 138-42.

Fernandes, C. J., Jr., N. Akamine, et al. (1999). "Cardiac troponin: a new serum marker of myocardial injury in sepsis." Intensive Care Med **25**(10): 1165-8.

Finn, A., S. Naik, et al. (1993). "Interleukin-8 release and neutrophil degranulation after pediatric cardiopulmonary bypass." J.Thorac.Cardiovasc.Surg. **105**(2): 234-241.

Fortin, C. F., P. P. McDonald, et al. (2009). "Sepsis, leukocytes and nitric oxide (NO): an intricate affair." Shock.

Fourrier, F., P. Lestavel, et al. (1990). "Meningococcemia and purpura fulminans in adults: acute deficiencies of proteins C and S and early treatment with antithrombin III concentrates." Intensive Care Med. **16**(2): 121-124.

Frenette, P. S. and D. D. Wagner (1996). "Adhesion molecules--Part 1." N Engl J Med **334**(23): 1526-9.

Frenette, P. S. and D. D. Wagner (1996). "Adhesion molecules--Part II: Blood vessels and blood cells." N Engl J Med **335**(1): 43-5.

Fried, I., B. Bar-Oz, et al. (2006). "Comparison of N-terminal pro-B-type natriuretic peptide levels in critically ill children with sepsis versus acute left ventricular dysfunction." Pediatrics **118**(4): e1165-8.

Friedman, G., G. Berlot, et al. (1995). "Combined measurements of blood lactate concentrations and gastric intramucosal pH in patients with severe sepsis." Crit Care Med **23**(7): 1184-93.

Fries, M., M. H. Weil, et al. (2006). "Increases in tissue Pco2 during circulatory shock reflect selective decreases in capillary blood flow." Crit Care Med **34**(2): 446-52.

Gando, S., T. Kameue, et al. (2005). "Serial changes in neutrophil-endothelial activation markers during the course of sepsis associated with disseminated intravascular coagulation." Thromb Res **116**(2): 91-100.

Geiger, R., A. Hammerer-Lercher, et al. (2007). "NT-proBNP concentrations indicate cardiac disease in pediatric patients." Int J Cardiol **123**(1): 63-5.

Gendrel, D., M. Assicot, et al. (1996). "Procalcitonin as a marker for the early diagnosis of neonatal infection." J Pediatr **128**(4): 570-3.

Gerard, C., C. Bruyns, et al. (1993). "Interleukin 10 reduces the release of tumor necrosis factor and prevents lethality in experimental endotoxemia." J.Exp.Med. **177**(2): 547-550.

Gerhardt, W., H. Katus, et al. (1991). "S-troponin T in suspected ischemic myocardial injury compared with mass and catalytic concentrations of S-creatine kinase isoenzyme MB." Clin Chem **37**(8): 1405-11.

Giamarellos-Bourboulis, E. J., A. Mega, et al. (2002). "Procalcitonin: a marker to clearly differentiate systemic inflammatory response syndrome and sepsis in the critically ill patient?" Intensive Care Med **28**(9): 1351-6.

Gibot, S., A. Cravoisy, et al. (2005). "Time-course of sTREM (soluble triggering receptor expressed on myeloid cells)-1, procalcitonin, and C-reactive protein plasma concentrations during sepsis." Crit Care Med **33**(4): 792-6.

Girardin, E., G. E. Grau, et al. (1988). "Tumor necrosis factor and interleukin-1 in the serum of children with severe infectious purpura." N.Engl.J.Med. **319**(7): 397-400.

Girardin, E., P. Roux-Lombard, et al. (1992). "Imbalance between tumour necrosis factor-alpha and soluble TNF receptor concentrations in severe meningococcaemia. The J5 Study Group." Immunology **76**(1): 20-23.

Girardin, E., P. Roux-Lombard, et al. (1992). "Imbalance between tumour necrosis factor-alpha and soluble TNF receptor concentrations in severe meningococcaemia. The J5 Study Group." Immunology **76**(1): 20-3.

Giroir, B. P., P. J. Scannon, et al. (2001). "Bactericidal/permeability-increasing protein--lessons learned from the phase III, randomized, clinical trial of rBPI21 for adjunctive treatment of children with severe meningococcemia." Crit Care Med. **29**(7 Suppl): S130-S135.

Glitza, I. C., I. Ehrhard, et al. (2008). "Longitudinal study of meningococcal carrier rates in teenagers." Int J Hyg Environ Health **211**(3-4): 263-72.

Goedhart, P. K. M., Bezemer R, Merza J, and Ince C (2007). "Sidestream Dark Field (SDF) imaging: a novel stroboscopic LED ring-based imaging modality for clinical assessment of the microcirculation." Optical Society of America **15**(23): 15101-15114.

Goldhill, D. R. (1997). "Calcium and Magnesium." Care Crit.Ill. **13**: 112-115.

Goldman, D., R. M. Bateman, et al. (2004). "Effect of sepsis on skeletal muscle oxygen consumption and tissue oxygenation: interpreting capillary oxygen transport data using a mathematical model." Am.J.Physiol Heart Circ.Physiol **287**(6): H2535-H2544.

Goodchild, C. S. and J. M. Serrao (1989). "Cardiovascular effects of propofol in the anaesthetized dog." Br J Anaesth **63**(1): 87-92.

Gray, S. J., C. L. Trotter, et al. (2006). "Epidemiology of meningococcal disease in England and Wales 1993/94 to 2003/04: contribution and experiences of the Meningococcal Reference Unit." J Med Microbiol **55**(Pt 7): 887-96.

Grocott-Mason, R. M. and A. M. Shah (1998). "Cardiac dysfunction in sepsis: new theories and clinical implications." Intensive Care Med **24**(4): 286-95.

Groner, W., J. W. Winkelman, et al. (1999). "Orthogonal polarization spectral imaging: a new method for study of the microcirculation." Nat.Med. **5**(10): 1209-1212.

Groner, W., J. W. Winkelman, et al. (1999). "Orthogonal polarization spectral imaging: a new method for study of the microcirculation." Nat Med **5**(10): 1209-12.

Grundmann, U., A. Zissis, et al. (1997). "In vivo effects of halothane, enflurane, and isoflurane on hepatic sinusoidal microcirculation." Acta Anaesthesiol Scand **41**(6): 760-5.

Gundersen, Y., C. O. Corso, et al. (1998). "The nitric oxide donor sodium nitroprusside protects against hepatic microcirculatory dysfunction in early endotoxaemia." Intensive Care Med **24**(12): 1257-63.

Gundersen, Y., T. Saetre, et al. (1996). "The NO donor sodium nitroprusside reverses the negative effects on hepatic arterial flow induced by endotoxin and the NO synthase inhibitor L-NAME." Eur.Surg.Res. **28**(5): 323-332.

Gurkan, F., A. Alkaya, et al. (2004). "Cardiac troponin-I as a marker of myocardial dysfunction in children with septic shock." Swiss Med Wkly **134**(39-40): 593-6.

Gutgesell, H. P., M. Paquet, et al. (1977). "Evaluation of left ventricular size and function by echocardiography. Results in normal children." Circulation **56**(3): 457-62.

Hackett, S. J., E. D. Carrol, et al. (2002). "Improved case confirmation in meningococcal disease with whole blood Taqman PCR." Arch Dis Child **86**(6): 449-52.

Hackett, S. J., A. P. Thomson, et al. (2001). "Cytokines, chemokines and other effector molecules involved in meningococcal disease." J.Med.Microbiol. **50**(10): 847-859.

Hagmolen of ten, H., A. Wiegman, et al. (2000). "Life-threatening heart failure in meningococcal septic shock in children: non-invasive measurement of cardiac parameters is of important prognostic value." Eur.J.Pediatr. **159**(4): 277-282.

Hagmolen of ten Have, W., A. Wiegman, et al. (2000). "Life-threatening heart failure in meningococcal septic shock in children: non-invasive measurement of cardiac parameters is of important prognostic value." Eur J Pediatr **159**(4): 277-82.

Hahne, S. J., A. Charlett, et al. (2006). "Effectiveness of antibiotics given before admission in reducing mortality from meningococcal disease: systematic review." Bmj **332**(7553): 1299-303.

Hall, C. (2005). "NT-ProBNP: the mechanism behind the marker." J Card Fail **11**(5 Suppl): S81-3.

Halstensen, A., M. Ceska, et al. (1993). "Interleukin-8 in serum and cerebrospinal fluid from patients with meningococcal disease." J.Infect.Dis. **167**(2): 471-475.

Handford S, F. A. J. a. R. M. E. (2007). Surveillance Network for Invasive Neisseria meningitidis in Europe - 2002. Final report. 2003.

Harada, K., M. Tamura, et al. (2002). "Comparison of the right ventricular Tei index by tissue Doppler imaging to that obtained by pulsed Doppler in children without heart disease." Am J Cardiol **90**(5): 566-9.

Harbarth, S., K. Holeckova, et al. (2001). "Diagnostic value of procalcitonin, interleukin-6, and interleukin-8 in critically ill patients admitted with suspected sepsis." Am J Respir Crit Care Med **164**(3): 396-402.

Hardman, J. M. and K. M. Earle (1969). "Myocarditis in 200 fatal meningococcal infections." Arch.Pathol. **87**(3): 318-325.

Harris, A. G., I. Sinitsina, et al. (2000). "The Cytoscan Model E-II, a new reflectance microscope for intravital microscopy: comparison with the standard fluorescence method." J Vasc Res **37**(6): 469-76.

Harris, A. G., I. Sinitsina, et al. (2002). "Validation of OPS imaging for microvascular measurements during isovolumic hemodilution and low hematocrits." Am J Physiol Heart Circ Physiol **282**(4): H1502-9.

Harrison, L. H., M. A. Pass, et al. (2001). "Invasive meningococcal disease in adolescents and young adults." Jama **286**(6): 694-9.

Hart, C. A. and T. R. Rogers (1993). "Meningococcal disease." J Med Microbiol **39**(1): 3-25.

Hart, C. A. and T. R. Rogers (1993). "Meningococcal disease." Journal of Medical Microbiology **39**: 3-25.

Hart, C. A. and A. P. Thomson (2006). "Meningococcal disease and its management in children." Bmj **333**(7570): 685-90.

Hawkins, R. C. and H. L. Tan (1999). "Comparison of the diagnostic utility of CK, CK-MB (activity and mass), troponin T and troponin I in patients with suspected acute myocardial infarction." Singapore Med J **40**(11): 680-4.

Hazelzet, J. A., I. M. Risseeuw-Appel, et al. (1996). "Age-related differences in outcome and severity of DIC in children with septic shock and purpura." Thromb.Haemost. **76**(6): 932-938.

Hazelzet, J. A., d. V. van, et al. (1994). "Relation between cytokines and routine laboratory data in children with septic shock and purpura." Intensive Care Med. **20**(5): 371-374.

Heger M, B. J., Stenback K, Faber DJ, and van Gemert MJC. (2005). "Darkfield orthogonal polarized spectral imaging for studying endovascular laser-tissue interactions in vivo – a preliminary study." Opt. Express **13**: 702-715.

Herbertson, M. J., H. A. Werner, et al. (1996). "Nitric oxide synthase inhibition partially prevents decreased LV contractility during endotoxemia." Am J Physiol **270**(6 Pt 2): H1979-84.

Hersch, M., A. A. Gnidec, et al. (1990). "Histologic and ultrastructural changes in nonpulmonary organs during early hyperdynamic sepsis." Surgery **107**(4): 397-410.

Heyderman, R. S., Y. Ben-Shlomo, et al. (2004). "The incidence and mortality for meningococcal disease associated with area deprivation: an ecological study of hospital episode statistics." Arch Dis Child **89**(11): 1064-8.

Heyderman, R. S., Y. Ben-Shlomo, et al. (2004). "The incidence and mortality for meningococcal disease associated with area deprivation: an ecological study of hospital episode statistics." Arch.Dis.Child **89**(11): 1064-1068.

Hiarada, K., T. Orino, et al. (2000). "Tissue doppler imaging of left and right ventricles in normal children." Tohoku J Exp Med **191**(1): 21-9.

Hollenberg, S. M., M. Broussard, et al. (2000). "Increased microvascular reactivity and improved mortality in septic mice lacking inducible nitric oxide synthase." Circ Res **86**(7): 774-8.

Holzmann, A., H. Schmidt, et al. (1995). "Propofol-induced alterations in the microcirculation of hamster striated muscle." Br J Anaesth **75**(4): 452-6.

Hunt, P. J., E. A. Espiner, et al. (1996). "Differing biological effects of equimolar atrial and brain natriuretic peptide infusions in normal man." J Clin Endocrinol Metab **81**(11): 3871-6.

Hussain, N., D. Hodson, et al. (2008). "The biphasic transmittance waveform: an early marker of sepsis in patients with neutropenia." Thromb Haemost **100**(1): 146-8.

Ince, C. (1999). "Mechanism of impaired oxygen extraction in sepsis. Shunt and the pO2 gap." Minerva Anestesiol **65**(6): 337-9.

Ince, C. (2005). "The microcirculation is the motor of sepsis." Crit Care **9 Suppl 4**: S13-9.

Ince, C. and M. Sinaasappel (1999). "Microcirculatory oxygenation and shunting in sepsis and shock." Crit Care Med **27**(7): 1369-77.

Ince, C. and M. Sinaasappel (1999). "Microcirculatory oxygenation and shunting in sepsis and shock." Crit Care Med. **27**(7): 1369-1377.

Jafri, S. M., S. Lavine, et al. (1990). "Left ventricular diastolic function in sepsis." Crit Care Med **18**(7): 709-14.

Jakobsen, P. H., S. Morris-Jones, et al. (1994). "Increased plasma concentrations of sICAM-1, sVCAM-1 and sELAM-1 in patients with Plasmodium falciparum or P. vivax malaria and association with disease severity." Immunology **83**(4): 665-669.

Januzzi, J. L., Jr., C. A. Camargo, et al. (2005). "The N-terminal Pro-BNP investigation of dyspnea in the emergency department (PRIDE) study." Am J Cardiol **95**(8): 948-54.

Januzzi, J. L., R. van Kimmenade, et al. (2006). "NT-proBNP testing for diagnosis and short-term prognosis in acute destabilized heart failure: an international pooled analysis of 1256 patients: the International Collaborative of NT-proBNP Study." Eur Heart J **27**(3): 330-7.

Jensen, J. U., L. Heslet, et al. (2006). "Procalcitonin increase in early identification of critically ill patients at high risk of mortality." Crit Care Med **34**(10): 2596-602.

Jensen, J. U., B. Lundgren, et al. (2007). "Meta-analysis of procalcitonin for sepsis detection." Lancet Infect Dis **7**(8): 499-500; author reply 502-3.

Jobsis, F. F. (1977). "Noninvasive, infrared monitoring of cerebral and myocardial oxygen sufficiency and circulatory parameters." Science **198**(4323): 1264-7.

Katus, H. A., A. Remppis, et al. (1991). "Diagnostic efficiency of troponin T measurements in acute myocardial infarction." Circulation **83**(3): 902-12.

Kirsch, E. A., R. P. Barton, et al. (1996). "Pathophysiology, treatment and outcome of meningococcemia: a review and recent experience." Pediatr.Infect.Dis.J. **15**(11): 967-978.

Kirshbom, P. M., J. M. Forbess, et al. (2007). "Cerebral near infrared spectroscopy is a reliable marker of systemic perfusion in awake single ventricle children." Pediatr Cardiol **28**(1): 42-5.

Kleiber, M. and T. A. Rogers (1961). "Energy metabolism." Annu Rev Physiol **23**: 5-36.

Klein, N. J., G. I. Shennan, et al. (1992). "Alteration in glycosaminoglycan metabolism and surface charge on human umbilical vein endothelial cells induced by cytokines, endotoxin and neutrophils." J.Cell Sci. **102 (Pt 4)**: 821-832.

Klinkhammer, M. D. and J. E. Colletti (2008). "Pediatric myth: fever and petechiae." Cjem **10**(5): 479-82.

Knotzer, H., S. Maier, et al. (2007). "Oscillation frequency of skin microvascular blood flow is associated with mortality in critically ill patients." Acta Anaesthesiol Scand **51**(6): 701-7.

Koch, M., D. De Backer, et al. (2008). "Effects of propofol on human microcirculation." Br J Anaesth **101**(4): 473-8.

Koj, A. (1996). "Initiation of acute phase response and synthesis of cytokines." Biochim Biophys Acta **1317**(2): 84-94.

Kolar, F. and L. Jansky (1984). "Oxygen consumption in rat skeletal muscle at various rates of oxygen delivery." Experientia **40**(4): 353-4.

Kornelisse, R. F., J. A. Hazelzet, et al. (1996). "The relationship between plasminogen activator inhibitor-1 and proinflammatory and

counterinflammatory mediators in children with meningococcal septic shock." J.Infect.Dis. **173**(5): 1148-1156.

Kowluru, A. (2001). "Adenine and guanine nucleotide-specific succinyl-CoA synthetases in the clonal beta-cell mitochondria: implications in the beta-cell high-energy phosphate metabolism in relation to physiological insulin secretion." Diabetologia **44**(1): 89-94.

Krown, K. A., M. T. Page, et al. (1996). "Tumor necrosis factor alpha-induced apoptosis in cardiac myocytes. Involvement of the sphingolipid signaling cascade in cardiac cell death." J Clin Invest **98**(12): 2854-65.

Krueger, M., A. Heinzmann, et al. (2007). "Adhesion molecules in pediatric intensive care patients with organ dysfunction syndrome." Intensive Care Med **33**(2): 359-63.

Krupicka, J., T. Janota, et al. (2008). "Natriuretic peptides- physiology, pathophysiology and clinical use in heart failure." Physiol Res.

Kumar, A., V. Thota, et al. (1996). "Tumor necrosis factor alpha and interleukin 1beta are responsible for in vitro myocardial cell depression induced by human septic shock serum." J Exp Med **183**(3): 949-58.

Kvalsvig, A. J. and D. J. Unsworth (2003). "The immunopathogenesis of meningococcal disease." J.Clin.Pathol. **56**(6): 417-422.

Lack, J. A. and M. E. Stuart-Taylor (1997). "Calculation of drug dosage and body surface area of children." Br J Anaesth **78**(5): 601-5.

Lacroix, J. and J. Cotting (2005). "Severity of illness and organ dysfunction scoring in children." Pediatr Crit Care Med **6**(3 Suppl): S126-34.

Lam, C., K. Tyml, et al. (1994). "Microvascular perfusion is impaired in a rat model of normotensive sepsis." J.Clin.Invest **94**(5): 2077-2083.

Lambert, A. J., B. Wang, et al. (2004). "Exogenous insulin can reverse the effects of caloric restriction on mitochondria." Biochem Biophys Res Commun **316**(4): 1196-201.

Lampugnani, M. G., L. Caveda, et al. (1993). "Endothelial cell-to-cell junctions. Structural characteristics and functional role in the regulation of vascular permeability and leukocyte extravasation." Baillieres Clin.Haematol. **6**(3): 539-558.

Langer, S., P. Biberthaler, et al. (2001). "In vivo monitoring of microvessels in skin flaps: introduction of a novel technique." Microsurgery **21**(7): 317-24.

Langer, S., F. Born, et al. (2002). "Orthogonal polarization spectral imaging versus intravital fluorescent microscopy for microvascular studies in wounds." Ann Plast Surg **48**(6): 646-53.

Langer, S., A. G. Harris, et al. (2001). "Orthogonal polarization spectral imaging as a tool for the assessment of hepatic microcirculation: a validation study." Transplantation **71**(9): 1249-56.

Leach, R. M. and D. F. Treacher (1992). "The pulmonary physician and critical care. 6. Oxygen transport: the relation between oxygen delivery and consumption." Thorax **47**(11): 971-8.

Leach, R. M. and D. F. Treacher (1998). "Oxygen transport-2. Tissue hypoxia." Bmj **317**(7169): 1370-3.

Leclerc, F., S. Leteurtre, et al. (2002). "Procalcitonin as a prognostic marker in children with meningococcal septic shock." Arch Dis Child **87**(5): 450.

Ledingham, I. M. and C. S. McArdle (1978). "Prospective study of the treatment of septic shock." Lancet **1**(8075): 1194-1197.

Leteurtre, S., A. Martinot, et al. (2003). "Validation of the paediatric logistic organ dysfunction (PELOD) score: prospective, observational, multicentre study." Lancet **362**(9379): 192-7.

Levin, E. R., D. G. Gardner, et al. (1998). "Natriuretic peptides." N Engl J Med **339**(5): 321-8.

Levy, M. M., M. P. Fink, et al. (2003). "2001 SCCM/ESICM/ACCP/ATS/SIS International Sepsis Definitions Conference." Crit Care Med **31**(4): 1250-6.

Lidington, D., K. Tyml, et al. (2002). "Lipopolysaccharide-induced reductions in cellular coupling correlate with tyrosine phosphorylation of connexin 43." J.Cell Physiol **193**(3): 373-379.

Lifely, M. R., S. C. Roberts, et al. (1991). "Immunogenicity in adult males of a Neisseria meningitidis group B vaccine composed of polysaccharide complexed with outer membrane proteins." Vaccine **9**(1): 60-6.

Lindsay CA, B. P., Lawless S, Kitchen L, Zorka A, Garcia J et al (1998). "Pharmacokinetics and pharmacodynamics of milrinone lactate in pediatric patients with septic shock.

." J Pediatr. **132**: 329-34.

Lodha, R., S. Arun, et al. (2009). "Myocardial cell injury is common in children with septic shock." Acta Paediatr **98**(3): 478-81.

Loke, K. E., P. I. McConnell, et al. (1999). "Endogenous endothelial nitric oxide synthase-derived nitric oxide is a physiological regulator of myocardial oxygen consumption." Circ Res **84**(7): 840-5.

Lominadze, D. and G. McHedlishvili (1999). "Red blood cell behavior at low flow rate in microvessels." Microvasc Res **58**(2): 187-9.

Lopez, A., J. A. Lorente, et al. (2004). "Multiple-center, randomized, placebo-controlled, double-blind study of the nitric oxide synthase inhibitor 546C88: effect on survival in patients with septic shock." Crit Care Med **32**(1): 21-30.

Ma, K. K., T. Ogawa, et al. (2004). "Selective upregulation of cardiac brain natriuretic peptide at the transcriptional and translational levels by pro-inflammatory cytokines and by conditioned medium derived from mixed lymphocyte reactions via p38 MAP kinase." J Mol Cell Cardiol **36**(4): 505-13.

Maat, M., C. M. Buysse, et al. (2007). "Improved survival of children with sepsis and purpura: effects of age, gender, and era." Crit Care **11**(5): R112.

Machado, M., L. M. Falcao, et al. (2004). "The clinical role of natriuretic peptides--importance of BNP and NT-proBNP. Implications in heart failure and acute coronary syndrome." Rev Port Cardiol **23**(7-8): 1005-32.

Magga, J., M. Marttila, et al. (1994). "Brain natriuretic peptide in plasma, atria, and ventricles of vasopressin- and phenylephrine-infused conscious rats." Endocrinology **134**(6): 2505-15.

Mair, G., S. Dunhill, et al. (2008). "Prognostic implications of a biphasic waveform for APTT analysis in a district general hospital." Int J Lab Hematol **30**(6): 467-72.

Maisel, A. S., P. Krishnaswamy, et al. (2002). "Rapid measurement of B-type natriuretic peptide in the emergency diagnosis of heart failure." N Engl J Med **347**(3): 161-7.

Marechal, X., R. Favory, et al. (2008). "Endothelial glycocalyx damage during endotoxemia coincides with microcirculatory dysfunction and vascular oxidative stress." Shock **29**(5): 572-6.

Marik, P. E. (2005). "Regional carbon dioxide monitoring to assess the adequacy of tissue perfusion." Curr Opin Crit Care **11**(3): 245-51.

Marik, P. E. and A. Bankov (2003). "Sublingual capnometry versus traditional markers of tissue oxygenation in critically ill patients." Crit Care Med **31**(3): 818-22.

Marik, P. E. and A. Lorenzana (1996). "Effect of tube feedings on the measurement of gastric intramucosal pH." Crit Care Med **24**(9): 1498-500.

Marra, M. N., C. G. Wilde, et al. (1992). "The role of bactericidal/permeability-increasing protein as a natural inhibitor of bacterial endotoxin." J.Immunol. **148**(2): 532-537.

Martins, P. S., E. G. Kallas, et al. (2003). "Upregulation of reactive oxygen species generation and phagocytosis, and increased apoptosis in human neutrophils during severe sepsis and septic shock." Shock **20**(3): 208-212.

Marzouk, O., K. Bestwick, et al. (1993). "Variation in serum C-reactive protein across the clinical spectrum of meningococcal disease." Acta Paediatr. **82**(9): 729-733.

Marzouk, O., A. P. Thomson, et al. (1991). "Features and outcome in meningococcal disease presenting with maculopapular rash." Arch Dis Child **66**(4): 485-7.

Mathura, K. R., K. C. Vollebregt, et al. (2001). "Comparison of OPS imaging and conventional capillary microscopy to study the human microcirculation." J Appl Physiol **91**(1): 74-8.

Mathura, K. R., K. C. Vollebregt, et al. (2001). "Comparison of OPS imaging and conventional capillary microscopy to study the human microcirculation." J.Appl.Physiol **91**(1): 74-78.

Matsumoto, T., H. Wada, et al. (2006). "Frequency of abnormal biphasic aPTT clot waveforms in patients with underlying disorders associated with disseminated intravascular coagulation." Clin Appl Thromb Hemost **12**(2): 185-92.

McLaurin, M. D., F. S. Apple, et al. (1997). "Cardiac troponin I, cardiac troponin T, and creatine kinase MB in dialysis patients without ischemic heart disease: evidence of cardiac troponin T expression in skeletal muscle." Clin Chem **43**(6 Pt 1): 976-82.

McMahon, T. (1973). "Size and shape in biology." Science **179**(79): 1201-4.

Mehta, N. J., I. A. Khan, et al. (2004). "Cardiac troponin I predicts myocardial dysfunction and adverse outcome in septic shock." Int J Cardiol **95**(1): 13-7.

Mercier, J. C., F. Beaufils, et al. (1988). "Hemodynamic patterns of meningococcal shock in children." Crit Care Med **16**(1): 27-33.

Mercier, J. C., F. Beaufils, et al. (1988). "Hemodynamic patterns of meningococcal shock in children." Crit Care Med. **16**(1): 27-33.

Merz, A. J., C. A. Enns, et al. (1999). "Type IV pili of pathogenic Neisseriae elicit cortical plaque formation in epithelial cells." Mol Microbiol **32**(6): 1316-32.

Merz, A. J. and M. So (1997). "Attachment of piliated, Opa- and Opc- gonococci and meningococci to epithelial cells elicits cortical actin rearrangements and clustering of tyrosine-phosphorylated proteins." Infect Immun **65**(10): 4341-9.

Merz, A. J. and M. So (2000). "Interactions of pathogenic neisseriae with epithelial cell membranes." Annu Rev Cell Dev Biol **16**: 423-57.

Mills, G. D., H. M. Lala, et al. (2006). "Elevated procalcitonin as a diagnostic marker in meningococcal disease." Eur J Clin Microbiol Infect Dis **25**(8): 501-9.

Molesworth, A. M., M. C. Thomson, et al. (2002). "Where is the meningitis belt? Defining an area at risk of epidemic meningitis in Africa." Trans.R.Soc.Trop.Med.Hyg. **96**(3): 242-249.

Monsalve, F., L. Rucabado, et al. (1984). "Myocardial depression in septic shock caused by meningococcal infection." Crit Care Med. **12**(12): 1021-1023.

Monsalve, F., L. Rucabado, et al. (1984). "Myocardial depression in septic shock caused by meningococcal infection." Crit Care Med **12**(12): 1021-3.

Morin, M. J., N. Unno, et al. (1998). "Differential expression of inducible nitric oxide synthase messenger RNA along the longitudinal and crypt-villus axes of the intestine in endotoxemic rats." Crit Care Med. **26**(7): 1258-1264.

Mulier, K. E., D. E. Skarda, et al. (2008). "Near-infrared spectroscopy in patients with severe sepsis: correlation with invasive hemodynamic measurements." Surg Infect (Larchmt) **9**(5): 515-9.

Muller, B., M. Schmidtke, et al. (1987). "Action of the stable prostacyclin analogue iloprost on microvascular tone and -permeability in the hamster cheek pouch." Prostaglandins Leukot Med **29**(2-3): 187-98.

Munt, B., J. Jue, et al. (1998). "Diastolic filling in human severe sepsis: an echocardiographic study." Crit Care Med **26**(11): 1829-33.

Murthy, V. V. and A. Karmen (1997). "Troponin-T as a serum marker for myocardial infarction." J Clin Lab Anal **11**(3): 125-8.

Nadeau, R. G. and W. Groner (2001). "The role of a new noninvasive imaging technology in the diagnosis of anemia." J Nutr **131**(5): 1610S-4S.

Nadeau, R. G., W (2000). "Orthogonal polarization spectral imaging: State of the Art." Orthogonal polarization spectral imaging. Messmer K (ed). Karger, Basel **24**: 9-20.

Nadel, S., B. Goldstein, et al. (2007). "Drotrecogin alfa (activated) in children with severe sepsis: a multicentre phase III randomised controlled trial." Lancet **369**(9564): 836-43.

Nadel, S., M. Levin, et al. (1995). Treatment of meningococcal disease in childhood. Meningococcal Disease. Chichester, John Wiley and Sons: 207-243.

Nagueh, S. F., K. J. Middleton, et al. (1997). "Doppler tissue imaging: a noninvasive technique for evaluation of left ventricular relaxation and estimation of filling pressures." J Am Coll Cardiol **30**(6): 1527-33.

Nagueh, S. F., I. Mikati, et al. (1998). "Doppler estimation of left ventricular filling pressure in sinus tachycardia. A new application of tissue doppler imaging." Circulation **98**(16): 1644-50.

Narula, J., B. A. Khaw, et al. (1993). "Brief report: recognition of acute myocarditis masquerading as acute myocardial infarction." N Engl J Med **328**(2): 100-4.

Narula, J., J. F. Southern, et al. (1991). "Myocarditis simulating myocardial infarction." J Nucl Med **32**(2): 312-8.

Nasser, N., Z. Perles, et al. (2006). "NT-proBNP as a marker for persistent cardiac disease in children with history of dilated cardiomyopathy and myocarditis." Pediatr Cardiol **27**(1): 87-90.

Nikolaou, N. I., C. Goritsas, et al. (2007). "Brain natriuretic peptide increases in septic patients without severe sepsis or shock." Eur J Intern Med **18**(7): 535-41.

Ninis, N., C. Phillips, et al. (2005). "The role of healthcare delivery in the outcome of meningococcal disease in children: case-control study of fatal and non-fatal cases." Bmj **330**(7506): 1475.

Nir, A. and N. Nasser (2005). "Clinical value of NT-ProBNP and BNP in pediatric cardiology." J Card Fail **11**(5 Suppl): S76-80.

Nishida, J., R. S. McCuskey, et al. (1994). "Protective role of NO in hepatic microcirculatory dysfunction during endotoxemia." Am.J.Physiol **267**(6 Pt 1): G1135-G1141.

Oki, T., T. Tabata, et al. (1997). "Clinical application of pulsed Doppler tissue imaging for assessing abnormal left ventricular relaxation." Am J Cardiol **79**(7): 921-8.

Ommen, S. R. (2001). "Echocardiographic assessment of diastolic function." Curr Opin Cardiol **16**(4): 240-5.

Ommen, S. R. and R. A. Nishimura (2003). "A clinical approach to the assessment of left ventricular diastolic function by Doppler echocardiography: update 2003." Heart **89 Suppl 3**: iii18-23.

Osterud, B. and T. Flaegstad (1983). "Increased tissue thromboplastin activity in monocytes of patients with meningococcal infection: related to an unfavourable prognosis." Thromb.Haemost. **49**(1): 5-7.

Osthaus, W. A., D. Boethig, et al. (2009). "First experiences with intraoperative Levosimendan in pediatric cardiac surgery." Eur J Pediatr **168**(6): 735-40.

Otero, R. M., H. B. Nguyen, et al. (2006). "Early goal-directed therapy in severe sepsis and septic shock revisited: concepts, controversies, and contemporary findings." Chest **130**(5): 1579-95.

Oyamada, J., M. Toyono, et al. (2008). "Noninvasive estimation of left ventricular end-diastolic pressure using tissue Doppler imaging combined with pulsed-wave Doppler echocardiography in patients with ventricular septal defects: a comparison with the plasma levels of the B-type natriuretic Peptide." Echocardiography **25**(3): 270-7.

Pahernik, S., A. G. Harris, et al. (2002). "Orthogonal polarisation spectral imaging as a new tool for the assessment of antivascular tumour treatment in vivo: a validation study." Br J Cancer **86**(10): 1622-7.

Parker, M. M., J. H. Shelhamer, et al. (1987). "Serial cardiovascular variables in survivors and nonsurvivors of human septic shock: heart rate as an early predictor of prognosis." Crit Care Med **15**(10): 923-9.

Parthasarathi, K. and H. H. Lipowsky (1999). "Capillary recruitment in response to tissue hypoxia and its dependence on red blood cell deformability." Am J Physiol **277**(6 Pt 2): H2145-57.

Pathan, N., C. A. Hemingway, et al. (2004). "Role of interleukin 6 in myocardial dysfunction of meningococcal septic shock." Lancet **363**(9404): 203-9.

Pathan, N., C. A. Hemingway, et al. (2004). "Role of interleukin 6 in myocardial dysfunction of meningococcal septic shock." Lancet **363**(9404): 203-209.

Pathan, N., C. Sandiford, et al. (2002). "Characterization of a myocardial depressant factor in meningococcal septicemia." Crit Care Med **30**(10): 2191-8.

Pathan, N., C. Sandiford, et al. (2002). "Characterization of a myocardial depressant factor in meningococcal septicemia." Crit Care Med. **30**(10): 2191-2198.

Pathan, N., E. J. Williams, et al. (2005). "Changes in the interleukin-6/soluble interleukin-6 receptor axis in meningococcal septic shock." Crit Care Med **33**(8): 1839-44.

Pearson, J. D. (2000). "Normal endothelial cell function." Lupus **9**(3): 183-8.
Pellett, A. A., W. G. Tolar, et al. (2004). "The Tei index: methodology and disease state values." Echocardiography **21**(7): 669-72.
Pennings, F. A., G. J. Bouma, et al. (2004). "Direct observation of the human cerebral microcirculation during aneurysm surgery reveals increased arteriolar contractility." Stroke **35**(6): 1284-1288.
Peters, M., A. Petros, et al. (2002). "Genuine reduction in meningococcal deaths results from teamwork." Arch Dis Child **87**(6): 560-1; author reply 361.
Pinto, B. B., S. Rehberg, et al. (2008). "Role of levosimendan in sepsis and septic shock." Curr Opin Anaesthesiol **21**(2): 168-77.
Pittet, J. F., J. S. Lacroix, et al. (1992). "Different effects of prostacyclin and phentolamine on delivery-dependent O2 consumption and skin microcirculation after cardiac surgery." Can.J.Anaesth. **39**(10): 1023-1029.
Pittet, J. F., J. S. Lacroix, et al. (1990). "Prostacyclin but not phentolamine increases oxygen consumption and skin microvascular blood flow in patients with sepsis and respiratory failure." Chest **98**(6): 1467-1472.
Poderoso, J. J., M. C. Carreras, et al. (1996). "Nitric oxide inhibits electron transfer and increases superoxide radical production in rat heart mitochondria and submitochondrial particles." Arch Biochem Biophys **328**(1): 85-92.
Poelaert, J., C. Declerck, et al. (1997). "Left ventricular systolic and diastolic function in septic shock." Intensive Care Med **23**(5): 553-60.
Poeze, M. (2006). "Tissue-oxygenation assessment using near-infrared spectroscopy during severe sepsis: confounding effects of tissue edema on StO2 values." Intensive Care Med **32**(5): 788-9.
Pollack, M. M., U. E. Ruttimann, et al. (1988). "Pediatric risk of mortality (PRISM) score." Crit Care Med **16**(11): 1110-6.
Pollard, A. J. and M. C. Maiden (2003). "Epidemic meningococcal disease in sub-Saharan Africa--towards a sustainable solution?" Lancet Infect.Dis. **3**(2): 68-70.
Povoas, H. P., M. H. Weil, et al. (2001). "Decreases in mesenteric blood flow associated with increases in sublingual PCO2 during hemorrhagic shock." Shock **15**(5): 398-402.
Powars, D. R., Z. R. Rogers, et al. (1987). "Purpura fulminans in meningococcemia: association with acquired deficiencies of proteins C and S." N.Engl.J.Med. **317**(9): 571-572.
Pradier, O., C. Gerard, et al. (1993). "Interleukin-10 inhibits the induction of monocyte procoagulant activity by bacterial lipopolysaccharide." Eur.J.Immunol. **23**(10): 2700-2703.
Pries, A. R. and W. M. Kuebler (2006). "Normal endothelium." Handb Exp Pharmacol(176 Pt 1): 1-40.
Protti, A. and M. Singer (2006). "Bench-to-bedside review: potential strategies to protect or reverse mitochondrial dysfunction in sepsis-induced organ failure." Crit Care **10**(5): 228.
Rees, D. D., J. E. Monkhouse, et al. (1998). "Nitric oxide and the haemodynamic profile of endotoxin shock in the conscious mouse." Br J Pharmacol **124**(3): 540-6.
Remedi, M. S., C. G. Nichols, et al. (2006). "The mitochondria and insulin release: Nnt just a passing relationship." Cell Metab **3**(1): 5-7.

Revelly, J. P., T. Ayuse, et al. (1996). "Endotoxic shock alters distribution of blood flow within the intestinal wall." Crit Care Med. **24**(8): 1345-1351.

Rey, C., A. M. Los, et al. (2007). "Procalcitonin and C-reactive protein as markers of systemic inflammatory response syndrome severity in critically ill children." Intensive Care Med. **33**(3): 477-484.

Rich, N., N. West, et al. (2003). "Milrinone in meningococcal sepsis." Pediatr Crit Care Med **4**(3): 394-5.

Riordan, A., A. Thomson, et al. (1995). "Hearing assessment after meningitis and meningococcal disease." Arch Dis Child **72**(5): 441-2.

Riordan, F. A., O. Marzouk, et al. (1995). "The changing presentations of meningococcal disease." Eur J Pediatr **154**(6): 472-4.

Riordan, F. A., O. Marzouk, et al. (1996). "Proinflammatory and anti-inflammatory cytokines in meningococcal disease." Arch.Dis.Child **75**(5): 453-454.

Riordan, F. A., A. P. Thomson, et al. (1999). "Admission cortisol and adrenocorticotrophic hormone levels in children with meningococcal disease: evidence of adrenal insufficiency?" Crit Care Med. **27**(10): 2257-2261.

Rivers, E., B. Nguyen, et al. (2001). "Early goal-directed therapy in the treatment of severe sepsis and septic shock." N Engl J Med **345**(19): 1368-77.

Rivers, E. P. (2006). "Early goal-directed therapy in severe sepsis and septic shock: converting science to reality." Chest **129**(2): 217-8.

Rivers, E. P., H. B. Nguyen, et al. (2004). "Early goal-directed therapy." Crit Care Med **32**(1): 314-5; author reply 315.

Roberson, D. A., W. Cui, et al. (2007). "Annular and septal Doppler tissue imaging in children: normal z-score tables and effects of age, heart rate, and body surface area." J Am Soc Echocardiogr **20**(11): 1276-84.

Roch, A., J. Allardet-Servent, et al. (2005). "NH2 terminal pro-brain natriuretic peptide plasma level as an early marker of prognosis and cardiac dysfunction in septic shock patients." Crit Care Med **33**(5): 1001-7.

Rosenstein, N. E., B. A. Perkins, et al. (2001). "Meningococcal disease." N.Engl.J.Med. **344**(18): 1378-1388.

Rudiger, A., S. Gasser, et al. (2006). "Comparable increase of B-type natriuretic peptide and amino-terminal pro-B-type natriuretic peptide levels in patients with severe sepsis, septic shock, and acute heart failure." Crit Care Med **34**(8): 2140-4.

Sakr, Y., M. J. Dubois, et al. (2004). "Persistent microcirculatory alterations are associated with organ failure and death in patients with septic shock." Crit Care Med **32**(9): 1825-31.

Sakr, Y., M. J. Dubois, et al. (2004). "Persistent microcirculatory alterations are associated with organ failure and death in patients with septic shock." Crit Care Med. **32**(9): 1825-1831.

Sanders, S., A. Barnett, et al. (2008). "Systematic review of the diagnostic accuracy of C-reactive protein to detect bacterial infection in nonhospitalized infants and children with fever." J Pediatr **153**(4): 570-4.

Schmidt-Nielsen, K. and P. Pennycuik (1961). "Capillary density in mammals in relation to body size and oxygen consumption." Am J Physiol **200**: 746-50.

Sharkey, I., A. V. Boddy, et al. (2001). "Body surface area estimation in children using weight alone: application in paediatric oncology." Br J Cancer **85**(1): 23-8.

Shipley, J. B., D. Tolman, et al. (1996). "Milrinone: basic and clinical pharmacology and acute and chronic management." Am J Med Sci **311**(6): 286-91.

Simon, L., F. Gauvin, et al. (2004). "Serum procalcitonin and C-reactive protein levels as markers of bacterial infection: a systematic review and meta-analysis." Clin.Infect.Dis. **39**(2): 206-217.

Sinaasappel, M., I. M. van, et al. (1999). "Microvascular oxygen pressure in the pig intestine during haemorrhagic shock and resuscitation." J.Physiol **514 (Pt 1)**: 245-253.

Sinclair, J. F., C. H. Skeoch, et al. (1987). "Prognosis of meningococcal septicaemia." Lancet **2**(8549): 38.

Sirithunyanont, C., W. Leowattana, et al. (2003). "Role of the plasma brain natriuretic peptide in differentiating patients with congestive heart failure from other diseases." J Med Assoc Thai **86 Suppl 1**: S87-95.

Skarda, D. E., K. E. Mulier, et al. (2007). "Dynamic near-infrared spectroscopy measurements in patients with severe sepsis." Shock **27**(4): 348-53.

Skippen, P. W. and G. E. Krahn (2005). "Acute renal failure in children undergoing cardiopulmonary bypass." Crit Care Resusc **7**(4): 286-91.

Slack, R., K. C. Hawkins, et al. (2005). "Long-term outcome of meningococcal sepsis-associated acute renal failure." Pediatr Crit Care Med **6**(4): 477-9.

Smedegard, G., J. Bjork, et al. (1985). "An intravital microscopy model for studies of immune complex induced inflammation at the microvascular level." Int J Tissue React **7**(1): 55-60.

Smith, E. Y., L. A. Charles, et al. (2004). "Biphasic activated partial thromboplastin time waveform and adverse events in non-intensive care unit patients." Am J Clin Pathol **121**(1): 138-41.

Snell, R. S. (2003). "Clinical Anatomy (Snell Clinical Anatomy) ".

Snider AR, S. G. (1990). "Echocardiography in Pediatric Heart Disease." Year Book Medical Publishers.

Sohn, D. W., I. H. Chai, et al. (1997). "Assessment of mitral annulus velocity by Doppler tissue imaging in the evaluation of left ventricular diastolic function." J Am Coll Cardiol **30**(2): 474-80.

Spies, C., V. Haude, et al. (1998). "Serum cardiac troponin T as a prognostic marker in early sepsis." Chest **113**(4): 1055-63.

Springer, T. A. (1994). "Traffic signals for lymphocyte recirculation and leukocyte emigration: the multistep paradigm." Cell **76**(2): 301-14.

Spronk, P. E., C. Ince, et al. (2002). "Nitroglycerin in septic shock after intravascular volume resuscitation." Lancet **360**(9343): 1395-6.

Spronk, P. E., C. Ince, et al. (2002). "Nitroglycerin in septic shock after intravascular volume resuscitation." Lancet **360**(9343): 1395-1396.

Spronk, P. E., D. F. Zandstra, et al. (2004). "Bench-to-bedside review: sepsis is a disease of the microcirculation." Crit Care **8**(6): 462-468.

Spronk, P. E., D. F. Zandstra, et al. (2004). "Bench-to-bedside review: sepsis is a disease of the microcirculation." Crit Care **8**(6): 462-8.

Sprung, C. L., D. Annane, et al. (2008). "Hydrocortisone therapy for patients with septic shock." N Engl J Med **358**(2): 111-24.

Stephens, D. S. (1999). "Uncloaking the meningococcus: dynamics of carriage and disease." Lancet **353**(9157): 941-942.

Stephens, D. S., L. H. Hoffman, et al. (1983). "Interaction of Neisseria meningitidis with human nasopharyngeal mucosa: attachment and entry into columnar epithelial cells." J.Infect.Dis. **148**(3): 369-376.

Stuart, J. M., P. N. Monk, et al. (1997). "Management of clusters of meningococcal disease. PHIS Meningococcus Working Group and Public Health Medicine Environmental Group." Commun.Dis.Rep.CDR Rev. **7**(1): R3-R5.

Subbaswamy, A., A. A. Hsu, et al. (2008). "Correlation of Cerebral Near-Infrared Spectroscopy (cNIRS) and Neurological Markers in Critically Ill Children." Neurocrit Care.

Sudoh, T., K. Kangawa, et al. (1988). "A new natriuretic peptide in porcine brain." Nature **332**(6159): 78-81.

Suffredini, A. F., R. E. Fromm, et al. (1989). "The cardiovascular response of normal humans to the administration of endotoxin." N Engl J Med **321**(5): 280-7.

Suga, S., K. Nakao, et al. (1992). "Receptor selectivity of natriuretic peptide family, atrial natriuretic peptide, brain natriuretic peptide, and C-type natriuretic peptide." Endocrinology **130**(1): 229-39.

Tang, B. M., S. J. Huang, et al. (2007). "Predictive value of N-terminal pro-brain natriuretic peptide in sepsis." Crit Care Med **35**(10): 2464.

Tavernier, B., J. M. Li, et al. (2001). "Cardiac contractile impairment associated with increased phosphorylation of troponin I in endotoxemic rats." Faseb J **15**(2): 294-6.

Taylor, K. R. and R. L. Gallo (2006). "Glycosaminoglycans and their proteoglycans: host-associated molecular patterns for initiation and modulation of inflammation." Faseb J **20**(1): 9-22.

Tedder, T. F., D. A. Steeber, et al. (1995). "The selectins: vascular adhesion molecules." Faseb J **9**(10): 866-73.

Tei, C. (1995). "New non-invasive index for combined systolic and diastolic ventricular function." J Cardiol **26**(2): 135-6.

Tei, C., L. H. Ling, et al. (1995). "New index of combined systolic and diastolic myocardial performance: a simple and reproducible measure of cardiac function--a study in normals and dilated cardiomyopathy." J Cardiol **26**(6): 357-66.

Theilen, U., L. Wilson, et al. (2008). "Management of invasive meningococcal disease in children and young people: summary of SIGN guidelines." Bmj **336**(7657): 1367-70.

Thiru, Y., N. Pathan, et al. (2000). "A myocardial cytotoxic process is involved in the cardiac dysfunction of meningococcal septic shock." Crit Care Med **28**(8): 2979-83.

Thiru, Y., N. Pathan, et al. (2000). "A myocardial cytotoxic process is involved in the cardiac dysfunction of meningococcal septic shock." Crit Care Med. **28**(8): 2979-2983.

Thomale, U. W., K. D. Schaser, et al. (2001). "Visualization of rat pial microcirculation using the novel orthogonal polarized spectral (OPS) imaging after brain injury." J Neurosci Methods **108**(1): 85-90.

Thomson, A. P., J. A. Sills, et al. (1991). "Validation of the Glasgow Meningococcal Septicemia Prognostic Score: a 10-year retrospective survey." Crit Care Med **19**(1): 26-30.

Thomson APJ, R. F. (2000). "The management of meningococcal disease." Current Paediatrics **10**: 104-9.

Thorburn, K. and P. Baines (2002). "Predicting mortality or recognizing death in meningococcal disease? Pediatric Risk of Mortality (PRISM) and Pediatric Index of Mortality (PIM)." Crit Care Med **30**(7): 1675-6.

Thorburn, K., P. Baines, et al. (2001). "Mortality in severe meningococcal disease." Arch Dis Child **85**(5): 382-5.

Tikhomirov, E., M. Santamaria, et al. (1997). "Meningococcal disease: public health burden and control." World Health Stat.Q. **50**(3-4): 170-177.

Toet, M. C., A. Flinterman, et al. (2005). "Cerebral oxygen saturation and electrical brain activity before, during, and up to 36 hours after arterial switch procedure in neonates without pre-existing brain damage: its relationship to neurodevelopmental outcome." Exp Brain Res **165**(3): 343-50.

Toh, C. H., J. Samis, et al. (2002). "Biphasic transmittance waveform in the APTT coagulation assay is due to the formation of a Ca(++)-dependent complex of C-reactive protein with very-low-density lipoprotein and is a novel marker of impending disseminated intravascular coagulation." Blood **100**(7): 2522-9.

Toh, C. H., L. O. Ticknor, et al. (2003). "Early identification of sepsis and mortality risks through simple, rapid clot-waveform analysis. Implications of lipoprotein-complexed C reactive protein formation." Intensive Care Med **29**(1): 55-61.

Toller, W. G. and C. Stranz (2006). "Levosimendan, a new inotropic and vasodilator agent." Anesthesiology **104**(3): 556-69.

Tomaru Ki, K., M. Arai, et al. (2002). "Transcriptional activation of the BNP gene by lipopolysaccharide is mediated through GATA elements in neonatal rat cardiac myocytes." J Mol Cell Cardiol **34**(6): 649-59.

Top, A., C. Ince, et al. (2011). "Persistent low microcirculatory vessel density in nonsurvivors of sepsis in pediatric intensive care." Crit Care Med **39**(1): 8-13.

Top, A. P., C. Ince, et al. "Persistent low microcirculatory vessel density in nonsurvivors of sepsis in pediatric intensive care." Crit Care Med **39**(1): 8-13.

Toth, M., K. H. Vuorinen, et al. (1994). "Hypoxia stimulates release of ANP and BNP from perfused rat ventricular myocardium." Am J Physiol **266**(4 Pt 2): H1572-80.

Treacher, D. L., RM (1998). "ABC of oxygen. Oxygen transport—1. Basic principles." BMJ **317**: 1302-6.

Trzeciak, S., I. Cinel, et al. (2008). "Resuscitating the microcirculation in sepsis: the central role of nitric oxide, emerging concepts for novel therapies, and challenges for clinical trials." Acad Emerg Med **15**(5): 399-413.

Trzeciak, S., R. P. Dellinger, et al. (2006). "Translating research to clinical practice: a 1-year experience with implementing early goal-directed therapy for septic shock in the emergency department." Chest **129**(2): 225-32.

Trzeciak, S., R. P. Dellinger, et al. (2007). "Early microcirculatory perfusion derangements in patients with severe sepsis and septic shock: relationship to hemodynamics, oxygen transport, and survival." Ann Emerg Med **49**(1): 88-98, 98 e1-2.

Turhan, H., A. R. Erbay, et al. (2005). "Plasma soluble adhesion molecules; intercellular adhesion molecule-1, vascular cell adhesion molecule-1 and E-selectin levels in patients with isolated coronary artery ectasia." Coron Artery Dis **16**(1): 45-50.

Turner, A., M. Tsamitros, et al. (1999). "Myocardial cell injury in septic shock." Crit Care Med **27**(9): 1775-80.

Uji, Y., H. Sugiuchi, et al. (1992). "[Evaluation of serum troponin T measurement in acute myocardial infarction]." Rinsho Byori **40**(7): 775-82.

Umans, J. G., M. E. Wylam, et al. (1993). "Effects of endotoxin in vivo on endothelial and smooth-muscle function in rabbit and rat aorta." Am Rev Respir Dis **148**(6 Pt 1): 1638-45.

Uzzan, B., R. Cohen, et al. (2006). "Procalcitonin as a diagnostic test for sepsis in critically ill adults and after surgery or trauma: a systematic review and meta-analysis." Crit Care Med **34**(7): 1996-2003.

Vallet, B. (2002). "Endothelial cell dysfunction and abnormal tissue perfusion." Crit Care Med. **30**(5 Suppl): S229-S234.

Van Amersfoort, E. S., T. J. Van Berkel, et al. (2003). "Receptors, mediators, and mechanisms involved in bacterial sepsis and septic shock." Clin Microbiol Rev **16**(3): 379-414.

van den, B. G., P. Wouters, et al. (2001). "Intensive insulin therapy in the critically ill patients." N.Engl.J.Med. **345**(19): 1359-1367.

Van der Kaay, D. C., E. D. De Kleijn, et al. (2002). "Procalcitonin as a prognostic marker in meningococcal disease." Intensive Care Med **28**(11): 1606-12.

Van der Poll, T., J. A. Romijn, et al. (1991). "Tumor necrosis factor mimics the metabolic response to acute infection in healthy humans." Am J Physiol **261**(4 Pt 1): E457-65.

van der Poll, T., S. J. van Deventer, et al. (1992). "Effects on leukocytes after injection of tumor necrosis factor into healthy humans." Blood **79**(3): 693-8.

van Deuren, M., J. van der Ven-Jongekrijg, et al. (1995). "Correlation between proinflammatory cytokines and antiinflammatory mediators and the severity of disease in meningococcal infections." J Infect Dis **172**(2): 433-9.

Van Zee, K. J., T. Kohno, et al. (1992). "Tumor necrosis factor soluble receptors circulate during experimental and clinical inflammation and can protect against excessive tumor necrosis factor alpha in vitro and in vivo." Proc.Natl.Acad.Sci.U.S.A **89**(11): 4845-4849.

Varani, J. and P. A. Ward (1994). "Mechanisms of neutrophil-dependent and neutrophil-independent endothelial cell injury." Biol.Signals **3**(1): 1-14.

Varpula, M., K. Pulkki, et al. (2007). "Predictive value of N-terminal pro-brain natriuretic peptide in severe sepsis and septic shock." Crit Care Med **35**(5): 1277-83.

Victor, V. M., M. Rocha, et al. (2004). "Immune cells: free radicals and antioxidants in sepsis." Int Immunopharmacol. **4**(3): 327-347.

Vila, G., M. Resl, et al. (2008). "Plasma NT-proBNP increases in response to LPS administration in healthy men." J Appl Physiol **105**(6): 1741-5.

Vincent, J. L., D. C. Angus, et al. (2003). "Effects of drotrecogin alfa (activated) on organ dysfunction in the PROWESS trial." Crit Care Med **31**(3): 834-40.

Vink, H. and B. R. Duling (1996). "Identification of distinct luminal domains for macromolecules, erythrocytes, and leukocytes within mammalian capillaries." Circ Res **79**(3): 581-9.

von Dobschuetz, E., P. Biberthaler, et al. (2003). "Noninvasive in vivo assessment of the pancreatic microcirculation: orthogonal polarization spectral imaging." Pancreas **26**(2): 139-43.

Voss, R., F. R. Matthias, et al. (1990). "Activation and inhibition of fibrinolysis in septic patients in an internal intensive care unit." Br.J.Haematol. **75**(1): 99-105.

Waage, A., P. Brandtzaeg, et al. (1989). "The complex pattern of cytokines in serum from patients with meningococcal septic shock. Association between interleukin 6, interleukin 1, and fatal outcome." J.Exp.Med. **169**(1): 333-338.

Waage, A., A. Halstensen, et al. (1987). "Association between tumour necrosis factor in serum and fatal outcome in patients with meningococcal disease." Lancet **1**(8529): 355-7.

Waage, A., A. Halstensen, et al. (1987). "Association between tumour necrosis factor in serum and fatal outcome in patients with meningococcal disease." Lancet **1**(8529): 355-357.

Waage, A., A. Halstensen, et al. (1989). "Local production of tumor necrosis factor alpha, interleukin 1, and interleukin 6 in meningococcal meningitis. Relation to the inflammatory response." J.Exp.Med. **170**(6): 1859-1867.

Walley, K. R. (1996). "Heterogeneity of oxygen delivery impairs oxygen extraction by peripheral tissues: theory." J Appl Physiol **81**(2): 885-94.

Wang, P., Z. F. Ba, et al. (1995). "Endothelium-dependent relaxation is depressed at the macro- and microcirculatory levels during sepsis." Am J Physiol **269**(5 Pt 2): R988-94.

Wang, T. J., M. G. Larson, et al. (2004). "Plasma natriuretic peptide levels and the risk of cardiovascular events and death." N Engl J Med **350**(7): 655-63.

Watson, R. S., J. A. Carcillo, et al. (2003). "The epidemiology of severe sepsis in children in the United States." Am J Respir Crit Care Med **167**(5): 695-701.

Weibel, E. R. and H. Hoppeler (2005). "Exercise-induced maximal metabolic rate scales with muscle aerobic capacity." J Exp Biol **208**(Pt 9): 1635-44.

Weil, M. H., Y. Nakagawa, et al. (1999). "Sublingual capnometry: a new noninvasive measurement for diagnosis and quantitation of severity of circulatory shock." Crit Care Med **27**(7): 1225-9.

Weisel, R. D., L. Vito, et al. (1977). "Myocardial depression during sepsis." Am J Surg **133**(4): 512-21.

Weisinger, J. R. and E. Bellorin-Font (1998). "Magnesium and phosphorus." Lancet **352**(9125): 391-396.

Weiss, J., P. Elsbach, et al. (1978). "Purification and characterization of a potent bactericidal and membrane active protein from the granules of human polymorphonuclear leukocytes." J.Biol.Chem. **253**(8): 2664-2672.

Wells, L. C., J. C. Smith, et al. (2001). "The child with a non-blanching rash: how likely is meningococcal disease?" Arch Dis Child **85**(3): 218-22.

West, G. B., J. H. Brown, et al. (1999). "The fourth dimension of life: fractal geometry and allometric scaling of organisms." Science **284**(5420): 1677-9.

Westendorp, R. G., J. A. Langermans, et al. (1995). "Release of tumor necrosis factor: an innate host characteristic that may contribute to the outcome of meningococcal disease." J.Infect.Dis. **171**(4): 1057-1060.

Whalen, M. J., L. A. Doughty, et al. (2000). "Intercellular adhesion molecule-1 and vascular cell adhesion molecule-1 are increased in

the plasma of children with sepsis-induced multiple organ failure." Crit Care Med **28**(7): 2600-7.

Witthaut, R., C. Busch, et al. (2003). "Plasma atrial natriuretic peptide and brain natriuretic peptide are increased in septic shock: impact of interleukin-6 and sepsis-associated left ventricular dysfunction." Intensive Care Med **29**(10): 1696-702.

Wong, H. R., J. A. Carcillo, et al. (1996). "Nitric oxide production in critically ill patients." Arch Dis Child **74**(6): 482-9.

Wood, M. J. and M. H. Picard (2004). "Utility of echocardiography in the evaluation of individuals with cardiomyopathy." Heart **90**(6): 707-12.

Wright, S. P., R. N. Doughty, et al. (2003). "Plasma amino-terminal pro-brain natriuretic peptide and accuracy of heart-failure diagnosis in primary care: a randomized, controlled trial." J Am Coll Cardiol **42**(10): 1793-800.

Wu, A. H., Y. J. Feng, et al. (1998). "Characterization of cardiac troponin subunit release into serum after acute myocardial infarction and comparison of assays for troponin T and I. American Association for Clinical Chemistry Subcommittee on cTnI Standardization." Clin Chem **44**(6 Pt 1): 1198-208.

Xu, H., J. A. Gonzalo, et al. (1994). "Leukocytosis and resistance to septic shock in intercellular adhesion molecule 1-deficient mice." J Exp Med **180**(1): 95-109.

Yamamoto, K., M. M. Redfield, et al. (1996). "Analysis of left ventricular diastolic function." Heart **75**(6 Suppl 2): 27-35.

Yvonne-Tee, G. B., A. H. Rasool, et al. (2005). "Reproducibility of different laser Doppler fluximetry parameters of postocclusive reactive hyperemia in human forearm skin." J Pharmacol Toxicol Methods **52**(2): 286-92.

Zakariah, A. N., S. M. Cozzi, et al. (2008). "Combination of biphasic transmittance waveform with blood procalcitonin levels for diagnosis of sepsis in acutely ill patients." Crit Care Med **36**(5): 1507-12.

Zenz, W., B. Zoehrer, et al. (2004). "Use of recombinant tissue plasminogen activator in children with meningococcal purpura fulminans: a retrospective study." Crit Care Med. **32**(8): 1777-1780.

Zhou, M., A. J. Arthur, et al. (2001). "The small intestine plays an important role in upregulating CGRP during sepsis." Am.J.Physiol Regul.Integr.Comp Physiol **280**(2): R382-R388.